MULTIMODE STELLAR PULSATIONS

MULTIMODE STELLAR PULSATIONS

Proceedings of the Workshop held in Budapest,
Hungary, 1– 3 September 1987

Editors:
G. KOVÁCS
L. SZABADOS
B. SZEIDL

KONKOLY OBSERVATORY · KULTURA · BUDAPEST, 1988

Joint edition published by
the KONKOLY OBSERVATORY of the HUNGARIAN ACADEMY of SCIENCES
and KULTURA, Budapest

Editors:
G. KOVÁCS
L. SZABADOS
B. SZEIDL

ISBN 963 8361 29 8

Printed in Hungary

CONTENTS

PREFACE ix

LIST OF PARTICIPANTS xi

MULTI-MODE PULSATION IN CEPHEIDS AND OTHER SUPERGIANTS 1
L. Szabados

PULSATION TYPES IN MAGELLANIC CLOUD CEPHEIDS 13
J. O. Petersen and G.K. Andreasen

NEW OBSERVATIONS OF THE DOUBLE-MODE CEPHEIDS AP VEL AND BK CEN 19
M. Jerzykiewicz

DOUBLE-MODE PULSATORS WITH UNUSUAL LIGHT CURVES 27
E. Antonello, E. Poretti, and R. F. Stellingwerf

IS THREE-MODE RESONANCE ABLE TO SUPPORT BEAT CEPHEID-TYPE PULSATION? 33
G. Kovács and Z. Kolláth

RR LYRAE STARS: BEAT AND BLAZHKO EFFECT 45
B. Szeidl

DEPENDENCE OF THE PERIOD AND AMPLITUDE FLUCTUATION OF RR LYRAE STARS ON THE BLAZHKO PERIOD 67
S. Kanyó

THE AMPLITUDE EQUATION FORMALISM APPLIED TO STELLAR PULSATIONS 71
J. R. Buchler

THE HISTORY AND DEVELOPMENT OF NONLINEAR STELLAR PULSATION CODES 87
C. G. Davis

MULTIPLE-MODE PULSATION IN δ SCUTI STARS 95
D. W. Kurtz

MULTIPLE-MODE AND NON-LINEAR PULSATION IN RAPIDLY OSCILLATING Ap STARS 107
D. W. Kurtz

SPECTRAL LINE VARIATION DUE TO NON-RADIAL PULSATION 119
W. W. Weiss and H. Schneider

NONLINEAR EFFECTS IN LOW AMPLITUDE VARIABLES 127
W. Dziembowski

LIMITING AMPLITUDE EFFECT OF THE PARAMETRIC RESONANCE IN ROTATING MAIN SEQUENCE STARS 141
M. Królikowska and W. Dziembowski

STABILITY OF THE THREE-MODE LIMIT CYCLES IN THE MULTIMODE PARAMETRIC RESONANCE CASE 149
P. Moskalik

EXCITATION OF SOLAR OSCILLATIONS: THEORETICAL POSSIBILITIES AND OBSERVATIONAL CONSEQUENCES 153
J. Christensen-Dalsgaard

THEORY AND OBSERVATIONS OF PULSATING WHITE DWARF STARS 181
D. E. Winget

ZZ CETI MODE TRAPPING REVISITED 199
M. A. Wood and D. E. Winget

SECULAR EVOLUTION OF THE 516s PERIOD IN THE PRESENCE OF NEW MODES IN PG 1159-035 205
D. E. Winget and S. O. Kepler

THE STRUCTURE OF STELLAR QUANTUM CHAOS 209
J. Perdang

CHAOTIC PULSATIONS IN STELLAR MODELS 265
J. R. Buchler, G. Kovács, and M.-J. Goupil

A NONADIABATIC OSCILLATOR PRODUCING CHAOS 277
M. Takeuti

TESTING FOR CHAOS IN LONG PERIOD VARIABLES 283
S. Blacher and J. Perdang

SECULAR EVOLUTION OF THE 5/6s PERIOD IN THE PRESENCE OF NEW MODES IN PG 1159-035 203
D. E. Winget and S. O. Kepler

THE STRUCTURE OF STELLAR QUANTUM CHAOS 209
J. Perdang

CHAOTIC PULSATIONS IN STELLAR MODELS 265
J. R. Buchler, G. Kovács, and M.-J. Goupil

A NONADIABATIC OSCILLATOR PRODUCING CHAOS 277
M. Takeuti

TESTING FOR CHAOS IN LONG PERIOD VARIABLES 283
S. Blacher and J. Perdang

PREFACE

The subject of *multimode stellar pulsation* has become one of the the most intensively studied fields of variable star astronomy. It is not difficult to list the reasons why this is so. The reasons are:

(i) development of data acquisition systems and data analysis has given us efficient tools for studying the temporal variation of the light and/or radial velocity of various types of pulsators.

(ii) A very large portion of the observed pulsators have proved to be multi-periodic, and it is quite possible that in certain types of pulsators (Sun, white dwarfs, Delta Scuti and rapidly oscillating Ap stars) this is the usual (and maybe the only) way of pulsation.

(iii) In almost all cases the time variation can be represented by the finite Fourier sum of constant amplitudes and phases. This fact makes variable star astronomy feasible since, by a mere increase in the duration of the observations, we are able to achieve a greater accuracy and, eventually, resolve the Fourier spectrum.

(iv) Since the linear nonadiabatic eigenmode frequencies usually give an adequate representation of the observed frequency spectra, very important information on the internal structure of the pulsators can be inferred without resorting to the unsolved problem of nonlinear nonradial pulsation.

(v) The great progress in the powerful application of the methods of seismology and pulsation theory to the solar data has led to the recognition of the possibility of applying the methods to other multimode pulsators.

(vi) The testing of the internal structure of stars through their pulsational frequencies (i.e. *stellar seismology*) is the only way to understand the internal constitution of the individual stars. Of course, this also leads to other data of astrophysical and cosmological interest (i.e. better estimation of the chemical composition, information on the elementary particle processes in the stellar core, convection in stars, rotation, magnetic field, etc.).

Despite the promising progress achieved in some fields of multimode stellar pulsation (e.g. white dwarfs, rapidly oscillating Ap stars but especially the Sun), there remain plenty of unanswered problems which keep everyone busy working on stellar pulsation. Without attempting to provide comprehensive details, here we should like to list only a few outstanding problems.

Strictly speaking, our first attempt to utilize double-periodic stellar pulsation to obtain better stellar parameters has failed. We still do not know the reason for the mass discrepancy of the beat Cepheids nor, on the whole, why nonlinear pulsational stellar models are unable to model sustained double-periodic pulsations as observed in the case of beat Cepheids, dwarf Cepheids and RR Lyrae stars. In general, though

some progress has been made during the past few years mostly in the phenomenological interpretation of nonlinear stellar pulsation, much more work is needed both on the mode coupling theory and on the development of the nonlinear pulsation codes. The difficult problem of the hydrodynamic modelling of nonlinear nonradial pulsation is probably attackable in the not very distant future, due to the rapid development of supercomputers.

It is clear that in the overwhelming majority of the multimode stellar pulsators, finite amplitude pulsation is established by nonlinear effects, consequently nonlinear theories are indispensable in understanding their basic behaviour.

The situation in the field of the linear pulsation theory is better, though problems like the excitation mechanism of the pulsations of Beta Cephei and Ap stars and the Sun, and the pulsation-convection interaction are still unsolved.

As to the observations, besides the discovery of further multimode variables, it is immensely important to study the individual objects in detail. Long base international observations have already been made in the case of the Sun, white dwarfs and rapidly oscillating Ap stars but little is known about the small amplitude Delta Scuti stars, which constitute the overwhelming majority of these variables. Finally, we mention that for long period variables such as W Vir, RV Tau, semiregular and Mira variables, the basic question whether they are multiperiodic or chaotic is still unanswered, mainly because of the paucity and poor quality of the available data.

International conferences on various types of variable stars are organized almost every year. Because of the rapid development in the study of solar oscillations, experts on this and related fields gather especially often. The last international conference focusing on multiperiodic stellar oscillation, however, was held (in Budapest) more than 10 years ago. Since that time considerable progress has been made both in the theory and observations, which explains the timeliness of the present workshop.

It is a pleasant duty to acknowledge the financial support of the Committee of the International Theoretical Physics Workshop (NEFIM) operated in the Central Research Institute for Physics of the Hungarian Academy of Sciences, and the helpful assistance of Mrs. Emilia Szabó, the secretary of this organization. The active cooperation of the Scientific Organizing Committee: J. Robert Buchler, Jørgen Christensen-Dalsgaard and Wojtek Dziembowski meant a considerable contribution to the successful organization of this workshop. Mr. Harvey Shenker is thanked for the linguistic revision, and Mrs. Éva Végvári for her painstaking camera ready typing. We are grateful to Mrs. Ilona Kálmán for the excellent arrangements during the meeting.

Editors

LIST OF PARTICIPANTS

Elio ANTONELLO	Osservatorio Astronomico di Brera Via E. Bianchi 46 I–22055, Merate, Italy
László BAKSAY	Union College Department of Physics Schenectady, NY 12308, USA
J. Robert BUCHLER	University of Florida Department of Physics 215 Williamson Hall Gainesville, FL 32611, USA
Jørgen CHRISTENSEN-DALSGAARD	Institute of Astronomy University of Aarhus DK 8000 Aarhus C, Denmark
Cecil G. DAVIS	Los Alamos National Laboratory Box 1163, Los Alamos, NM 87545, USA
N. DOLEZ	Observatoires du Pic-Du-Midi et de Toulouse, 14, Avenue Edouard-Belin F–31400 Toulouse, France
Wojtek DZIEMBOWSKI	Copernicus Astronomical Center ul. Bartycka 18, 00–716 Warsaw, Poland
Marie-Jo GOUPIL	Observatoire de Nice, BP 139 F–06003 Nice Cedex, France
András HOLL	Konkoly Observatory 1525 Budapest XII. Box 67, Hungary

Mikolaj JERZYKIEWICZ	Wroclaw University Observatory ul. Kopernika 11, 51–622 Wroclaw, Poland
Sándor KANYÓ	Konkoly Observatory 1525 Budapest XII. Box 67, Hungary
Zoltán KOLLÁTH	Konkoly Observatory 1525 Budapest XII. Box 67, Hungary
Géza KOVÁCS	Konkoly Observatory 1525 Budapest XII. Box 67, Hungary
Malgosia KRÓLIKOWSKA	Copernicus Astronomical Center ul. Bartycka 18, 00–716 Warsaw, Poland
Don W. KURTZ	Department of Astronomy University of Cape Town Rondebosch 7700, South Africa
Miklós MARIK	Eötvös Loránd University Department of Astronomy 1083 Budapest, Kun B. tér 2.
Pawel MOSKALIK	Copernicus Astronomical Center ul. Bartycka 18, 00–716 Warsaw, Poland
Margit PAPARÓ	Konkoly Observatory 1525 Budapest XII. Box 67, Hungary
Jean PERDANG	Institut d'Astrophysique Avenue de Cointe, 5 B–4200 Cointe-Ougrée, Belgium
J. Øtzen PETERSEN	Copenhagen University Observatory Oster Voldgade 3 DK–1350, Copenhagen K, Denmark

Norio SAITO

Astronomical Institute
Faculty of Science,
Tôhoku University,
Sendai 980, Japan

László SZABADOS

Konkoly Observatory
1525 Budapest XII. Box 67, Hungary

Károly SZATMÁRY

József Attila University
Department of Experimental Physics
6720 Szeged, Dóm tér 9., Hungary

Béla SZEIDL

Konkoly Observatory
1525 Budapest XII. Box 67, Hungary

Mine TAKEUTI

Astronomical Institute
Faculty of Science,
Tôhoku University,
Sendai 980, Japan

Frank VERHEEST

Institut voor Theoretische Mechanica
Gebouw S 9, Krijgslaan 271
B–9000 Gent, Belgium

Balázs VETŐ

Konkoly Observatory
1525 Budapest XII. Box 67, Hungary

Werner W. WEISS

Institut für Astronomie
Universität Wien
Türkenschanzstrasse 17
A–1180 Wien, Austria

Don E. WINGET

University of Texas
Department of Astronomy
Austin, TX 78712, USA

Matt A. WOOD

University of Texas
Department of Astronomy
Austin, TX 78712, USA

Jan ZALEWSKI

Copernicus Astronomical Center
ul. Bartycka 18,
00–716 Warsaw, Poland

Endre ZSOLDOS

Konkoly Observatory
1525 Budapest XII. Box 67, Hungary

MULTI-MODE PULSATION IN CEPHEIDS AND OTHER SUPERGIANTS

L. Szabados
Konkoly Observatory, Budapest, Hungary

Abstract

The pulsating supergiants with more than one excited mode include the beat Cepheids, the bump Cepheids of both populations, as well as some other pulsating variables in which mode switching occurs, e.g. RV Tauri stars, UU Her variables, R CrB variables, and other peculiar stars. The recent results concerning their multi-mode behaviour, both observational and theoretical are reviewed.

1. Beat Cepheids

The small but important group of beat Cepheids is still a mistery and no spectacular progress has been reached since *Balona's* (1985) review. There are, however, some results to be mentioned.

EW Scuti turned out to be a new member of this group (*Cuypers* 1985). Its fundamental period is almost the longest (5.8 days) and the period ratio of the two co-existing modes is in accordance with the typical values of other beat Cepheids. Moreover, its recent spectral classification resulted in a spectral type of F8 II (*Antonello, Mantegazza* and *Poretti* 1987), while the out-of-date spectral type given in the GCVS is K0.

CO Aur is not a new member but its membership among the double-mode Cepheids has been questioned (*Balona* 1985). As a matter of fact, its periods give a ratio quite different from the typical values for beat Cepheids. When revealing the double periodicity, *Mantegazza* (1983) interpreted those as the simultaneously excited first and second overtones. This conclusion has been confirmed in three more recent papers: *Fuhrmann, Luthardt* and *Schult* (1984) analysed the light variation of CO Aur using the Sonneberg plate collection, *Antonello, Mantegazza* and *Poretti* (1986) performed new photoelectric measurements, while *Babel* and *Burki* (1987) published both photoelectric radial velocity and photometric data.

The number of known beat Cepheids in our galaxy now totals 13. Table I contains some basic information on each of them. The respective columns contain the following data: the name of the star; the value of the fundamental period; the ratio of the two periods; the ratio of the respective amplitudes of the light variation; the ratio of the amplitudes of the radial velocity variations; and the remarks. It is clearly

seen from these data that although the amplitude of the light variation in the first overtone is usually less than the light amplitude of the fundamental mode pulsation (AX Vel is the only exception), the ratio of the amplitudes is not much less than unity. In this respect the question whether there exist double-mode Cepheids with a very small amplitude secondary oscillation is of importance both from observational and theoretical points of view. The proposed candidates for slightly modulated pulsation are the Cepheids AS Cas (*Henden* 1980), EU Tau (*Gieren* 1985; *Gieren* and *Matthews* 1987), and EV Sct (*Mermilliod, Mayor* and *Burki* 1987). Extensive photometry of these stars would certainly help solve this puzzling situation.

Table I. Double-mode Cepheids

Name	P_0	P_1/P_0	$(\Delta V)_1/(\Delta V)_0$	$(\Delta v_r)_1/(\Delta v_r)_0$	Remark
CO Aur	$1^d.78301$	0.8008	0.178	0.20	1
TU Cas	2.13931	0.7097	0.353	0.49	
U TrA	2.56843	0.7105	0.421	0.51	
VX Pup	3.0109	0.7104	0.867	1.43	
AP Vel	3.12776	0.7033	0.502	0.74	
BK Cen	3.17387	0.7004	0.433	0.76	
UZ Cen	3.33435	0.7064	0.227	0.42	
Y Car	3.63981	0.7032	0.451	0.61	2
AX Vel	3.67317	0.7059	1.276	2.08	
GZ Car	4.15885	0.7054	0.573	1.34	
BQ Ser	4.27073	0.7053	0.585		
EW Sct	5.8195	0.6984	0.815		
V 367 Sct	6.29307	0.6967	0.958		3

Remarks:
1. P_1 and P_2 are excited instead of P_0 and P_1
2. Binary
3. Cluster member

The data concerning CO Aur are taken from *Babel* and *Burki* (1987); BQ Ser: *Balona* and *Engelbrecht* (1985); EW Sct: *Cuypers* (1985); the other stars: *Balona* (1985), where the error of the entries is also listed.

Since the double-mode Cepheids are normal Cepheids, one would expect them to exist in the Magellanic Clouds, too. Apart from one not very convincing example (W3 in LMC, with a period probably less than one day – *Connolly* 1982), other searches failed to find extragalactic beat Cepheids. This situation is now changed. *Andreasen* (1987) reported that he had succeeded in finding one Cepheid in LMC (HV 2345) with two simultaneous periods.

The problem of Hα emission in beat Cepheids is another important but still unanswered question. *Barrell* (1978) found Hα emission of varying strength in seven out of nine beat Cepheids when spectroscopic observations were made during the ascending branch or the maximum of the light variation. Later on (*Balona* 1985) these emissions were attributed to an instrumental effect and, similarly, no Hα emission was found in TU Cas (*Henden, Cornett* and *Schmidt* 1984). Upon my request a spectrum of TU Cas covering the red region including the Hα line was taken by Drs. K.P. Tsvetkova and L. Iliev with the coudé-spectrograph of the 2-m telescope in Rozhen (Bulgaria) on 23/24 November 1983 (mid-exposure: J.D. 2444662.430). The profile of the Hα line is shown in Figure 1. A weak emission in the core can clearly be seen. This line profile recalls that of VX Pup published by *Barrell* (1978). When the emission was observed, TU Cas was near its minimum brightness. The presence of this emission means that such emissions can occur in beat Cepheids – at least in certain phases – and the behaviour of the Hα line in double-mode Cepheids deserves further attention. It is difficult to predict the proper phases if one wants to observe emission, because *Barrell* (1978) did not publish the phases according to the overtone (or the beat period). The emission found by her occurred mostly between the phases 0.75 and 0.10 if the zero phase corresponds to maximum light in the primary pulsation period. The only exception is Y Car where the Hα emission was observed at phases 0.13 and 0.69 of the fundamental period. Y Car might, however, be an atypical beat Cepheid because it is a component of a binary system (*Stobie* and *Balona* 1979). Due to the proximity of the companion to the pulsating atmosphere of the Cepheid (the projected orbit has a value of $a \sin i = 10^8$ km – *Balona* 1983), emissions due to mass transfer cannot be excluded during the phases when the single beat Cepheids are not able to produce an emission.

An interesting relationship between the period and a parameter based on the observable amplitudes of the beat Cepheids can be revealed with the help of the data gathered in Table I. The parameter mentioned is the ratio of the amplitude ratios $AR = \Delta V/\Delta v_r$ for the overtone and the fundamental periods, where ΔV is the amplitude of the light variation and Δv_r is that of the radial velocity variation. When plotting AR_1/AR_0 *vs.* the fundamental period (subscript 1 denotes the first overtone, 0 refers to the fundamental mode variations), a systematic decrease of this ratio toward the longer periods is seen (Figure 2). The error bars are rather large due to the error propagation, therefore it would be extremely important that the three longest period known beat Cepheids be included in the diagram. To this end radial velocity observations have to be performed since the light amplitudes of BQ Ser, EW Sct, and V 367 Sct are more or less accurately known. If the effect is real, it can be interpreted that in the case of two simultaneously excited modes the relative

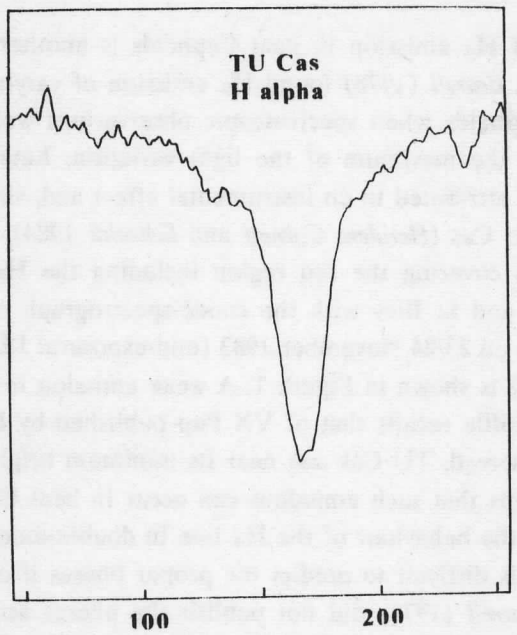

Fig. 1. Profile of the Hα line of TU Cas. The scales are arbitrary on both axes. The emission in core is clearly visible.

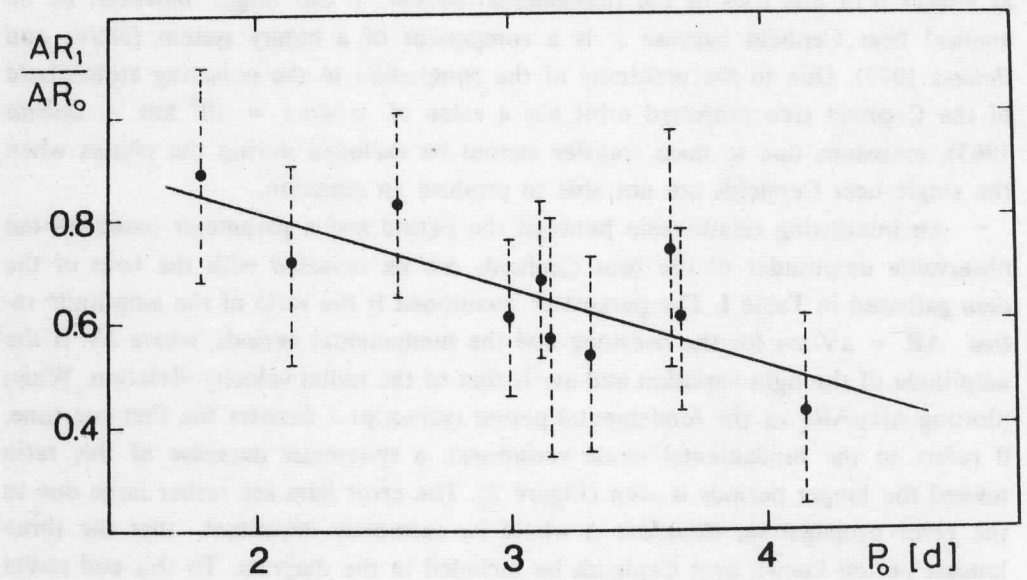

Fig. 2. Ratio of $\Delta V_1/\Delta V_0$ and $(\Delta v_r)_1/(\Delta v_r)_0$ vs. the fundamental period (for detailed discussion, see text).

importance of the overtone diminishes with increasing period, as far as the light variation is concerned. In other words, there is some effect working in these stars which allows the periodic displacement of the atmospheric layers by the overtone period but inhibits the accompanying light variations. This trend of the amplitude ratios gives a plausible explanation for the fact that the beat phenomenon in Cepheids is confined to the fundamental periods shorter than about six days, but nothing can be said about the underlying physical process. The linear least squares fit to the data points in Figure 2 resulted in the formula:

$$AR_1/AR_0 = -0.150\ P_0 + 1.120$$
$$\pm .042 \qquad \pm .131$$

CO Aur has been treated here as if it were a fundamental and first overtone pulsator. For the time being the above relationship is only suspected, its reality needs to be supported by additional or higher accuracy data.

In addition to the radial velocity observations, in most cases we are in need of new, high quality photometric data, too. The list of recent papers that contain photometric observations of "bona fide" double-mode Cepheids is very short: *Moffett* and *Barnes* (1984) (TU Cas, VX Pup, V 367 Sct, BQ Ser), *Balona* and *Engelbrecht* (1985) (BQ Ser). The problem of secular photometric amplitude variation (changes in modal amplitudes), phase jitter of the overtone, additional periodicities (see *Balona* 1985, and references therein) can only be solved with new observational data.

The long period (1400 days) modulation of both the light and radial velocity curves of V 473 Lyrae (=HR 7308) is unique among the Cepheids. Based on the period ratio, its classification as a double-mode pulsator can be excluded. The pulsation period of 1.491 d is stable but the amplitude of pulsation varies by at least a factor of 15. When the amplitude is at minimum, the shape of the radial velocity curve is simply sinusoidal, and it becomes asymmetric with increasing amplitude. Under the hypothesis that the star is a classical Cepheid, its radius ($>30\ R_\odot$) implies radial pulsation in a high (at least the 2nd) overtone. However, the possibility that the star is a Population II Cepheid of lower pulsation mode cannot be ruled out (*Burki et al.* 1986), although V 473 Lyrae shows normal solar abundance. The star is situated to the red of the instability strip and this fact also increases our confidence in the hypothesis by *Auvergne* (1986) who calculated the instability of the limit-cycle in a one-zone model, as a possible explanation of the strange modulation of V 473 Lyrae.

2. Resonances in Bump Cepheids

Bumps in the light curves are now interpreted as the result of near resonance between the fundamental mode and the second overtone periods as discussed by *Simon* and *Schmidt* (1976). The resonance is clearly seen when the light and/or radial velocity curves of classical Cepheids are decomposed into their Fourier components (*Simon* and *Lee* 1981; *Simon* and *Davis* 1983; *Simon* and *Teays* 1983; *Simon* and *Moffett* 1985). The light curves of the small amplitude Cepheids have been Fourier decomposed by *Antonello* and *Poretti* (1986). The same authors (1987) found that unlike the classical Cepheids, where the resonance condition $P_2/P_0 = 0.5$ is fulfilled, the s-Cepheids are subjected to a resonance between the third overtone and the fundamental mode, or if the small amplitude Cepheids are first overtone pulsators, then the fourth overtone is in resonant mode coupling with the lower harmonic, *i.e.* $P_4/P_1 = 0.5$.

The Hertzsprung sequence of the light curve shapes, seen so well for the classical Cepheids (with periods between about 5 and 15 days), and for the small amplitude Cepheids (with periods between 2 and 8 days), shows up for the lower mass, Population II Cepheids, as first noticed by *Stobie* (1973). Recently, a number of studies were performed where Fourier decomposition was applied to the light curves of BL Herculis type variables (*Petersen* and *Diethelm* 1986; *Simon* 1986; *Petersen* and *Andreasen* 1987; *Carson* and *Lawrence* 1987), but there is disagreement in the seemingly simple problem of where the resonance centre (*i.e.* $P_2/P_0 = 0.5$) occurs. The values 1.6 days and 2.0 days have been deduced in the literature.

According to *Fokin* (1986), the mechanism leading to the appearance of the bump is evidently complex and includes not only resonant excitation of the second overtone but also generation of a travelling wave (or pulse). In their latest paper on stellar acoustics, however, *Aikawa* and *Whitney* (1985) conclude that the mode-resonance is a more apt description of the bump phenomenon instead of the simultaneous presence of the pulse resonance and the mode-resonance.

The non-linear hydrodynamic models calculated by *Fadeyev* and *Fokin* (1985) revealed the resonance $P_0 = 2 \cdot P_1$ for the W Vir models with a period of 10 days and longer. This resonance causes the flat top on the light curve at a period of 10 days and appearance of a shallow alternating minimum at longer periods as is observed in the RV Tauri variables. In their recent models, *Buchler* and *Kovács* (1987) have demonstrated that the hydrodynamic behaviour of radiative W Vir models shows a typical period doubling sequence leading to chaos, with the effective temperature being the control parameter. These latter models involve two types of third order resonance.

3. RV Tauri and Related Supergiant Variables

The first attempt to model the occurrence of the alternating deep and shallow minima in RV Tau stars as a result of resonance between the fundamental mode and the first overtone was made by *Takeuti* and *Petersen* (1983). The linear adiabatic theory, however, was unable to give the overall explanation of RV Tauri pulsation properties because of strong non-adiabatic and non-linear effects. The most prominent feature of the non-linear pulsation model calculated by *Fadeyev* (1984) is that the innermost layers oscillate as a standing wave whereas the oscillations of outer layers occur in the form of running waves. The ratio of the frequency of the standing wave to that of running waves is about 2. This fact leads to an alternation of deep and shallow minima in the kinetic energy and radius variations and it explains the nature of RV Tauri variables.

Linear, non-adiabatic pulsation models including convection have been developed by *Worrell* (1987). Only those RV Tauri stars could successfully be modelled in which the alternation of deep and shallow light minima continues without reversal over many cycles. The overwhelming majority of RV Tauri variables, however, is not associated with the critical period ratios (e.g. $P_1/P_0 = 1/2$).

The models calculated by *Buchler* and *Kovács* (1987) are able to simulate the RV Tauri phenomenon at certain effective temperatures. It is interesting to note that this behaviour could be achieved by neglecting convection.

From the observational point of view, the difficulty is that extensive series of observations covering long time intervals are not available in the literature. The only detailed study of an RV Tauri variable is that of V 453 Oph (*Mantegazza* 1985). For this star, the complex light variation could be decomposed into a few periodic terms. Three of these terms are exactly in integer ratios but they are not Fourier harmonics of the same wave, i.e. they are resonant independent waves. Moreover, some of the terms are split into two which could indicate the presence of non-radial pulsations. Analysis of the light curves of other RV Tauri variables is still inconclusive (*Mantegazza* 1986).

There is one more interesting observational fact concerning multiple periodicity in RV Tauri stars, viz. the periodic (or cyclic) variability of the mean light of RVb stars. The relationship between the fundamental period and the long-term modulation is surprisingly linear (*Fokin* 1984). Somewhat similar behaviour but with a different slope can be seen in the corresponding diagram for the doubly periodic semiregular variables of spectral type M (*Fokin* 1984).

Mode switching and resonance can occur in red variables. Small amplitude secondary periods of length twice the primary pulsation period, which can be explained in terms of a $P_0 = 2P_1$ resonance between the first overtone and the fundamental mode, have been noted in some cases (*Wood* 1981). An example of gradual switch-

ing from mode to mode over many pulsation cycles is the SRd variable Z Aur. This transition might correspond to a switching from P_3 to P_2 (*Wood* 1975). The pulsating component of the ε Aurigae system shows a number of simultaneously present periods (*Arellano Ferro* 1985; *Kraus et al.* 1987).

There are some F-type, Cepheid-like supergiants in the halo with interesting properties (*Sasselov* 1985): roughly normal composition, yet these stars are found at high galactic latitudes; small amplitude and long period light variation; two (or three) distinct, alternating modes switching from one to the other, with a shorter interval of erratic fluctuations in between; short standstills, i.e. unpredictable abrupt cessation of pulsation for a couple of months. Their classification as a separate type of variables has been proposed by Sasselov, but in the GCVS the prototype stars (UU Her) itself is classified as an SRd star, with the remark that its light curve resembles that of RV Tauri variables. Another recent common practice is to refer to them as 89 Her stars (*Arellano Ferro* 1984; *Worrell* 1986) – though the variable star name V 441 Her has long been assigned to 89 Her. Curiously enough, V 441 Her is also classified as an SRd star in the latest edition of the GCVS.

The mode switching is best seen in HD 161 796 (= V 814 Her). In 1979/80 the star had two non-simultaneous pulsation periods of 62 and 43 days, while in 1984 the periods were shorter: 54 and 38 days but their ratio has remained the same (*Fernie* 1986). As Fernie noted, the modes do not represent the fundamental and first harmonic modes, they are rather non-radial modes. It is worth mentioning that the star is able to switch on its pulsation instantaneously at full amplitude with no growth being visible. On the basis of pulsational calculations the low mass (and highly evolved star) hypothesis is preferred (*Worrell* 1986; *Zalewski* 1986) but the spectroscopic binary nature of V 441 Her (*Arellano Ferro* 1984) would imply a high mass (~ 20 $M_\odot$) for this supergiant star.

The case of V 810 Cen is unique. In this long period Cepheid- like star (Sp: G0 Ia; according to the GCVS the star belongs to the SRd type) there are five frequencies necessary to describe the observed variation in V light (*Burki* 1984). The periods involved are: 80, 105, 133, 182, and 476 days. The largest amplitude belongs to the 105 day oscillation. If the 182 day period corresponds to the fundamental mode of the oscillation, then the observed period ratios P_i/P_0 for overtones are as follows: $P_1/P_0 = 0.73$, $P_2/P_0 = 0.58$, $P_3/P_0 = 0.44$, while theoretical predictions give the values 0.74, 0.57, and 0.46 for these ratios respectively. This is the only known supergiant star which pulsates in the first four radial modes simultaneously (*Burki* 1984). This interpretation, however, needs further confirmation.

4. Other Supergiants

Multi-mode pulsation is also present in the rapidly rotating B supergiants (*Maeder* 1986, and references therein), *e.g.* γ Arae. The line profile variation of this star provides convincing evidence of stable non-radial pulsations. *Baade* and *Ferlet* (1984) found two stable periods of non-radial pulsations $P_1 = 0.87$ d and $P_2 = 0.17$ d identified as corresponding to two sectorial modes.

The R CrB variables falling into the instability strip form a distinct group of pulsating supergiants. Their pulsation period is near 40 days (RY Sgr: 38.6 d, R CrB: 44 or 49 days, UW Cen: 43 days - *Feast* 1986). S Aps now has a pulsation period near 40 days, although it used to pulsate with a period of 120 days (*Kilkenny* 1983). This may be due to a change from the fundamental mode of pulsation to an overtone. The period change analyses of pulsating R CrB stars performed by *Kilkenny* (1982), and *Kilkenny* and *Flanagan* (1983) suggest that these stars are evolving from red to blue in the HR diagram. According to theoretical results (*Saio* and *Wheeler* 1985) rapid mass loss occurs in the low effective temperature region, if the mass is less than 1.6 $M_\odot$. The decrease of the envelope mass would increase the effective temperature of the star. Since the amplitude of the pulsation decreases rapidly as the effective temperature increases, the mass loss rate may be reduced as the star travels bluewards. This suggests that the rate of blueward evolution is slower in a higher effective temperature region in the HR diagram which may explain the fact that the pulsating R CrB stars are crowded around $T \approx 7000$ K, or period $\approx$ 40 days. The mode switching of S Apodis discovered by *Kilkenny* (1983) can also be considered as a result of the blueward evolution, if the overtones become more dominant at higher temperatures.

Just the opposite direction of evolution characterizes the peculiar supergiant variable FG Sagittae, the central star of a planetary nebula. This star has been pulsating since the sixties with enormously rapid increase in the period. Changes in its spectral type and effective temperature also give evidence of rapid redward evolution in the HR diagram (*Jurcsik* and *Szabados* 1981, and references therein). According to the nonlinear, radial pulsational model computed by *Aikawa* (1985a,b), FG Sge started its pulsation in the third overtone mode when entering the instability strip from the blue side, then a mode switching might have occurred to the fundamental mode. Aikawa's theoretical light curve shows a sub-structure that would correspond to the interaction of the third overtone with the fundamental mode pulsation. Such a pattern of the light curves of FG Sge was observed in 1970 (*Jurcsik* and *Szabados* 1981). The effective temperature of FG Sge, however, was higher in 1970 ($\sim$8000 K) than the theoretical value at which the mode switching was expected to occur (between 6000 and 5400 K).

A word of warning is appropriate here: *Harmanec* (1987) showed that the interpretation of the observed semi-periodic light or radial velocity variations of supergiants in terms of (non-radial) pulsations is not as straightforward as is often believed. He demonstrated that the observed semi-period – luminosity – colour relationship can also be derived under the assumption of orbital motion in a binary system. Therefore it cannot be excluded that some of the variable supergiants are in fact contact or nearly contact more massive components of unrecognized binary systems of low mass ratio. The existence of multiple periodic supergiants, however, serves as a convincing evidence in favour of the explanation of their variation in terms of pulsation, keeping in mind that Harmanec's hypothesis cannot be ruled out in some other supergiants.

Acknowledgements. A part of this review was prepared during the author's stay at Union College (Schenectady, NY), as the Dudley Visiting Professor. The generous support from the Dudley Board and hospitality at the Department of Physics, Union College are gratefully acknowledged. Thanks are also due to Drs. K.P. Tsvetkova and L. Iliev for kindly taking the spectrum of TU Cas.

References

Aikawa, T. 1985a, *Ap. Space Sci.*, **112**, 125.

Aikawa, T. 1985b, *Ap. Space Sci.*, **116**, 401.

Aikawa, T., and Whitney, C.A. 1985, *Ap.J.*, **296**, 165.

Andreasen, G.K. 1987, *Astr. Ap.*, **186**, 159.

Antonello, E., Mantegazza, L., and Poretti, E. 1986, *Astr. Ap.*, **159**, 269.

Antonello, E., Mantegazza, L., and Poretti, E. 1987, in: *Stellar Pulsation*, Lecture Notes in Physics, vol. 274, eds. A.N. Cox, W.M. Sparks, and S.G. Starrfield; Springer, Berlin, p.191.

Antonello, E., and Poretti, E. 1986, *Astr. Ap.*, **169**, 149.

Antonello, E., and Poretti, E. 1987, in: *Stellar Pulsation* (see Antonello et al. 1987), p. 176.

Arellano Ferro, A. 1984, *Pub. A.S.P.*, **96**, 641.

Arellano Ferro, A. 1985, *M.N.R.A.S.*, **216**, 571.

Auvergne, M. 1986, *Astr. Ap.*, **159**, 197.

Baade, D., and Ferlet, R. 1984, *Astr. Ap.*, **140**, 72.

Babel, J., and Burki, G. 1987, preprint.

Balona, L.A. 1983, *Observatory*, **103**, 163.

Balona, L.A. 1985, in: *Cepheids: Theory and Observations*, Proc. IAU Coll. No.82, ed. B.F. Madore, Cambridge Univ. Press, Cambridge, p. 17.

Balona, L.A., and Engelbrecht, C.A. 1985, *Inf. Bull. Var. Stars*, No. 2758.

Barrell, S.L. 1978, *Ap.J.* (Letters), **226**, L141.

Buchler, J.-R., and Kovács, G. 1987, *Ap.J.* (Letters), **320**, L57.

Burki, G. 1984, in: *Space Research Prospects in Stellar Activity and Variability*, eds. A. Mangeney, F. Praderie, Obs. Paris- Meudon, p.69.

Burki, G., Schmidt, E.G., Arellano Ferro, A., Fernie, J.D., Sasselov, D., Simon, N.R., Percy, J.R., and Szabados, L. 1986, Astr. Ap., **168**, 139.

Carson, T.R., and Lawrence, S.P.A. 1987, in: *Stellar Pulsation* (see Antonello et al. 1987), p. 293.

Connolly, L. 1982, in: *Pulsation in Classical and Cataclysmic Variable Stars*, ed. J.P. Cox, C.J. Hansen, JILA, Boulder, p. 188.

Cuypers, J. 1985, *Astr. Ap.*, **145**, 283.

Fadeyev, Yu.A. 1984, *Ap. Space Sci.*, **100**, 329.

Fadeyev, Yu.A., and Fokin, A.B. 1985, *Ap. Space Sci.*, **111**, 355.

Feast, M.W. 1986, in: *Hydrogen Deficient Stars and Related Objects*, eds. K. Hunger et al., Reidel, Dordrecht, p. 151.

Fernie, J.D. 1986, *Ap.J.*, **306**, 642.

Fokin, A.B. 1984, *Nauchnye Informatsii*, No. 57, 17.

Fokin, A.B. 1986, *Astrofizika*, **24**, 109.

Fuhrmann, B., Luthardt, R., and Schult, R.H. 1984, *Mitt. veränderl. Sterne*, **10**, H4, 79.

Gieren, W.P. 1985, in: *Cepheids: Theory and Observations* (see Balona 1985), p. 98.

Gieren, W.P., and Matthews, J.M. 1987, *A.J.*, **94**, 431.

Harmanec, P. 1987, *Bull. Astr. Inst. Czechosl.*, **38**, 52.

Henden, A.A. 1980, *M.N.R.A.S.*, **192**, 621.

Henden, A.A., Cornett, R.H., and Schmidt, E.G. 1984, *Pub. A.S.P.*, **96**, 310.

Jurcsik, J., and Szabados, L. 1981, *Acta Astr.*, **31**, 213.

Kilkenny, D. 1982, *M.N.R.A.S.*, **200**, 1019.

Kilkenny, D. 1983, *M.N.R.A.S.*, **205**, 907.

Kilkenny, D., and Flanagan, C. 1983, *M.N.R.A.S.*, **203**, 19.

Kraus, D.J., Kemp, J.C., Henson, G.D., Dunaway, M.H., Hopkins, S.L., and Schmidtke, P.C. 1987, *B.A.A.S.*, **19**, 752.

Maeder, A. 1986, in: *Highlights of Astronomy*, ed. J.-P. Swings, Reidel, Dordrecht, p. 273.

Mantegazza, L. 1983, *Astr. Ap.*, **118**, 321.

Mantegazza, L. 1985, *Astr. Ap.*, **151**, 270.

Mantegazza, L. 1986, *Milano Preprint Series in Astrophysics*, No. 10, 56.

Mermilliod, J.-C., Mayor, M., and Burki, G. 1987, *Astr. Ap. Suppl.*, **70**, 389.
Moffett, T.J., and Barnes, T.G. 1984, *Ap.J. Suppl.*, 55, 389.
Petersen, J.O., and Andreasen, G.K. 1987, *Astr. Ap.*, **176**, 183.
Petersen, J.O., and Diethelm, R. 1986, Astr. Ap., **156**, 337.
Saio, H., and Wheeler, J.C. 1985, *Ap.J.*, **295**, 38.
Sasselov, D.D. 1985, in: *Cepheids: Theory and Observations* (see Balona 1985), p. 85.
Simon, N.R. 1986, *Ap.J.*, **311**, 305.
Simon, N.R., and Davis, C.G. 1983, *Ap.J.*, **266**, 787.
Simon, N.R., and Lee, A.S. 1981, *Ap.J.*, **248**, 291.
Simon, N.R., and Moffett, T.J. 1985, *Pub. A.S.P.*, **97**, 1078.
Simon, N.R., and Schmidt, E.G. 1976, *Ap.J.*, **205**, 162.
Simon, N.R., and Teays, T.J. 1983, *Ap.J.*, **265**, 997.
Stobie, R.S. 1973, *Observatory*, **93**, 111.
Stobie, R.S., and Balona, L.A. 1979, *M.N.R.A.S.*, **189**, 627.
Takeuti, M., and Petersen, J.O. 1983, *Astr. Ap.*, **117**, 352.
Wood, P.R. 1975, in: *Multiple Periodic Variable Stars*, Proc. IAU Coll. No.29, ed. W.S. Fitch, Reidel, Dordrecht, Vol. I, p. 69.
Wood, P.R. 1981, in: *Physical Processes in Red Giants*, eds. I. Iben Jr., A. Renzini, Reidel, Dordrecht, p. 205.
Worrell, J.K. 1986, *M.N.R.A.S.*, **223**, 787.
Worrell, J.K. 1987, in: *Stellar Pulsation* (see Antonello et al. 1987), p. 289.
Zalewski, J. 1986, *Acta Astr.* **36**, 63.

PULSATION TYPES IN MAGELLANIC CLOUD CEPHEIDS

J. O. Petersen and G. K. Andreasen
Copenhagen University Observatory, Copenhagen K, Denmark

Abstract

The occurrence of different types of Cepheid pulsation in the Magellanic Clouds is studied by means of Fourier decompositions. Comparison with results for Cepheids in the Milky Way confirms the similarity in pulsation properties in these stellar systems. Double-mode Cepheids are shown to occur in LMC, and s-Cepheids and Type II variables are briefly discussed.

1. Introduction

In recent years the theoretical understanding of modal selection and multimode pulsation has been much improved by application of modern methods for analyzing general non-linear systems (*e.g. Buchler* and *Kovács,* 1986; *Takeuti* 1984). The best observational material for testing these theories is the large number of available investigations of pulsation properties of Cepheid variables. Comparison of pulsation properties of Cepheids in the Galaxy and in the Magellanic Clouds can be expected to give interesting new possibilities for such tests, as the metal content of the stars in the Clouds is considerably smaller than typical galactic values.

While the pulsation properties of Cepheids in the Milky Way system are relatively well studied, and several Cepheid groups of different pulsation types have been identified, the material available for the Magellanic Clouds is more sparse and much more uncertain. We have started a systematic discussion of the available photographic light curves of Cepheids in the Clouds, using Fourier decomposition techniques (*Andreasen* and *Petersen* 1987; *Andreasen* 1987, 1988). Due to the relatively low accuracy of these data, it is essential to take uncertainties calculated for individual Fourier parameters into account in the analysis. Here we will discuss the occurrence of different pulsation types in Magellanic Cloud Cepheids, making a comparison with the well established pulsation types in the Milky Way.

2. Pulsation types in the Milky Way system

Let us start by summarizing the situation in our Galaxy (see Table 1).

The vast majority of the classical Cepheids (Type I) clearly oscillate in the fundamental mode and follow the Hertzsprung progression sequence with a center period of about 10^d. The Fourier diagrams show a great regularity along this sequence, especially for periods 3^d-9^d (*e.g. Simon* and *Lee* 1981). *Simon* (1987) emphasizes that this regularity argues strongly against the presence of any mechanism (*e.g.* He-poor winds or significant mass loss) which increases the physical complexity of stellar evolution.

Table 1. Pulsation types of Cepheids in the Galaxy and in the Magellanic Clouds. The first three columns give information on physical properties of three galactic Cepheid groups and the next three columns summarize their pulsation characteristics. Fundamental and (first) overtone oscillation modes are indicated by F and O, respectively. When a Hertzsprung-type progression sequence is known/suspected, the center period is given. The last two columns give present status with respect to establishment of the occurrence of the relevant pulsation type among Magellanic Cloud Cepheids and the presence of a progression sequence. Results marked by a colon need confirmation.

Milky Way System						Magellanic Clouds	
Name of variables	Age (10^9y)	Mass ($M_\odot$)	Pulsation type	Modes	Center period	Type known	Pro-gression
Classical Cepheids Type I	<1	> 4	Normal Cδ	F	10^d	Yes	Yes
			S-type	F/O	$3^d.0$:	Yes:	No
			Double-mode	F+O	-	Yes	-
Type II Cepheids	5-15	0.5-0.6	BL Her and W Vir	F	$1^d.5$:	Yes	No
Anomalous Cepheids	?	1-2:	Anomalous	F/O	?	Yes:	No

Several theoretical studies have explained the Hertzsprung progression by the resonance $\Pi_2/\Pi_0 = 0.5$ at about 10^d. We note that present standard stellar models predict this resonance at somewhat higher period, and that homogeneous standard models also fail to give the observed period ratio $\cong 0.70$ for the double-mode Cepheids. *Simon* (1987) suggests opacity changes as the proper explanation.

Recently, *Antonello* and *Poretti* (1986) discussed the structural properties of the light curves of s-Cepheids. A well defined sequence with a discontinuity in the Fourier phase diagram at 3^d was found. An attractive explanation could be that all s-type

Cepheids oscillate in the first overtone and that a resonance (*e.g.* $\Pi_4/\Pi_1 = 0.5$) occurs at 3^d. However, according to Antonello and Poretti, most s-Cepheids probably oscillate in the fundamental mode rather than in overtones.

The double-mode Cepheids have been discussed in numerous papers (*e.g. Balona* 1985). As mentioned above it is still not possible to reconcile the observed period ratios with the properties of generally accepted standard stellar models.

The observed properties of Type II Cepheids agree remarkably well with theoretical predictions from standard stellar pulsation and evolution theories (when a suitable mass loss in the red giant stage is introduced). In contrast to the case for classical Cepheids the observed period ratios of RR Lyrae variables here provide an accurate mass determination in agreement with other kinds of information (*e.g. Cox, Hodson,* and *Clancy* 1983). *Petersen* and *Diethelm* (1986), and *Carson* and *Lawrence* (1987) find the center period of the bump progression sequence at 1.5^d, while *Simon* (1986) prefers an alternative interpretation with a center period of 2^d.

Besides the above mentioned Type I and Type II Cepheids *anomalous* Cepheids have been discussed in the literature (*e.g. Zinn* and *King* 1982). Anomalous Cepheids are known in SMC and in a few dwarf elliptical galaxies. The (possible) existence of this group is predicted by stellar evolution theory, but only one or two (V19 in NGC 5466 and perhaps XZ Ceti) seem to be known in the Milky Way.

3. Pulsation types in the Magellanic Clouds

Using Fourier decompositions for analysis of about 250 LMC and SMC Cepheids, we have shown that the basic pulsation properties are very similar in the Clouds and in the Milky Way system (*Andreasen* and *Petersen* 1987; *Andreasen* 1988). For the interesting period interval 2^d-9^d the well defined Hertzsprung sequences are virtually identical, the progression center occurring at a slightly larger period in the Clouds. For periods longer than 11^d we find no significant differences.

The fact that stars in LMC have the same (known) distance, give new possibilities for discussion of the s-Cepheids. The period-luminosity diagram (Fig. 3 in *Andreasen* and *Petersen* 1987) give some evidence for the hypothesis that most of the s-Cepheids in LMC of periods less than 9^d are first overtone pulsators. However, since our sample contains only 7 stars in this group, this result needs confirmation; and the rather uncertain Fourier phases give no possibility for discussion of the presence of a progression sequence.

In the Galaxy almost one third of the Cepheids with period 2^d-4^d are double-mode pulsators. If the double-mode Cepheids constitute the same fraction in the Clouds, they should contain many (> 100) such objects. As far as we know, none

has been reported in the literature until now, and this has been considered a strange fact.

Searching the LMC sample, *Andreasen* (1987) discovered two stars which can safely be identified as double-mode Cepheids. Thus the present studies indicate that although double-mode Cepheids do occur in LMC, their relative abundance is much smaller in the Clouds than in the Galaxy. However, this result is based upon photographic light curves containing only about 40 observations each, and therefore needs confirmation.

The LMC and SMC samples considered in our investigations do not seem to contain Type II Cepheids. They should show conspicuous deviations from the P-L relation for Type I. We do not find stars with the deviation expected for Type II Cepheids. In principle, Fourier parameters could also be used for selection of Type II variables. But this problem has not yet been addressed, even for the much more accurate data available for galactic Cepheids.

We have not attempted discussion of anomalous Cepheids by means of the Fourier decomposition technique. Probably the available observational material is too sparse and too uncertain to allow a useful analysis.

4. Conclusion

We have started comparisons of pulsation properties of Cepheids in the Magellanic Clouds and the Milky Way, making Fourier decompositions of photographic light curves of about 250 Cepheids in LMC and SMC. We confirm the well known similarities in basic Cepheid properties in these galaxies. Double-mode Cepheids – for a long time expected to be present in the Clouds – were discovered in LMC by *Andreasen* (1987).

Comparisons between period distribution and relative numbers of stars of different pulsation types in the Magellanic Clouds and in the Milky Way indicate significant differences. For example, we find fewer double-mode Cepheids in LMC and SMC than expected from extrapolation of galactic data, and also Type II Cepheids seem to be rare in the Clouds. We emphasize that much better observational data is required for a secure decision of these important problems.

The fact that Magellanic Cloud Cepheids have known distances gives new possibilities for analysis of their pulsation properties. Therefore we expect future detailed investigations of variable stars in the Clouds to yield both new insight in stellar pulsation and interesting information on the physical properties of stellar populations in the Magellanic Clouds.

References

Andreasen, G.K. 1987, *Astr. Ap.*, in press.

Andreasen, G.K. 1988, *Astr. Ap.*, in press.

Andreasen, G.K., and Petersen, J.O. 1987, *Astr. Ap.* **180**, 129.

Antonello, E., and Poretti, E. 1986, *Astr. Ap.* **169**, 149.

Buchler, J.R., and Kovács, G. 1986, *Ap. J.* **303**, 749.

Balona, L.A. 1985, in: *Cepheids: Theory and Observations*, IAU Coll. **82**, ed. Madore, B.F., Cambridge Univ. Press, p. 17.

Carson, T.R., and Lawrence, S.P.A. 1987, in *Stellar Pulsation*, Cox, A.N. Sparks, W.M., and Starrfield, S.G. (eds.), *Lecture Notes in Physics*, Vol. 274, p. 293.

Cox, A.N., Hodson, S.W., and Clancy, S.P. 1983, *Ap. J.* **266**, 94.

Petersen, J.O., and Diethelm, R. 1986, *Astr. Ap.* **156**, 337.

Simon, N.R. 1986, *Ap. J.* **311**, 305.

Simon, N.R. 1987, in *Stellar Pulsation,* Cox, A.N., Sparks, W.M., and Starrfield, S.G. (eds.), *Lecture Notes in Physics*, Vol. 274, p. 148.

Simon, N.R., and Lee, A.S. 1981, *Ap. J.* **248**, 291.

Takeuti, M. 1984, in *Non-linear phenomena in stellar outer-layers*, Sendai Report No. 265, p. 1.

Zinn, R., and King, C.R. 1982, *Ap. J.* **262**, 700.

NEW OBSERVATIONS OF THE DOUBLE-MODE CEPHEIDS AP VEL AND BK CEN*

M. Jerzykiewicz
Wroclaw University Observatory, Wroclaw, Poland

Abstract

The *uvby* observations of AP Vel and BK Cen are presented and analyzed. The wavelength dependence of the fundamental and first-overtone amplitudes and mean epochs of maximum light is derived. In addition, on the basis of all available data, the stability of the pulsations of AP Vel and BK Cen is studied. No long-term variations of the component amplitudes and periods are found.

1. Introduction

Although main observational properties of the double-mode Cepheids are quite well known, especially since the extensive work of *Stobie* and *Balona* (1979a, b), these objects should still be observed from time to time in order to monitor the long-term stability of the component oscillations. Ideally, all double-mode Cepheids should be checked at regular intervals of several years. Such a program may, perhaps, be carried out in the future. For the time being we selected for observing just two double-mode Cepheids, AP Vel and BK Cen.

According to *Stobie* and *Balona* (1979b), the fundamental and first-overtone frequencies of AP Vel are $f_0 = 0.319718 \pm 0.000010$ c/d and $f_1 = 0.454578 \pm 0.000010$ c/d. The frequencies of BK Cen are similar, $f_0 = 0.315073 \pm 0.000010$ c/d and $f_1 = 0.449848 \pm 0.000010$ c/d. In both cases, the fundamental V light amplitude, amounting to $0^m.275 \pm 0^m.007$ and $0^m.245 \pm 0^m.013$ for AP Vel and BK Cen respectively, is about twice as large as the first-overtone amplitude.

---

* Based on observations collected at the European Southern Observatory, La Silla, Chile.

2. Observations

AP Vel and BK Cen were included in the Long-Term Photometry of Variables project, a coordinated photometric program at the European Southern Observatory (*Sterken* 1983). They were observed on eight runs, from January to March 1985 and from November 1985 to July 1986, by means of the *uvby* photometers, attached to the ESO and Danish 50-cm telescopes. The observers were: H. Duerbeck, O. Stahl, A. Reitermann, F.-J. Zickgraf, M. Burger, A. Jorissen, H. Steenman, and R. Madejski. As a rule, each star was observed once per night, AP Vel on 110 nights, and BK Cen on 104 nights. The photometric reductions were carried out by J. Manfroid. A description of the reduction procedure can be found in *Manfroid* and *Heck* (1983).

3. Analysis

3.1. Fourier Decomposition

The data selected for analysis consist of 114 differential *uvby* magnitudes, AP Vel *minus* HR 3404, and 108 differential *uvby* magnitudes, BK Cen *minus* HR 4634. Following *Fitch* (1966), we assume that the differential magnitudes can be represented by means of the double Fourier polynomial

$$\Delta m = A_0 + \Sigma_{i,j}\ A_{ij}\ \cos\ [2\pi f_{ij}(t\text{-}t_0) + \phi_{ij}] \quad , \qquad (1)$$

where $f_{ij} = |if_0 + jf_1|$, with i and j being whole numbers such that $i \geq 0$ and $i^2 + j^2 > 0$.

After a number of trial least-square fits to equation (1), we found that retaining ten strongest sinusoidal components was sufficient to adequately represent the data. As an example, parameters of a ten-component least-squares fit of the differential y magnitudes of AP Vel are listed in Table 1.

A comparison of the differential y magnitudes of AP Vel with the synthetic light-curve, computed using the parameters listed in Table 1, is shown in Figure 1.

The standard deviation in Table 1, equal to $0^m.019$, although quite small, is much too large to be accounted for by the random photometric errors and the cumulative effect of the neglected high order terms. As it turned out, the problem can be traced to small systematic differences between the differential magnitudes, obtained on different observing runs. The same problem was encountered in the case of BK Cen. The origin of the systematic differences is, so far, unclear.

Table 1. The Δy variation of AP Vel: ten strongest components

Number of observations = 114 $\Delta t = 516^d$

t_o = JD 2446070.5

std. dev. = $0^m.019$ (original std. dev. = $0^m.231$)

$A_o = 3^m.6125 \pm 0^m.0020$

i	j	f_{ij}	A_{ij}	ph of max.
1	0	0.319718	$0^m.2775 \pm 0^m.0026$	0.892 ± 0.002
0	1	0.454578	0.1431 ± 0.0026	0.411 ± 0.003
2	0	0.639436	0.0851 ± 0.0026	0.623 ± 0.005
1	1	0.774296	0.0555 ± 0.0035	0.160 ± 0.010
2	1	1.094014	0.0364 ± 0.0038	0.794 ± 0.015
1	-1	0.134860	0.0358 ± 0.0026	0.295 ± 0.012
3	0	0.959154	0.0312 ± 0.0037	0.342 ± 0.019
0	2	0.909156	0.0232 ± 0.0035	0.566 ± 0.025
1	2	1.228874	0.0103 ± 0.0037	0.319 ± 0.054
1	-3	1.044016	0.0100 ± 0.0039	0.689 ± 0.057

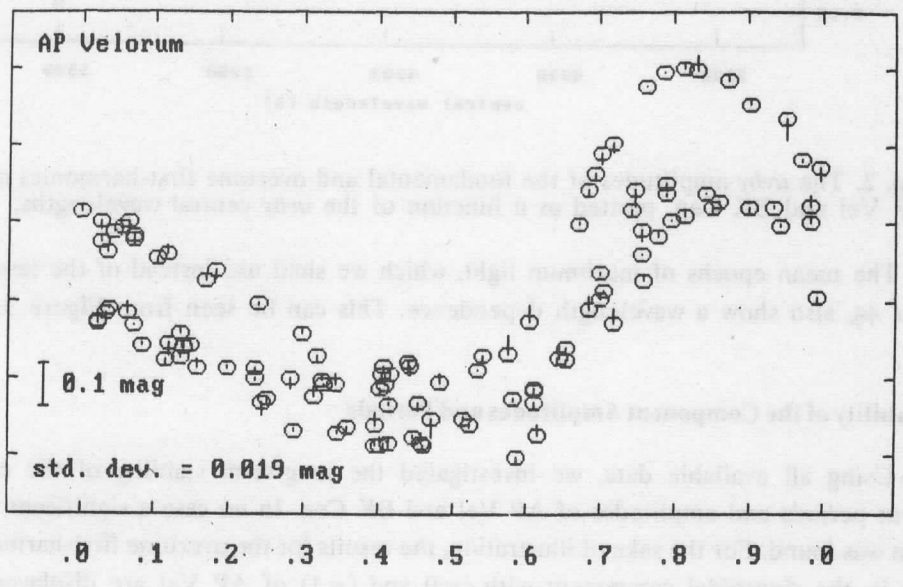

Fig. 1. The differential *y* magnitudes of AP Vel, plotted as a function of phase of the fundamental frequency, $f_0 = 0.319718$ c/d. Phase zero corresponds to JD 2446070.5 . Comparison star: HR 3404. The vertical bars represent deviations from a synthetic ten-component light-curve, computed using the parameters listed in Table 1.

3.2 Amplitudes and the Mean Epochs of Maximum Light

The light amplitudes of AP Vel and BK Cen show a wavelength dependence. For the two strongest sinusoidal components this is illustrated in Figure 2, where the fundamental first-harmonic amplitude, A_{10}, and the overtone first-harmonic amplitude, A_{01}, are plotted as a function of the central wavelength of the *uvby* filters.

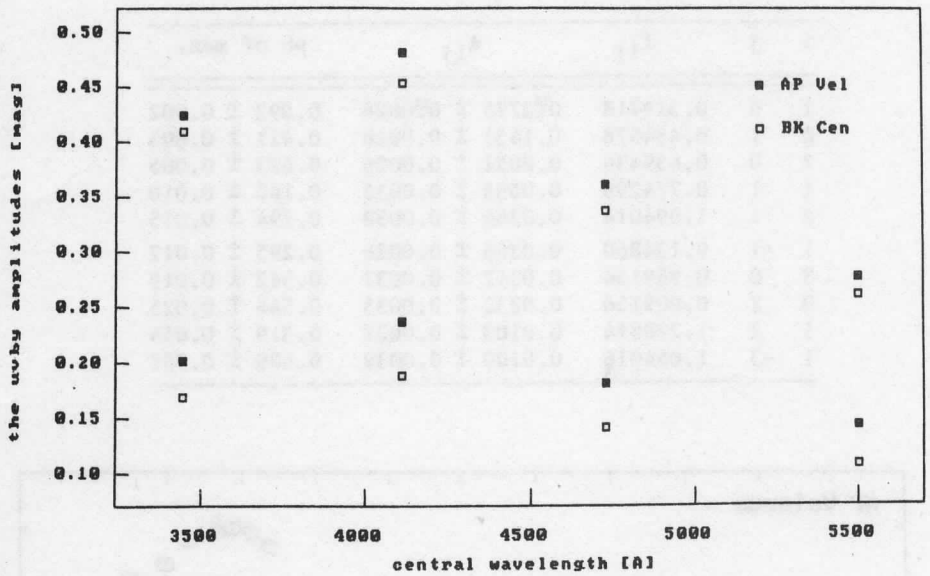

Fig. 2. The *uvby* amplitudes of the fundamental and overtone first-harmonics of AP Vel and BK Cen, plotted as a function of the *uvby* central wavelengths.

The mean epochs of maximum light, which we shall use instead of the less familiar ϕ_{ij}, also show a wavelength dependence. This can be seen from Figure 3.

4. Stability of the Component Amplitudes and Periods

Using all available data, we investigated the long-term stability of the component periods and amplitudes of AP Vel and BK Cen. In no case a significant variation was found. For the sake of illustration, the results for the overtone first-harmonic (that is, the sinusoidal component with $i=0$ and $j=1$) of AP Vel are displayed in Figures 4 and 5. In both figures, the leftmost points were derived from the photographic observations of *Hertzsprung* (1936), taking into account the wavelength dependences discussed in the preceding chapter. The filled squares correspond to an assumed central wavelength of 4400 Å for the Hertzsprung's photometric system,

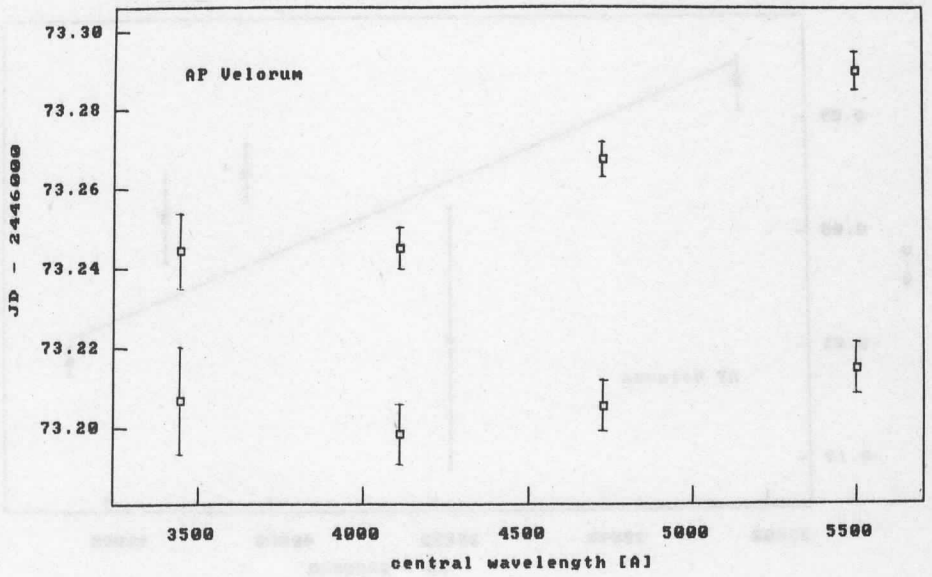

Fig. 3. The mean *uvby* epochs of maxima of the fundamental and overtone first-harmonics of AP Vel (top) and BK Cen (bottom), plotted as a function of the *uvby* central wavelengths. Each vertical bar is equal to twice the corresponding standard deviation. The overtone epochs of maxima (bottom each panel) were shifted by arbitrary amounts in order to fit the panels.

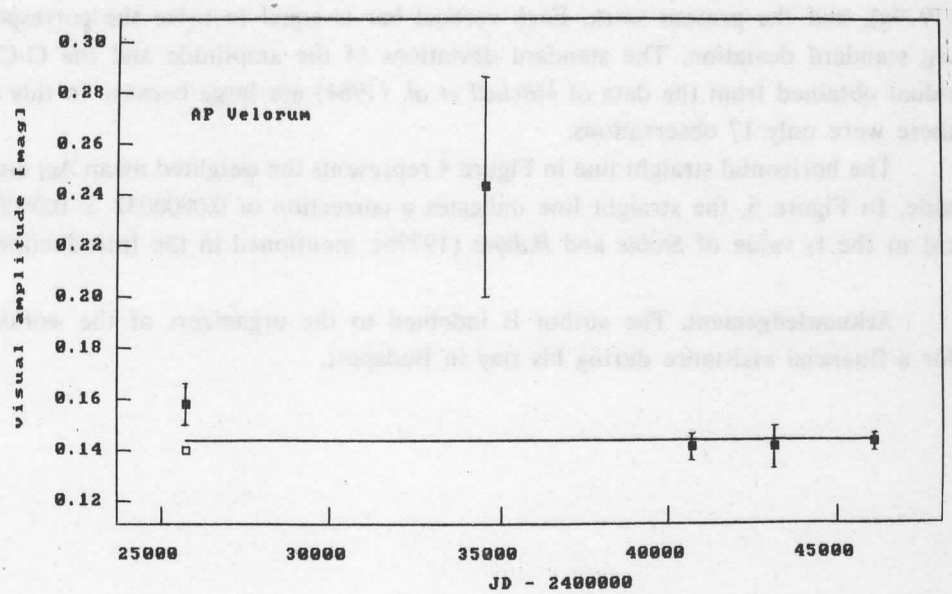

Fig. 4. The overtone first-harmonic visual amplitude of AP Vel, plotted as a function of time.

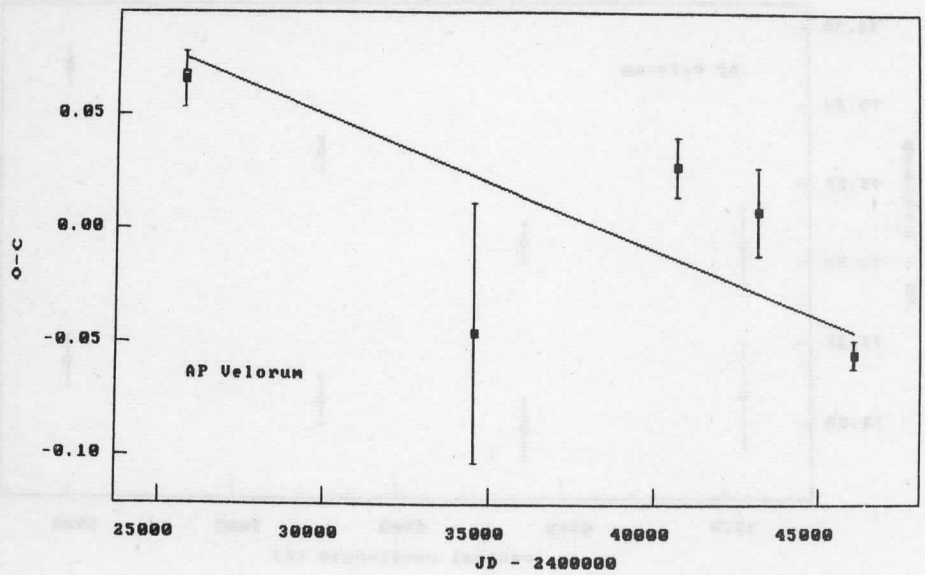

Fig. 5. The O-C diagram for the overtone first-harmonic maximum light of AP Vel.

while the open squares, to $\lambda_c = 4200$ Å. The remaining points, from left to right, are based on the observations of *Mitchell et al.* (1964), *Pel* (1976), *Stobie* and *Balona* (1979a), and the present work. Each vertical bar is equal to twice the corresponding standard deviation. The standard deviations of the amplitude and the O-C residual obtained from the data of *Mitchell et al.* (1964) are large because in this case there were only 17 observations.

The horizontal straight line in Figure 4 represents the weighted mean A_{01} amplitude. In Figure 5, the straight line indicates a correction of 0.0000032 ± 0.0000007 c/d to the f_1 value of *Stobie* and *Balona* (1979b), mentioned in the Introduction.

Acknowledgement. The author is indebted to the organizers of the workshop for a financial assistance during his stay in Budapest.

References

Fitch, W.S. 1966, *Ap. J.*, **143**, 852.

Hertzsprung, E. 1936, *B.A.N.*, **7**, 333.

Manfroid, J., and Heck, A. 1983, *Astr. Ap.*, **120**, 302.

Mitchell, R.I., Iriarte, B., Steinmetz, D., and Johnson, H.L. 1964, *Bol. Obs. Tonantzintla Tacubaya*, **3**, 153.

Pel, J. 1976, *Astr. Ap. Suppl.*, **24**, 413.

Sterken, C. 1983, *ESO Messenger*, **33**, 10.

Stobie, R. S., and Balona, L. A. 1979a, *M.N.R.A.S.*, **188**, 595.

Stobie, R. S., and Balona, L. A. 1979b, *M.N.R.A.S.*, **189**, 627.

DOUBLE-MODE PULSATORS WITH UNUSUAL LIGHT CURVES

E. Antonello and E. Poretti,
Osservatorio Astronomico di Brera, Merate, Italy
and
R.F. Stellingwerf
Mission Research Corporation, Albuquerque, New Mexico, USA

Abstract

The case of the ultra-short period pulsating stars V1719 Cyg and V798 Cyg is discussed taking into account the observational results and the indications of the one-zone model. The He depletion in the envelope is suggested as the possible cause of unusual light curve shapes of these δ Scuti stars, but other observational and theoretical tests are needed.

1. Introduction

Generally, the (multi-) periodic pulsating stars such as RR Lyrae, high amplitude δ Scuti and SX Phoenicis stars, and Cepheids, have light curves characterized by a rising branch steeper than the descending one. Recently, however, we pointed out the unusual light curve shape of the double-mode pulsator V1719 Cyg (*Antonello, Mantegazza,* and *Poretti* 1986a), which is characterized by a descending branch steeper than the rising one. Also *Johnson* and *Joner* (1986) remarked this fact and made an interesting photometric study which revealed several unusual features of this star.

Last year, starting a program for the observation of short period pulsating (δ Scuti and RR Lyrae) stars with high amplitude in order to confirm the existence of two families of light curves for the δ Scuti stars (*Antonello et al.* 1986b), the variable star V798 Cyg was observed. Also this star shows an unusual light curve similar to that of V1719 Cyg. In the present note we will discuss briefly these two cases which could represent a subclass of pulsating stars.

2. Data on V1719 Cyg and V798 Cyg

The analysis of the photometric observations of V1719 Cyg showed that it pulsates in two modes with periods of 0.267 and 0.214 d, the period ratio being 0.80 (*Mantegazza* and *Poretti* 1986). Johnson and Joner observed this star in the Strömgren-Crawford photometric system, and pointed out the unusual behavior of the m_1 index. The authors considered two possible explanations: a) microturbulence excited

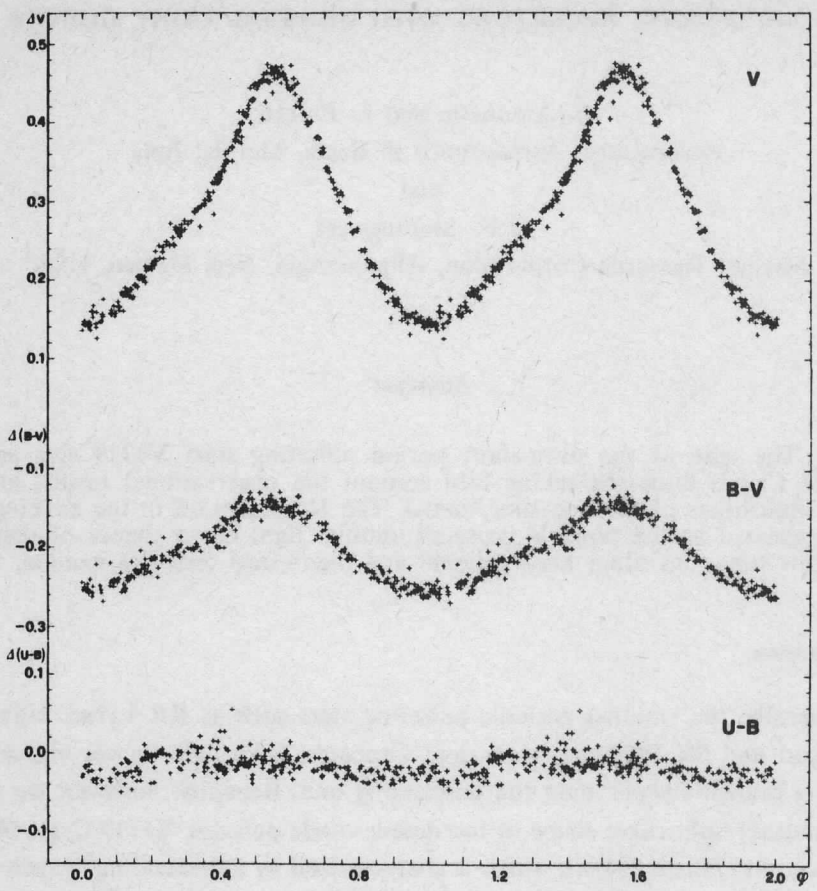

Fig.1. V, B-V and U-B curves of V1719 Cyg for the first period. These curves were obtained by subtracting the second period and the combination frequencies from the original data (*Poretti* and *Antonello* 1987).

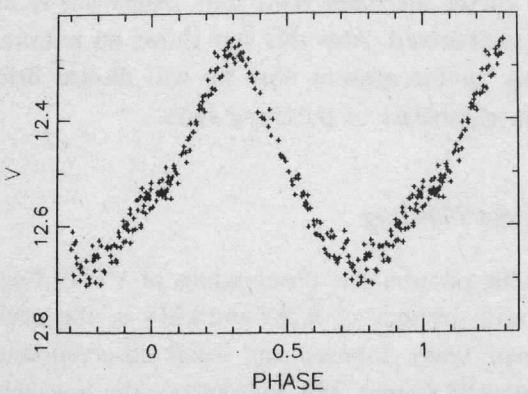

Fig. 2. V curve of V798 Cyg. The period is 0.195 d.

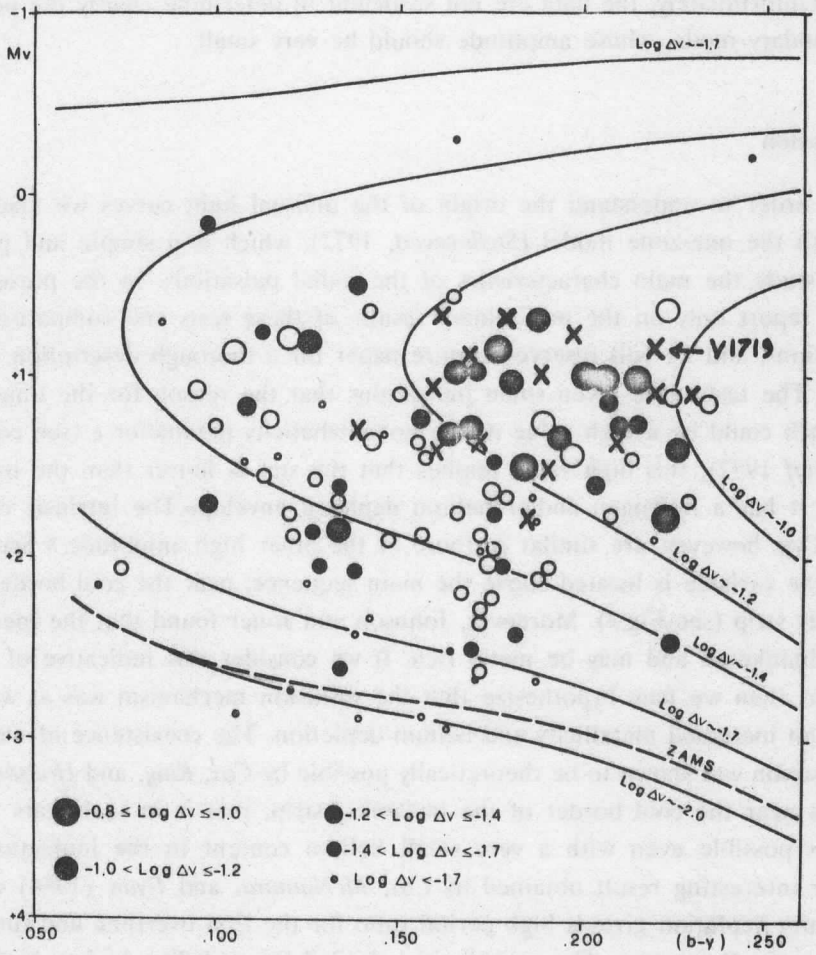

Fig. 3. Color-magnitude diagram of the lower part of the instability strip with the marked position of V1719 Cyg. The filled circles are δ Scuti stars with light amplitude $\Delta V < 0.3$ and many observed pulsation cycles, the open circles are the other δ Scuti stars with $\Delta V < 0.3$. The sizes of the circles correspond to different ΔV ranges. The crosses are δ Scuti stars with $\Delta V \geq 0.3$ (see *Antonello* 1983).

by the secondary pulsation mode which affects the metallicity index; b) Am/Fm phenomenon, that is the star has metal abundance anomalies. V798 Cyg was observed at Catania Observatory for three nights during an interval of seven days. From the data analysis it resulted that the light curve of V798 Cyg is similar to that of V1719

Cyg, and possibly it is another double-mode pulsator (see Figures 2 and 1 respectively). Unfortunately, the data are not sufficient to determine clearly the period of the secondary mode, whose amplitude should be very small.

3. Discussion

In order to understand the origin of the unusual light curves we made some tests with the one-zone model (*Stellingwerf*, 1972), which is a simple and powerful tool to study the main characteristics of the radial pulsations. In the present note we will report only on the preliminary results of these tests and comparisons with observations, and we will reserve a future paper for a thorough description and discussion. The tests have given some indications that the reason for the unusual rising branch could be a high value of the nonadiabaticity parameter ζ (see eq.(15) in *Stellingwerf* 1972); this high value implies that the star is hotter than the instability strip or it has a hydrogen and/or helium depleted envelope.The intrinsic colors of V1719 Cyg, however, are similar to those of the other high amplitude δ Scuti stars, that is the variable is located above the main sequence, near the cool border of the instability strip (see Fig.3). Moreover, Johnson and Joner found that the spectrum is heavily blanketed and may be metal rich. If we consider this indicative of an Fm-type star, then we may hypothesize that the diffusion mechanism was at work and yielded an increased metallicity and helium depletion. The coexistence of metallicity and pulsation was shown to be theoretically possible by *Cox*, *King*, and *Hodson* (1979) for stars near the cool border of the instability strip; that is in such stars the pulsation is possible even with a very small helium content in the ionization zone. Another interesting result obtained by *Cox, McNamara*, and *Ryan* (1984) was that the helium depletion gives a high period ratio for the first overtone and fundamental mode of δ Scuti stars. The period ratio of 1719 Cyg is 0.80, which is higher than the canonical one (0.77); moreover, as the main period is rather long (0.267 d), it is difficult to believe it to be the period of the first overtone, hence one should exclude that the pulsation modes of V1719 Cyg are the first and second overtones.

On the whole, the observations and theory are concurring to form a plausible scenario for the V1719 Cyg phenomenon. However, more observational and theoretical tests are needed in order to confirm the metallicity of V1719 Cyg and V798 Cyg, to exclude that the m_1 behavior is due to the second period itself, and to study the influence of other possible parameters (*e.g.* radiation pressure; *Stellingwerf* and *Gautschy* 1987) on the light curve shape.

References

Antonello, E. 1983, *Hvar Obs. Bull.* **7**, 329.

Antonello,E., Mantegazza, L.. and Poretti, E. 1986a, in *Stellar Pulsation*, Cox, A.N., Sparks, W.M., Starrfield, S.G.,(eds.) Lect.Not. in Physics, Vol. 274, p. 191.

Antonello, E., Broglia, P., Conconi, P., and Mantegazza, L. 1986b, *Astr.Ap.***169**, 122.

Cox, A.N., King, D.S., and Hodson, S.W. 1979, *Ap. J.* **231**, 798.

Cox, A.N., McNamara,B.J. and Ryan, W. 1984, *Ap.J.* **284**, 250.

Johson, S.B., and Joner, M.D. 1986, Publ. *A. S. P.* **98**, 581.

Mantegazza, L., and Poretti, E. 1986, *Astr.Ap.* **158**, 389.

Poretti, E., and Antonello, E. 1987, in preparation.

Stellingwerf, R.F. 1972, *Astr. Ap.*, **21**, 91.

Stellingwerf, R.F., and Gautschy, A. 1987, in preparation.

IS THREE-MODE RESONANCE ABLE TO SUPPORT BEAT CEPHEID-TYPE PULSATION?

G. Kovács and Z. Kolláth
Konkoly Observatory, Budapest, Hungary

Abstract

The general case of resonant three-mode coupling including non-resonant (cubic) mode interaction is studied in the context of beat Cepheid-type pulsation. It is shown that even small non-adiabaticity in the resonant coupling can lead to steady three-mode (i.e. double-periodic) pulsation, which is the only stable solution. Large differences in the non-adiabaticity of the resonant coupling can easily lead to substantial period ratio change, which may serve as an explanation of the period ratio-mass discrepancy of the beat Cepheids. Besides the three-mode steady solution, the relevant equations offer a whole wealth of different solutions for various (physically possible) parameter combinations. These solutions include single-mode steady pulsation, three-mode solution with periodically modulated amplitudes and phases, period-doubling, and chaos.

The long-standing problem of modelling steady double-periodic stellar pulsation has posed a very difficult puzzle for theoreticians ever since their first efforts to solve it (*Stellingwerf* 1975a,b; *Cox, Hodson,* and *Davey* 1976; *Cox* 1982). In addition, in the case of beat Cepheids, even the observed period ratio does not fit that computed by linear pulsational codes, if evolutionary masses are assumed (*e.g. Petersen* 1973).

Simon's (1979) hypothesis, that double-periodic pulsation is connected with the lowest order resonance among the two directly observable modes and a higher order one, stimulated further studies in this field. Unfortunately, direct checking of this hypothesis by means of a hydrodynamic code led to a negative result (*Simon, Cox,* and *Hodson* 1980). Moreover, a subsequent study of the amplitude equations describing the resonant mode interaction with adiabatic coupling coefficients showed that three-mode resonance supports single-mode pulsation rather than three-mode (*i.e.* double-periodic) pulsation (*Dziembowski* and *Kovács* 1984; hereinafter DK). The same authors, however, also showed that a 2:1 resonance between one of the observable modes and a higher order one can easily lead to double-periodic pulsation in some neighbourhood of the resonance centre. The subsequent hydrodynamic survey of *Kovács* and *Buchler* (1988) has confirmed this result, and led to the first, easy to reproduce beat RR Lyrae model. The problem here, however, is that in order to

satisfy the resonance condition and get unstable first overtone single-mode pulsation (the necessary conditions for double-periodic pulsation to be the only one which is stable), one needs to assume relatively high mass and low temperature for the model. This leads to wrong period ratios, which are not compatible with the observations. The same authors conclude that existing radiative hydrocodes are unable to reproduce the observed beat RR Lyrae pulsation, in view of which one needs to include additional physical and mathematical features (convection, better shock-treatment, difference scheme, less artificial dissipation) in order to tackle the problem again (see also *Cox* 1987; and *Davis* 1988).

The purpose of the present note is to study again the effect of three-mode resonance with the aid of a more general set of equations – as was used by DK. One of their main simplifications, *i.e.* omission of the non-adiabatic effect in the resonant coupling, was criticized by *Klapp, Goupil, and Buchler* (1985) on the ground of the consistency of the series development when the amplitude equations are derived. Here we include all effects of the mode interaction up to the cubic terms, except for the nonresonant period change (*i.e.* the quadratic terms in the equations for the phases). With this assumption and by introducing normalized time, amplitudes and relative phases, the amplitude equations for three-mode resonance read as follows

$$a_1' = \bar{\varkappa}_1 a_1 + a_2 a_3 \cos\alpha \quad , \tag{1}$$

$$a_2' = \bar{\varkappa}_2 a_2 + a_1 a_3 \cos(\alpha+\beta_2) \quad , \tag{2}$$

$$a_3' = \bar{\varkappa}_3 a_3 - a_1 a_2 \cos(\alpha+\beta_3) \quad , \tag{3}$$

$$a_1\alpha_1' = a_2 a_3 \sin\alpha \quad , \tag{1a}$$

$$a_2\alpha_2' = a_1 a_3 \sin(\alpha+\beta_2) \quad , \tag{2a}$$

$$a_3\alpha_3' = a_1 a_2 \sin(\alpha+\beta_3) \quad , \tag{3a}$$

where $\bar{\varkappa}_i = \varkappa_i(1+\alpha_{i1}a_1^2+\alpha_{i2}a_2^2+\alpha_{i3}a_3^2)$.

Primes denote derivation by the normalized time τ which is related to the physical time by $\tau=\varkappa_1 t$, where $\varkappa_1$ is the linear growth-rate of the first mode, and

it is assumed to be positive. The normalized amplitude is defined by $a_i=A_i/f_i$, where A_i is the physical amplitude, and the factor f_i is computed by the equation $f_i^2=\varkappa_i^2(c_j c_k)$ where c_i is the modulus of the resonant coupling coefficient. The indices are different in f_i, c_j and c_k and $1\le i, j, k\le 3$. The resonant and the non-resonant coupling coefficients (c_i, β_i and α_{ij} respectively) are complicated integrals of the various products of the linear non-adiabatic (LNA) eigenfunctions and the static stellar parameters over the envelope. Evaluation of the resonant coupling coefficients is relatively easy in the adiabatic case ($\beta_2=\beta_3=0$); for radial pulsation it is given by *Takeuti* and *Aikawa* (1981); and for the non-radial case by *Dziembowski* (1982) and by *Dziembowski* and *Królikowska* (1985). The general non-adiabatic case is treated analytically by *Buchler* and *Goupil* (1984), and numerically (for 2:1 resonance) by *Klapp et al.* (1985). Because, except for their order of magnitude, we do not know much about their values, we treat them as (almost) free parameters. It is important, however, that all α_{ij} are negative (*Buchler* and *Kovács* 1987) and that c_i are in the order of the LNA-eigenfrequencies (*Takeuti* and *Aikawa* 1981; *Dziembowski* and *Królikowska* 1985).

The phase variables α, α_i are related by $\alpha=\Delta\nu\,\tau+\alpha_3-\alpha_1-\alpha_2$, where $\Delta\nu=(\omega_3-\omega_1-\omega_2)/\varkappa_1$ and ω_i is the LNA eigenfrequency of the *i*-th mode. We see that for non-zero amplitudes, equations (1a), (2a), (3a) can be combined into one equation

$$\alpha'=\Delta\nu+\frac{a_1 a_2}{a_3}\sin(\alpha+\beta_3)-\frac{a_2 a_3}{a_1}\sin(\alpha)-\frac{a_1 a_3}{a_2}\sin(\alpha+\beta_2) \quad . \tag{4}$$

This equation, together with equations (1), (2), (3) forms a closed set for the four unknown functions a_1, a_2, a_3 and α, which are applicable for the multimode (non-vanishing) solutions of the original equations.

Assuming that the eigenfunctions are normalized to unity at the surface, the surface radius variation is given by

$$\Delta R/R_o=A_1\sin(\omega_1 t+\varphi_1)+A_2\sin(\omega_2 t+\varphi_2)+A_3\sin(\omega_3+\varphi_3) \quad , \tag{5}$$

where R_o is the static radius, $\varphi_1=\alpha_1, \varphi_2=\alpha_2$ and $\varphi_3=\alpha_3-\Phi_1$ with Φ_1 being an arbitrary phase.

Since we are interested in beat Cepheid-type pulsation, we assume throughout the following discussion that the growth-rates of the low-frequency modes are positive, whereas that of the highest-frequency one is negative. The case when the highest-frequency mode is linearly excited and the other two are damped was treated (in

second order adiabatic approximation) by *Moskalik* (1985) and by *Dziembowski* and *Królikowska* (1985) in the context of white dwarf and δ Scuti pulsations respectively.

DK treated equations (1), (2), (3) and (4) in the adiabatic approximation of the second order coupling coefficients ($\beta_2=\beta_3=0$). They concluded that this type of resonance leads to a situation when at least one of the single-mode constant-amplitude (*i.e.* fixed point) solutions is stable. For some very restricted parameters one might get a stable three-mode (*i.e.* double-periodic) solution coexisting with (at least) one of the single-mode solutions. In addition, only the very close neighbourhood of the three-mode fixed point attracts, therefore, one of the single-mode solutions is the most probable observable limiting state.

First we deal with the case when all $\alpha_{ij}=0$. *Dziembowski* (1982) has shown that if $\beta_2=\beta_3=0$, there is no stable fixed point solution. Here we prove the following property; In the general case, stable fixed point solutions exist for quite large ranges of β_2, β_3 . However, for small frequency mismatch the parameter regions $0<\beta_2<\pi$, $\pi<\beta_3<2\pi$ and $\pi<\beta_2<2\pi$, $0<\beta_3<\pi$ surely yield unbounded solutions. Indeed, for $\Delta\nu=0$ the fixed point solution is symmetric to the point $\beta_2=\beta_3=\pi$, therefore, it is enough to study that class of solutions for which $\sin\alpha>0$. The positivity of the amplitudes yields $\cos\alpha<0$, $\cos(\alpha+\beta_2)<0$, $\cos(\alpha+\beta_3)>0$. The last inequality implies $0<\beta_3<\pi$. The stability condition (one of the Routh-Hurwitz criteria, see *e.g. Kubicek* and *Marek* 1983), requires $\tan(\alpha+\beta_2)>0$, therefore $0<\beta_2<\pi$. We remark that one can put more restricted limits on β_2 , by the thorough examination of one of the coefficients of the characteristic equation for the stability roots.

We searched numerically for the stable fixed point solutions of equations (1)-(4). For a fixed parameter set ($\Delta\nu$, $\varkappa_2$, $\varkappa_3$, β_2, β_3) the equilibrium condition (*i.e.* all time derivatives equal zero) led to a cubic equation for the tangent of the phase α. Subsequent computation of the equilibrium amplitudes was straightforward. Linearized stability analysis was performed by the application of the Routh-Hurwitz criteria on the resulting characteristic equation. Figures 1 and 2 show the regions of the stable three-mode solution in the (β_3, β_2) plane for zero and large frequency mismatches respectively. Each box corresponds to different ($\varkappa_2$, $\varkappa_3$) values. It is seen that the basic property we have proved is clearly exhibited. We would mention that in the less relevant case for beat Cepheids, *i.e.* when $\varkappa_2<1$, the situation is very similar to the ones shown. Besides the stable fixed point solutions (black shaded areas) we also show the regions where only the last Routh-Hurwitz criterion is not satisfied (hatched areas). In these regions the fixed point solution may bifurcate to a limit cycle solution (Hopf bifurcation, see *e.g. Marsden* and *McCracken* 1976). Straightforward numerical integrations of the equation have shown that the fixed point solutions indeed bifurcate to limit cycles in these regions. In addition, the limit cycles further bifurcate at the border of these regions to chaos via period-doubling bifurcations. Further away from the limit cycle and/or fixed point regions however, the solutions

blow up. (This happens in the regions mentioned for the proved property, for example.)

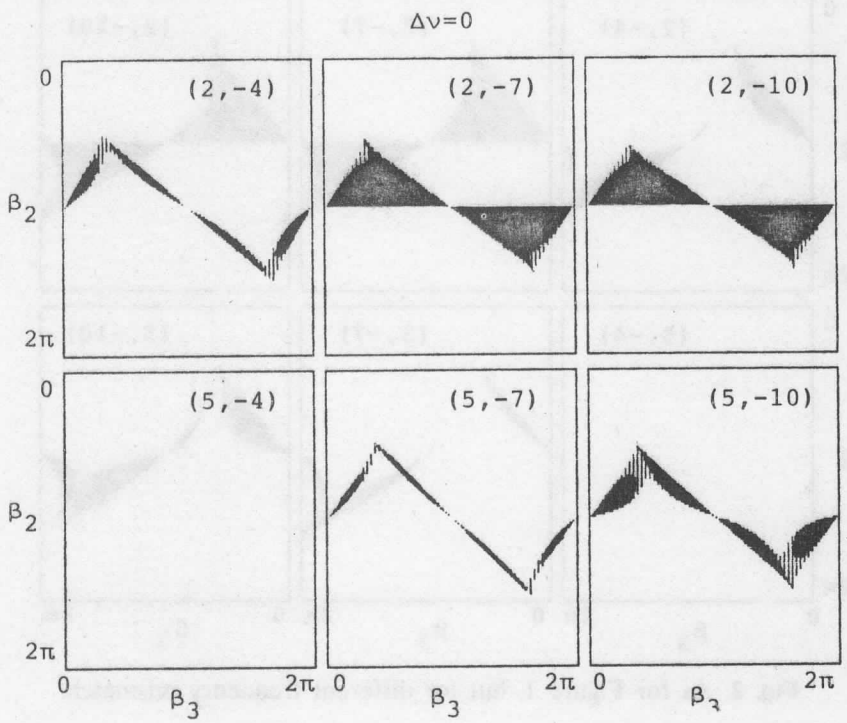

Fig. 1. Regions of stable fixed point (black) and limit cycle solution (hatched) of the general three-mode resonance equation in second order approximation. All computations were performed with the same frequency mismatch as shown at the top of the figure. Numbers in parentheses denote the values of $(\varkappa_2,\varkappa_3)$, kept constant in each case plotted in separate boxes. Notations are the same in equations (1) – (4).

We now turn to the discussion of the general case, when all α_{ij} are kept in equations (1) – (4). The first question we ask is whether it is possible to destabilize both single-mode solutions by introducing non-adiabatic phase shifts (β_2, β_3) in the resonant coupling. Following the same procedure as in DK, the criteria for the stability of the single-mode solution $a_1\neq 0$, $a_2=a_3=0$ are

$$\varkappa_2^* + \varkappa_3^* < 0 \quad , \tag{6}$$

$$\varkappa_2^*\varkappa_3^*((\varkappa_2^*+\varkappa_3^*)^2+(\Delta\nu)^2)+a_{10}^2(\varkappa_2^*+\varkappa_3^*)^2\cos\beta- \tag{7}$$

$$-a_{10}^4\sin^2\beta-\Delta\nu(\varkappa_2^*-\varkappa_3^*)a_{10}^2\sin\beta>0\,.$$

Here $a_{10}^2=-1/\alpha_{11}$, $\varkappa_i^*=\varkappa_i(1+\alpha_{11}a_{10}^2)$ and $\beta=\beta_2-\beta_3$.

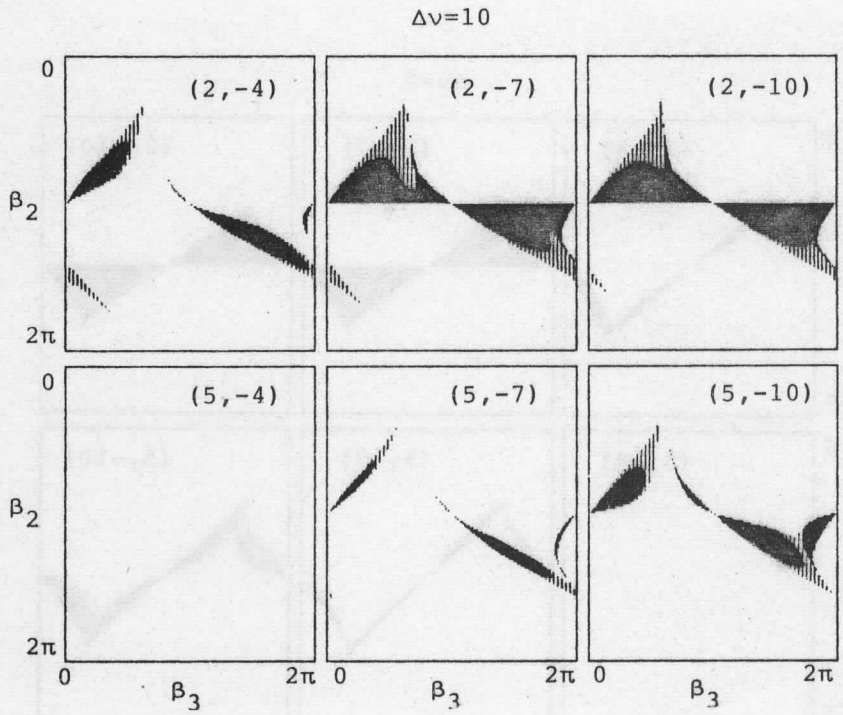

Fig. 2. As for Figure 1, but for different frequency mismatch.

Stability criteria for the $a_2 \neq 0$; $a_1 = a_3 = 0$ solution can be obtained by the interchange of the indices 1 and 2 (*i.e.* $\beta = \beta_3$) in the above formulae. It is clear that even if the single-mode state is stable in the non-resonant case ($\varkappa_2^* < 0$), the three-mode resonance may be able to destabilize this state if $\beta \neq 0$. The question whether this property will also lead to stable three-mode solution can only be studied by numerical means.

If we wish to perform a numerical survey of the possible fixed point solutions of equations (1) – (4), we cannot follow the same technique used in the discussion of the second order case since the resulting equation for the equilibrium phase would have been of very high order and thus very difficult to tackle both analytically and numerically. Instead, for fixed $\varkappa_2, \varkappa_3$ and α_{ij} $(1 \leq i, j \leq 3)$ we choose some equilibrium values of a_1, a_2 and a_3 and compute (by very simple algebra) the equilibrium phase and the corresponding $\Delta\nu$, β_2 and β_3. On performing this computation many thousand times with different (a_1, a_2, a_3) values, one can map the possible stable fixed points.

We show in Figure 3 one of our representative results. The different stable fixed point solutions are plotted with different symbols; vertical line ($a_2 \neq 0$, $a_1 = a_3 = 0$), horizontal line ($a_1 \neq 0$, $a_2 = a_3 = 0$), crosses ($a_1 \neq 0$, $a_2 \neq 0$, $a_3 \neq 0$)). In order to compare the underlying physical model with the parameters listed, assuming $c_i \approx \omega_i$, $\varkappa_1 \approx 0.01$ (dimensionless, see *Stellingwerf* 1975a) the relative radius variation is in the range of 0.01 – 0.5 and the maximum of the normalized frequency distance (see *Petersen* 1979) is $|1-(\omega_1+\omega_2)/\omega_3| \leq 0.1$.

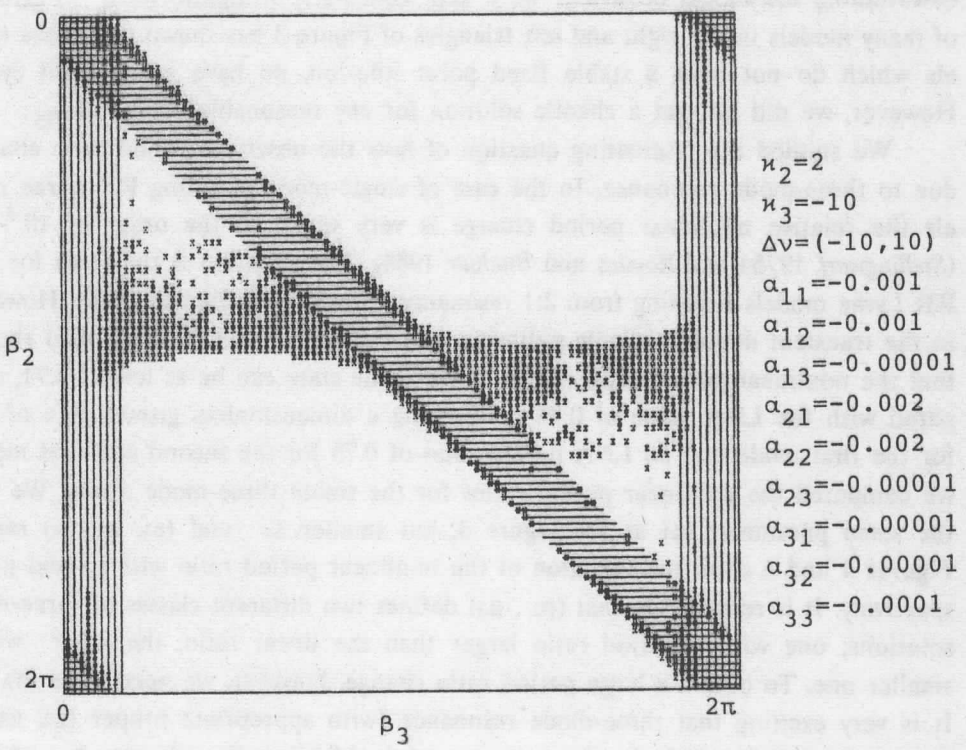

Fig. 3. Regions of the stable fixed point solutions of general three-mode resonance equation. The set of parameters used is shown beside the figure. Ranges of equilibrium amplitudes were the same for all three amplitudes, *i.e.* 1–61. Vertical lines correspond to the single-mode solutions $a_2 \neq 0$, $a_1 = a_3 = 0$, horizontal lines to $a_1 \neq 0$, $a_2 = a_3 = 0$, and crosses to the three-mode solution.

We see that all possible combinations of the stable fixed point solutions are observable. We mention however, that since $\Delta\nu$ is not fixed, there is an ambiguity in identifying the models on the basis of this figure. (Direct check of the output of the stability analysis, however, showed the existence of simultaneously stable single- and three-mode fixed points.) Similarly to the special case discussed by DK, there are coexisting stable single mode (both) and three-mode states close to the origo $(\beta_2, \beta_3) \approx (0,0)$. Also the models are of "either-or"-type (*Stellingwerf* 1975a) in the

corners of the (β_2, β_3) plane, though the non-resonant parameters correspond to "first mode only" ($\kappa_1^*>0$, $\kappa_2^*<0$). This result is also in agreement with that of DK. The new feature, however, is the appearance of regions where only the three-mode state is stable. This can even happen with small (β_2, β_3) values, but is quite common for larger (β_2, β_3) values. We see that it is possible to have a situation when the system continuously changes from one single-mode state to the other through a three-mode state. (It is mentioned that the figure is not appropriate for modelling such an evolutionary change as the important parameters (*i.e.* κ_2, κ_3, $\Delta\nu$) primarily determining the modal behaviour were kept constant). Straightforward integration of many models in the right and left triangles of Figure 3 has shown that those models which do not have a stable fixed point solution, do have stable limit cycles. However, we did not get a chaotic solution for any reasonable choice of a_{ij}.

We studied the fascinating question of how the observed period ratio changes due to three-mode resonance. In the case of single-mode pulsating RR Lyrae models the relative nonlinear period change is very small, of the order of 10^{-2}–10^{-5} (*Stellingwerf* 1975a and *Kovács* and *Buchler* 1988). The situation is the same for beat RR Lyrae models resulting from 2:1 resonance (*Kovács* and *Buchler* 1988). However, in the transient double-periodic pulsation of a Cepheid model *Uji-Iye* (1986) showed that the nonlinear period ratio in the mixed-mode state can be as low as 0.71, compared with the LNA value of 0.74 . Assuming a dimensionless growth rate of 0.01 for the first mode and an LNA period ratio of 0.75 for the second and first modes, we computed the nonlinear period ratios for the stable three-mode states. We used the same parameter set as for Figure 3, but smaller $\Delta\nu$ and (a_1, a_2, a_3) ranges. Figures 4 and 5 show the variation of the nonlinear period ratio with β_2 and β_3 respectively. It is remarkable that (β_2 , β_3) defines two different classes of three-mode solutions; one with a period ratio larger than the linear ratio, the other with a smaller one. To obtain a large period ratio change, however, we need large (β_2, β_3). It is very exciting that three-mode resonance (with appropriate proper (β_2, β_3)) is able to account not only for the existence of double-periodic pulsators, but also for the explanation of the beat Cepheid mass anomaly.

We conclude that three-mode resonance can, in principle, cause beat Cepheid-type pulsations if we allow some (proper) non-adiabatic phase shift in the resonant coupling. If, however these phase shifts are small, three-mode resonance supports single-mode rather than three-mode pulsations. There is no direct evidence that the non-adiabatic phase shift in the resonant coupling is large in the beat Cepheids (no numerical results are available). However, in the case of bump Cepheids, both analytical (*Buchler* and *Kovács* 1986) and numerical results (*Klapp et al.* 1985) indicate that non-adiabaticity in the resonant coupling might be important. Nonlinear hydrodynamic computations, however, have not shown the desired effect of three-mode res-

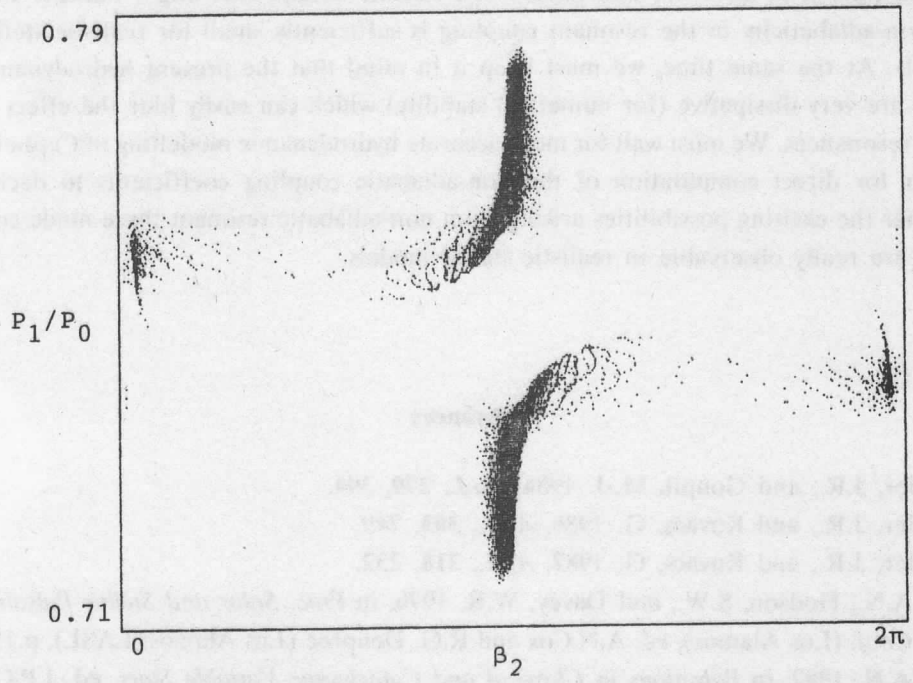

Fig. 4. Variation of the nonlinear period ratio with the non-adiabatic resonant phase shift β_2. The same parameters were used as for the ranges of the equilibrium amplitudes, which were 3–41 for all three amplitudes. The LNA period ratio of 0.75 and the dimensionless growth rate of the first mode of 0.01 were used.

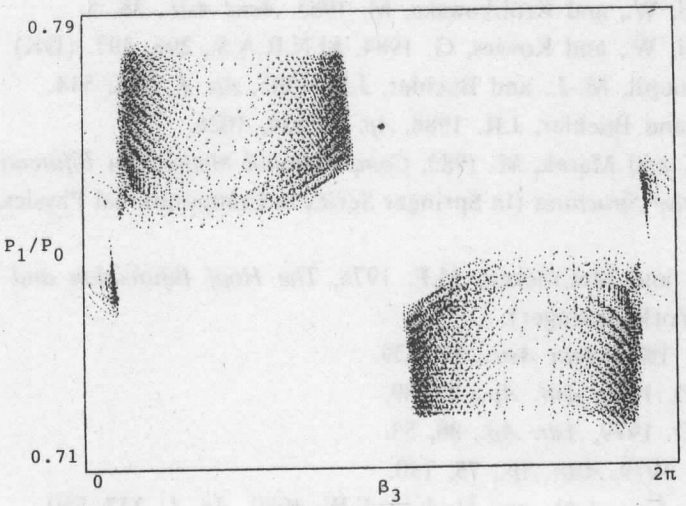

Fig. 5. Variations of the nonlinear period ratio with the non-adiabatic phase shift β_3 . Parameters as in Figure 4.

onance (*Simon et al.* 1980; and *Kovács* and *Buchler* 1988). This might indicate that the non-adiabaticity in the resonant coupling is sufficiently small for realistic stellar models. At the same time, we must keep it in mind that the present hydrodynamic codes are very dissipative (for numerical stability) which can easily blur the effect of some resonances. We must wait for more accurate hydrodynamic modelling of Cepheids and/or for direct computation of the non-adiabatic coupling coefficients to decide whether the exciting possibilities arising from non-adiabatic resonant three mode coupling are really observable in realistic stellar models.

References

Buchler, J.R., and Goupil, M.-J. 1984, *Ap.J.*, **279**, 394.

Buchler, J.R., and Kovács, G. 1986, *Ap.J.*, **303**, 749.

Buchler, J.R., and Kovács, G. 1987, *Ap.J.*, **318**, 232.

Cox, A.N., Hodson, S.W., and Davey, W.R. 1976, in *Proc. Solar and Stellar Pulsation Conf.* (Los Alamos), ed. A.N.Cox and R.G. Deupree (Los Alamos; LASL), p.157.

Cox, A.N. 1982, in *Pulsations in Classical and Cataclysmic Variable Stars*, ed. J.P.Cox and C.J.Hansen (Boulder; JILA), p.157.

Cox, A.N. 1987, preprint: "Modes, Masses, Metallicities, and Magnitudes of RR Lyrae Stars", in Proc. IAU Coll. No. 95., Tucson, Arizona.

Davis, C.G. 1988, these Proceedings.

Dziembowski, W. 1982, *Acta Astr.*, **32**, 147.

Dziembowski, W., and Królikowska, M. 1985, *Acta Astr.*, **35**, 5.

Dziembowski, W., and Kovács, G. 1984, M.N.R.A.S., **206**, 497. (DK)

Klapp, J., Goupil, M.-J., and Buchler, J.R. 1985, *Ap. J.*, **296**, 514.

Kovács, G., and Buchler, J.R. 1988, *Ap. J.*, **324**, 1026.

Kubicek, M., and Marek, M. 1983, *Computational Methods in Bifurcation Theory and Dissipative Structures* (in Springer Series in Computational Physics, Springer New York).

Marsden, J., and McCracken, M.F. 1976, *The Hopf Bifurcation and its Application* (New York; Springer).

Moskalik, P. 1985, *Acta Astr.*, **35**, 229.

Petersen, J.O. 1973, *Astr. Ap.*, **27**, 89.

Petersen, J.O. 1979, *Astr. Ap.*, **80**, 53.

Simon, N.R. 1979, *Astr. Ap.*, **75**, 140.

Simon, N.R., Cox, A.N., and Hodson, S.W. 1980, *Ap. J.*, **237**, 550.

Stellingwerf, R.F. 1975a, *Ap. J.*, **195**, 441.

Stellingwerf, R.F. 1975b, *Ap. J.*, **199**, 705.

Takeuti, M., and Aikawa, T. 1981, *Science. Rep. Tohoku University,Eighth Series*, Vol.2, p.106.

Uji-Iye K.-i. 1986, *Sendai Astronomiaj Raportoj*, No. 292.

RR LYRAE STARS: BEAT AND BLAZHKO EFFECT

B. Szeidl
Konkoly Observatory, Budapest, Hungary

Abstract

About one third of the RR Lyrae stars show non-repetitive nature. At present two effects are known, which produce this behaviour: double-mode pulsation and Blazhko effect. A concise description of these phenomena is given and attention is called to some important problems of the RRd and Blazhko stars, and the possible relationship between them.

1. Introduction

The RR Lyrae stars are regularly pulsating stars. Investigation of their period changes has shown that their periods are remarkably constant. The change in their periods is usually less than some tenths of a second over several decades. Nevertheless a number of RR Lyrae stars exhibit some kind of non-repetitive features in their light curves from cycle to cycle. As far back as 80 years ago *Blazhko* (1907) had already taken note of this phenomenon. He noticed that the times of maximum light of RW Dra could not be represented by a linear formula, a cosine term had to be added to it, i.e. a periodic change with a secondary period of 41.6 days had to be postulated in the fundamental period. *Shapley* (1916, 1918) was the first to show that the periodic oscillation of time of maximum was always accompanied by changes in the heights of light maximum and in the shape of light curve with the same long period. Later on this kind of long periodic, secondary variation was found in a number of RR Lyrae stars. Usually the large scatter on the folded light curves, especially around light maxima, calls attention to the existence of this effect. Since Blazhko was the first to observe this phenomenon, it is called Blazhko effect. Recently the effect is frequently referred to as *amplitude modulation*, because during the course of a long (around 1-3 months) secondary cycle the most striking feature is the oscillation of the light amplitude.

Because the existence of the Blazhko effect in some RRab stars is unquestionable, attempts have been made to identify the changes in the light curves (in amplitudes, heights of maxima, etc.) of those RRc stars exhibiting the Blazhko phenomenon. It is still questionable whether the RRc stars exhibit light curve variations with a long, 20-100 days, period.

It is indeed surprising that during the seventy years of observations of RR Lyrae stars nobody recognized earlier that these stars might possess another kind of double periodicity, viz. *double-mode pulsation*. In this case the modulation or beat period is very short, around one day, and a large scatter characterizes the whole light curve folded according to phase. The first and so far the only known field RR Lyrae star of this sort, AQ Leo, was discovered about ten years ago by *Jerzykiewicz* and *Wenzel* (1977).

Sandage, Katem and *Sandage* (1981) noticed that there was an abrupt increase in scatter of the photometry of c type stars of M15 in the very narrow period range $0.390 \text{ day} < P < 0.429 \text{ day}$. The amplitudes of these variables vary from cycle to cycle and this gives rise to the scattered nature of the folded light curves. Because this narrow period range occurs just at the transition period between c and ab variables, the cited authors presumed the phenomenon to be due to a mixing between the fundamental mode and the first overtone.

The double-mode RR Lyrae pulsators are often called RRd variables.

2. Frequency of RR Lyrae stars with non-repetitive nature

The observed light curve variations indicate that the star possesses some sort of non-repetitive feature. Further detailed investigations are likely to be able to clarify whether this feature is caused by the Blazhko effect or by double-mode pulsation. Probably the RRab stars showing non-repetitive character in their light variation exhibit the Blazhko effect, whereas the RRc stars of this sort are double-mode pulsators.

The most reliable estimation of the frequency of RR Lyrae stars showing light curve variation can be obtained by using the fairly homogeneous photographic data of the cluster variables. For example, in M3 the effect was shown in 35 out of 104 RRab stars, this corresponds to a frequency of 34% (*Szeidl*, 1965, 1973). *Smith* (1981) extended the statistics to the RRab stars of a further three clusters (M5, M15, ω Cen) and the Draco dwarf galaxy, and obtained a frequency of 25% for the RRab stars with Blazhko effect. Table 1 summarizes all the reliable data available in the literature for the cluster variables in M3, M5, M15 and ω Cen and Draco dwarf galaxy. The results are in good agreement with the earlier estimates, the frequency of the stars in question is between 25 and 30%. These results are well supported by the study of *Kinman et al.* (1984) who investigated the RR Lyrae stars in the field RRI (MWF 361A). Of the 42 ab type variables in their sample "7 (16%) definitely and 5 (12%) probably have more scatter in their light curves than can be accounted for by observational error".

Table 1. RR Lyrae stars in M3, M5, M15, ω Cen and Draco dwarf galaxy (r < 5'40")

period range	all		non-rep.		%	
	ab	c	ab	c	ab	c
0d22 - 0d26	-	1	-	-	-	0.0
0.26 - 0.30	-	14	-	1	-	7.1
0.30 - 0.34	-	33	-	3	-	9.1
0.34 - 0.38	-	37	-	10	-	27.0
0.38 - 0.42	-	42	-	22	-	52.4
0.42 - 0.46	7	5	1	4	14.3	80.0
0.46 - 0.50	30	3	12	-	40.0	0.0
0.50 - 0.54	57	1	19	-	33.3	0.0
0.54 - 0.58	66	-	27	-	40.9	-
0.58 - 0.62	69	-	19	-	27.5	-
0.62 - 0.66	50	-	11	-	22.0	-
0.66 - 0.70	33	-	3	-	9.1	-
0.70 - 0.74	9	-	-	-	0.0	-
0.74 - 0.78	10	-	-	-	0.0	-
0.78 - 0.82	3	-	-	-	0.0	-
0.82 - 0.86	6	-	-	-	0.0	-
0.86 - 0.90	3	-	-	-	0.0	-
0.90 - 0.94	1	-	-	-	0.0	-
all	344	136	92	40	26.7	29.4

We come to the same conclusion if we investigate the field RR Lyrae stars. The 3rd Edition of the GCVS and its first, second and third Supplements list more than 4000 RR Lyrae stars, but refer to the Blazhko effect in only 180 cases. This would mean a frequency of about 4-5%. The data of the GCVS are, however, very inhomogeneous, especially towards fainter stars. This selection effect is clearly shown in Table 2. In this table the numbers of RR Lyrae stars contained in the 3rd Edition of the GCVS and its Supplements down to 19th magnitude are given by magnitude intervals. The Blazhko effect is mentioned in only 135 cases from among the 3207 RRab stars. Table 2 strongly suggests that the data of the GCVS for stars fainter than the 12th magnitude are incomplete and for a reliable estimate of the frequency of RRab stars with Blazhko effect only stars brighter than 12th magnitude can be used. The result for these stars is around 30%.

Smith (1981) called attention to a very interesting and important fact: the absence of Blazhko effect among the long period RRab stars. Table 1 clearly indicates that the RRab stars in clusters with a fundamental period longer than 0.7 day always have a stable light curve. In the field, four RRab stars with periods longer than 0.7 day and with supposed Blazhko effect are mentioned in the GCVS. These stars are XX And (0.7227 d), CF Com (0.7392 d), SW For (0.8037) and AT Ser (0.7466 d).

Table 2. Field RRab stars

mean brightness	all RRab	Blazhko effect	%
$7^{m}.00 - 7^{m}.99$	1	1	100.0
8.00 - 8.99	0	0	-
9.00 - 9.99	4	2	50.0
10.00 - 10.99	29	8	27.6
11.00 - 11.99	94	30	31.9
12.00 - 12.99	179	25	14.0
13.00 - 13.99	283	18	6.4
14.00 - 14.99	650	19	2.9
15.00 - 15.99	963	11	1.1
16.00 - 16.99	688	11	1.6
17.00 - 17.99	257	10	3.9
18.00 - 18.99	59	0	0.0
all	3207	135	4.2

The light curve variation of XX And ($P_B = 36$ days) was found by *Lange* (1962) from visual observations, while AT Ser is only reported in the GCVS as exhibiting the Blazhko effect. *Hoffmeister* (1956) claimed that the light curve of SW For had a changing form. However, photoelectric observations by *Fitch, Wisniewski* and *Johnson* (1966), by *Kinman* (1960) and by members of Konkoly Observatory (unpublished) prove that these stars are monoperiodic. The possible Blazhko effect of CF Com was mentioned by *Meinunger* and *Wenzel* (1968). Their photographic observations exhibited some changes in the form of the light maxima of CF Com. As long as photoelectric observations do not confirm the presence of Blazhko effect in this star we can take it as a fact that amplitude modulation is able to take place only in RRab stars with periods of less than 0.7 day.

The occurrence of Blazhko effect in some of the RRc stars is a matter of dispute. Some doubtful cases have been reported. For example *Ficarrotta* and *Romoli* (1979) using *Todoran's* (1974) observations derived a secondary period of 29.88 days for RZ Cep whereas *Paczynski's* (1965b) and our unpublished photoelectric observations show that the light curve of RZ Cep is very stable. Moreover *Glovnia* (1983) reanalysed Todoran's data more rigorously and could not find clear evidence for the presence of a long term amplitude modulation in RZ Cep. So the question whether RRc stars have the Blazhko effect is open for further study.

On the other hand, the presence of double-mode pulsation in a significant fraction of RRc stars is a common feature. Table 1 shows that about 1/3 of the RRc stars in clusters are double-mode pulsators, and their frequency increases with increas-

ing period. There are four single periodic RRc stars with periods between 0.46 and 0.54 day. A rigorous and detailed investigation of these stars and a search for double periodicity in them seems to be reasonable.

The first double-mode field RR Lyrae star, AQ Leo, was discovered by *Jerzykiewicz* and *Wenzel* (1977). There are some other RRc stars which exhibit strong light curve variations and are good candidates for double-mode variables (e.g. BV Aqr, $P = 0.364$ day; AH Cam, $P = 0.369$ day; BT Aqr, $P = 0.407$ day). Recently *Peniche et al.* (1987) carried out a thorough period analysis of the RRc type star ST CVn. They came to the conclusion that ST CVn is a multiperiodic star and were able to identify three periods in its pulsation.

3. The Blazhko effect

The most significant feature of the Blazhko effect is the long term (20-100 days) amplitude modulation of the pulsational light variation. During the long modulation cycle or Blazhko period, the light curve undergoes a very characteristic variation, in particular around light maxima both in shape and height. As an example, a series of light curves of RR Lyr at different phases of the Blazhko cycle is shown in Figure 1. Since observers have, in general, found the changes of the ascending branch and maximum light most interesting and most characteristic of the Blazhko effect, the observations have always been concentrated on this part of the light curves and photometry has not been extended to the whole light curves. Hence, period analysis of RR Lyrae stars with Blazhko effect meets very serious difficulties.

The Blazhko effect has been observed in a number of RRab stars, however, in many cases we should accept the results with reserve. In the previous section some examples have already been mentioned. In the following some further, intriguing examples are given.

Chumak (1965) reported that AT And ($P = 0.617$ d) showed the Blazhko effect with a secondary period of 82.7 days. Our photoelectric observations (*Oláh* and *Szeidl*, 1978) refute the existence of any secondary changes in this star. *Lange* (1962) stated that AA Aql ($P = 0.362$ d, $P_B = 18$ days or > 100 days) belonged to the group of RRab stars with the *Blazhko* effect whereas *Paczynski's* (1965a, 1966) accurate photoelectric observations contradict this statement. On the basis of her visual observations, *Kanishcheva* (1971) suggested that DX Del ($P = 0.473$ d, $P_B = 35$ days) had light curve variation. The earlier photoelectric observations by *Fitch, Wisniewski* and *Johnson* (1966) and by *Preston* (1961) do not support this suggestion. *Firmanyuk* (1974) visually investigated KX Lyr ($P = 0.441$ d) and concluded that it had strong secondary variations with a period of 132.7 days. No sign of any light curve varia-

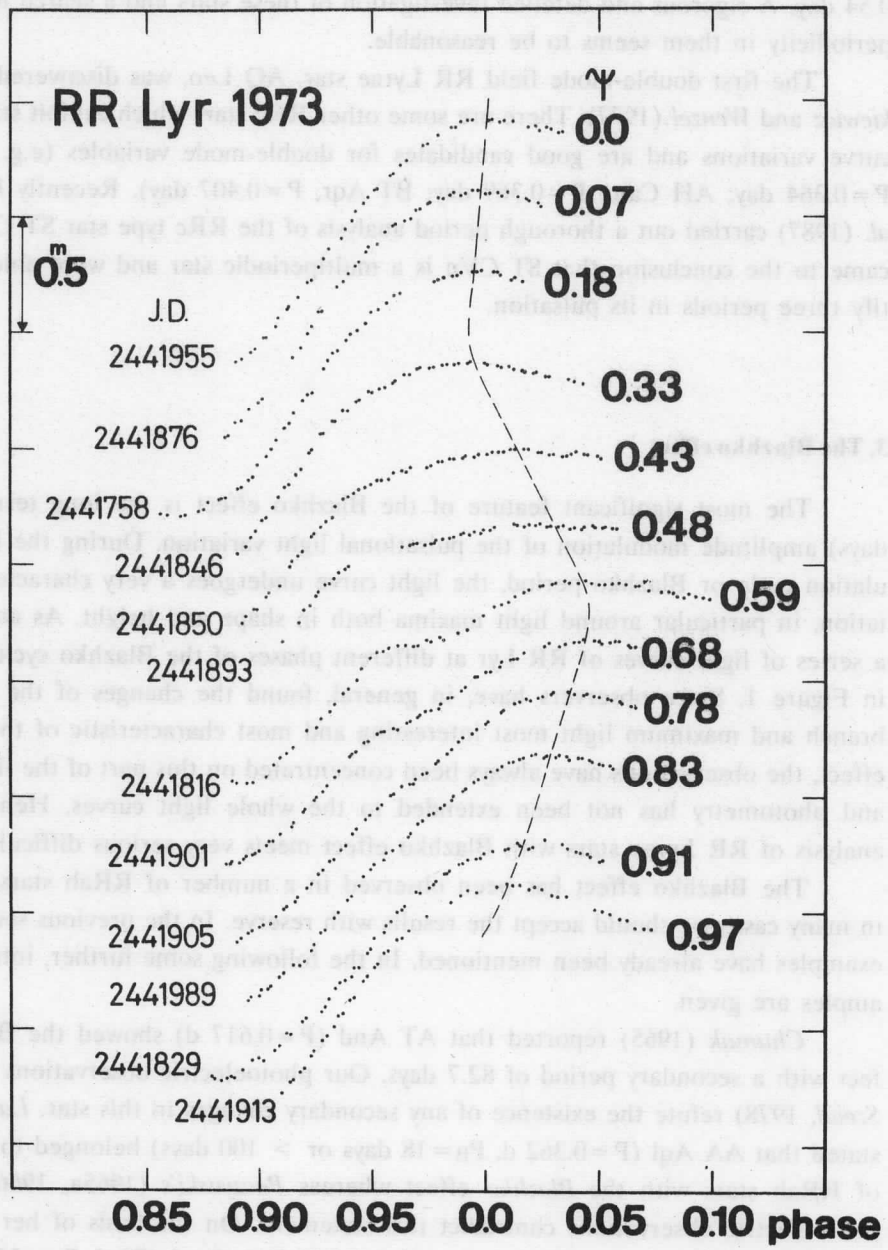

Fig. 1. Light curves of RR Lyr at different phases of the Blazhko cycles. The phases of the secondary cycles have been computed by the formula $C_B = JD\ 2414905.0 + 40.8\ N$. The light curves are shifted by 0.3 mag on the vertical axis.

tions of KX Lyr could, however, be found in *Fitch, Wisniewski* and *Johnson's* (1966), nor in *Stepien's* (1972) photoelectric observations. *Batyrev* (1957) used his visual observations in a discussion on AN Ser and claimed that this star also exhibited Blazhko effect with $P_B = 22.94$ days. Our long series of photoelectric observations (*Szeidl*, 1968b), however, shows AN Ser to be a stable, single periodic RRab star. All these (and other, here not mentioned) erroneous results were probably the consequence of the inferiority of visual observations.

There are two interesting stars (SW And and RR Gem), which deserve more attention. *Shapley* (1921) observed an 0.4 mag oscillation in the height of light maxima of SW And in 1920, while forty years later only a small variation in the shape of the hump on the ascending branch could be detected. RR Gem showed the Blazhko effect according to Detre's photographic observations in the thirties. However, the photoelectric observations carried out in the last thirty years have shown the star to be single periodic. The behaviour of these stars indicates that there may be no sharp distinction between RR Lyrae stars with or without Blazhko effect.

The RR Lyrae stars with known Blazhko period are listed in Table 3 using only reliable data. An inspection of the data of this table suggests that no connection exists between the fundamental (P) and the Blazhko (P_B) period. In Figure 2 $\log P_B$ is plotted against logP. This figure demonstrates and supports the former statement. In some of the Blazhko stars (Table 4) a second long period has also been identified. In Figure 2 the logarithm of the other long period is also indicated. The problem of reality of the two long periods needs further thorough investigation, namely P_{B2} is about of the same length as the observational season. Probably, RS Boo is the only exception. The two long periods observed in this star are certainly real, but the behaviour of RS Boo differs from the remaining Blazhko stars in other aspects, too.

The oscillation of the heights and times of maximum light of Blazhko stars during the secondary period is very characteristic (see figures 5a-e in *Szeidl*, 1976). The amplitudes and asymmetries of these curves are marked with A_{max}, A_{O-C}, μ_m and μ_{O-C}, and the phase difference between the two curves with $\Delta\psi$. Table 5 summarizes these data for ten stars. No connections seem to exist among the different parameters. It is interesting to note that the characteristics may change in the same star from one year to the other (*e.g.* RR Lyr). But there does exist an important connection between the amplitudes of the RRab stars with Blazhko effect and that of the single periodic RRab stars. On the period-amplitude plot, the highest light amplitude of the Blazhko star always fits in the period-amplitude diagram of the single periodic RRab stars. In the lower part of Figure 3 the period-amplitude diagram of the RRab stars in M3 is given. In some cases the largest amplitude of the

Table 3. RRab stars with known or presumed Blazhko period

Star	P(day)	P_B(days)	Reference
BM Del	0.351	∿100	Ahnert et al. (1947)
RS Boo	0.377	537	Oosterhoff (1946)
RR Gem	0.397	37	Budapest, unpublished
MW Lyr	0.398	33.3	Mandel (1970)
DM Cyg	0.420	26.0	Lysova and Firmanyuk (1980)
SW And	0.442	36.8	Balázs and Detre (1954)
RW Dra	0.443	41.6	Blazhko (1907)
RV Cap	0.448	223.8	Tsesevich (1943)
BI Cen	0.453	∿ 70	Kinman (1960)
TU Com	0.461	∿ 75	Ureche (1965)
XZ Cyg	0.467	57.4	Blazhko (1922)
RV UMa	0.468	90.1	Balázs and Detre (1957)
AR Her	0.470	31.5	Balázs and Detre (1939)
XZ Dra	0.476	76	Balázs and Detre (1941)
RY Col	0.479	∿ 90	Kinman (1960)
V14 in M5	0.487	75.0	Goranskij (1980a)
X Ret	0.492	≥ 45	Hoffmeister (1956)
V674 Cen	0.494	29.4	Hoffmeister (1956)
V63 in M5	0.498	146.8	Goranskij (1980b)
KM Lyr	0.500	∿ 30	Hoffmeister (1951)
V5 in M3	0.506	194.6	Panov (1980)
RZ Lyr	0.511	116.7	Romanov (1967)
V434 Her	0.514	26.1	Rozhavski (1964)
SW Psc	0.521	34.5	Ureche (1971)
Y LMi	0.524	33.4	Martynov (1940)
V2 in M5	0.526	∿132	Goranskij (1980b)
V30 in M53	0.535	37.0	Wachmann (1968)
SZ Hya	0.537	25.8	Kanyó (1970)
UV Oct	0.543	∿ 80	Hoffmeister (1956)
V788 Oph	0.547	∿115	Mandel (1969)
RW Cnc	0.547	87	Blazhko (1922)
AD UMa	0.548	35-40	Hoffmeister (1958)
TT Cnc	0.563	89	Szeidl (1968a)
RR Lyr	0.567	40.6	Hertzsprung (1922)
V829 Oph	0.569	∿165	Mandel (1969)
AR Ser	0.575	105	Szeidl (1967)
WY Dra	0.589	14.3	Chis et al. (1975)
DL Her	0.592	33.6	Szeidl (1963)
V365 Her	0.613	40.6	Tsesevich (1961)
ST Boo	0.622	284	Lange and Firmanyuk (1975)
BH Peg	0.641	39.8	Kudryashova (1978)
Z CVn	0.654	22.7	Kanyó (1966)

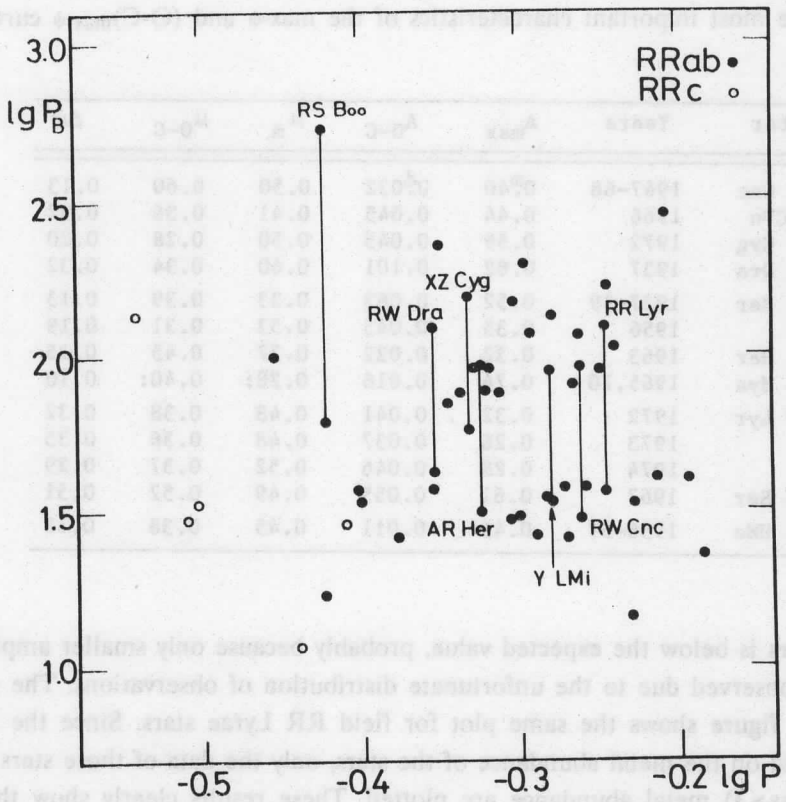

Fig. 2. Relationship between the P main and P_B Blazhko period. The uncertain results for RRc stars are indicated by circles.

Table 4. Blazhko stars with two long periods

Star	P(day)	P_{B1}(days)	P_{B2}(days)	Reference
RS Boo	0.377	62	533	Kanyó (1980)
RW Cnc	0.547	29.6	91.1	Balázs and Detre (1950)
XZ Cyg	0.467	57.25	153.8	Muller (1953)
RW Dra	0.443	41.61	121.4	Balázs and Detre (1952)
AR Her	0.470	31.55	90.83	Almár (1961)
Y LMi	0.524	33.4	89.2	Balázs (1956)
RR Lyr	0.567	40.7	122.1	Walraven (1949)

Table 5. The most important characteristics of the max-ψ and $(O-C)_{max-\psi}$ curves.

Star	Years	A_{max}	A_{O-C}	μ_m	μ_{O-C}	$\Delta\psi$
TT Cnc	1967-68	$0^m.40$	$0^d.032$	0.50	0.60	0.13
Z CVn	1966	0.44	0.045	0.41	0.56	0.92
XZ Cyg	1972	0.59	0.045	0.50	0.28	0.20
RW Dra	1937	0.82	0.101	0.40	0.34	0.32
AR Her	1937-39	0.52	0.063	0.33	0.39	0.13
	1956	0.35	0.045	0.53	0.31	0.19
DL Her	1963	0.32	0.022	0.37	0.45	0.15
SZ Hya	1965,70	0.74	0.016	0.28:	0.40:	0.10
RR Lyr	1972	0.32	0.041	0.48	0.38	0.32
	1973	0.26	0.037	0.48	0.36	0.35
	1974	0.28	0.046	0.52	0.37	0.29
AR Ser	1967	0.61	0.055	0.49	0.52	0.51
RV UMa	1956-57	0.49	0.011	0.45	0.38	0.12

Blazhko stars is below the expected value, probably because only smaller amplitudes have been observed due to the unfortunate distribution of observations. The upper part of the figure shows the same plot for field RR Lyrae stars. Since the amplitudes depend on the metal abundance of the stars, only the data of those stars which have low ($\Delta s \geq 3$) metal abundance are plotted. These results clearly show that the Blazhko effect is connected with a mechanism which tries to suppress the normal pulsational features (amplitudes) of the star.

The most thoroughly observed Blazhko star is RR Lyr itself. The long series of observations have made it possible to investigate the changes in the intensity of the Blazhko effect. In the years 1963, 1967, 1971 and 1975 the intensity of the Blazhko effect became very weak. Hence it became obvious that the Blazhko effect in RR Lyr has a four-year cycle. By means of old visual and photographic observations we were able to trace back this four-year cycle to 1935 (*Detre* and *Szeidl*, 1973; *Szeidl*, 1976). The cycle lengths varied between 3.8 and 4.8 years. At the end of an old four-year cycle the amplitude of the light maximum variations is smaller than 0.1 mag and then it very rapidly becomes as large as 0.2-0.3 mag. The transition from an old four-year cycle to a new one is always accompanied by a phase shift of about 10 days in the 41-day Blazhko period, and these shifts may be both positive or negative. After each discontinuity in the O-C diagram of the 41-day cycle the secondary period remains constant during the following four-year cycle.

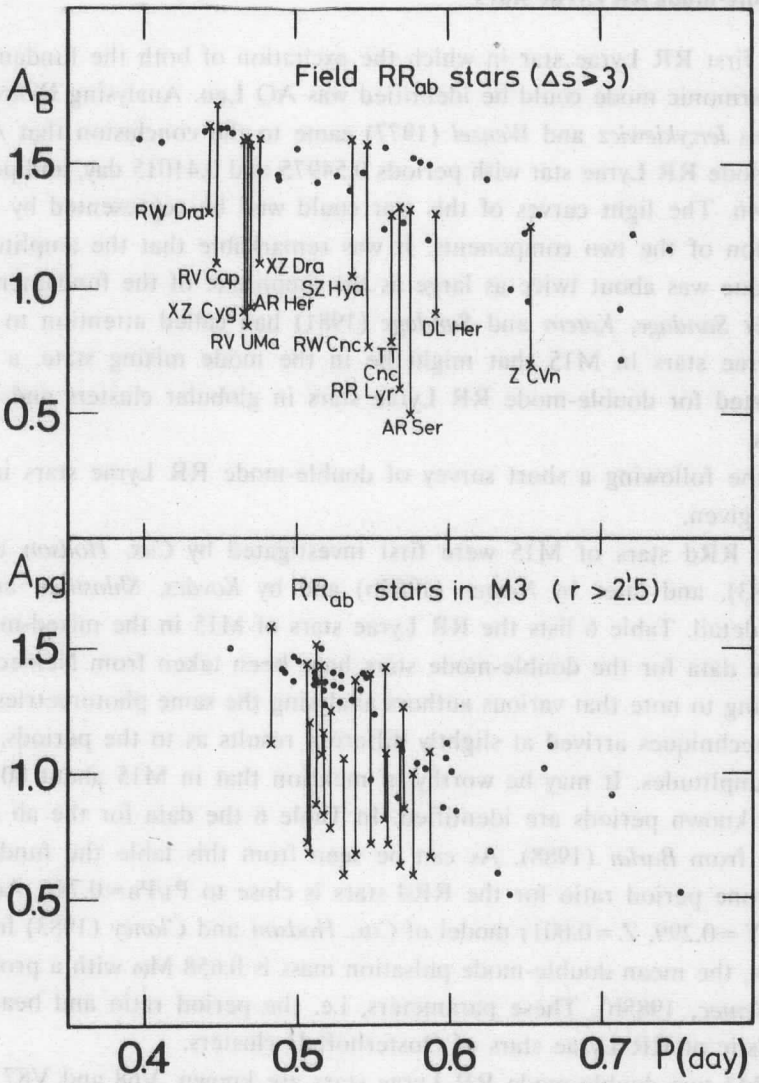

Fig. 3. Period-amplitude diagram for RRab stars in M3 and in the field. The highest and smallest amplitude of the Blazhko stars observed are also indicated.

Other Blazhko RRab stars may also possess this kind of long period cycle (XZ Cyg: 9.2 years; RW Dra: 7.4 years; Y LMi: 7.7 years) which reminds us of the solar activity cycle. In this respect it may be worth mentioning that *Babcock* (1958) observed a strong, variable magnetic field in RR Lyr.

4. The double-mode RR Lyrae stars

The first RR Lyrae star in which the excitation of both the fundamental and the first harmonic mode could be identified was AQ Leo. Analysing *Wenzel's* (1976) observations *Jerzykiewicz* and *Wenzel* (1977) came to the conclusion that AQ Leo is a double-mode RR Lyrae star with periods 0.54975 and 0.41015 day, and period ratio $P_1/P_0 = 0.746$. The light curves of this star could well be represented by non-linear superposition of the two components. It was remarkable that the amplitude of the first overtone was about twice as large as the amplitude of the fundamental mode.

After *Sandage, Katem* and *Sandage* (1981) had called attention to a number of RR Lyrae stars in M15 that might be in the mode mixing state, a systematic search started for double-mode RR Lyrae stars in globular clusters and extragalactic systems.

In the following a short survey of double-mode RR Lyrae stars in different systems is given.

The RRd stars of M15 were first investigated by *Cox, Hodson* and *Clancy* (1981, 1983), and later by *Nemec* (1985b) and by *Kovács, Shlosman* and *Buchler* (1986) in detail. Table 6 lists the RR Lyrae stars of M15 in the mixed-mode period range. The data for the double-mode stars have been taken from Nemec's study. It is interesting to note that various authors analysing the same photometries, but using different techniques arrived at slightly different results as to the periods, period ratios and amplitudes. It may be worthy of mention that in M15 about 80 RR Lyrae stars with known periods are identified. In Table 6 the data for the ab and c stars are taken from *Barlai* (1988). As can be seen from this table the fundamental to first overtone period ratio for the RRd stars is close to $P_1/P_0 = 0.746$. Adopting the King Ia ($Y = 0.299$, $Z = 0.001$) model of *Cox, Hodson* and *Clancy* (1983) for the mass calibration, the mean double-mode pulsation mass is 0.658 $M_\odot$ with a probable error of 5% (*Nemec*, 1985b). These parameters, i.e. the period ratio and beat mass, are characteristic of RR Lyrae stars of Oosterhoff II clusters.

In M3 two double-mode RR Lyrae stars are known, V68 and V87 (*Goranskij*, 1981; *Cox, Hodson* and *Clancy*, 1983). Table 7 presents the data for the RR Lyrae stars of M3 in the mixed-mode range. The stars are listed according to increasing period. The periods of single periodic ab and c stars have been compared by adopting the period ratio $P_1/P_0 = 0.745$. If a definite trend in the change of the periods of these stars has been observed, the β values ($\Delta P/P$) (*Szeidl*, 1965, 1973) are also indicated in Table 7. These values do not support the hysteresis suggestion concerning the transition through the mode mixing period interval. Further investigation of period changes in the mode-mixing period interval may contribute to our better understanding of the pulsational modes in this period interval. From the period ratios

of the two RRd stars in M3 *Cox, Hodson* and *Clancy* (1983) derived a beat mass of about 0.55 $M_\odot$ for these stars. This mass value is characteristic of Oosterhoff type I RR Lyrae stars.

Table 6. RR Lyrae stars of M15 in the mixed-mode range

Var	Type	P_1	P_0	P_1/P_0	A_1	A_0	A_1/A_0
3	c	$0^d.3887$	–	–	$0^m.59$	–	–
39	d	0.3896	$0^d.5216$	0.7469	0.44	$0^m.20$	2.2
41	d	0.3918	0.5240:	0.7476	0.48	0.15:	3.2:
16	c	0.3992	–	–	0.47	–	–
43	c	0.3960	–	–	0.66	–	–
96	d	0.3963	0.5309	0.7465	0.517	0.188	2.7
51	d	0.3970	0.5337	0.7439	0.53	0.12	4.4
78	c	0.3989	–	–	0.60	–	–
54	d	0.3996	0.5377:	0.743	0.46	0.10	4.6
61	d	0.3996	0.5361	0.7454	0.51	0.23	2.2
101	d	0.4007	0.5376:	0.7454:			
26	d	0.4023	0.5391	0.7461	0.41	0.10	4.1
67	d	0.4046	0.5425	0.7459	0.37	0.20	1.9
30	d	0.4060	0.5446	0.7455	0.32	0.18	1.8
100	c	0.4061	–	–	0.70	–	–
58	d	0.4073	0.5459	0.7460	0.51	0.24	2.1
31	d	0.4082	0.5472	0.7460	0.44	0.18	2.4
59	ab	–	0.5548	–	–	0.85	–
104	c	0.4141	–	–	0.70	–	–
53	d	0.4141	0.5553	0.7458	0.52	0.19	2.7
56	ab	–	0.5704	–	–	0.92	–
19	abBl	–	0.5723	–	–	1.31	–
17	d	0.4289	0.5748	0.7462	0.35	0.16	2.2
13	ab	–	0.5750	–	–	1.11	–
29	abBl?	–	0.5750	–	–	0.85	–
52	ab	–	0.5756	–	–	1.08	–
15	abBl	–	0.5836	–	–	1.24	–
33	abBl	–	0.5839	–	–	0.80	–
12	abBl	–	0.5929	–	–	0.78	–
44	abBl	–	0.5956	–	–	0.88	–

IC 4499 is found to be unusually rich in RR Lyrae stars. *Coutts Clement, Dickens* and *Epps Bingham* (1979) investigated the RR Lyrae stars in the cluster and presented periods and light curves for 52 ab type and 23 c type stars. The cluster clearly belongs to Oosterhoff type I. In a recent paper *Clement et al.* (1986) discuss the double-mode RR Lyrae stars in this cluster. Thirteen RRd stars have been identified which have surprisingly uniform properties and are considerably different from the RRd stars found in M15, in an Oosterhoff type II system. The mean ratio of the first overtone period to the fundamental one is $<P_1/P_0> = 0.7444 \pm 0.0002$ and the

mean double-mode pulsation mass for the 13 stars, using the King Ia mass calibration, is 0.538 $M_\odot$. Table 8 collects the data for RR Lyrae stars of IC 4499 in the mixed-mode period range based on the results of *Coutts Clement, Dickens* and *Epps Bingham* (1979) and *Clement et al.* (1986).

Table 7. RR Lyrae stars of M3 in the mixed-mode period range

Var	Type	P_1	P_0	P_1/P_0	$10^{10}\beta$(d/d)
140	c	$0^d.3331$	-	-	0.0
97	c	0.3349	-	-	+1.6
72	ab	-	$0^d.4561$	-	+2.0
77	ab	-	0.4593	-	+1.7
177	c	0.3483	-	-	(cyclic)
126	c	0.3484	-	-	(cyclic)
125	c	0.3498	-	-	+2.9
28	abBl	-	0.4706	-	(cyclic)
85	c	0.3558	-	-	(cyclic)
68	d	0.3560	0.4779	0.7449	-
87	d	0.3575	0.4797	0.7452	-
25	abBl?	-	0.4801	-	+6.3
22	abBl	-	0.4814	-	(strong irreg.)
13	abBl?	-	0.4830	-	-9.4
79	abBl	-	0.4833	-	(strong irreg.)
41	abBl?	-	0.4850	-	(cyclic)

Clement, Ip and *Robert* (1984) looked for double-mode pulsation in three RRc variables of M9. Two of them turned out to be single periodic, but for the third star, V5 ($P_1 = 0.3786$ d), there was a weak evidence for its double-mode nature with a period ratio $P_1/P_0 = 0.747$.

The double-mode nature of V3 in M68 was discovered by *Andrews* (1980). This RRd star has periods $P_1 = 0.392$ day and $P_0 = 0.526$ day, and the period ratio 0.745.

A very interesting and remarkable result was obtained by *Nemec, Linnell Nemec* and *Norris* (1986) when searching for double-mode RR Lyrae stars in ω Cen. Using *Martin's* (1939) extensive photometry, the brightness variation of 55 RR Lyrae stars was thoroughly analysed, and in the period interval 0.35 day to 0.50 day there appeared to be no doubly periodic RR Lyrae stars.

Double-mode RR Lyrae stars have also been found in extragalactic systems. For a number of RR Lyrae stars in and around NGC 2257 – an LMC globular cluster – *Nemec, Hesser* and *Ugarte* (1985) found that the light curves of these stars showed

greater than average scatter and in some cases the scatter could not be explained by the effects of crowding or background starlight or both. These stars (V18, V43, V2952, V2948, V2945) may be RRd stars.

Table 8. RR Lyrae stars of IC 4499 in the mixed-mode period range

Var	Type	P_1	P_0	P_1/P_0	A_1	A_0	A_1/A_0
69	c	$0^d.3402$	–	–	$0^m.62$	–	–
78	d	0.3519	$0^d.4726$	0.7445	0.43	$0^m.32$	1.3
18	d	0.3523	0.4734	0.7442	0.55	0.33	1.7
65	d	0.3528	0.4740	0.7442	0.57	0.23	2.5
103	c	0.3530	–	–	0.57	–	–
10	d	0.3532	0.4746	0.7441	0.53	0.44	1.2
21	d	0.3533	0.4748	0.7441	0.55	0.26	2.1
77	c	0.3546	–	–	0.59	–	–
92	c	0.3547	–	–	0.50	–	–
89	c	0.3554	–	–	0.52	–	–
109	d	0.3555	0.4776	0.7444	0.48	0.26	1.8
98	c	0.3556	–	–	0.51	–	–
59	d	0.3573	0.4800	0.7443	0.49	0.27	1.8
111	c	0.3573	–	–	0.61	–	–
87	d	0.3577	0.4805	0.7444	0.49	0.35	1.4
63	d	0.3577	0.4807	0.7441	0.53	0.17	3.1
96	c	0.3584	–	–	0.54	–	–
55	c	0.3585	–	–	0.50	–	–
73	d	0.3591	0.4825	0.7443	0.58	0.38	1.5
32	c	0.3600	–	–	0.43	–	–
3	ab	–	0.4832	–	–	1.47	–
42	d	0.3615	0.4852	0.7450	0.54	0.28	1.9
31	d	0.3617	0.4861	0.7442	0.55	0.39	1.4
95	d	0.364	0.491	0.74:			
40	ab	–	0.4923	–	–	1.47	–
2	ab	–	0.493	–	–	1.47	–
8	d	0.3674	0.4935	0.7445	0.46	0.34	1.4
34	ab	–	0.4936	–	–	1.53	–
14	ab	–	0.500	–	–		–
49	ab	–	0.500	–	–	1.41	–
58	ab	–	0.5006	–	–	1.35	–
33	ab	–	0.5064	–	–	1.59	–
27	ab	–	0.5067	–	–	1.50	–
23	ab	–	0.507	–	–	1.30	–

The photometry of RR Lyrae stars in the Draco dwarf galaxy by *Baade* and *Swope* (1961) was used by *Nemec* (1985a) to search for RRd stars in the system. Previously *Goranskij* (1982) had identified three RRd stars in the system, but *Nemec* found seven further members of the group. He derived the physical characteristics of these stars and compared them with those of the double-mode RR Lyrae stars

in the Galaxy. The periods and period ratios (0.7448-0.7466) are consistent with the simultaneous radial pulsation in the fundamental and first overtone modes. The average beat mass is shown to be 0.65 M⊙ for nine stars, and 0.55 M⊙ for the tenth star (V165). Metal abundances for the stars, estimated from their position in the period-amplitude diagram, suggest that V165 is more metal rich than the other nine. The Draco stars are indistinguishable from the RRd stars discovered in M15 and M3. The first nine stars belong to Oosterhoff type II, while the tenth belongs to Oosterhoff type I stars. The data for the RR Lyrae stars of the Draco dwarf galaxy in the mixed-mode period range are presented in Table 9.

Table 9. RR Lyrae stars of the Draco system in the mixed-mode period range

Var	Type	P_1	P_0	P_1/P_0	A_1	A_0	A_1/A_0
97	c	$0^d.3148$	–	–	$0^m.80$	–	–
121	c	0.3365	–	–	0.84	–	–
165	d	0.3580	$0^d.4807$	0.7448	0.55	$0^m.33$	1.7
113	c	0.3627	–	–	0.67	–	–
173	c	0.3695	–	–	0.77	–	–
44	c	0.3844	–	–	0.64	–	–
190	d	0.3965	0.5315	0.7460	0.66	0.31	2.1
83	d	0.4008	0.5372	0.7460	0.59	0.40	1.5
169	d	0.4031	0.5405	0.7458	0.59	0.29	2.0
143	d	0.4032	0.5401	0.7466	0.54	0.21	2.6
34	abBl	–	0.5451	–	–	0.81	–
72	d	0.4071	0.5460	0.7457	0.52	0.32	1.6
138	d	0.4077	0.5468	0.7456	0.58	0.18	3.2
156	d	0.4087	0.5486	0.7450	0.57	0.26	2.2
11	d	0.4110	0.5510	0.7460	0.61	0.26	2.3
136	ab	–	0.5549	–	–	0.96	–
163	abBl	–	0.5605	–	–	0.90	–
112	d	0.4284	0.5742	0.7458	0.54	0.27	2.0
177	ab	–	0.5924	–	–	0.80	–
184	abBl	–	0.5944	–	–	1.04	–
189	ab	–	0.5944	–	–	1.06	–
75	abBl	–	0.6027	–	–	0.74	–

The candidates for double-mode oscillation in the Ursa Minor dwarf galaxy were investigated by *Nemec* (1984) using van *Agt's* (1967, 1968) photometry, and it was found that V44, V49, V57, V58 and V83 might be double-mode pulsators, but more accurate photometry is needed to derive the period ratios of these stars and to estimate their masses.

5. Conclusions and comments

i) The RRd stars are of fundamental importance when investigating the physical properties of RR Lyrae stars. According to the idea first presented by *Jorgensen* and *Petersen* (1967), it is possible to use the period ratio to derive a mass for each star. It is noteworthy that there is no significant discrepancy among the beat, evolutionary and pulsation masses of the RR Lyrae stars whereas there is a mysterious mass anomaly for the double-mode Cepheids.

ii) Both of the Oosterhoff type clusters may have a fairly large number of double-mode RR Lyrae stars (*e.g.* M15 - type II, IC 4499 - type I). This suggests that double-mode pulsation may be a stable mode of pulsation. The theoretical time scale of mode switching is too short to explain the existence of the large number of RRd stars. The constancy of the modal content of the RRd stars in M15 during a twenty year interval has been proved by *Kovács, Shlosman* and *Buchler* (1986).

iii) The above notwithstanding, there are clusters (*e.g.* ω Cen) which contain many RR Lyrae stars with a pure overtone only and pure fundamental periods, but no double-mode stars. *Nemec, Linnell Nemec* and *Norris* (1986) try to explain this fact by the higher rotational velocities of stars in those clusters. *Cox* (1987) deals with this peculiarity by assuming that the helium abundance of the RR Lyrae stars of these clusters is too small to produce double-mode pulsation.

iv) The periods of the first overtone pulsation of RRd stars are in the interval 0.35 to 0.45 day, but not all the c type stars of the same cluster in that period interval are doubly periodic. There exist some ab type stars with strongly repetitive character (*i.e.* pulsating only in the fundamental mode) in the mode-mixing period interval. These stars have a shorter period than the longest RRd fundamental period observed or than the period calculated from the longest, observed pure overtone period if we assume a reasonable value for the period ratio (see Tables 6-9). The simultaneous occurrence of ab, c and d type stars in the mode-mixing period interval raises some problems.

v) In all cases of RRd stars investigated so far, the dominant mode of pulsation is the first overtone. The amplitudes of the first overtone pulsation of the RRd stars are about the same as the amplitudes of the pure overtone pulsation and are about twice as large as the amplitudes of the pulsation of RRd stars in the fundamental mode. *Cox, Hodson* and *Clancy* (1983) suspect that "the shorter periods have more overtone content with larger A_1/A_0 than for longer periods", but the modal content in each double-mode RR Lyrae stars seems to be unchanged over two decades.

The possible relationship between double-mode and Blazhko stars was discussed in detail by *Nemec* (1985a). Here I should like to stress some problems I think important.

i) The frequency of Blazhko stars is greater among RRab variables of shorter period, *viz.* near or in the period interval of double-mode RR Lyrae stars. It is, however, somewhat disturbing that *not all* the RRab stars have Blazhko effect in or near that interval. Long-period ab type stars (as was first noted by *Smith*, 1981) are usually non-Blazhko stars.

ii) The frequency of Blazhko variables in each cluster is around 25-30%. At the same time the frequency of RRd stars may vary from 0 to about 15% (*e.g.* in ω Cen there are many Blazhko and no RRd stars, M15 contains many Blazhko and many RRd variables). Concerning this fact *Nemec, Linnell Nemec* and *Norris* (1986) remark that "the presence of Blazhko stars in a system does not necessarily imply that RRd stars will be present, although both types of variables may be stars in the process of switching modes".

iii) The interpretation of the period-amplitude diagram of Blazhko stars (see Figure 3) may encounter some difficulties. Moreover, the amplitude of the lowest maximum of a Blazhko cycle may vary over some years.

iv) If the Blazhko phenomenon were in some way related to the double-mode pulsation or some mode-switching process, one would expect that some relationships should exist among the different parameters characterizing the Blazhko effect (P, PB Δs, etc.).

v) The behaviour of the long period cycle (four-year cycle in RR Lyr) raises a special problem. Do these long cycles have some relationship with other parameters of the Blazhko effect?

Even though the double-mode pulsation of RR Lyrae stars is well understood, the basic mechanism responsible for the amplitude modulation is unknown. More theoretical work is needed to get an idea about the physics of the Blazhko effect. *Moskalik's* (1986) recent work on the internal resonances, which may cause amplitude modulation, raises some hope. Nevertheless the oblique rotator hypothesis (*Detre* and *Szeidl*, 1973; *Cousens*, 1983) still seems to be a reasonable means of explaining the Blazhko effect.

References

Ahnert, P., Hoffmeister, C., Rohlfs, E., and van de Voorde, A. 1947, *Veröff. Sternw. Sonneberg*, **1**, 45.

Almár, I. 1961, *Mitt. Sternw. (Konkoly Obs.) Budapest*, Ung. Akad. Wiss. Nr. 51.

Andrews, P.J. 1980, in *Star Clusters*, Proc. IAU Symp. 85, ed. J.E. Hesser, Reidel-Dordrecht, p. 425.

Baade, W., and Swope, H.H. 1961, *A. J.*, **66**, 300.

Babcock, H.W., 1958, *Ap. J. Suppl.*, **3**, 141.

Balázs, J. 1956, *Mitt. Sternw. (Konkoly Obs.) Budapest*, Ung. Akad. Wiss. Nr. 39.

Balázs, J., and Detre, L. 1939, *Mitt. Sternw. (Konkoly Obs.) Budapest*, Ung. Akad. Wiss. Nr. 8.

Balázs, J., and Detre, L. 1941, *Astr. Nachr.*, **271**, 231.

Balázs, J., and Detre, L. 1950, *Mitt. Sternw. (Konkoly Obs.) Budapest*, Ung. Akad. Wiss. Nr. 23.

Balázs, J., and Detre, L. 1952, *Mitt. Sternw. (Konkoly Obs.) Budapest*, Ung. Akad. Wiss. Nr. 27.

Balázs, J., and Detre, L. 1954, *Mitt. Sternw. (Konkoly Obs.) Budapest*, Ung. Akad. Wiss. Nr. 33.

Balázs, J., and Detre, L. 1957, *Mitt. Sternw. (Konkoly Obs.) Budapest*, Ung. Akad. Wiss. Nr. 34.

Barlai, K. 1988, to be published in *Comm. Konkoly Obs.*, Budapest.

Batyrev, A.A. 1957, *Peremennye Zvezdy*, **12**, 137.

Blazhko, S. 1907, *Astr. Nachr.*, **175**, 325.

Blazhko, S. 1922, *Astr. Nachr.*, **216**, 103.

Chis, D., Chis, G., and Mihoc, I. 1975, *Inf. Bull. Var. Stars*, No. 960.

Chumak, O.B. 1965, *Peremennye Zvezdy*, **15**, 569.

Clement, C.M., Ip, P., and Robert, N. 1984, *A. J.*, **89**, 1707.

Clement, C.M., Nemec, J.M., Robert, N., Wells, T., Dickens, R.J., and Bingham, E.A. 1986, *A. J.*, **92**, 825.

Cousins, A. 1983, *M.N.R.A.S.*, **203**, 1171.

Coutts Clement, C., Dickens, R.J., and Bingham, E. 1979, *A. J.*, **84**, 217.

Cox, A.N. 1987, in *Proc. IAU Coll.* No. 95 (preprint).

Cox, A.N., Hodson, S.W., and Clancy, S.P. 1981, in *Astrophysical Parameters for Globular Clusters*, Proc. IAU Coll. 68 (eds. A.G. Davis Philip and D.S. Hayes), L. Davis Press, Inc. Schenectady, New York, p. 337.

Cox, A.N., Hodson, S.W., and Clancy, S.P. 1983, *Ap. J.*, **266**, 94.

Detre, L., and Szeidl, B. 1973 in *Variable Stars in Globular Clusters and Related Systems*, IAU Coll. 21, ed. J.D. Fernie, Reidel-Dordrecht, p. 31.

Ficarrotta, F., and Romoli, C. 1979, *Inf. Bull. Var. Stars* No. 1642.

Firmanyuk, B.N. 1974, *Astr. Tsirk.* No. 828.

Fitch, W.S., Wisniewski, W.Z., and Johnson, H.L. 1966 *Comm. Lunar and Planetary Lab.*, No. 71, Vol. 5., Part 2.

Glownia, Z. 1983, *Astr. Nachr.*, **304**, 45.

Goranskij, V.P. 1980a, *Astr. Tsirk.*, No. 1096.

Goranskij, V.P. 1980b, *Astr. Tsirk.*, No. 1111.

Goranskij, V.P. 1981, *Inf. Bull. Var. Stars*, No. 2007.

Goranskij, V.P. 1982, *Astr. Tsirk.*, No. 1216.
Hertzsprung, E. 1922, *Bull. Astr. Inst. Netherlands*, **1**, 139.
Hoffmeister, C. 1951, *Veröff. Sternw. Sonneberg*, **1**, 409.
Hoffmeister, C. 1956, *Veröff. Sternw. Sonneberg*, **3**, 3.
Hoffmeister, C. 1958, *Astr. Nachr.*, **284**, 165.
Jerzykiewicz, M., and Wenzel, W. 1977, *Acta Astr.*, **27**, 35.
Jorgensen, J.E., and Petersen, J.O. 1967, *Zs.* Astrophys., **67**, 377.
Kanishcheva, R.K. 1971, *Peremennye Zvezdy*, **18**, 105.
Kanyó, S. 1966, *Inf. Bull. Var. Stars*, No. 146.
Kanyó, S. 1970, *Inf. Bull. Var. Stars*, No. 490.
Kanyó, S. 1980, *Inf. Bull. Var. Stars*, No. 1832.
Kinman, T.D. 1960, *Roy. Obs. Bull.*, 37E149.
Kinman, T.D., Wong-Swanson, B., Wenz, M., and Harlan, E.A., 1984, *A. J.*, **89**, 1200.
Kovács, G., Shlosman, I., and Buchler, J.R. 1986, *Ap. J.*, **307**, 593.
Kudryashova, L.A. 1978, *Astr. Tsirk.*, No. 1012.17
Lange, G.A. 1962, *Astr. Tsirk.*, No. 227.19
Lange, G.A., and Firmanyuk, B.N. 1975, *Astr. Tsirk.*, No. 864.7
Lysova, L.E., and Firmanyuk, B.N. 1980, *Astr. Tsirk.*, No. 1122.3
Mandel, O.E., 1969, *Peremennye Zvezdy*, **16**, 628.
Mandel, O.E., 1970, *Peremennye Zvezdy*, **17**, 335.
Martin, W.C., 1939, *Ann. Sternw. Leiden*, **17**, Part 2., p. 1.
Martynov, D.Y. 1940, *Engelhard Bull.*, **18**, 3.
Meinunger, L., and Wenzel, W. 1968, *Veröff. Sternw. Sonneberg*, **7**, 387.
Moskalik, P. 1986, *Acta Astr.*, **36**, 333.
Muller, A.B. 1953, *Bull. Astr. Inst. Netherlands*, **12**, 11.
Nemec, J.M. 1984, in *Observational Tests of Stellar Evolution*, Proc. IAU Symp. 105, eds. A. Maeder and A. Renzini, Reidel- Dordrecht, p. 465.
Nemec, J.M. 1985a, *A. J.*, **90**, 204.
Nemec, J.M. 1985b, *A. J.*, **90**, 240.
Nemec, J.M., Hesser, J.E., and Ugarte, P.P. 1985, *Ap. J. Suppl.*, **57**, 287.
Nemec, J.M., Linnell Nemec, A.F., and Norris, J. 1986, *A. J.*, **92**, 358.
Oláh, K., and Szeidl, B. 1978, *Mitt. Sternw. (Konkoly Obs.) Budapest*, Ung. Akad. Wiss., Nr. 71.
Oosterhoff, P.T. 1946, *Bull. Astr. Inst. Netherlands*, **10**, 101.
Paczynski, B. 1965a, *Acta Astr.*, **15**, 103.
Paczynski, B. 1965b, *Acta Astr.*, **15**, 115.
Paczynski, B. 1966, *Acta Astr.*, **16**, 97.
Panov, K. 1980, *Peremennye Zvezdy*, **21**, 391.
Peniche, R., Gomez, T., Parrao, L., and Pena, J.H. 1987, preprint.

Preston, G.W. 1961, *Ap. J.*, **134**, 633.
Romanov, Y. 1967, *Inf. Bull. Var. Stars*, No. 205.
Rozhavski, F.G. 1964, *Peremennye Zvezdy*, **15**, 211.
Sandage, A., Katem, B., and Sandage, M. 1981, *Ap. J. Suppl.*, **46**, 41.
Shapley, H. 1916, *Ap. J.*, **43**, 217.
Shapley, H. 1918, *Publ. Am. Astr. Soc.*, **3**, 16.
Shapley, H. 1921, *M.N.R.A.S.*, **81**, 209.
Smith, H.A. 1981, *Publ. A.S.P.*, **93**, 721.
Stepien, K. 1972, *Acta Astr.*, **22**, 175.
Szeidl, B. 1963, *Inf. Bull. Var. Stars*, No. 36.
Szeidl, B. 1965, *Mitt. Sternw. (Konkoly Obs.) Budapest*, Ung. Akad. Wiss. Nr. 58.
Szeidl, B. 1967, *Inf. Bull. Var. Stars*, No. 220.
Szeidl, B. 1968a, *Inf. Bull. Var. Stars*, No. 278.
Szeidl, B. 1968b, *Inf. Bull. Var. Stars*, No. 291.
Szeidl, B. 1973, *Mitt. Sternw. (Konkoly Obs.) Budapest*, Ung. Akad. Wiss. Nr. 63.
Szeidl, B. 1976, in *Multiply Periodic Variable Stars*, Proc. IAU Coll. 29, ed. W. Fitch, Vol. I., p. 133.
Todoran, I. 1974, *Inf. Bull. Var. Stars*, No. 915.
Tsesevich, V.P. 1943, *Astr. Tsirk.*, No. 17.
Tsesevich, V.P. 1961, *Astron. Zhurnal*, **38**, 293.
Ureche, V. 1965, *Babes-Bolyai Stud. fasc.*, **1**, 73.
Ureche, V. 1971, *Inf. Bull. Var. Stars*, No. 532.
Van Agt, S.L.T.J. 1967, *Bull. Astr. Inst. Netherlands*, **19**, 275.
Van Agt, S.L.T.J, 1968, *Bull. Astr. Inst. Netherlands Suppl.* **2**, 237.
Wachmann, A.A. 1968, *Abhand. Hamburg*, **8**, 105.
Walraven, T. 1949, *Bull. Astr. Inst. Netherlands*, **11**, 17.
Wenzel, W. 1976, in *Multiply Periodic Variable Stars*, Proc. IAU Coll. 29, ed. W. Fitch, Vol. II., p. 221.

DEPENDENCE OF THE PERIOD AND AMPLITUDE FLUCTUATION OF RR LYRAE STARS ON THE BLAZHKO PERIOD

S. Kanyó
Konkoly Observatory, Budapest, Hungary

Abstract

The topic of this note is the dependence of some parameters on the Blazhko period in a selected sample of RR Lyrae stars. It is shown that there is a certain correlation between the size of the period noise and the frequency of RRab stars with Blazhko effect.

The more luminous field RRab stars (brighter than 12 mag) offer the most advantageous sample for considering the distribution and the stability of the Blazhko effect in the Blazhko gap. The Blazhko gap is the period interval in which all secondary periods produced by the Blazhko effect can be found. In this note we select the more luminous field RRab variables because these have been observed for about 50 years and the observed points are evenly distributed along this relatively long period of time.

There are three relationships by means of which we can consider the above mentioned situation:

– $\delta_A = \Delta A / \bar{A}$ relative amplitude variation of the fundamental period, where ΔA is the amplitude variation and $\bar{A}$ is the averaged fundamental amplitude.

– σ_F^2 is the mean square value of the phase fluctuations

$$\sigma_F^2 = \int_{-\infty}^{\infty} f^2 \Psi(f) df \quad ,$$

where $\psi(f)$ is the probability density function of the f phase fluctuation. It was shown by *Balázs-Detre* and *Detre* (1965), that standard deviation σ_F derived from the structure of O–C curves of the variable stars is an important parameter of the period instability of variable stars.

The fundamental period (P_0), the Blazhko period (P_B) and δ_A, σ_F are listed in Table 1 for a selected sample of RRab stars.

The δ_A–P_B relation is shown in Figure 1. The protruding three points issue from RRab stars which have double secondary amplitudes and periods (RW Cnc) or have a variable secondary amplitudes (XZ Cyg). The third point (RV Cap) has a special long secondary period. The dependence of δ_A on the P_B is not remarkable. The phase fluctuations σ_F for stable RR Lyrae and other kinds of variable stars

Table 1

Var.	P_o(d)	P_B(d)	σ_F(%)	δ_A
Z CVn	0.654	22.7	0.25	0.46
SZ Hya	0.537	25.8	0.40	0.50
RW Cnc	0.547	29.9	-	0.92
AR Her	0.470	31.6	0.30	0.40
RR Lyr	0.567	40.8	0.22	0.36
RW Dra	0.443	41.7	0.38	0.40
XZ Cyg	0.466	57.0	0.25	0.29
XZ Dra	0.476	77.0	0.09	0.25
RV UMa	0.468	90.1	0.02	0.33
AR Ser	0.575	108.4	-	0.57
RZ Lyr	0.511	116.7	0.04	0.42
RV Cap	0.448	225.5	0.10	0.76

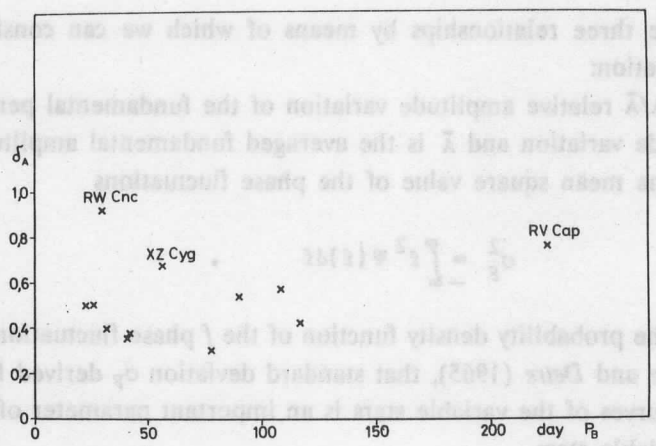

Fig. 1

were calculated by *Balázs-Detre* and *Detre* (1965). It was demonstrated that the average $\bar{\sigma}_F$ for stable RRab is very low, less than 0.1%, whereas $\bar{\sigma}_F$ for those with Blazhko effect exhibits a value which is about five times greater.

The distribution of σ_F of RRab stars with Blazhko effect inside the Blazhko gap was earlier considered by *Kanyó* (1975) and it was demonstrated that there was

some correlation between σ_F and P_B (Fig. 2). There is a trend to get higher values of σ_F for shorter P_B, that is to say the period noise of variable stars of shorter P_B is greater than that of longer one. This result is in accordance with the frequency of brighter RRab with Blazhko effect in the Blazhko gap (Fig. 3). The most populated portion of the Bkashko gap is the shorter period side ($P_B < 70^d$), where σ_F gets a relatively great value.

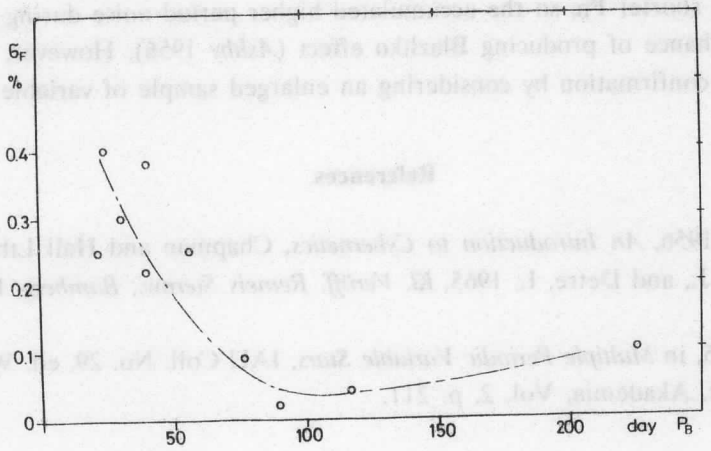

Fig. 2

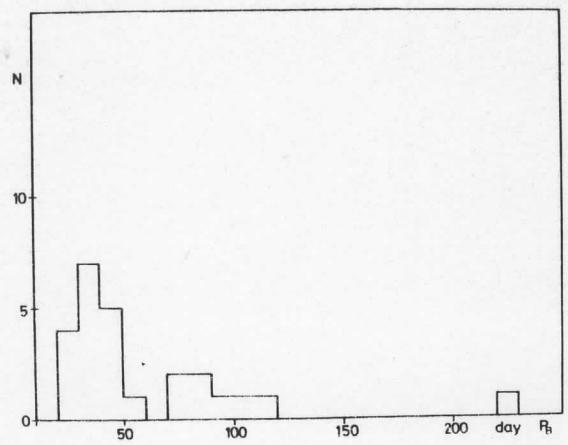

Fig. 3

The main points of this note are as follows.

Let us suppose that σ_F phase fluctuation or period noise of RRab is amplified by the perturbing influence of the Blazhko effect. It is suggested by Figure 2, that the appearance of the Blazhko effect in an RR Lyrae is due to a considerable perturbation that develops typically on the shorter side of P_B of Blazhko gap. If σ_F is smaller, the smaller perturbation yields a smaller chance of forming Blazhko effect. If σ_F becomes smaller, the P_B secondary period becomes longer. A possible explanation may be that because the longer P_B period consists of more pulsation events than does the shorter P_B, so the accumulated higher period noise during the longer P_B stands a chance of producing Blazhko effect (*Ashby* 1956). However, this suspicion requires confirmation by considering an enlarged sample of variable stars.

References

Ashby, R.W. 1956, *An Introduction to Cybernetics*, Chapman and Hall Ltb, London.

Balázs-Detre, J., and Detre, L. 1965, *Kl. Veröff. Remeis Sternw., Bamberg*, **IV**, No. 40, p. 184.

Kanyó, S. 1975, in *Multiple Periodic Variable Stars*, IAU Coll. No. 29, ed. W. S. Fitch, Budapest, Akadémia, Vol. 2, p. 211.

THE AMPLITUDE EQUATION FORMALISM APPLIED TO STELLAR PULSATIONS

J. R. Buchler
Physics Department, University of Florida, Gainesville, Florida, USA

Abstract

The assumptions underlying the amplitude equation formalism are discussed. The successes of the formalism in describing the nonlinear behavior of the classical Cepheids (Bump Cepheids, RR Lyrae) are reviewed. Further challenges which consist in describing the behavior of the more dissipative stars such as the Semi-Regulars and the Irregulars are briefly discussed.

1. Introduction

Amplitude equations have been used for quite a while in diverse areas of physics, such as plasma physics, nonlinear optics, fluid dynamics. In applied mathematics they are known as normal form equations (*Guckenheimer* and *Holmes* 1983). In astrophysics they have also been used for a number of years (*e.g., Dziembowski* 1982, *Takeuti* and *Aikawa* 1981, *Regev* and *Buchler* 1981). There exist a variety of ways to derive amplitude equations. Their form, which depends on the nature of the physical problem, is often trivial to write down. The difficulty generally lies in relating the coefficients which appear in the amplitude equations to the original physical system and in computing them ab initio, a process which often involves overwhelming algebra. However, useful astrophysical results have been derived from the mere knowledge of the form of the appropriate amplitude equations. A general derivation of the amplitude equations and their coefficients from the original partial differential system (of hydrodynamics and heat transfer) in the context of radial stellar pulsations has been given by *Buchler* and *Goupil* (1984) and can readily be generalized to the nonradial case as well. An alternate, very elegant derivation can be found in *Coullet* and *Spiegel* (1984) although their amplitude equations have some subtle differences with ours.

2. The dimensional reduction technique and amplitude equations

In the following I shall discuss the general conditions of validity of the dimensional reduction techniques which lead to amplitude equations. I will do that in the

context of radial stellar pulsations. The hydrodynamical equations in Lagrangean form are given by

$$d^2R/dt^2 = -4\pi R^2 \, \partial p/\partial m - Gm/R^2 \quad , \tag{1}$$

$$T \, ds/dt = - \partial L/\partial m \quad , \tag{2}$$

$$\partial R^3/\partial m = (4\pi\rho)^{-1} \quad , \tag{3}$$

$$L = (4\pi R^2)^2 \, (ac/3\kappa) \, (\partial T^4/\partial m) \quad , \tag{4}$$

$$p = p(\rho, s) \quad , \tag{5}$$

$$\kappa = \kappa(\rho, s) \quad , \tag{6}$$

where $R(m)$ denotes the distance from the stellar center of that spherical shell, which contains an amount of mass m and $s(m)$ is the specific entropy at m. In our realistic models the equation of state $p(\rho,s)$ and the opacity $\kappa(\rho,s)$ are complicated functions as they take into account the ionization of hydrogen and the two ionic states of helium; they have to be evaluated through a numerical solution of the Saha equation. In the models of interest to us convection does not play a dominant role and diffusive heat transport has been assumed in equation 4.

A model is said to be in full equilibrium when all time-derivatives in equations 1 and 2 vanish. If we introduce the velocity

$$dR/dt = v \quad , \tag{7}$$

then the partial differential system can be cast into a first order system. If we also introduce deviations from equilibrium for the radius, $\delta R(m)$, for the velocity, $\delta v(m)$, and for the entropy, $\delta s(m)$, and define a deviation vector in their product space, *i.e.* $|z(m)> \; = (\delta R, \, \delta v, \, \delta s)$, we can cast the original system into a very compact form

$$d/dt \; |z> = \mathbf{A} \; |z> + \mathbf{N}_2 \; |zz> + \mathbf{N}_3 \; |zzz> + \ldots \quad . \tag{8}$$

In equation (8) we have expanded around equilibrium. The spatial operators, $\mathbf{A}$, $\mathbf{N}_2$, $\mathbf{N}_3$, *etc.*, denote the linear, quadratic, cubic, *etc.*, contributions. In practice one discretizes the star into N mass-shells so that the quantity $|z>$ becomes a $3N$-dimensional vector. The operator $\mathbf{A}$ becomes a non-selfadjoint $3N$ by $3N$ matrix.

Implicit in equation (8) is the *first assumption* which one is the weak nonlinearity.

In order to proceed we need to examine the spectrum of the linear eigenvalue problem associated with system (8). Introducing a time-dependence of the form $exp(\sigma t)$ we obtain

$$\mathbf{A}\,|\alpha> \;=\; \sigma_\alpha\,|\alpha> \quad , \tag{9a}$$

$$<\alpha|\mathbf{A} \;=\; \sigma_\alpha\,<\alpha| \quad , \tag{9b}$$

(we note in parentheses that because of the non-selfadjointness of **A** the lefthand eigenvectors $<\alpha|$ are not just hermitean conjugates of the righthand $|\alpha>$, and one needs to use a dual basis of eigenvectors). Because **A** is real the eigenvalues are either purely real (secular and thermal modes) or they come in complex conjugate pairs (vibrational modes).

The *second assumption* is that we can split the modes into two groups; the first group contains the very stable modes, sometimes called *slave*-modes, for which $\kappa = Re(\sigma)$ is very negative whereas the second group contains those modes for which $|\kappa|$ is small. We shall call the latter marginally stable and unstable modes the *principal* modes. The situation is schematically depicted in Figure 1.

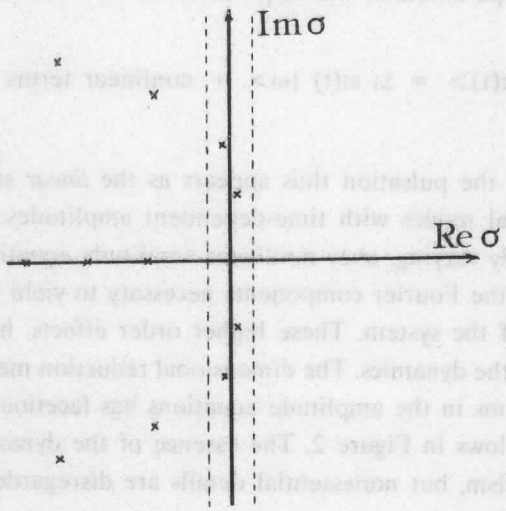

Fig. 1. Schematic representation of the spectrum in the complex plane. The modes within the strip delineated by dashed lines are the principal modes, whereas the others are the slave modes.

When both assumptions are satisfied one can play off the weak nonlinearities against the weak dissipation and obtain some balance at a small but finite saturation amplitude. This is the gist of asymptotic perturbation methods and of the re-

sulting amplitude equation formalism. The same two assumptions underlie the formalism of Coullet and Spiegel.

Other small parameters may exist in the problem, such as the nearness to a resonance (detuning parameter) and need to be taken into account in the derivation of amplitude equations. (The disregard of a resonance would lead to divergent coefficients in the amplitude equations.)

We shall not discuss here the dimensional reduction method, but simply quote the results. The amplitude equations are of the general form

$$\begin{aligned} da_0/dt &= \sigma_0\, a_0 + \textit{essential}\ \text{nonlinearities}\ (\{a_i\}) \quad , \\ da_1/dt &= \sigma_1\, a_1 + \textit{essential}\ \text{nonlinearities}\ (\{a_i\}) \quad , \\ &\cdots\cdots \\ &\cdots\cdots \\ da_i/dt &= \sigma_i\, a_i + \textit{essential}\ \text{nonlinearities}\ (\{a_i\}) \quad , \end{aligned} \tag{10}$$

where the order of the system depends on the number of small parameters, the so-called *co-dimension*. The form of the essential nonlinear terms is determined by the nature of the small parameters. Our approximation to the solution is given by

$$|z(t)> \;=\; \Sigma_i\, a_i(t)\ |\alpha_i> \;+\; \text{nonlinear terms} \quad . \tag{11}$$

In *lowest order* the pulsation thus appears as the *linear* superposition of pulsations in the principal modes with time-dependent amplitudes. The latter, which by assumption are slowly varying, obey nonlinear amplitude equations. The higher order terms contribute to the Fourier components necessary to yield the actual, more complicated, behavior of the system. These higher order effects, however, do not determine the essence of the dynamics. The dimensional reduction method and the omission of "nonessential" terms in the amplitude equations has facetiously been illustrated by *Coullet* (1981) as follows in Figure 2. The essence of the dynamic is captured in low order by the formalism, but nonessential details are disregarded.

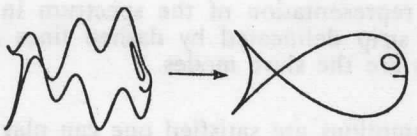

Fig. 2. The dimensional reduction method.

The dimensional reduction method is more than a mere truncation of a modal expansion (such as the famous Lorenz system). It takes into account the deformation of the dynamic due to the presence of the slave modes. This is schematically illustrated in Figure 3. The horizontal and vertical axes represent the spaces R_p and R_s, spanned by the eigenvectors of the principal modes and of the stable modes, respectively. After very short-lived transients the system moves on the principal manifold M which is tangent to the space spanned by the principal modes for small amplitudes.

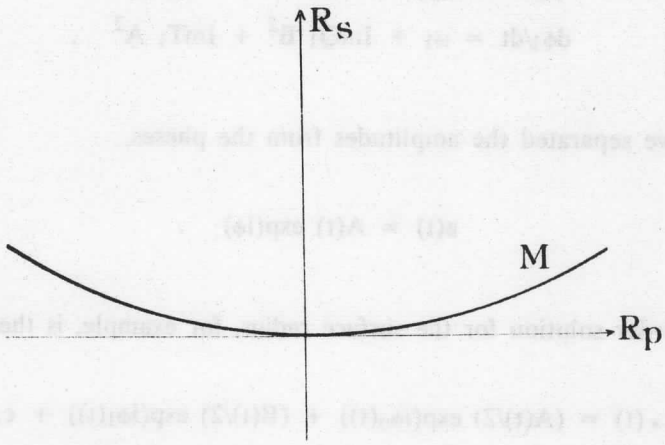

Fig. 3. Schematic representation of the spaces of the principal modes R_p and the slave modes R_s and of the manifold of the dynamic M.

One of the nice features of the amplitude equation formalism is that its basic quantities, namely the amplitudes and their phases, can be directly related to those obtained from a Fourier analysis of observations or of numerical hydrodynamics. One of its limitations is that it is limited to the description of those situations in which the amplitude modulations are slow compared to the basic pulsation.

In the following I shall review some of the successes of the amplitude equation formalism in the study of nonlinear radial stellar pulsations. The application to the nonradial case is discussed by *Dziembowski* (1988).

2.1 RR Lyrae

The majority of the RR Lyrae stars pulsate either in the fundamental mode (RRa and RRb), in the first overtone (RRc) or in both of these modes simultaneously (the so-called double-mode RR Lyrae, RRd). Some also exhibit the Blazhko effect

(*Szeidl* 1988). Since there seem to be no low-order resonances inside the range of interest of RR Lyrae, *Buchler* and *Kovács* (1986b) used the nonresonant amplitude equations for just two modes to see if the general "modal" selection could be understood in the framework of amplitude equations. They truncated the amplitude equations at the lowest (cubic) nonlinearities. The corresponding amplitude equations are given by

$$dA/dt = \kappa_0 A + ReQ_0 A^3 + ReT_0 AB^2 \quad , \tag{12a}$$

$$dB/dt = \kappa_1 B + ReQ_1 B^3 + ReT_1 BA^2 \quad , \tag{12b}$$

$$d\phi_0/dt = \omega_0 + ImQ_0 A^2 + ImT_0 B^2 \quad , \tag{12c}$$

$$d\phi_1/dt = \omega_1 + ImQ_1 B^2 + ImT_1 A^2 \quad , \tag{12d}$$

where we have separated the amplitudes from the phases,

$$a(t) = A(t) \exp(i\phi) \quad . \tag{13}$$

The lowest order solution for the surface radius, for example, is then

$$\delta R_*(t) = (A(t)/2) \exp(i\phi_0(t)) + (B(t)/2) \exp(i\phi_1(t)) + c.c. \quad , \tag{14}$$

where the phases ϕ contain a rapidly oscillating part ωt and a slowly varying one (eqs. 12c, d).

The result of the study of *Buchler* and *Kovács* (1986b) is that with the assumption of the negativity of the cubic terms the observed modal behavior could easily be understood in terms of the fixed points of the amplitude equations. They have also shown that a discriminant determines whether either double-mode behavior or fundamental and first overtone pulsations occur. Further recent studies of these amplitude equations can be found in *Dziembowski* and *Kovács* (1984) and *Verheest* (1987). Although these studies were very encouraging they remained qualitative.

In order to assess the quantitative usefulness of amplitude equations in the context of the nonlinear pulsations of RR Lyrae, *Buchler* and *Kovács* (1987a) have performed a comparison of numerical hydrodynamic computations with the amplitude equations. A stellar model in full equilibrium is perturbed and its subsequent hydrodynamical evolution is followed numerically for some time. Taking a purely phenomenological approach Buchler and Kovács then fit the coefficients of the amplitude equations (12) to match the hydrodynamical behavior. Amplitudes and phases are extracted from the latter through a time-dependent Fourier analysis.

The results of that study are as follows: (1) the fit is almost indistinguishable from the hydrodynamics. (2) The location and stability properties of the final attractor, predicted from the fitted coefficients agree remarkably well with those obtained from a direct computation of the stable nonlinear pulsations. This is illustrated in the following figures for an RR Lyrae model of 0.65 solar masses, a luminosity of 60 solar luminosities and an effective temperature of 7000K.

Figures 4a and 4b show the temporal behavior of the amplitudes A and B of the fundamental and the first overtone, respectively, for two different initializations with 2% and with 10% overtone perturbation. The first evolution leads toward a pulsation in the fundamental mode and the second evolution toward an overtone pulsation.

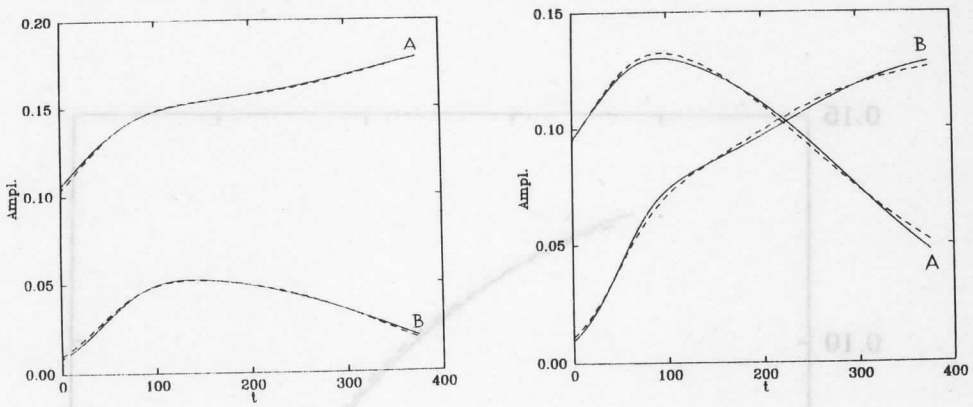

Fig. 4. Temporal behavior of amplitudes of the fundamental mode *(A)* and of the first overtone *(B)* for two different initializations. The dashed lines are derived from the hydrodynamical computations and the solid line represents the fit with the amplitude equations.

In Figures 5a and 5b we show the corresponding behavior of the phases ϕa and ϕb of the two modes. Finally in Figure 6 we show the same two evolutions in an amplitude-amplitude plot. It can clearly be seen that one evolution is towards the fundamental attractor (on the horizontal axis) and the other is towards the overtone attractor (vertical axis).

The conclusion is thus reached that nonresonant amplitude equations for just two modes, the fundamental and the first overtone, truncated at the lowest order (cubic) nonlinearities give a remarkably good description of the nonlinear pulsations of RR Lyrae models.

One of the highlights of the amplitude equation formalism is that it yields new insight into the pulsation mechanism on a more fundamental level (topology of phase-space, bifurcations of attractors, *etc.*).

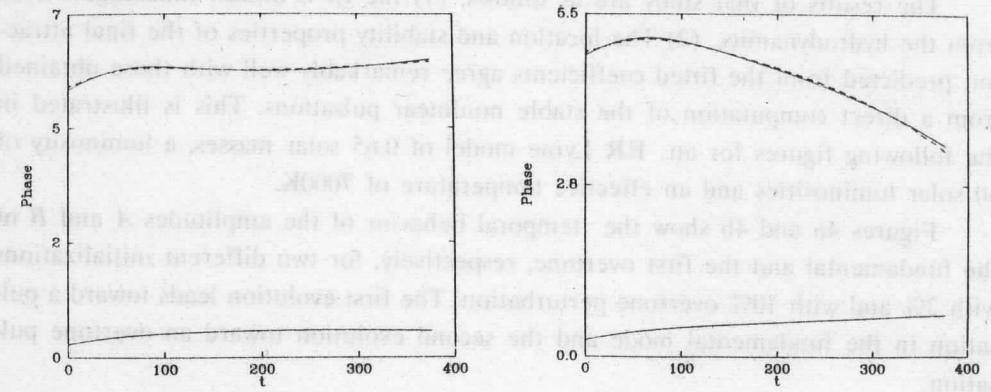

Fig. 5. Temporal behavior of the phases for the same models as in Figure 4.

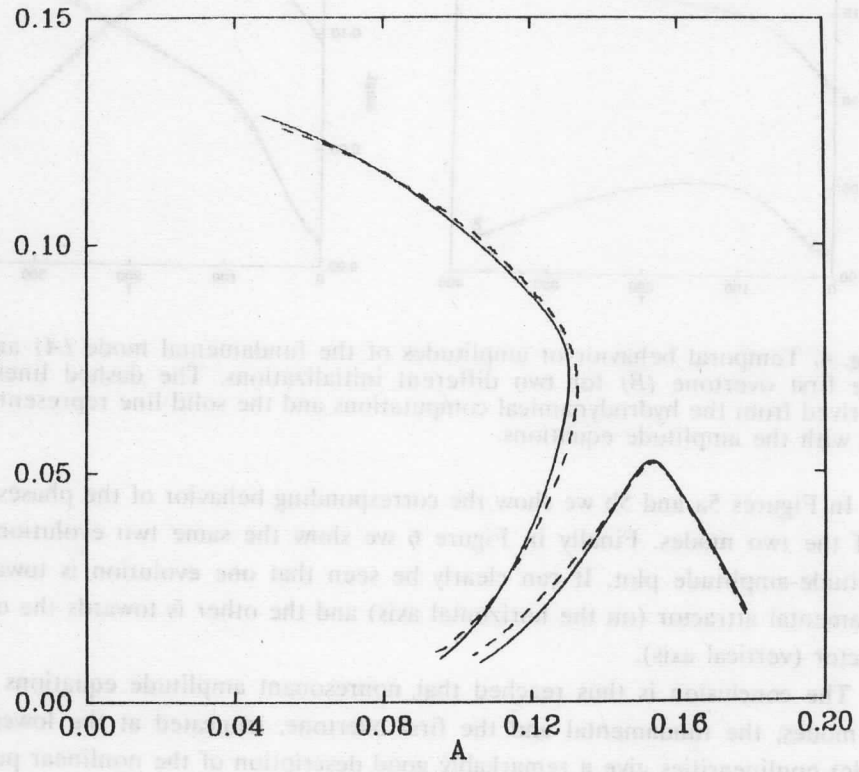

Fig. 6. Amplitude-amplitude plot for the two initializations of Figures 4 and 5. One evolution is towards the fundamental pulsation (fixed point on the horizontal axis) and the other towards the first overtone pulsation (fixed point on the vertical axis).

I would also like to mention in passing that the amplitude equation formalism has guided *Kovács* and *Buchler* (1988) in their search for and discovery of numerical hydrodynamical RR Lyrae models which pulsate simultaneously in the fundamental and in the first overtone modes with constant amplitudes and phases.

A so far unsolved problem in RR Lyrae concerns the explanation of the Blazhko effect which consists of a slow periodic modulation of the amplitude of the fundamental pulsations in some RRa and RRb stars (*Szeidl* 1988). Their possible explanation in terms of a 2:1 resonance of the fundamental with a higher overtone (*Buchler* and *Kovács* 1986a, *Moskalik* 1987) awaits confirmation with numerical hydrodynamical modelling.

2.2 Bump Cepheids

It has been known for quite a while (*Ludendorff* 1919) that Cepheids have secondary bumps on their lightcurves in the vicinity of a 10d period, and that the location of these bumps moves with the period forming the so-called Hertzsprung progression. *Payne-Gaposhkin* (1947) already noticed that the Fourier phases show abrupt features near 10d. *Christy* (1966) was able to reproduce this bump behavior with numerical hydrodynamical models and, for their explanation, he invoked some echo mechanism which however is fraught with difficulties. Progress was made when Simon and Schmidt (1976) noticed that the linear models go through a resonance of the type $2\omega_0 \approx \omega_2$ in the vicinity of a 10d period. Later *Simon* and *Lee* (1981) and *Simon* and *Teays* (1982, 1983) plotted the phase difference $\phi_{21} = \phi_2 - 2\phi_1$ versus the period and found an almost universal curve, both for the light curves and for the radial velocities of Cepheids.

It was then suggested by *Klapp*, *Goupil* and *Buchler* (1985; see also *Buchler* and *Kovács* 1986a) that the striking behavior of the phases could be explained with the help of amplitude equations appropriate for the case of a 2:1 resonance

$$da/dt = \sigma_0 a + P_0 a^* b \quad , \tag{15a}$$

$$db/dt = \sigma_1 b + P_1 a^2 \quad . \tag{15b}$$

Klapp et al. (1985) performed an ab initio computation of the quadratic coefficients P_0 and P_1 from the hydrodynamical equations for a series of Cepheid stellar models and computed the fixed points of the amplitude equations which correspond to the nonlinear pulsation with constant amplitudes. The models were chosen to be as close as possible to Cepheid models whose hydrodynamical behavior had been studied and Fourier analyzed by *Simon* and *Davis* (1983). (We note in passing that

the amplitudes and phases of the amplitude equations are in direct correspondence with those of a Fourier fit to the observational data or to hydrodynamical output.) The overall agreement was excellent, but two major discrepancies showed up: first, the amplitude equations do not have any fixed points beyond approximately 10d and, second, towards low periods the amplitudes and phases deviate from the numerical ones.

The remedy for both of these problems was shown to be the inclusion of cubic terms in the amplitude equations (*Buchler* and *Kovács* 1986a). Since an ab initio computation of cubic terms is very tedious and has not yet been attempted they performed a parameter study with cubic terms and showed that for reasonable values one can get good qualitative agreement with the observation and with the numerical models.

It is interesting to note that the mere existence of bump Cepheids and the shape of the ϕ_{21} curve put some contraints on the coefficients of the amplitude equations, and thus on the models themselves, namely $\kappa_0+\kappa_2<0$, $2\kappa_0+\kappa_2<0$, and $q=tan(arg(P_0/P_1))<0$.

The amplitude equations give a nice ϕ_{21} versus period relation if one keeps their coefficients constant and one varies only the detuning parameter. Real Cepheid stars come with a variety of structures and even the P_2/P_0 versus period relation necessarily has some spread. It is therefore remarkable that Cepheids show such a clean characteristic behavior of ϕ_{21} which must be an indication that they form a rather homogeneous group.

The amplitude equation formalism gives the following physical picture of the occurrence of the bump progression: For low periods the saturation of the amplitude occurs through the cubic nonlinear terms, *i.e.* it is provided by the nonlinear effects of the fundamental mode itself and all the slave modes. As the 10d period is approached the resonance singles out the second overtone among the other slave modes and this mode starts to become a principal mode itself. The quadratic terms provide the energy transfer to the linearly stable second overtone mode. While this happens the saturation amplitude of the fundamental mode gets depressed. Near 10d a bifurcation occurs in which the stable fixed point of the amplitude equations merges with an unstable fixed point and disappears. Beyond the bifurcation point the saturation is provided by the cubic terms. At first the resonance still has an effect on the fixed point, but as one moves to higher periods its influence diminishes and the saturation is again provided by the cubic terms as on the other far side of the resonance.

The systematic behavior of the Cepheids can be understood from the *fixed points* of the amplitude equations. However, for other parameter values different solutions can exist. One type of solution, which arises from a Hopf bifurcation of the fixed

point, gives rise to periodically modulated amplitudes and phases. Another type of solution is chaos which gives rise to erratic modulations of the amplitudes and phases. These solutions may well be the explanation of the Blazhko effect mentioned in the previous section.

3. Other possible applications

3.1 Coupling with secular modes

The dimensional reduction method shows that, in principle, it is necessary to include *all* the marginally stable or unstable modes in the principal manifold, including the secular modes which have small decay-rates. The reason we seem to be able to get away without them in the previous description of RR Lyrae and Cepheids may be one of degree. If the coupling between the vibrational and the secular modes is weak, as one may expect because of a poor overlap between the corresponding eigenvectors, then the effect of these modes cannot be very large. However, there may be cases where these secular modes play a nonnegligible role and give rise to a small regular or irregular modulation of the amplitudes and phases.

The opposite amplitude equations for the coupling of a vibrational mode with a couple of secular modes are given (*Buchler* 1985)

$$dA/dt = \kappa_0 A + Q_0 A^3 + P_1\, b_1 A + P_2\, b_2 A \quad , \tag{16a}$$

$$db_1/dt = \sigma_1 b_1 + R_1 A^2 + S_1 b_1^2 + T_1 b_2^2 + U_1 b_1 b_2 \quad , \tag{16b}$$

$$db_2/dt = \sigma_2 b_2 + R_2 A^2 + S_2 b_2^2 + T_2 b_1^2 + U_2 b_1 b_2 \quad . \tag{16c}$$

The observed signal, say for the surface radius is then given by

$$\delta R_*(t) \sim A(t)\cos(\omega t) + b_1(t) + b_2(t) \quad . \tag{17}$$

As expected the secular modes add a slowly varying constant component to the oscillatory signal. Whether this coupling is important and leads to observable consequences awaits numerical modelling. This is a considerably more involved project than the usual pulsational calculations. The reason is that only the envelope is involved in the pulsations whereas the secular models extend into the core and the burning shells.

3.2 Semi-regular and irregular variability

Models of red giant envelopes which have been studied in the context of planetary nebula formation (*Keeley* 1970, *Tuchman, Sack* and *Barkat* 1979, *Fox* and *Wood* 1982) have shown that because of the extended regions of partial ionization these models can be near a dynamical instability, *i.e.* the fundamental frequency of oscillation can be very small. At the same time numerical hydrodynamical computations show a very erratic temporal behavior. This can be understood in terms of amplitude equations. Let us assume for simplicity that only two vibrational modes are involved, namely the fundamental and an overtone. Because of the nearness of the dynamical instability one now has an additional small parameter, namely ω_0, in addition to the two growthrates. The smallness of ω_0 causes the two corresponding eigenvectors to become linearly dependent and the nonresonant amplitude equations (12) have to be modified to read (*Buchler* and *Goupil* 1988)

$$dx/dt = y \quad , \tag{18a}$$

$$dy/dt = -2\kappa_0 y - (\omega_0^2 + \kappa_0^2)\, x + k_1 x + k_2 |b|^2 + k_3 xy \quad , \tag{18b}$$

$$db/dt = (i\omega_1 + \kappa_1)\, b + k_5 xb \quad , \tag{18c}$$

where the real variables x and y correspond to the fundamental mode and b denotes the complex amplitude of the overtone.

The surface radius, for example, then behaves like

$$\delta R_*(t) \sim x(t) + |b(t)| \cos(\omega_1 t) + \text{higher order terms} \quad . \tag{19}$$

The system of equations (18) again has fixed points, limit cycles and chaotic solutions. A typical chaotic solution is shown in Figures 7a and 7b.

Of interest is the fact that during part of the irregular cycling the amplitude $B = |b|$ of the pulsation vanishes. In other words the pulsations continuously grow and then completely decay away. In Figure 8 we have plotted a sample of the temporal behavior one may expect of the surface radius.

It is clear that to get this kind of intermittency, which seems to occur in the Irregular stars, one needs the strong coupling between either a vibrational mode and one or several real modes or between two or more vibrational modes one of which has a very small frequency.

The red giant envelopes of interest here are generally very nonadiabatic and the growthrates are not small. This violates one of the assumptions of our amplitude equation formalism. However the formalism is of an asymptotic nature and its

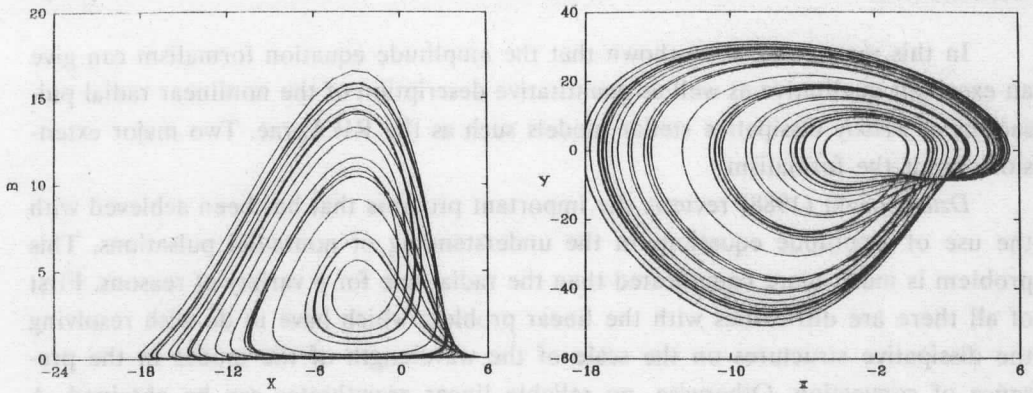

Fig. 7. Typical solution of equations (18) in the chaotic domain of parameters, (a) for $B = |b|$ versus x and (b) for y versus x.

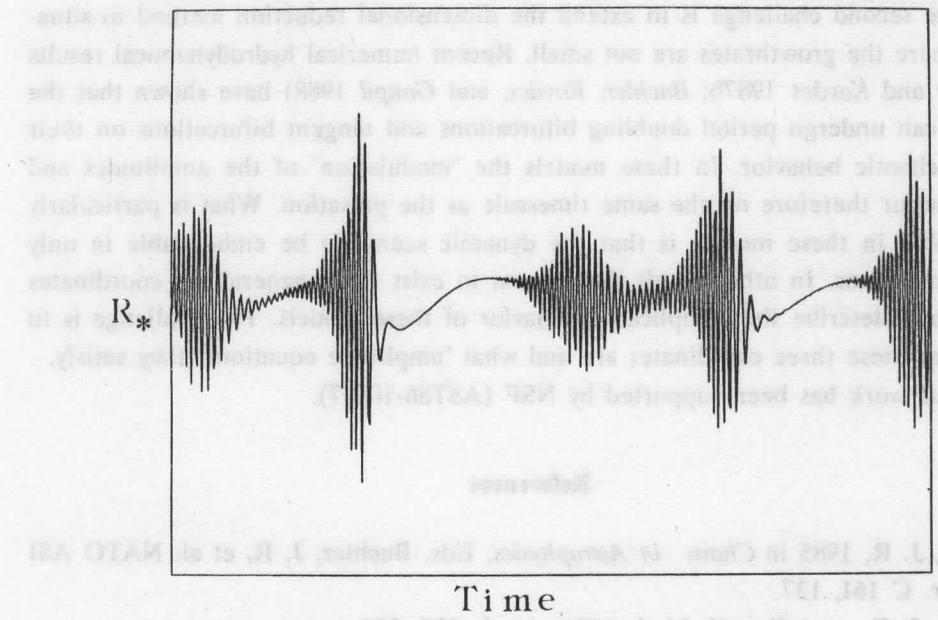

Fig. 8. Sample of the reconstructed signal, *e.g.* a surface radius variation.

range of validity is therefore expected to be large, at least in a qualitative sense. It is therefore not clear a priori to what extent amplitude equations can describe the behavior of these models. Numerical hydrodynamical work is in progress to test the predictions of the amplitude equations.

4. Conclusions

In this review we have shown that the amplitude equation formalism can give an excellent qualitative as well as quantitative description of the nonlinear radial pulsations of *weakly* dissipative stellar models such as the RR Lyrae. Two major extensions await the formalism.

Dziembowski (1988) reviews the important progress that has been achieved with the use of amplitude equations in the understanding of nonradial pulsations. This problem is much more complicated than the radial one for a variety of reasons. First of all there are difficulties with the linear problem which have to do with resolving the dissipative structures on the scale of the wavelength of the modes in the presence of convection. Otherwise, no reliable linear growthrates can be obtained. A second poblem has to do with the large dimension of the principal manifold because of the large number of modes which seem to be excited. And, finally, one can have spatial as well as temporal chaos with the chaotic formation, propagation and dissolution of nonlinear structures.

The second challenge is to extend the dimensional reduction method to situations where the growthrates are not small. Recent numerical hydrodynamical results (*Buchler* and *Kovács* 1987b; *Buchler, Kovács,* and *Goupil* 1988) have shown that the models can undergo period doubling bifurcations and tangent bifurcations on their way to chaotic behavior. In these models the "modulation" of the amplitudes and phases occur therefore on the same timescale as the pulsation. What is particularly remarkable in these models is that the dynamic seems to be embeddable in only *three* dimensions. In other words there seem to exist three generalized coordinates which fully describe the complicated behavior of these models. The challenge is to find what these three coordinates are and what "amplitude equations" they satisfy.

This work has been supported by NSF (AST86-10097).

References

Buchler, J. R. 1985 in *Chaos in Astrophysics*, Eds. Buchler, J. R. et al. NATO ASI Ser. C **161**, 137.

Buchler, J. R., and Goupil, M. J. 1984, *Ap. J.*, **279**, 394.

Buchler, J. R., and Goupil, M. J. 1988, *Astr. Ap.*, in press.

Buchler, J. R., and Kovács, G. 1986a, *Ap. J.*, **303**, 749.

Buchler, J. R., and Kovács, G. 1986b, *Ap. J.*, **308**, 661.

Buchler, J. R., and Kovács, G. 1987a, *Ap. J.*, **318**, 232.

Buchler, J. R., and Kovács, G. 1987b, *Ap. J., (Letters)*, **320**, L57.

Buchler, J. R., Kovács, G., and Goupil, M. J., 1988, these proceedings.

Christy, R. F. 1966, *Ap. J.*, **144**, 108.

Coullet, t, P. 1981, *Summer Study Program at Woods Hole Oceanographic Institute, Tech. Rep.* WHOI-81-102.

Coullet, P., and Spiegel, E. A. 1984, *SIAM J. Appl. Math.*, **43**, 776.

Dziembowski, W. 1982, *Acta Astron.*, **32**, 147.

Dziembowski, W. 1988, these proceedings.

Dziembowski, W. and Kovács, G. 1984, M. N. R. A. S., **206**, 497.

Fox, M. W., and Wood, P. R. 1982, *Ap. J.*, **259**, 198.

Guckenheimer, J., and Holmes, P. 1983, *Nonlinear Oscillations, Dynamical Systems and Bifurcation Theory*, New York, Springer.

Keeley, D. A. 1970, *Ap. J.*, **161**, 643.

Klapp, J., Goupil, M. J., and Buchler, J. R. 1985, *Ap. J.*, **296**, 514.

Kovács, G., and Buchler, J. R. 1988, *Ap. J.*, **324**, 1026.

Ludendorff, H. 1919, *Astron. Nach.*, **209**, 217.

Moskalik, P. 1986, *Acta Astr.*, **36**, 333.

Payne-Gaposhkin, C. 1947, *A. J.*, **52**, 218.

Regev, O., and Buchler, J. R. 1981, *Ap. J.*, **250**, 769.

Simon, N. R., and Davis, C. G. 1983, *Ap. J.*, **266**, 787.

Simon, N. R., and Lee, A. S. 1981, *Ap. J.*, **248**, 291.

Simon, N. R., and Schmidt, E. G. 1976, *Ap. J.*, **205**, 162.

Simon, N. R., and Teays, T. 1982, *Ap. J.*, **261**, 586.

Simon, N. R., and Teays, T. 1983, *Ap. J.*, **265**, 996.

Szeidl, B. 1988, these proceedings.

Takeuti, M., and Aikawa, T. 1981, *Sci. Rept. Tohoku Univ., 8th ser.* **4**, 129.

Tuchmann, Y., Sack, N., and Barkat, Z. 1979, *Ap. J.*, **234**, 217.

Verheest, F. 1987, preprint: "Discussion of Nonlinear Interaction Models for Stellar Pulsations", Rijksuniversiteit Gent, Belgium.

THE HISTORY AND DEVELOPMENT OF NONLINEAR STELLAR PULSATION CODES*

C. G. Davis
Physics Division, Los Alamos National Laboratory, Los Alamos, USA

Abstract

This review is limited to the history and development of nonlinear stellar pulsation codes and methods. Starting with the digital computer and the method of pseudo-viscosity, that made it feasible to solve the equations of hydrodynamics coupled with heat flow, till the present time with our super computers and new techniques of hydrodynamics the discussion proceeds. The narrative includes examples of practical interest in the application of these numerical methods to problems in stellar pulsation such as Cepheid mass discrepancy, the delineation of the RR Lyrae instability strip, and the question of the development of double-mode pulsation as observed in Cepheids, RR Lyrae and other variable stars.

1. Introduction

The history of nonlinear pulsation codes really begins with the development of the computer. Previous to this time, Baker and others had established one-zone models of pulsation but it wasn't until the 50s when the digital computers became available that a solution to a set of nonlinear difference equations of coupled hydrodynamics and radiation flow were possible. Previous to this time Eddington, Zhevakin, Cox and Whitney, and others had determined that the de-stabilization in stars, that caused the observed pulsations, was due to the ionization of hydrogen and helium in the atmospheres of such variables as Cepheids, RR Lyrae and W Virginis. The finite difference equations of nonlinear hydrodynamics were first used on the CPC, the Eniac and the Maniac at Los Alamos. This work was the genesis of the early pulsation codes of Christy and Cox, et al. The first nonlinear pulsation calculations were probably done on the IBM 704. We will discuss these early developments as well as the more recent improvements in hydro and radiative transfer that have made important contributions to our understanding of the properties of stellar pulsation.

In Section 2, we discuss the pioneering work of Christy and Cox as they battled with machine language coding and the IBM 704 computers. In Section 3, we discuss

* Work performed under the auspices of the U.S. Department of Energy

the improvements to solve the equations of multigroup transfer coupled with hydrodynamics and the development of a relaxation scheme to study limiting amplitude and improvements in the hydrodynamics (non-Lagrangian). In Section 4, we discuss the present status of nonlinear stellar pulsation and its application to details of light curves, "resonance" and the vexing problem of double-mode pulsation. Finally in Section 5, we detail some possible improvements to present codes and the need for time dependent convection and the possibility of two-dimensional models.

References will be limited to the Los Alamos, Goddard Conferences (*LG*), to the original publication of the various codes and a review article by *J. Cox* (1974).

2. Early Developments

With the advent of the computer and the establishment of methods to solve the equations of hydrodynamics (pseudo viscosity) the first nonlinear pulsation calculations were made. Some of the pioneers were *Christy* (1964) at Cal Tech and *Cox*, *Brownlee*, and *Eilers* (1969) at Los Alamos. Their codes were based on the early work of Richtmyer and Von Neumann and the development of the method of pseudo viscosity, which made it possible to automatically treat the growth of compression waves into shocks in the nonlinear equations while maintaining stability. Christy studied questions of mode transition, limiting amplitude and the Hertzsprung sequence for mass determination. Developing a series of RR Lyrae models he determined the transition from the first overtone at the blue edge of the instability strip through an either/or condition to the fundamental pulsators at the red edge of a strip. The idea of a transition line from the 1st overtone to fundamental in period was confirmed by some more recent calculations of Stellingwerf. These lines are sensitive to pseudo viscosity as well as the addition of radiation pressure in the equations. Christy at first did not include the radiation pressure in his equations, which shifted his transition line somewhat (*LG-1*). Another of Christy's studies addressed the question of the "bump" sequence as observed in Cepheid variables (Hertzsprung). Using a series of Cepheid models he determined that the phase of the observed "bumps" depended on luminosity in the Hertzsprung-Russell diagram in the following way,

$$\pi_{tr} = 0.057\ L^{0.6}\ \text{(days)},$$

where L is the luminosity in solar units.

Following Christy's work *Stobie* (1969) completed a detailed study where he considered the effects of zoning, pseudo-viscosity and the weighting of the opacities on the bump phase, his results are generally in support of Christy. A more recent report by *Fadeyev* and *Tutukov* (1981) supports these earlier results, which means that the question of the Cepheid "bump" masses still remains.

The Cox's approached the problem of nonlinear pulsation from the idea of understanding the mechanisms of pulsation rather than to study the modes of pulsation in stars. In the Cox's study, they included only a shallow envelope (10% of the mass) in their models and limited the excitation to only the Helium region. The results of a study by Cox, et al. on the instability strip for Cepheids is discussed in *LG-2.* The strip is expected to be wider than observed since they did not include the effects of convection on pulsation, which limits the red edge of the strip. In their detailed work on the mechanisms for pulsation, they studied the growth of pulsation from noise for a Cepheid model called BK7, from Baker and Kippenhahn's earlier work. They initiated the model without any driving, except noise, and it started as a first overtone pulsator. At some later stage, it switched over to the fundamental mode of pulsation at which it stayed in until limiting amplitude. The switch-over may have occurred due to a surge on the computer, at a time sooner than they might have expected, around 350 periods in the fundamental. The maximum kinetic energy in the first harmonic was 3.0×10^{36} ergs as compared to 1.1×10^{43} ergs for the fundamental.

Other developments in nonlinear pulsation codes were pursued in these early days by *Aleshin* (1964) and *Hillendahl* (1969). Aleshin apparently used a sinusoidal inner boundary condition that artificially pumped his models while Hillendahl studied the question of the shocks in the atmosphere of Cepheids but only to a limited extent.

3. Further Developments in Stellar Pulsation Codes

As a continuation of the work of Christy and Cox the author of this review and J. Castor at Cal Tech began working on improved radiative transfer techniques for use in the stellar pulsation codes. Castor's approach was to use the integral method of Schwartzschild while Davis applied the variable Eddington methods of *Freemen* and *Davis (LG-1).*Castor was limited in machine-time and only completed one cycle of pulsation with his radiative transfer code (*Castor* 1966). *Bendt* and *Davis* (1971) on the other hand used as a boundary condition the flux and velocity from the diffusion code to study the effects of frequency grouping, zoning, and the weighting of the opacities across the zone interfaces to establish models of Cepheids. The results, in agreement with Castor, showed that the effects of improved radiative transfer in models of Cepheids was minimal. Following this initial work we studied models of RR Lyrae and W Virginis stars using standard boundary conditions, (*i.e.* u(inside) = 0.0) instead of results from the diffusion code. The result for SW Andromedae was an improvement in U-B *vs.* phase when compared to the observations. For W Virginis the results were more dramatic (see *J. Cox's* review 1974). Using a

model first developed by Christy, Davis noted that shocks formed in the atmosphere of the star resulted in a shoulder on the light curve not present in the diffusion model. This model was also an improvement in that alterations in light maximum and minimum occurred in contrast to only variations in light minimum in Christy's diffusion model. Following the work of Christy and Castor, *Hill* (1972) studied transfer effects in the extended atmosphere of Christy's RR Lyrae model 5G. He found that a series of shocks formed that could be related to observable lines. The observation of more than one shock forming in the atmosphere of an RR Lyrae model is supported by the earlier work of Hillendahl.

With the ability to do frequency resolved radiative transfer, Cox and Davis looked into the question of the proper averages for the colors from B-V to obtain the temperature of pulsating stars. The results for a model of RR Lyrae supports the observers' method of taking $<B>-<V>$ averages to obtain the temperature from the standard relation of Oke, Giver, and Searle where the opacity was the standard King 1 A and for Cepheids a new opacity table (CD1) was developed that contained molecules and gave good agreement with the Kraft relation. Other applications of improved radiative transfer techniques were made by *Spangenberg,* using non-equilibrium diffusion, and *Karp,* using a modified Henyey method *(LG-1).*

A study conducted by *Vermury* and *Stothers* (1978) and *Stothers (LG-4)* concluded that Carson opacities and/or the use of tangled magnetic field may explain the "bump" sequence using evolutionary masses.

During this development period a method to relax the equations to the periodic solution was devised by *Baker* and *Von Sengbusch* (1969). The periodic solution of a stellar envelope is calculated using an eigenvalue method. From the resulting Floquet matrix, one obtains the conditions of growth for the various modes of pulsation contained in the model. For an RR Lyrae model Von Sengbusch found the blue edge of the instability at limiting amplitude. This method looks very powerful for studies in modal content of pulsation. *Stellingwerf* (1974) modified the relaxation method to make it more adaptable to the initial value technique. For problems in which e-folding times are long, the method is clearly needed to reduce the number of integrations. Using this method *Stellingwerf (LG-1)* determined the transition lines and growth rates for a series of RR Lyrae and beat Cepheid models. For a model with $M = 0.578 M_{\odot}$, $L = 63 L_{\odot}$, and $T_{eff} = 6500K$, he believed he had established a mixed-mode model, but later attempts by A. Cox et al., using DYNSTAR *(LG-4)* were unsuccessful. It appears that efforts to find double-mode pulsators using nonlinear methods have proven to be limited to regions in the Hertzsprung-Russell diagram outside those accepted from linear theory for either/or pulsation. Apparently the Stellingwerf code uses an adiabatic spring as an inner boundary condition. *Cox (LG-3)* found that effects due to this boundary condition appeared in other zones that could have caused problems in the results.

Realizing that standard Lagrangian codes did not resolve the light curves very well a new approach using non-Lagrangian techniques was developed. The original work on dynamic zoning was carried out by Castor but applied by *Castor, Davis* and *Davison* (1977) to Cepheid pulsation. Before this work one usually used the calculated velocity profiles for comparison to the bumps observed in the Hertzsprung sequence. The dynamic zoning algorithm improved the light curves considerably. The ability to place zones in the ionization region, which is spatially very thin, results in smoother light curves. Recently, a similar code using temperature instead of mass, as the dependent variable was developed by *Aikawa* and *Simon* (1983). Details in the light curves of long period Cepheids have been seen in the results of Moffett and Barnes. For X Cygni, the non-Lagrangian code gives a "dip" as observed on the rising part of the light curve (0.85 in phase). Interestingly enough the resulting mass is the evolutionary mass ($7.0M_\odot$) *(LG-3)*.

Methods for treating convection in nonlinear Lagrangian codes have not changed much since the earlier work of *Cox et al.*, (1969). The standard mixing length theory has been modified somewhat by the addition of time dependent terms but still a number of parameters must be fixed to establish the proper effects due to convection. It has been accepted that convection has a small effect near the blue edge of the instability strip but it probably causes the occurrence of the red edge. More recent studies on the effects of convection on the pulsational development of the nonlinear models will be discussed in the next section.

4. Present Status in Nonlinear Pulsation

Probably the most exciting part of this review is the discussion of the present status and interest in methods of nonlinear pulsation as applied to problems of "resonance", double-mode pulsation and mass discrepancies. We will consider the various efforts to attack these problems with the use of analytic means, amplitude equations and the use of the very sophisticated relaxation direct integration methods. Probably the most exciting area of research in stellar pulsation at present is the search for the cause of nonlinear development of multimode pulsation as observed in RR Lyrae, beat Cepheids, δ Scuti and possibly other variable stars in the instability strip. Since the early attempts of Stellingwerf (see Section 3) many have tried but few have succeeded in producing double-mode pulsation with their nonlinear codes. One exception is the recent model of Buchler and Kovács with $M = 0.85M_\odot$, $L = 35L_\odot$, and $T_{eff} = 6200K$. The period ratio of $P_1/P_0 = 0.756$ does not agree with ratio of 0.746 as observed for this class of double-mode RR Lyrae stars. To obtain this result they had to make a careful selection of the artificial viscosity parameters. We should mention again that attempts to duplicate Stellingwerf's results were unsuccessful (see Sec-

tion 3). Recently, *Cox* and *Ostlie* have included a form of time-dependent convection in their code *(LG-7)* with the expectation that the effects of convection will reduce the amplitude and enhance the occurrence of double-mode pulsators. At present their convective flux differs from Stellingwerf's in an unexplained manner. A good review on various techniques applied to convection is given by *Toomre (LG-5)*. A new approach to nonlinear pulsation is the use of an asymptotic method by *Buchler* and *Goupil* and along with *Klapp (LG-7)* they have studied the occurrence of resonance in Cepheid pulsation and find good agreement with a set of DYN calculations done by *Simon* and *Davis (LG-5)*. *Davis, Kovács* and *Buchler (LG-7)* have studied an RR Lyrae model that contains fundamental and first harmonic modes in pulsation. Initiating the model in both fundamental and first harmonic amplitudes (20 km/s) and without "pumping" they observed the detailed growth to limiting amplitude. Using the Maximum Entropy Method (MEM), they analyzed the results at various stages to study the modal content of the model. The method provides an accurate practical test for assessing whether a model has relaxed to a steady pulsation and produces time-dependent amplitudes and phases that can be analyzed within the amplitude equation formalism of Buchler and Goupil.

A recent study of interest to this author is that by *Aikawa* and *Simon* (1983) where they Fourier analyzed a convection model of an RR Lyrae star, due to Stellingwerf and a radiative transfer model due to *Hill* (1972). They conclude that the comparisons, for the light and velocity amplitudes, from the convective model agree with their results for a radiative (diffusion) model but the results for the radiative transfer model are in better agreement with observations for RRab variables. They had incorrectly assumed that no other radiative transfer models existed for RR Lyrae (see *Davis* 1975). This result though supports the suggestion by Davis that transfer effects are important in models of RR Lyrae stars.

In these studies on modal selection, we need to mention the work of *Uji-iye, Aikawa, Ishida,* and *Takeuti (LG-7)*. They found that increases in artificial viscosity dissipated the kinetic energy of the first overtone mode much more than the fundamental mode. They were also unsuccessful in constructing a double-mode pulsator. Their Cepheid models had masses from $6.71M_\odot$ to $3.5M_\odot$ with constant luminosity, $L = 2280L_\odot$ and $T_{eff} = 5850K$.

It appears from these studies that our codes are missing some relevant physics in order to model double-mode pulsators. In this review, many suggestions were made that should be included in one code. First, we should use the direct integration methods coupled with relaxation methods and then add improvements to resolve the shock and ionization fronts (like dynamic zoning) and also improve the radiative transfer prescription as well as the time-dependent convection. With multiprocessing, vectorization, and the new super computers we may be able to assemble a code of this nature in the near future.

Recently, we have also seen a re-birth in an interest to understand the light curves of BL Her and W Virginis stars (not to mention δ Scuti and Ap stars). Recent work by *Bridger* on W Virginis, and *Fadeyev* and *Fokin* on BL Her and W Virginis stars *(LG-6),* have resulted in new insights into the structure of these pulsators. From this reviewer's point of view, we believe that improved radiative transfer techniques are needed in order to properly model Pop II class variables (higher luminosity to mass). Radiative transfer is needed in models of these stars to handle the extended atmospheres that results from the stronger shocks that transit during certain phases. The δ Scuti and Ap stars seem to require methods of non-radial pulsation that are not discussed in this review.

Another improvement in our understanding of modal interactions was gained by Whitney and others in the observation that the "echo" description of Christy's for the bump Cepheids is consistent with the resonance ideas of Simon and others.

5. The Future of Stellar Pulsation Codes

With the era of multiprocessing and higher speed computers at hand, the possibilities of many improvements to our nonlinear stellar pulsation codes exist. Improvements in radiative transfer techniques, including the treatment of line transfer, for a more direct comparison to the observations is now possible. The area I believe needs the most improvement and results can already be seen in other applications of astrophysical interest, is in the use of improved hydrodynamics. For one-dimensional Lagrangian codes we can expect improvements in methods of adaptive zoning, mass advection and shock treatments. The recent work of Winkler, Van Leer, Woodward and others is indicative of the improvements possible. The more robust adaptive mesh schemes of Winkler along with improved advection along the lines of MUSCL (Van Leer) or PPM (Woodward) should be incorporated into our nonlinear pulsation codes. The adaptation of Gudonov's method to improve the shock structure is also a possibility. In this new era of development, we can consider thousands of zones or adaptive meshing to resolve the ionization regions and the shocks, as well as improved radiative transfer and the use of tensor viscosities in the treatment of shocks. In the near future, two- and three-dimensional codes will be available with capabilities to do rotation and treat magnetic fields. The time-dependent convection problem may be more tractable in two or three dimensions (Dupree). Methods for treating turbulence are being formulated in two-dimensional codes at present and new techniques such as free Lagrange or Arbitrary Lagrangian Eulerian (ALE), may make the treatment of turbulence and mixing possible.

References

Aikawa, T., and Simon, N. 1983, *Ap. J.*, **273**, 346.

Aleshin, B. 1964, *Russ. A. J.*, **41**, 201.

Baker, N., and Von Sengbusch, K. 1969, *Mitteilungen der Astronomischen Gesellschaft*, 27.

Bendt, J., and Davis, C. 1971, *Ap. J.*, **169**, 333.

Castor, J. 1966, PhD Dissertation, Cal Tech, Pasadena.

Castor, J. Davis, C., and Davison, D. 1977, Los Alamos report LA-6664.

Christy, R. 1964, *Rev. of Modern Physics*, **36**, 555.

Cox, A., Brownlee, R., and Eilers, D. 1969. *Ap. J.*, **144**, 1024.

Cox, J. 1974, *Reports on Progress in Physics*, **37**, 563.

Davis, C.G. 1975, in *Multiple Periodic Variable Stars*, IAU Coll. No. 29, ed. W.S. Fitch (Akadémia Kiadó, Budapest), Vol II., p. 195.

Fadeyev, Yu., and Tutukov, A. 1981, *M.N.R.A.S.*, **195**, 811.

Hillendahl, R. 1969, PhD Dissertation, U. of C. Berkeley.

Hill, S. 1972, *Ap. J.*, **178**, 793.

Stellingwerf, R. 1974, *Ap. J.*, **192**, 139.

Stobie, R. 1969, *M.N.R.A.S.* **144**, 461.

Vermury, S., and Stothers, R. 1978, *Ap. J.*, **225**, 939.

These conferences are generally referred to as the Los Alamos/Goddard (LG) conferences, which originally started in 1972 at Los Alamos

(1) Cepheid Modeling, July 1974, NASA SP-383.

(2) Solar and Stellar Pulsation, August 1976, LA-6544C.

(3) Current Problems in Stellar Pulsation, June 1978, NASA Tech. Mem. 80625.

(4) Stellar Hydrodynamics, August 1980, IAU Coll. 58, Space Science Reviews **27**, (3).

(5) Pulsation in Classical and Cataclysmic Variable Stars, June 1984, JILA rept. J. Cox and C. Hansen eds.

(6) Cepheids: Theory and Observations, May-June 1984, IAU Coll. 82, B.F. Madore ed., Cambridge Press.

(7) Stellar Pulsation, A memorial to John Cox, August 1986, Lecture Notes in Physics, 274.

MULTIPLE-MODE PULSATION IN δ SCUTI STARS

D. W. Kurtz
Department of Astronomy, University of Cape Town, South Africa

Abstract

The δ Scuti stars are reviewed. It is emphasized that few successful frequency analyses have been done on multi-periodic, non-radially oscillating δ Scuti stars. Some successful analyses are discussed. Future observational effort needs to be on intensive multisite campaigns. Future theoretical effort needs to model specific stars for which there are frequency solutions.

1. Introduction

In the last 12 years helioseismology, the study of the interior structure of the sun by the analysis of its surface oscillations, has blossomed. Conferences devoted to the topic and its relative, asteroseismology, are now an annual affair of which this workshop is a part. The spectacular successes of helioseismology (see *Christensen-Dalsgaard*, these proceedings; *Toomre* 1986; *Christensen-Dalsgaard* 1986) have led to the desire to apply the theory developed for the sun to other stars.

It is probable that the δ Scuti stars are the most numerous nondegenerate pulsating stars in the galaxy which can presently be observed. They are Population I, A and F main sequence and giant stars which show light variations with amplitudes of a few mmag up to many tenths of a mag and periods in the range of about 30 minutes up to many hours. Some of the δ Scuti stars are singly or doubly periodic radial pulsators, but most are multiperiodic and pulsate in a mixture of radial and non-radial modes. They constitute at least 20% of all A stars; the low amplitude pulsators are much more numerous which means that as photometric accuracy improves, the fraction of A stars known to be δ Scuti stars will increase.

Many reviews of these stars have been written in the last dozen years. The most extensive are those of *Fitch* (1976), *Breger* (1979), *Eggen* (1979) and *Wolff* (1983). Shorter reviews are those of *Breger* and *Stockenhuber* (1983), *Kurtz* (1986) and *Shibahashi* (1987). Lists of δ Scuti stars and references to studies of individual stars can be found in *Breger* (1979), *Eggen* (1979) and *Halprin* and *Moon* (1983) and, of course, the indispensable *Astronomy and Astrophysics Abstracts*. With the exception of *Shibahashi* (1987), the above reviews emphasise observations rather than theory. Theoretical discussions, stability analyses, discussion of the role of resonances, and

models can be found in *Lee* (1985), *Andreasen, Hejlesen,* and *Petersen* (1983a,b), *Dziembowski* (1977, 1980, 1982), *Fitch* (1981) and *Stellingwerf* (1979).

The theoretical asteroseismologist should see the δ Scuti stars as a gold mine: many of them are naked-eye stars and easy to observe, they are common, many pulsate in non-radial modes and some pulsate in many non-radial modes simultaneously. This latter characteristic is most important since it is the variety of spherical-harmonic modes which gives us the ability to resolve the interior structure of a pulsating star.

Yet asteroseismologists pay scant attention to the δ Scuti stars. The reason for this is simple: there are few δ Scuti stars with solved frequency spectra. The most pressing need in δ Scuti star research is for solved frequency spectra of multiperiodic, non-radially oscillating, single, non-magnetic, normal abundance δ Scuti stars. In Section 5 I make a specific suggestion for a multi-site observing project to do this.

Before that, however, I would like to look at the developments in the field over the last dozen years, the complications which make the study of individual δ Scuti stars difficult, and the details of the few successful frequency analyses which have been done.

2. Twelve years ago...

Twelve years ago IAU colloquium 29, "Multiple (*sic*) Periodic Variable Stars", was held here in Budapest. *Fitch* (1976), in his review of the δ Scuti stars at that meeting, said that the controversies at that time centred "on three specific questions:

1) Are δ Scuti stars really periodic, or only quasi-periodic?

2) Are tidal modulations responsible for the slow cyclic variations observed in many of these stars...?

3) Are there any real physical differences between [dwarf Cepheids and δ Scuti stars] ...?"

The first question remains unresolved, although I have repeatedly emphasised the difficulty in distinguishing between unresolved frequencies in an inadequate data set on a multi-mode pulsator and modes with lifetimes short with respect to the time-span of the observations (*Kurtz* 1980, 1986). *Fitch* (1976) made that same point 12 years ago; both of us have expressed the prejudice that the δ Scuti stars will probably all be shown to pulsate in stable modes with frequencies which only change on evolutionary time-scales. *Breger* and *Stockenhuber* (1983) reviewed the δ Scuti stars at a recent conference and in the published discussion which followed their paper Breger ruled out the possibility of "meandering periods" based on the evidence

that frequency analyses of δ Scuti stars show peaks in the periodograms which are no wider than expected from the spectral windows.

Paparó and *Kovács* (1984) analysed 43 hr of photometry of HR 4684 and suggested that the periodograms of their data supported the contention that the amplitudes of the pulsation frequencies in HR 4684 may change significantly on a time-scale as short as days. They point out that this is much too short a time-scale for evolutionary changes and is also much shorter than theoretically calculated excitation and damping times (see *Dziembowski* 1977 and *Lee* 1985). So they suggest that perhaps non-linear coupling between resonant modes might be the cause of the mode changes.

Antonello et al. (1985) analysed another small data set for HR 4684, assumed stable periods, and concluded that three frequencies are present in the variations of this star, although the authors are uncertain amongst many possibilities what those three frequencies are. Nevertheless, they conclude that their data are consistent with *Dziembowski's* (1980, 1982) calculations of non-linear coupling between resonant frequencies. Dziembowski suggests that such mode-coupling may explain the profound difference of the multi-mode pulsation of many of the δ Scuti stars and the single or double mode pulsation of a few δ Scuti stars and the RR Lyrae stars and Cepheids.

There is other support for the idea that some δ Scuti stars may pulsate in modes with short life-times. It is widely accepted that solar 5-min oscillation modes have lifetimes less than a few weeks so one might suspect that this could be true for δ Scuti stars, too. The amplitudes of the observed δ Scuti pulsation modes are orders of magnitude greater than the amplitudes of the solar oscillations, however, and different driving mechanisms are almost certainly involved.

Matthews, Kurtz and *Wehlau* (1987) have hundreds of hours of observations of the rapidly oscillating Ap star, HD 60435; their data tend to suggest that the many modes in this complex star may have lifetimes which are only a week or so. If that is possible in a rapidly oscillating Ap star, then why not in a δ Scuti star? However, other rapidly oscillating Ap stars have frequencies which are stable over the several years since their discovery (see my review of the rapidly oscillating Ap stars elsewhere in this volume) and the possibility remains that this may also be true for HD 60435.

Where does that leave us with respect to Fitch's first question: Are δ Scuti stars really periodic? I continue to maintain that, with sufficient data, stable periodicities will be found in all of the δ Scuti stars; *i.e.* I suggest that the δ Scuti stars pulsate in radial and non-radial eigenmodes with frequencies which only change on evolutionary time-scales. This dogma is not very good science, however, since it is impossible to disprove. If a frequency analysis of a very large data set fails to support my hypothesis, I can simply claim that more data are needed. *Paparó* and *Kovács*

(1984) allude to this when they point out that even with over 100 hr of high-quality data, I was unable to find a frequency solution for the light variations in HD 52788 (*Kurtz* 1981). *Matthews, Kurtz,* and *Wehlau* (1987) had little success in finding stable periodicities in the rapidly oscillating Ap star HD 60435 even with many hundreds of hours of observations from observatories on two continents.

Fitch's second question: "Are tidal modulations responsible for the slow cyclic variations observed in many of these stars...?" also remains unanswered and little attention has been paid to this idea for some years now. *Fitch* and *Wisniewski* (1979) dealt with it extensively in their analysis of the δ Scuti star 14 Aur which is also a single-lined, non-eclipsing spectroscopic binary with an orbital period of 3.788568 day and with δ Del spectral peculiarities (*Kurtz* 1976). *Balona* and *Stobie* (1980a) rejected the tidal modulation hypothesis for 1 Mon based on their radial velocity observations.

I would say that tidal modulation may still be a working hypothesis for pulsating stars in close binary systems, but that observational attention is best spent now on trying to solve the frequency spectra of single δ Scuti stars. When we have a better understanding of the single pulsators, we can then turn our attention to the more complex binary systems which may show tidal interactions.

Fitch's third question, "Are there any real physical differences between [dwarf Cepheids and δ Scuti stars]...?" is answered. *Breger* (1980) says, "The majority of Dwarf Cepheids resemble the Population I δ Scuti stars in nearly all respects... A small subgroup [of the dwarf Cepheids], led by SX Phe, show[s] systematically low metallicities, high space motions, and low luminosities, and deviate[s] from the observed and theoretical period-gravity relation in the low mass direction." To summarise that: most of the stars previously called Dwarf Cepheids are just high amplitude δ Scuti stars, but there are a few Population II pulsators in the δ Scuti instability strip.

In my opinion our primary goal in the near future in δ Scuti star research is to obtain complete frequency solutions for as many multimode pulsators as possible. In Section 3 I discuss some of the complications which make many δ Scuti stars unsuitable for this purpose. In Section 4 I present a small selection of successful frequency analyses which have already been done and in Section 5 I propose a specific research project.

3. Complications

It is not known what limits the pulsational amplitudes in δ Scuti stars nor is it known what factors select modes. There are some clear correlations. The largest amplitude pulsators tend to be giant stars; the largest amplitude pulsators tend to

be slow rotators. But then giant stars tend to be slow rotators. Some slowly rotating giant stars in the δ Scuti instability strip show little or no variation.

Most large amplitude δ Scuti stars pulsate in only one or a few modes; most small amplitude pulsators are multi-periodic, but there are some which are singly periodic. *Antonello* (1983) and *Antonello, Fracassini,* and *Pastori* (1981) have found some statistical correlations among the various physical parameters of the δ Scuti stars, but for any particular star it is not possible to predict pulsational characteristics based on any combination of known physical parameters.

Two further complications in the δ Scuti instability strip are the existence of the Am and Ap stars (see the appropriate chapters in *Wolff* (1983) for general discussions of these stars). The Am stars have atmospheric abundance anomalies, rotate slowly, are almost all in short period binary systems, and constitute at least 1/3 of all the stars in the δ Scuti instability strip; at A8 they constitute 1/2 of the stars. In general, Am stars do not pulsate. Some giant Am stars (δ Del stars) pulsate (*Kurtz* 1976) and three marginal Am stars are known to pulsate (*Kurtz* 1978, 1984), but it has long been thought that *classical* Am stars do not pulsate. (A classical Am star is one in which there are more than 5 spectral subtypes difference between the Ca K-line classification and the metal-line classification.) Even this is no longer true.

A few months ago I discovered a pulsating classical Am star, HD 1097. *Houk* (1982) classifies this star A3/5mF0-F5 which means that there are 10 subtypes difference between the K-line and metal-line types. Strömgren photometry of HD 1097 gives $b\text{-}y = 0.238$, $m_1 = 0.326$, $c_1 = 0.463$, and $\beta = 2.729$ (*Hauck* and *Mermilliod* 1985) which also indicates that this star has very strong metallicity. An analysis of light curves obtained over 5 hr on two nights in 1987 July shows that a single period, $P = 81.17 \pm 0.05$ minutes, with a semi-amplitude of 4.52 ± 0.15 mmag fits both light curves coherently. These observations will be discussed in detail in a future publication.

The Ap stars, which constitute $\leq 10\%$ of the stars in the δ Scuti instability strip, are mostly magnetic Si and SrCrEu stars. In general these Ap stars are not δ Scuti stars, but there are exceptions to this which are discussed by *Weiss* (1983a,b) and *Kreidl* (1987). There are also the rapidly oscillating Ap stars (*Kurtz*, this volume).

The largest amplitude δ Scuti stars are slowly rotating giant stars, but on the main sequence the slowly rotating stars are all, or mostly, Am and Ap stars which generally do not pulsate. It is thus very difficult to separate the effects of rotation and metallicity on pulsation and pulsation amplitude.

4. Successful frequency analyses

A completely successful frequency analysis is one in which all of the frequencies present in the observations (light curves, radial velocity curves, line-profile variations) have been identified and nothing is left in the periodogram of the residuals except white noise. In addition, there must be good confidence that aliases have caused no confusion and that the signal-to-noise was sufficient for secure frequency identifications. This means that an analysis of a new set of observations will produce the same results – the standard definition of a successful experiment.

This sort of success is rare in δ Scuti star research, but fortunately is not absolutely necessary in order to make progress in our physical understanding of these stars. It is sufficient to identify only some of the frequencies with confidence that new observations will confirm those identifications. This has been done in a number of cases for the higher amplitude δ Scuti stars.

4a AC And and VZ Cnc

A good example is the study of AC And by *Fitch* and *Szeidl* (1976). They find that the star pulsates with three principal frequencies which show good agreement with models when identified with the fundamental, first overtone and second overtone radial modes. While I consider Fitch and Szeidl's analysis of AC And to be successful, in that the three principal frequencies which they identify are probably correct, it is clear that there is a lot of variation in the light curves of AC And which their frequencies do not account for. They fitted their light curves with a fifth-order combination of f_1, f_2 and f_3 along with the harmonics and cross-terms between those three frequencies, and yet their fit deviates from the observations by up to 0.05 mag.

It is often implicitly assumed in discussions of the largest amplitude δ Scuti stars that the two or three frequencies present in their variations, which can be identified with radial modes, along with their harmonics and cross-terms are a complete description of the variations in the observations; *i.e.* no additional, low-amplitude non-radial modes are present. *Cox, King,* and *Hodson* (1979) have found that the observed frequencies in double-mode δ Scuti stars match the theoretical ones well for stars in a post-main sequence stage of evolution with reasonable masses. More information about the structure of these stars could be extracted, however, if non-radial modes were also excited. One wonders, for example, if that might not be the case in AC And where the Fitch and Szeidl's fitted curve deviates by such large amounts from the observations. Their 0.05 mag deviations are larger than the peak-to-peak amplitudes of most of the non-radially oscillating δ Scuti stars.

To test for the presence of non-radial modes in the large amplitude δ Scuti stars, a large set of high accuracy observations is needed. These observations must be sufficient to avoid severe alias problems and must cover the entire light curve so that a periodogram analysis can identify the harmonics and cross-terms without assumptions about their presence being necessary. Many of the earlier observations of high amplitude δ Scuti stars are not useful for this purpose since observations were predominantly made on the rising branches of the light curves only.

A successful analysis of this sort has been made by *Cox, McNamara,* and *Ryan* (1984). They analysed 16 nights of new observations of VZ Cnc obtained in 1983. They made no assumptions about the frequency content in the light variations and used a combination of periodogram analysis and least-squares fitting to find all of the frequencies in their data. They found two principal frequencies with a ratio of 0.80 and many harmonics and cross-terms between those two frequencies. Importantly, no other frequencies were found above a noise level in their periodogram of 2 mmag; all of the variation in VZ Cnc is explained well by the two principal frequencies, their harmonics and cross-terms. The light curve constructed from those frequencies fits the data to an accuracy of 8 mmag which is probably close to the error in their observations.

Fitch and *Szeidl* (1976) list VZ Cnc as pulsating in the first and second radial overtones based on the 0.80 ratio between its two principal frequencies. *Cox, McNamara,* and *Ryan* (1984) find that same frequency ratio, but reinterpret the pulsation modes to be the fundamental and first overtone radial modes in a star in which considerable helium depletion has occurred in the outer envelope due to gravitational settling. (*Andreasen, Hejlesen,* and *Petersen* (1983a,b) also discuss helium-settling in δ Scuti stars.) This suggestion worries me: helium-settling is the usual explanation for the near exclusion between the δ Scuti stars and the Am and Ap stars. How can helium-settling be significant in such a large amplitude δ Scuti star as VZ Cnc and still be the reason why Am and Ap stars either do not pulsate or only do so with very low amplitudes?

4b AI Vel

AI Vel was at one time considered to be the prototype of the Population II pulsating stars in the δ Scuti instability strip. *Balona* and *Stobie* (1980b) analysed three nights of simultaneous BVRI photometry and radial velocities of AI Vel to conclude that it is pulsating in the fundamental and first overtone radial modes and is a normal Population I star. Their Wesselink analysis gives a radius of about $3R_{\odot}$.

In this case, however, it has not been demonstrated that the two principal frequencies are all that are present in the variations. Balona and Stobie only had three nights of observations of AI Vel so they relied on *Simon's* (1979) frequencies; Simon's two principal frequencies were assumed to be *Walraven's* (1955) two frequencies – all of the other frequencies he found came from assuming that the harmonics and cross-terms of f_1 and f_2 are present in the data. No search for those frequencies was done in the manner of *Cox, McNamara,* and *Ryan's* (1984) analysis of VZ Cnc.

4c δ Sct

The prototype of this class of stars, δ Sct itself, is a multiperiodic variable which, in spite of its apparent brightness, still does not have a solved frequency spectrum. *Fitch* (1976) could not get independent identical solutions to Fath's 1935-1938 data and his own 1972-1973 data; he even considered that the two principal frequencies might not be strictly constant.

Balona, Dean and *Stobie* (1981) obtained simultaneous BVI and radial velocity observations of δ Sct on two nights in 1976 and 1977. When they combined their radial velocity measurements with previous ones, they found that the two principal frequencies, $f_0 = 5.160765$ day^{-1} and $f_1 = 5.354018$ day^{-1}, along with the first harmonic of f_0 fitted all of the observations to $\sigma = 1.9$ km s^{-1} which they felt was close to the observational error.

By analysing the phase shift between V and B-V, Balona, Dean and Stobie concluded that f_0 is unequivocally due to radial pulsation and f_1 is due to quadrupole pulsation. Measurements of line profile variations in δ Sct by *Campos* and *Smith* (1980) and *Smith* (1982) are in agreement with these mode identifications.

There are many other frequencies present in the variations of δ Sct, however (*Fitch* 1976). When one examines the frequencies which Fitch found and their fit to his data, it is clear that he does not have a complete frequency solution. In my opinion, that frequency solution could be obtained from a high accuracy, multi-site set of observations and a project to obtain such observations is encouraged.

4d 1 Mon

1 Mon is the best case of a multi-mode, non-radially pulsating δ Scuti star with well determined frequencies and mode identifications which show an understandable pattern. *Balona* and *Stobie* (1980b) analysed simultaneous BVRI photometry and radial velocities, which they obtained on three nights in 1977, along with the V observa-

tions of *Shobbrook* and *Stobie* (1974) and *Millis* (1973). They found six frequencies, $f_1 = 7.346146 \pm 0.000002$ day^{-1}, $f_2 = 7.475268 \pm 0.000002$ day^{-1}, $f_3 = 7.217139 \pm 0.000007$ day^{-1}, $f_1 + f_2$, $2f_1$ and $2f_2$ which fit the observations with a standard deviation of $\sigma = 9$ mmag per observation. This standard deviation is substantially greater than the expected errors in Shobbrook and Stobie's and Balona and Stobie's data of about 3 mmag indicating that those six frequencies are not a complete description of the variations of 1 Mon.

Balona and Stobie identify f_1 as a radial mode; f_2 and f_3 they find are due to a dipole mode with $m = -1$ for f_2 and $m = +1$ for f_3. *Smith* (1982) finds line profile variations which are consistent with these mode identifications. The non-equal splitting of these three frequencies is consistent with the central frequency not being the $m = 0$ component of the dipole oscillation. If second order terms in the rotational splitting of a dipole mode in 1 Mon are not important, then the $m = 0$ component of the dipole must be separated from the observed radial mode by 0.000058 ± 0.000008 day^{-1}. This should be a powerful diagnostic of the internal structure of 1 Mon, but to my knowledge it has not yet been exploited theoretically.

4e Θ^2*Tau*

As I emphasised earlier, the most pressing need in δ Scuti star research is for solved frequency spectra for multi-mode non-radial pulsators, preferably with many frequencies. It is the multitude of different non-radial modes which provides the discerning probe of a star's interior. Recently *Breger et al.* (1987) have attempted this, and possibly they have succeeded.

Breger et al. obtained observations of Θ^2 Tau, a δ Scuti star which is known to be in a 140.728 day binary system. From calculations of light time effects on the derived pulsation frequencies, they suggest that all of the light variations are due to pulsation in the primary even though the secondary (1.1 mag fainter) is also in the instability strip. The frequencies they derive are: $f_1 = 13.22970$ day^{-1}, $A_1 = 6.5$ mmag; $f_2 = 13.48090$ day^{-1}, $A_2 = 2.7$ mmag; $f_3 = 13.69362$ day^{-1}, $A_3 = 4.0$ mmag; and $f_4 = 14.31756$ day^{-1}, $A_4 = 3.2$ mmag. These frequencies fit the observations to an accuracy of $\sigma = 3$ mmag per observation which is close to the actual observational error. Thus the authors suggest that they may have found the complete frequency set which describes the light variations in Θ^2 Tau. There are caveats to this, as usual, which the authors discuss. Nevertheless, this is the best that has been done so far for a low-amplitude multi-mode δ Scuti star and *Breger et al.'s* frequencies now need theoretical interpretation. *Breger et al.* give $M = 2M_\odot$, $T_{eff} = 8200$ K, log $g = 3.8$, and $M_V = 0.5$. Simple

calculations of Q-values indicate that the frequencies must be associated with $n \geq 2$ overtones.

5. A proposal for new observations of Θ Tuc

Breger et al. (1987) have shown that the frequencies in multi-mode, non-radially oscillating δ Scuti stars can be solved if enough effort is put into obtaining the observations. To advance our understanding of these stars further we need many with solved frequency spectra so that the patterns in the frequencies become evident. With care and a judicious selection of program stars this should be possible.

Θ Tuc is a well studied southern δ Scuti star which *Stobie* and *Shobbrook* (1976) concluded changes frequencies on a time-scale as short as 1 day, but which I later showed has at least one stable frequency (*Kurtz* 1980). I was unable to solve the frequency spectrum in Θ Tuc with 70 hr of observations obtained on 21 nights in 1979, but most of that problem is due to the daily aliases inherent in observations obtained from one site.

Furthermore, in retrospect, those 70 hr of observations are spread over 3 months and only a few of the longest observing runs were over 5 hr. At the time I considered that to be a large data set; now I think it is not. What is needed for Θ Tuc is an observing run which is as nearly continuous as possible for two weeks which will suppress the daily aliases, plus additional data from at least one observatory for a longer period to resolve more closely spaced frequencies.

Θ Tuc transits at midnight at the end of September. With a declination of $\delta = -71^{\circ}$ it can be observed all night, about 9 hr, from southern observatories. At a minimum I propose to observe it from the South African Astronomical Observatory from 1988 September 27 to October 10 and for another week in 1988 November. I would like observers who would like to join this observing project and who have access to telescopes in the southern hemisphere to contact me to arrange the details of the observing.

If we can get good contemporaneous coverage of Θ Tuc from Chile, South Africa, and Australia or New Zealand for a time-span of two weeks, we should be able to solve the frequency spectrum of this star. It is not known to have any spectral peculiarities, and hence should not have suffered helium depletion which would complicate modelling it. It is not known to be binary as Θ^2 Tau and hence there should be no confusion over which star is pulsating. It is bright and easy to observe and is known to have amplitudes large enough to give a reasonable signal-to-noise ratio.

References

Andreasen, G.K., Hejlesen, P.M., and Petersen, J.O. 1983a, *Astr. Ap.*, **121**, 241.

Andreasen, G.K., Hejlesen, P.M., and Petersen, J.O. 1983b, *Astr. Ap.*, **121**, 250.

Antonello, E. 1983, *Hvar Obs. Bull.*, **7**, 329.

Antonello, E., Fracassini, M., and Pastori, L. 1981, *Astrophys. Space Sci.*, **78**, 435.

Antonello, E., Guerrero, G., Mantegazza, L., and Scardia, M. 1985, *Astr. Ap.*, **146**, 11.

Balona, L.A., and Stobie, R.S. 1980a, *M. N. R. A. S.*, **190**, 931.

Balona, L.A., and Stobie, R.S. 1980b, *M. N. R. A. S.*, **192**, 625.

Balona, L.A., Dean, J.F., and Stobie, R.S. 1981, *M. N. R. A. S.*, **194**, 125.

Breger, M. 1979, *Pub. A. S. P.*, **91**, 5.

Breger, M., 1980. *Ap. J.*, **235**, 153.

Breger, M., Huang Lin, Jiang Shi-yang, Guo Zi-he, Antonello, E., and Mantegazza, L. 1987, *Astr. Ap.*, **175**, 117.

Breger, M., and Stockenhuber, H. 1983, *Hvar Obs. Bull.*, **7**, 283.

Campos, A.J., and Smith, M.A. 1980, *Ap. J.*, **238**, 667.

Christensen-Dalsgaard, J., 1986, in *Seismology of the Sun and Distant Stars*, ed. D.O. Gough, D. Reidel Publ. Co., Dordrecht, Holland, p. 23.

Cox, A.N., King, D.S., and Hodson, S.W. 1979, *Ap. J.*, **228**, 870.

Cox, A.N., McNamara, B.J., and Ryan, W. 1984, *Ap. J.*, **284**, 250.

Dziembowski, W. 1977, *Acta Astr.*, **27**, 95.

Dziembowski, W. 1980, in *Non-radial and Non-linear Stellar Pulsation*, eds. H.A. Hill and W.A. Dziembowski, Springer-Verlag publ., p. 22.

Dziembowski, W. 1982, *Acta Astr.*, **32**, 147.

Eggen, O.J. 1979, *Ap. J. Suppl.*, **41**, 413.

Fitch, W.S. 1976, in *Multiple Periodic Variable Stars*, ed. W.S. Fitch, IAU Coll. 29, D. Reidel Publ. Co., Dordrecht, Holland, p. 167.

Fitch, W.S. 1981, *Ap. J.*, **249**, 218.

Fitch, W.S., and Szeidl, B. 1976, *Ap. J.*, **203**, 616.

Fitch, W.S., and Wisniewski, W. 1979, *Ap. J.*, **231**, 808.

Halprin, L. and Moon, T.T., 1983, *Astrophys. Space Sci.*, **91**, 43.

Hauck, B., and Mermilliod, M. 1985, *Astr. Ap. Suppl.*, **60**, 61.

Houk, N. 1982, *Michigan Spectral Catalogue*, Vol. 3, Department of Astronomy, University of Michigan, Ann Arbor.

Kreidl, T.J. 1987, *Lecture Notes in Physics*, **274**, 134.

Kurtz, D.W. 1976, *Ap. J. Suppl.*, **32**, 651.

Kurtz, D.W. 1978, *Ap. J.*, **221**, 869.

Kurtz, D.W. 1980, *M. N. R. A. S.*, **193**, 61.

Kurtz, D.W. 1981, *M. N. R. A. S.*, **194**, 69.
Kurtz, D.W. 1984, *M. N. R. A. S.*, **206**, 253.
Kurtz, D.W. 1986, in *Highlights in Astronomy*, ed. J.P. Swings, Reidel,Dordrecht, IAU, p. 237.
Lee, U. 1985, *Pub. A. S. J.*, **37**, 279.
Matthews, J., Kurtz, D.W., and Wehlau, W. 1987, *Ap. J.*, **313**, 782.
Millis, R.L. 1973, *Pub. A. S. P.*, **85**, 410.
Paparó, M. and Kovács, G. 1984, *Astrophys. Space Sci.*, **105**, 357.
Shibahashi, H. 1987, *Lecture Notes in Physics*, **274**, 112.
Shobbrook, R.R., and Stobie, R.S. 1974, *M. N. R. A. S.*, **169**, 643.
Simon, N.R. 1979, *Astr. Ap.*, **74**, 30.
Smith, M.A., 1982. *Ap. J.*, **254**, 242.
Stellingwerf, R.F. 1979, *Ap. J.*, **227**, 935.
Stobie, R.S., and Shobbrook, R.R. 1976, *M. N. R. A. S.*, **174**, 401.
Toomre, J. 1986, in *Seismology of the Sun and Distant Stars*, ed. D.O. Gough, D. Reidel Publ. Co., Dordrecht, Holland, p. 1.
Walraven, Th. 1955, *Bull. Astr. Inst. Neth.*, **12**, 223.
Weiss, W.W. 1983a, *Astr. Ap.*, **128**, 152.
Weiss, W.W. 1983b, *Hvar Obs. Bull.*, **7**, 263.
Wolff, S.C. 1983, *The A-type Stars*, publ. NASA, Washington, D. C., p. 93.

MULTIPLE-MODE AND NON-LINEAR PULSATION IN RAPIDLY OSCILLATING Ap STARS

D. W. Kurtz
Department of Astronomy, University of Cape Town, South Africa

Abstract

The rapidly oscillating Ap stars are reviewed. Dipole oscillation modes are identified in HD 6532 and HD 83368. Mode lifetimes are discussed for HD 60435. A brief progress report on multi-site observations of HD 24712 obtained in 1986 is given. Difficulties in obtaining the temperatures and luminosities of the rapidly oscillating Ap stars are discussed.

1. Introduction

The rapidly oscillating Ap stars are high-overtone ($n \sim 10$-30) p-mode pulsators which mostly lie within or near the observed δ Scuti instability strip. These stars are all cool magnetic Ap stars with SrCrEu line strength peculiarities. Some are well known oblique magnetic rotators and it is a reasonable presumption that they all are.

Figure 1 is a plot of the position of the δ Scuti stars in the HR diagram taken directly from *Breger* and *Stockenhuber* (1983) onto which I have plotted schematic positions for the rapidly oscillating Ap stars. I emphasize the uncertainty of these positions. They have little meaning in luminosity and are also uncertain in temperature. M_V is calculated from δc_1 in this diagram and all of the rapidly oscillating Ap stars have δc_1 indices which make them appear to lie on or below the main sequence. This is almost certainly due to the effects of their abnormal line strengths on the c_1 index and is not a true reflection of their luminosity. From the frequency spacing observed in both HR 1217 and HD 60435 we know they lie about 0.5 mag above the main sequence (*Shibahashi* and *Saio* 1985; *Matthews, Kurtz,* and *Wehlau* 1987). From the spectral type of the companion to the visual binary HR 3831 we know that it also lies about 0.5 mag above the main sequence (*Kurtz* 1982). Hence, for convenience, I have placed the rapidly oscillating Ap stars 0.5 mag above the main sequence in Figure 1, but this should not be taken too seriously.

The $(b\text{-}y)_0$ positions have been estimated from the Hβ index where possible since $b\text{-}y$ is also affected by abnormal line strengths. Even so, there are indications that the Hβ index also underestimates temperature, especially for the coolest stars

plotted. HD 101065 is the most extreme case where the Hβ index would put it way off scale to the right in Figure 1. I have plotted it as an open square near F0 since there are other arguments that its effective temperature is near 7500 K (*Kurtz* and *Wegner* 1979; *Wegner et al.* 1982).

Figure 1 really only shows that the rapidly oscillating Ap stars lie in or near to the δ Scuti instability strip. The $(b-y)_0$ positions are sufficiently uncertain that we cannot conclude that the three stars which lie cooler than the red edge are truly that cool. We also cannot conclude that HD 6532, the hottest rapidly oscillating Ap star, is hotter than any δ Scuti star, partly because of uncertainty in its temperature and partly because of the uncertainty in the blue edge of the δ Scuti instability strip (the hottest δ Scuti stars have relatively low amplitudes and hence are less likely to be detected). That is unfortunate because if we knew that some rapidly oscillating Ap stars lay well outside the δ Scuti instability strip, that would have important implications for their excitation mechanism.

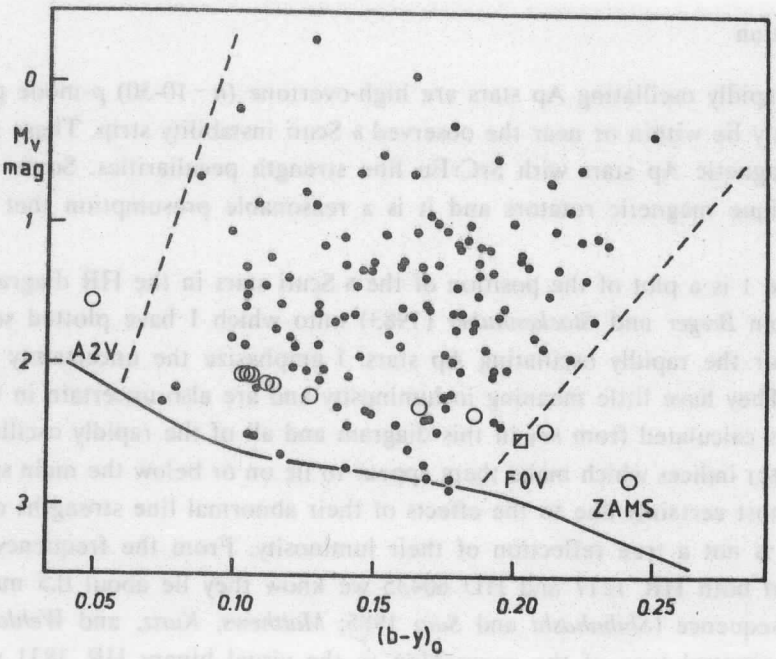

Fig. 1. The observed δ Scuti instability strip taken directly from *Breger* and *Stockenhuber* (1983) with the rapidly oscillating Ap stars schematically plotted as open circles (HD 101065 as an open square). Consult the text before drawing any conclusions.

It might be thought that atmospheric analyses of the rapidly oscillating Ap stars could resolve the problem of their temperatures and luminosities. Because of their extreme spectral peculiarities, however, this has not been possible to do with certainty. The temperature of HD 101065, the most difficult case, has been given to be as low as 6000 K and suggested to be as high as 8000 K. Confident determinations of the temperatures and luminosities of these stars will probably have to await accurate parallaxes from Hipparcos or perhaps the Hubble Space Telescope. Since many of the rapidly oscillating Ap stars are naked eye stars, their parallaxes will be easily measurable from space; that project should have a high priority.

The periods of the rapidly oscillating Ap stars lie in the range 3.5-15 min and the semi-amplitudes of the light variations due to individual pulsation modes are less than 6 mmag, generally much less – most are less than 1 mmag. Most of the observations of these stars have been of their light variations, but recently *Matthews et al.* (1987) have succeeded in measuring radial velocity variations with a semi-amplitude of about 200 m s^{-1} in HR 1217. *Baade* and *Weiss* (1986) have computed expected spectral line variations in an oblique pulsator and *Schneider et al.* (1987) have searched for such line variations in two rapidly oscillating Ap stars, α Cir and γ Equ. The reason for the observational emphasis on the light variations is that noise levels of 0.05-0.2 mmag are obtainable for these high frequencies which, with semi-amplitudes of mmag, give good signal-to-noise.

Recent reviews of the rapidly oscillating Ap stars have been given by *Kurtz* (1986), *Weiss* (1986) and *Shibahashi* (1987). For a more detailed guide to the literature on rapidly oscillating Ap stars, consult those reviews; Kurtz and Weiss emphasize the observations while Shibahashi gives a more thorough theoretical discussion.

There are several characteristics of these stars which make them particularly interesting in the context of this workshop: 1) They are multi-mode pulsators; in two cases, HR 1217 and HD 60435, high-overtone *p*-modes of alternating even and odd *l* are clearly present as in the sun. 2) Many of the rapidly oscillating Ap stars show the presence of harmonics of their principal frequencies. Non-linearities at such low amplitudes have never been seen in the δ Scuti stars. 3) The rapidly oscillating Ap stars are oblique pulsators which gives us a unique view of their non-radial pulsations.

This last characteristic is particularly interesting and promises to allow unprecedented probes of both the interior and exterior of these magnetic stars. *Kurtz* and *Shibahashi* (1986) and *Kurtz* and *Cropper* (1987) have shown for HR 3831 and HD 6532, respectively, that these two stars pulsate primarily in oblique dipole modes. In each of these cases it is possible to see the phase of the principal oscillation reverse by π radians as the star goes through quadrature.

Dziembowski and *Goode* (1985, 1986) calculate that it is the effect of the magnetic field on the pulsation modes which selects the magnetic axis as the pulsation axis. The modes cannot be only axisymmetric ($m = 0$) normal modes, however, as *Kurtz* (1982) first presumed. A normal mode with the magnetic axis as the pulsation axis is equivalent to a linear sum over m of all modes of the appropriate multiplet aligned along any other axis (say, for argument's sake, the rotation axis). A single normal mode should then drift with respect to the magnetic axis since the frequencies of rotationally split m-modes are split by an amount slightly different from the rotation frequency due to the effect of advection. *Dolez* and *Gough* (1982) pointed this out and suggested that perhaps the lifetimes of the pulsation modes were short with respect to the drift time and only modes currently in alignment with the magnetic field are excited to observable amplitudes.

Dziembowski and *Goode* (1985, 1986), *Kurtz* and *Shibahashi* (1986) and *Shibahashi* (1987) argued that each pulsation mode in a rapidly oscillating Ap star gives rise to a $(2l+1)^2$-multiplet of frequencies which keeps the pulsation axis and magnetic axis aligned. The study of the fine structure of the frequencies in each multiplet should yield information about the internal magnetic field strength in the star.

The excitation mechanism in the rapidly oscillating Ap stars is unknown. Since it is possible that they all lie in the δ Scuti instability strip, the simplest hypothesis is that they are excited by the κ-mechanism operating in the He II ionization zone as the δ Scuti stars are thought to be. *Dolez* and *Gough* (1982) found excitation in the 15th overtone (P = 15 min) in a simple A-star model. If this is the case, though, then why do the rapidly oscillating Ap stars pulsate in such high overtones and the δ Scuti stars in much lower ones? We might speculate that the magnetic field damps the lower overtone modes in the Ap stars, but then the lack of a magnetic field should not damp the higher overtone modes in the non-magnetic stars. I have searched for high-frequency oscillations in some δ Scuti stars without success. There are also a few Ap stars which show δ Scuti-like pulsation (*Weiss* 1983a,b; *Kreidl* 1987). How do those stars manage to pulsate in low overtone modes in the (presumed) presence of a global magnetic field?

Because of these problems *Shibahashi* (1983) and *Cox* (1984) suggested that the rapidly oscillating Ap stars are excited by magnetic overstability. If this were the case then we might expect to find rapidly oscillating Ap stars outside of the observed δ Scuti instability strip, especially hotter than the blue edge since the magnetic stars extend all the way up the main sequence to the early B stars. The positions of the rapidly oscillating Ap stars in Figure 1 suggest that some of them do lie outside of the δ Scuti instability strip, but from arguments given earlier, that is uncertain.

I have searched for rapid oscillations in many Ap stars much hotter than the blue border of the δ Scuti instability strip with only null results, but then these stars

are inherently brighter than the cooler Ap stars. A look at Figure 1 shows that an A0 main sequence star is about 1 mag brighter than an F0 main sequence star, hence, at a constant pulsation energy, the F0 star will have a signal-to-noise ratio 2.5 times greater than the A0 star.

Dolez, Gough, and *Vauclair* (1987) have suggested that helium concentrates at the magnetic poles in the rapidly oscillating Ap stars sufficiently to drive pulsation. In both their model and in Shibahashi's magnetic overstability, the alignment of the pulsation axis and magnetic axis is due to non-spherically symmetric driving at the magnetic poles.

The question of the pulsation mechanism in the rapidly oscillating Ap stars remains unanswered. *Shibahashi's* (1987) most recent review of the rapidly oscillating Ap stars contains a more extensive discussion of this question. In the year since that review was written there have been many observational advances. In the following sections I will summarise those new observations.

2. HD 24712 (HR 1217)

HR 1217 pulsates in six independent modes with frequencies which are approximately equally spaced (*Kurtz* and *Seeman* 1983). *Shibahashi* (1984), *Gabriel et al.* (1985) and *Shibahashi* and *Saio* (1985) pointed out that these frequencies could be interpreted as being due to pulsation in alternating even and odd l-modes with $n \sim 40$. Based on the assumption that the highest amplitude oscillations found by Kurtz and Seeman were due to dipole modes, Shibahashi and Saio suggested that the even-l modes were more likely to be radial than quadrupole modes based on the observed frequency spacings, theoretical A star models, and analogy with the solar p-mode spectrum. *Kurtz, Schneider,* and *Weiss* (1985) were able to show that none of the observed frequencies is due to pulsation in a radial mode.

Because of the similarity of the pattern of alternating even and odd l-modes in the amplitude spectrum of the variations in HR 1217 to that in the sun, it is very important to try to solve its frequency spectrum. That task is complicated by the fact that the natural frequency spacing is about 33 μ Hz which is close to 3 day^{-1}. Thus observations from a single site yield periodograms with frequencies and aliases hopelessly entangled. *Kurtz's* (1982) original analysis of this star suffered from this problem. HR 1217 also rotates with a period of $P_{rot} = 12.4572 \pm 0.0003$ day (0.92911 ± 0.00002 μ Hz) (*Kurtz* and *Marang* 1987a) and all of the pulsation frequencies are amplitude modulated with the rotation.

Hence, in order to solve the complex frequency spectrum of HR 1217, I organised an international collaboration to observe it as intensively as possible during 1986 October, November and December. That collaboration was successful. We (*Kurtz*

et al. 1988) obtained 365 hr of new observations of HR 1217 from eight observatories in Africa, Australia, Hawaii, North and South America and New Zealand. During one time-span of 36 days we had a 32% duty cycle, *i.e.* we averaged 8 hr of observations per day, with only two gaps as long as 24 hr during that span. The 33 μHz alias problem is almost eliminated in this new data set.

Analysis is now underway but, as of the time of this conference, it is not possible to report conclusively on the results of that analysis. As a preview I can say, however, that: 1) rotational sidelobes are observed. These may allow identification of the spherical harmonics of the pulsation modes and derivation of the rotational inclination and the magnetic obliquity. 2) The frequency of highest amplitude is the central one near 2.687 mHz, not the two on either side of it near 2.652 mHz and 2.721 mHz as *Kurtz* and *Seeman* (1983) found. If the central frequency is due to a dipole mode, then the frequency spacings which were previously so problematic now make sense. 3) There are indications of fine structure for the higher amplitude frequencies which may be due to the resolution of different spherical harmonics of the same parity, *i.e.* the resolution of $l=1$ and 3 or $l=2$ and 4, for example. If this is true, then we will have measurements of the second-order terms in the asymptotic p-mode dispersion relation – a potentially powerful structural diagnostic.

Including the new observations of HR 1217, we have a total of 579 hr of photometric observations obtained over a 6-year time span. If we can phase the data without alias ambiguity over the entire data set, then we will have a frequency resolution better than 100 pHz for the higher amplitude oscillations. This analysis should be completed and ready for public viewing during the next year.

3. HD 83368 (HR 3831)

New observations of HR 3831 in 1986 have allowed *Shibahashi, Kurtz,* and *Goode* (1988) to analyse all of the photometric observations obtained for this star from 1981 to 1986 without any alias ambiguity. Table 1 gives the 7 frequencies they derived.

The low frequency triplet, f_1, f_2 and f_3, is due to an oblique dipole pulsation. The proof of this lies in a plot of the pulsational phase of f_3 versus rotational phase which shows the π-radian phase reversals expected at quadrature (*Kurtz* and *Shibahashi* 1986). *Shibahashi, Kurtz,* and *Goode* (1988) show that this is the case over the entire 5-year time-span of the data they analysed.

Kurtz (1982) interpreted the high-frequency triplet, f_4, f_5 and f_6, as the three highest amplitude frequencies of a quintuplet associated with a quadrupole mode; that interpretation is still valid in terms of the generalized oblique pulsator model of *Dziembowski* and *Goode* (1985, 1986) and *Kurtz* and *Shibahashi* (1986).

The seventh frequency derived, $f_7 = 3f_3 + \Omega$. An initial speculation is that f_7 is part of a frequency septuplet due to pulsation in an $l = 3$ mode. Application of the generalized oblique pulsator model (*Shibahashi, Kurtz,* and *Goode* 1988) leads us to expect that $3f_3 - \Omega$ should be the highest amplitude frequency rather than $3f_3 + \Omega$ as is observed.

Table 1. A non-linear least-squares fit of the seven frequencies determined for the entire 1981-1986 data set for HD 83368

	frequency mHz	Amplitude mmag	Phase radians
f_1	1.42395445±0.00000002	2.098±0.021	-3.109±0.014
f_2	1.43207097±0.00000003	1.708±0.021	1.488±0.017
f_3	1.42801260±0.00000011	0.396±0.021	-2.824±0.074
f_4	2.85602537±0.00000011	0.419±0.021	-2.928±0.070
f_5	2.86414166±0.00000023	0.189±0.021	1.999±0.155
f_6	2.84790843±0.00000024	0.184±0.021	-1.102±0.159
f_7	4.28809664±0.00000041	0.108±0.020	-1.958±0.271

σ = 1.9796 mmag

$f_3 - f_1 = 4.05815 \pm 0.00011$ μHz
$f_2 - f_3 = 4.05837 \pm 0.00011$ μHz
$f_4 - f_6 = 8.11694 \pm 0.00026$ μHz = $2(4.05847 \pm 0.00013$ μHz)
$f_5 - f_4 = 8.11629 \pm 0.00033$ μHz = $2(4.05815 \pm 0.00017$ μHz)

$((f_4 - f_6) - (f_5 - f_4))/2 = 0.33 \pm 0.21$ pHz
$(f_3 - f_1) - (f_2 - f_3) = -0.22 \pm 0.16$ pHz
$2f_3 - f_4 = -0.17 \pm 0.25$ pHz
$f_7 - 3f_3 = 4.05884 \pm 0.00053$ μHz

$\Delta f = ((f_3-f_1)+(f_2-f_3)+(f_4-f_6)/2+(f_5-f_4)/2)/4 = 4.05829 \pm 0.00007$ μHz

$\Omega = 4.05829 \pm 0.00002$ μHz (Kurtz and Marang 1987b)

Note to Table 1: These parameters fit the relation
$\Delta B = \Sigma A_i \cos(2\pi f_i (t-t_0) + \varphi_i)$ where t_0 = JD 2444600.00000 .

Table 2. A non-linear least-squares fit of f_1, f_2, f_3 and f_4 to the JD2446256-6367 data for HD6532

	f mHz	A mmag	φ radians
f_1	2.396212±0.000002	0.98±0.02	0.57±0.09
f_2	2.402164±0.000002	0.74±0.02	2.45±0.08
f_3	2.408116±0.000003	0.60±0.02	-1.39±0.15
f_4	4.804299±0.000013	0.10±0.02	-0.17±0.60

σ = 1.47 mmag

$f_3 - f_2 = 5.952 \pm 0.004$ μHz
$f_2 - f_1 = 5.952 \pm 0.004$ μHz
$f_4 - 2f_2 = -0.029 \pm 0.013$ μHz

$\Omega = 5.952 \pm 0.006$ mHz (Kurtz and Marang 1987c)

Note to Table 2: These parameters fit the relation
$\Delta B = \Sigma A_i \cos(2\pi f_i(t-t_0)+\varphi_i)$ where t_0 = JD 2446256.00000 .

4. HD 6532

Kurtz and *Cropper* (1987) found an equally-spaced frequency triplet in the amplitude spectrum of 90 hr of photometric observations of HD 6532 obtained in 1985 from the South African Astronomical Observatory and the Mount Stromlo and Siding Spring Observatory. By plotting the phase of the pulsation versus rotational phase (determined from a new rotational ephemeris given by *Kurtz* and *Marang* 1987c), they showed that a π-radian phase reversal takes place at quadrature and hence the frequency triplet is due to oblique dipole pulsation. They also discovered the presence of the first harmonic of the low-frequency triplet at the remarkably high frequency of 4.804299 mHz, a point discussed further in Section 7. Table 2 gives the frequencies they derived.

An application of the generalized oblique pulsator model (*Dziembowski* and *Goode* 1985, 1986) indicates that the internal magnetic field strength in HD 6532

(*Kurtz* and *Cropper* 1987) is slightly less than that in HR 3831 (*Kurtz* and *Shibahashi* 1986). It is not known whether the same relationship will apply to the external magnetic field strengths. No magnetic measurements of HD 6532 (V = 8.45) have been made.

5. HD 60435

Matthews, Kurtz, and *Wehlau* (1986, 1987) obtained several hundred hours of photometric observations of HD 60435 from both the Carnegie Southern Observatory at Las Campanas in Chile and the South African Astronomical Observatory. They found a very rich spectrum of frequencies with a basic spacing of 25.8 μHz which they interpreted as a series of alternating even and odd *l*-modes much like that seen in the sun.

However, the behaviour of the oscillations in HD 60435 appears to be different from that in other rapidly oscillating Ap stars. The rotation period for HD 60435 is not known, but indications are that it is about 7-8 days. Frequencies are seen in the amplitude spectra of this star which increase and decrease in amplitude over a time-scale of about 7 days, but then they are not seen during the next 7-day time-span; they may or may not be re-observed later.

On JD2445728 Matthews, Kurtz, and Wehlau observed HD 60435 continuously for 13.5 hr. Four frequencies, 1.456 mHz, 1.431 mHz, 1.406 mHz and 1.382 mHz, were clearly present with a 25 μHz spacing and with amplitudes less than 1.6 mmag. At 1.367 mHz (25 μHz less than 1.382 mHz) on that night there is a local minimum in the amplitude spectrum, and yet the highest amplitude ever observed for a single frequency in a rapidly oscillating Ap star, 6.2 mmag, was at 1.37mHz in HD 60435 on JD2445383 (*Kurtz* 1984).

The dominant pulsation modes in HD 60435 have periods near 12 min, but other pulsation modes have been observed with periods near 15 min, 6 min and even 4 min. *Matthews, Kurtz,* and *Wehlau* (1987) suggest that these modes may be transient with lifetimes of only a few days. Such rapid growth and decay is not observed in other rapidly oscillating Ap stars and I continue to worry that the modes in HD 60435 may not be transient; the frequency spectrum may just be so complex that the modes appear transient due to complex beating patterns. I have made similar arguments concerning δ Scuti stars elsewhere in these proceedings.

The counter-argument to this line of thought is, of course, that the many hundreds of hours of observations of HD 60435 make the hypothesis of transient modes believable, and that, in turn, makes the same hypothesis believable in δ Scuti stars. I would like to analyse a data set for HD 60435 similar to the one discussed above for HR 1217 to test this hypothesis of transient modes further.

6. Non-linearities

Four of the twelve known rapidly oscillating Ap stars, HD 6532, HD 60435, HD 83368, and HD 101065, show the presence of the first harmonic of the principal frequency. In the case of HD 83368, as discussed in Section 3, the second harmonic is also present; in HD 60435 a second harmonic was observed during one week, but not again.

I originally argued (*Kurtz* 1982) that the first harmonic in HD 83368 is an independent $l=2$ pulsation mode which is excited by slight non-linearities in the principal $l=1$ mode. *Gabriel et al.* (1985) rejected that interpretation based on the fact that a $(2n,l=2)$ mode does not naturally have exactly twice the frequency of an $(n,l=1)$ mode. The original argument was, however, that the higher frequency mode is driven into a 2:1 resonance with the lower frequency mode. The natural frequency of the quadrupole mode is closest to that 2:1 resonance and hence that is the mode most likely to be excited.

Osaki and Shibahashi (private communication) also rejected the resonant driving hypothesis; they felt that the high frequency triplet in HD 83368 is just the first harmonic of the low frequency triplet and that it is expected that the first harmonic should look like a quadrupole mode. Further support for this hypothesis came from calculations by *Shibahashi* and *Saio* (1985) which showed that the rapidly oscillating Ap stars have frequencies near to, or even above, the critical frequency calculated from standard A-star models.

The highest frequency observed in a rapidly oscillating Ap star is the first harmonic in HD 6532 at 4.8 mHz. That frequency is very much greater than the critical frequency for even zero-age main sequence models and hence argues that it is not due to an independently driven mode. The same argument holds for the second harmonic in HD 83368.

However, even if these observed harmonics are non-linearities in the pulsation and not independent pulsation modes, they must belong to a different spherical harmonic than the principal mode and hence serve the same purpose diagnostically. In HD 83368 the arguments are very strong that the principal oscillation is an $l=1$ mode. The arguments are good that the first harmonic is a quadrupole mode and there are indications that the second harmonic is an $l=3$ mode. But, in any case, the second harmonic does *not* lie at three times the fundamental frequency; it lies at three times the fundamental frequency plus the rotation frequency; these harmonics do not have a simple ω, 2ω, 3ω etc. simplicity.

Three of the four rapidly oscillating Ap stars which show the presence of harmonics, HD 60435, HR 3831, and HD 101065, have principal frequencies near 1.4 mHz (P = 12 min). HR 1217 has its principal oscillations near 2.7 mHz (P = 6 min) and it definitely shows no evidence of any harmonic frequencies with amplitudes

above about 0.05 mmag. HD 134214 pulsates with only one frequency of 2.9 mHz which has a relatively large amplitude of 3.2 mmag; there is no evidence for any harmonic of that frequency. This makes it appear that there may be a high frequency limit to the harmonics; the second harmonics in HD 60435 and HR 3831 have periods of 4 min and the first harmonic in HD 6532 has a period of 3.5 min.

What does the presence of harmonics mean in the rapidly oscillating Ap stars? Are they independent pulsation modes? If so, in what way is the atmospheric structure of Ap stars altered from standard A-star models so that the critical frequencies are greater than 4-5 mHz? Do these harmonics represent non-linearities in the pulsation? If so, why are they seen in rapidly oscillating Ap stars with amplitudes of a few mmag and not in low-amplitude δ Scuti stars with amplitudes of many hundredths of a mag?

These harmonics should offer a great deal of information about the rapidly oscillating Ap stars and hence deserve some thought.

References

Baade, D., and Weiss, W.W. 1986 *Upper Main Sequence Stars with Anomalous Abundances*, IAU Coll. 90, ed. C.R. Cowley, M.M. Dworetsky, and C. Megessier, D. Reidel Publ. Co., Dordrecht, Holland, p. 234.

Breger, M., and Stockenhuber, H. 1983, Hvar Obs. Bull., **7**, 283.

Cox, J.P. 1984, *Ap. J.*, **280**, 220.

Dolez, N., and Gough, D.O. 1982, in *Pulsations in Classical and Cataclysmic Variables,* eds. J.P. Cox and C.J. Hansen, JILA, Boulder, p. 248.

Dolez, N., Gough, D.O., and Vauclair, S. 1987, in *Advances in Helio- and Asteroseismology,* IAU Symp. 123, in press.

Dziembowski, W., and Goode, P.R. 1985, *Ap. J.* (Letters), **296**, L27.

Dziembowski, W., and Goode, P.R. 1986, in *Seismology of the Sun and Distant Stars,* ed. D.O. Gough, D. Reidel Publ. Co., Dordrecht, Holland, p. 441.

Gabriel, M., Noels, A., Scuflaire, R., and Mathys, G., 1985, *Astr. Ap.*, **143**, 206.

Kreidl, T.J. 1987, *Lecture Notes in Physics,* **274**, 134.

Kurtz, D.W. 1982, *M. N. R. A. S.*, **200**, 807.

Kurtz, D.W. 1984, *M. N. R. A. S.*, **209**, 841.

Kurtz, D.W. 1986, in *Seismology of the Sun and Distant Stars*, ed. D.O. Gough, D. Reidel Publ. Co., Dordrecht, Holland, p. 417.

Kurtz, D.W., and Cropper, M.S. 1987, *M. N. R. A. S.*, in press.

Kurtz, D.W., and Marang, F. 1987a, *M. N. R. A. S.*, in press.

Kurtz, D.W., and Marang, F. 1987b, *M. N. R. A. S.*, in press.

Kurtz, D.W., and Marang, F. 1987c, *M. N. R. A. S.*, in press.

Kurtz, D.W., Matthews, J.M., Clemens, C., Cropper, M.S., Kawaler, S., Kepler, S.O., Kreidl, T.J., Martinez, P. Schneider, H., Seeman, J., Sterken, C., Sullivan, D., van der Peet, A., Wood, H. J., and Weiss, W.W. 1988, in preparation.

Kurtz, D.W., Schneider, H., and Weiss, W.W. 1985, *M. N. R. A. S.*, **215**, 77.

Kurtz, D.W., and Seeman, J. 1983, *M. N. R. A. S.*, **205**, 11.

Kurtz, D.W., and Shibahashi, H. 1986, *M. N. R. A. S.*, **223**, 557.

Kurtz, D., and Wegner, G. 1979, *Ap. J.*, **232**, 510.

Matthews, J., Kurtz, D.W., and Wehlau, W., 1986, *Ap. J.*, **300**, 348.

Matthews, J., Kurtz, D.W., and Wehlau, W. 1987, *Ap. J.*, **313**, 782.

Matthews, J.M., Wehlau, W.H., Walker, G.A.H., and Yang, S. 1987, preprint.

Schneider, H., Weiss, W.W., Kreidl, T.J., and Odell, A.P. 1987, *Lecture Notes in Physics*, **274**, 138.

Shibahashi, H. 1983, *Ap. J.* (Letters), **275**, L5.

Shibahashi, H. 1984, *Mem. Soc. Astron. Ital.*, **55**, 181.

Shibahashi, H. 1987, *Lecture Notes in Physics*, **274**, 112.

Shibahashi, H., Kurtz, D.W., and Goode, P.R. 1988, in preparation.

Shibahashi, H., and Saio, H. 1985, *Pub. A. S. J.*, **37**, 245.

Wegner, G., Cummins, D.J., Byrne, P.B., and Stickland, D.J. 1982, *Ap. J.*, **272**, 646.

Weiss, W.W. 1983a, *Astr. Ap.*, **128**, 152.

Weiss, W.W. 1983b, *Hvar Obs. Bull.*, **7**, 263.

Weiss, W.W. 1986, *Upper Main Sequence Stars with Anomalous Abundances*, IAU Coll. 90, ed. C.R. Cowley, M.M. Dworetsky, and C. Megessier, D. Reidel Publ. Co., Dordrecht, Holland, p. 219.

SPECTRAL LINE VARIATION DUE TO NON-RADIAL PULSATION*

W. W. Weiss
Intitute for Astronomy, Vienna, Austria
and
H. Schneider
Universitäts Sternwarte Göttingen, G.F.R.

Abstract

In astroseismology a reliable identification of modes is one of the fundamental problems where observations are of great importance. In the case of non-radially pulsating CP2 stars we tried to contribute to mode identification by applying high temporal and spectral resolution spectroscopy.

1. Introduction

The identification of individual peaks in power spectra of pulsating CP2 stars with radial or non-radial pulsation modes is important for the theoretical analysis concerning stellar structure and excitation mechanism. High speed photometry usually provides:

- pulsation frequencies
- pulsation amplitudes

In general, a solved frequency spectrum does not allow for an unambiguous identification of pulsation modes. It is therefore desirable to increase the amount of available information, for example by spectroscopy. Corresponding observations date back to 1984 (*Schneider et al.* 1987) as well as theoretical discussions of spectral line profile variations (*Odell* and *Kreidl* 1984; *Baade* and *Weiss* 1986).

To compute line profiles one has to take into account the superposition of

- velocity fields due to rotation
- velocity fields due to pulsation
- profile effects due to a magnetic field
- aspect effects

---

* Based in part on observations obtained at ESO, La Silla

Consequently, we have to deal with a large number of free parameters. In addition, we have to assume a homogeneous distribution of the element in the stellar atmosphere from which the spectral line under investigation originates.

In the best case, the contribution of some of these effects can be less than one percent in intensity. The requirements for corresponding spectral observations are therefore very high:

- Signal-to-Noise ratio of better than 1000
- Spectral resolution of better than 50 000
- Integration times of less than 1/10 of the pulsation period (*i.e.* 30 to about 90 seconds)
- Blend free spectral line

2. Observations

Currently, no equipment is available which would meet simultaneously all the requirements and we had to compromise. Our observations were obtained with the 1.4m CAT at ESO feeding a coude echelle spectrograph. A Reticon was used as a detector. We took many short exposures with each of the spectra having consequently only a poor S/N-ratio. To extract the required information we had two possibilities:

- Provide a simultaneous photoelectric photometry and coadd individual spectra with appropriate phases. Each of the mean spectra, averaged over a certain phase interval, allows to discuss line profile variations on a level of less than 1 percent.
- Fit a simple line profile to the individual low S/N spectra and discuss the temporal variation of the fit parameters. As was shown in *Baade* and *Weiss* (1986) a fit of a Gaussian profile might be useful despite the fact that a symmetric function is fitted to line profiles which in general will not be symmetric due to non-radial pulsation. However, the advantage is that only two free parameters are required and spectra of even poor S/N can be well fitted. These parameters allow to discuss variations of the line-centroid and line width and thus to restrict possible mode identifications (*Baade* and *Weiss* 1986)

3. α Cir

α Cir (HD 128898) was observed by us at ESO-La Silla during the nights from 1984 October 27/28 to 30/31. This CP2 star seems to be particularly suited since it seems to have a simple pulsation frequency spectrum (*Schneider* and *Weiss* 1983, *Weiss* and *Schneider* 1984; *Kurtz* and *Balona* 1984) with the main frequency being

6.8 hour^{-1}. About 1500 individual spectra were accumulated and reduced at ESO-Munich independently twice. Simultaneous 4-channel photometry was obtained with the 50cm Danish telescope and the Strömgren photometer.

Typical Gaussian fits are presented in Figure 1 for the line of CaI (multiplet 18) at 6471.9 Å. The spectrum at the top of this figure shows the mean spectrum deduced from all spectra obained during this night. Below this line we present ten mean spectra which are averaged for adjacent intervals of pulsation phases within a width of 0.1 in phase.

In order to detect possible systematic profile variation more easily, we plot in addition phase diagrams for bisectors which are computed for several intensity levels. In Figure 2 we present the results for the three CaI lines which originate from multiplet 18. As intensity level we have chosen a value (0.905) at the steepest part of the line profile, where effects due to pulsation will be more easily detectable.

As is evident from our Figure 1, a Gaussian fit is a reasonable approximation to the line profiles. We computed such fits for several individual spectral lines and for each of the individual, low S/N spectra. Line center and FWHM of the Gauss fit was Fourier analysed and power spectra were computed. As an example we present the results for the CaI line at 6471.9 Å in Figure 3. No clear positive evidence emerged for spectral line variations due to non-radial pulsation for all our reduction procedures.

4. γ Equ

γ *Equ* (HD 201601) was observed by us during the same period as was α Cir and analyzed in a similar way. In addition, T. Kreidl and A. Odell were able to observe this star with the Coude Feed at the KPNO on the night of 1984 July 08/09 (*Schneider et al.* 1987).Basically, we have obtained the same results as for α Cir.

5. HR 1217

Recently, *Mathews*, *Walker*, and *Wehlau* (1987) presented clear evidence for radial velocity variations in phase with pulsation for HR1217. They observed this star at Mauna Kea Observatory simultaneously in Johnson B and spectroscopically with the CFHT Coudé and Reticon equipment. Software modifications allowed them to read out the Reticon detector at certain pulsation phases and coadd the readout immediately in the computer. During the nights of 1986 Dec 15 and 16 observations were successful. For the first night, radial velocity variations with a peak-to-peak amplitude of about 100 m/s and in B of about 3 mmag are reported. The effects

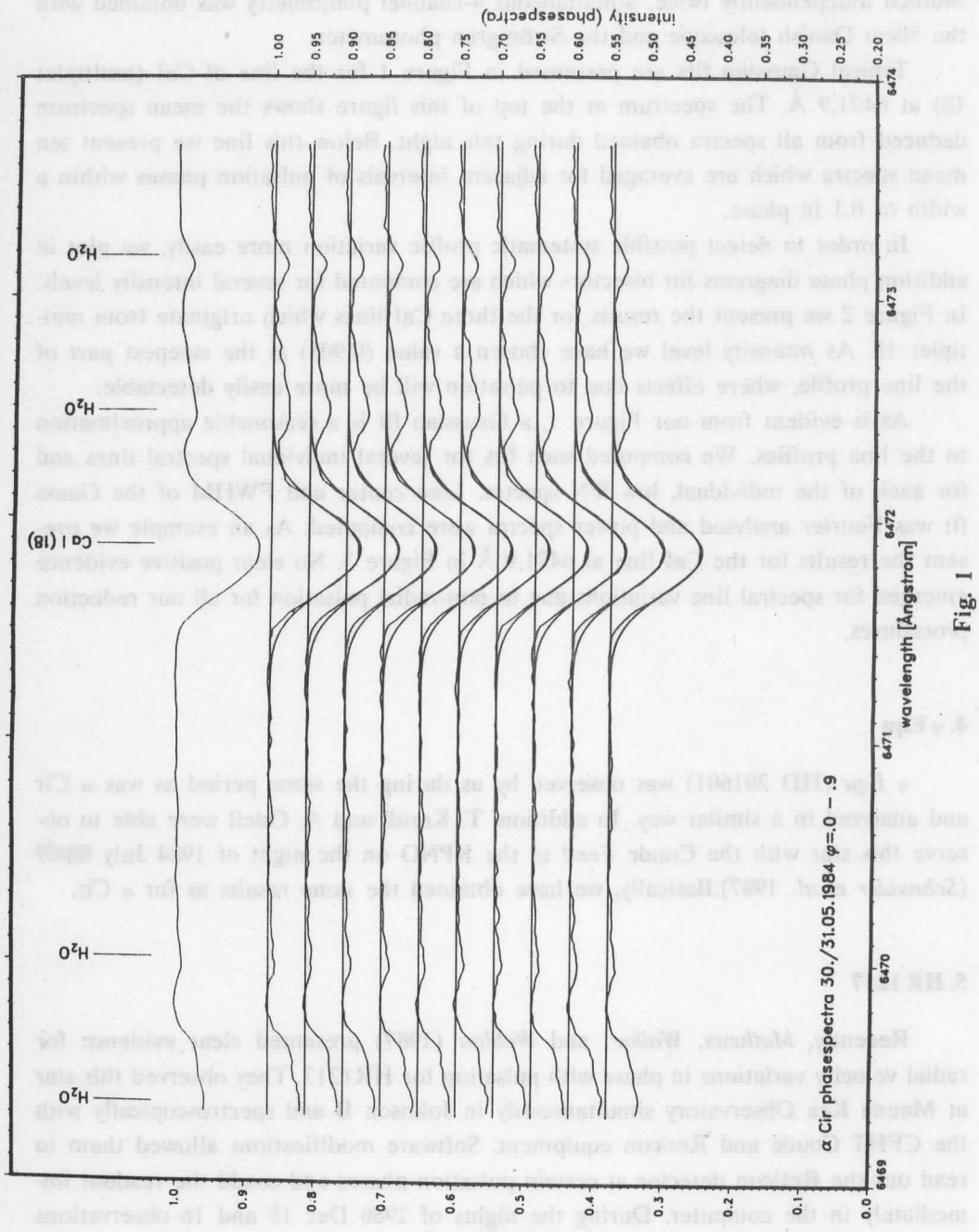
α Cir phasespectra 30./31.05.1984 φ=.0 – .9
intensity (spectrum)
intensity (phasespectra)
wavelength [Angstrom]
H2O
H2O
Ca I (18)
H2O
6469
6470
6471
6472
6473
6474

Fig. 1

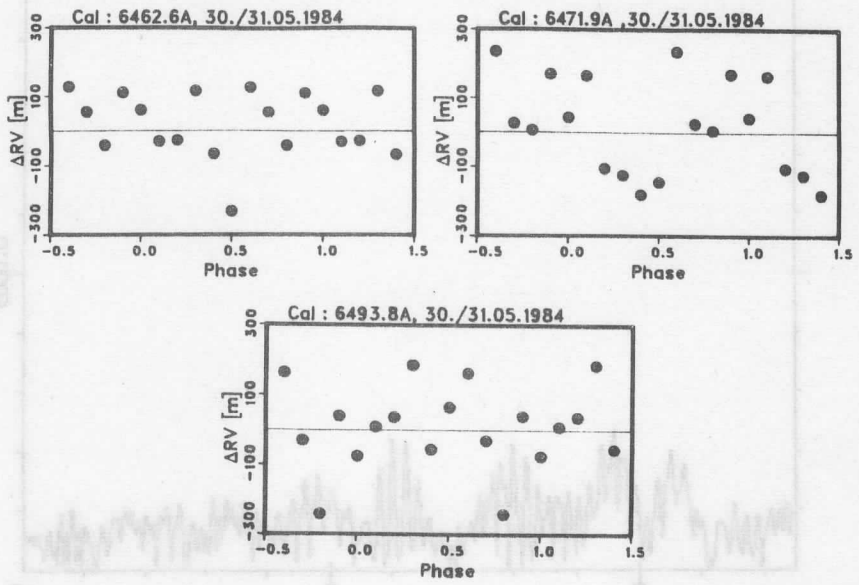

Fig. 2

were larger during the second night: 300 m/s and 7 mmag. In contrary to our procedure, Mathews et al. have obtained their RV values by crosscorrelating the entire spectra. Since several pulsation frequencies are present for this star (*Kurtz* 1988), the mentioned B-amplitude is related to what results from interference and it cannot be attributed to an individual pulsation mode.

6. Conclusion

Presently, different evidence are presented for spectrum variations due to non-radial pulsation of CP2 stars. One drawback in applying spectroscopic techniques to astroseismology of pulsating CP2 stars lies in the limits of the instrumentations currently available for observers. Access to larger telescopes definitely is needed even for such bright stars, in particular if one aims for a higher spectral resolution. Such efforts, however, seem to be justified in order to make use of as much information as possible which, on the other hand, is needed for an understanding of this group of stars.

Currently, the authors are preparing a more detailed and complete discussion of the observations at ESO for publication.

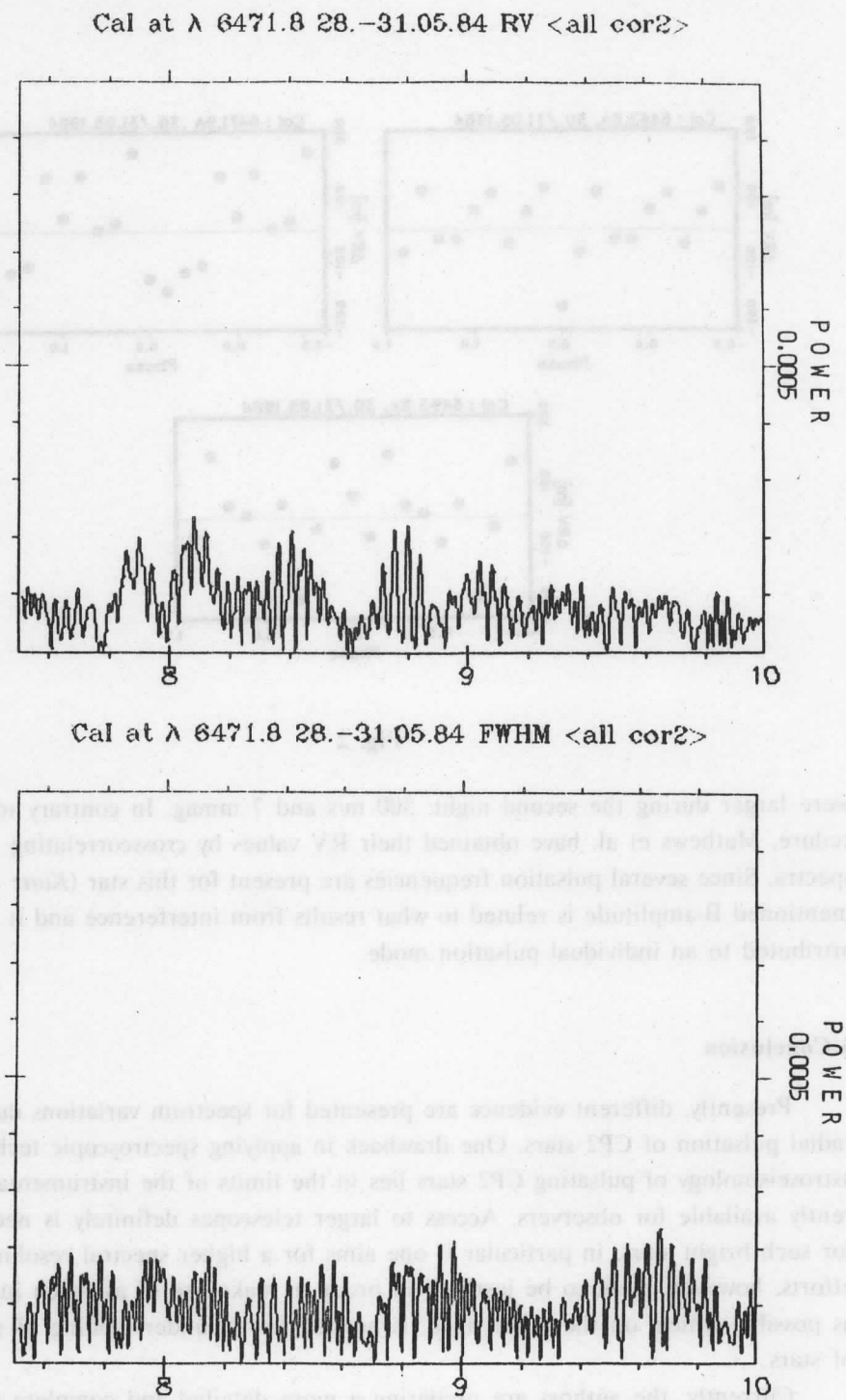
CaI at λ 6471.8 28.-31.05.84 RV <all cor2>
POWER
0.0005
8
9
10
CaI at λ 6471.8 28.-31.05.84 FWHM <all cor2>
POWER
0.0005
8
9
10
Frequency (1/h)

Fig. 3

References

Baade, D., and Weiss, W.W. 1986, *Astr. Ap. Suppl.*, **67**, 147.

Kurtz, D.W. 1988, this volume.

Kurtz, D.W., and Balona, L.A. 1984, *M.N.R.A.S.*, **210**, 779.

Mathews, J., Walker, G., and Wehlau, W. 1987, preprint.

Odell, A.P., and Kreidl, T.J. 1984, in *Theoretical Problems in Stellar Stability and Oscillations*, 25th Liege Internatl. Astrophys.Coll.,Liege, p.148.

Schneider, H., and Weiss, W.W. 1983, *Inf. Bull. Var. Stars*, No. 2306.

Schneider, H., Weiss, W.W., Kreidl, T.J., and Odell, A. 1987, in *Stellar Pulsation*, Lecture Notes in Physics, Vol. 274, Springer Berlin, p.138.

Weiss, W.W., and Schneider, H. 1984, *Astr. Ap.*, **135**, 148.

NONLINEAR EFFECTS IN LOW AMPLITUDE VARIABLES

W. Dziembowski
Copernicus Astronomical Center, Warsaw, Poland

Abstract

Resonant mode coupling is likely to play the dominant role in limiting the growth of unstable modes in main sequence stars and degenerate dwarfs. Within the framework of the lowest order nonlinear theory, I discuss possible forms of a finite amplitude development of the instabilities. Numerical results obtained for a ZAMS star model show that parametric excitation of linearly damped gravity modes must occur when the amplitude of linearly driven acoustic modes is of the order of 1–10 mmag. The nonlinear interaction of those modes may then result in the amplitude limitation at a similar level. Excitation of a higher frequency mode due to the 2:1 resonance can also limit the amplitude growth, but this is a much less important effect.

1. Introduction

Almost nine years ago at the workshop "Nonradial and Nonlinear Stellar Pulsation" I gave a review talk on the δ Scuti variables (*Dziembowski* 1980), I expressed then an idea that the difference in the behaviour between the dwarf and horizontal branch pulsators is a result of differences in the mechanism of amplitude limitation, which in the former case is the resonant mode coupling while in the latter one the nonlinear saturation of the driving mechanism.

It was my hope that we might soon achieve a basic understanding of variability in such stars like the δ Scuti or ZZ Ceti by applying the formalism of resonant mode interaction developed in different areas of physics to the problem of stellar pulsations. However, we are still far from the goal. In my review – which may be regarded as a progress report I still discuss possibilities and problems rather than definite results.

The observed properties of main sequence and degenerate variables are reviewed in this volume by *Kurtz* (1988a, b) and by *Winget* (1988). Outside of their discussions are β Cep and other upper main sequence stars. I will also not cover problems concerning specifically this group, but I believe that some results concerning amplitude limitation in the δ Scuti type reviewed later in this paper may be relevant to those objects as well.

2. Problems posed by observations

Calculations reveal that in main sequence stars and, even to greater extent, in white dwarfs pulsation instability usually appears in many modes of various radial orders, n, and various horizontal degrees, l. The number of observed periodicities in individual stars is much smaller and the deficit remains even after eliminating high-l modes ($l>4$) which suffer significant amplitude reduction due to the horizontal averaging. The patterns of observed frequencies are often difficult to understand on the ground of the linear theory. In δ Sct and δ Del, for instance, there are modes observed at frequencies corresponding to the fundamental radial mode and the second overtone, but there is nothing at the first overtone frequency. On the other hand, calculated growth rates exhibit a rapid increase with the mode order up to the fourth or fifth overtone.

This clearly demonstrates that in order to understand pulsational behaviour of low amplitude variables we need a nonlinear theory perhaps even more than in the case of high amplitude pulsating stars. The main question that such a theory must answer concerns the mechanism of amplitude limitation. In Cepheid-type variables the dominant role is played by the nonlinear saturation of the opacity mechanism. Both observations and model calculations show that this is done in most cases by a single pulsation mode even if there are more linearly unstable modes. It is clear that in the low amplitude variables nonlinear effects must operate in a different way, but I am less sure now than in 1979 that the resonant mode coupling is the only important effect in all these stars.

Of all types of variable stars in which we are interested here, δ Scutis are best understood. The vast majority of them have light amplitudes less than 0.1 mag. Those few with larger amplitudes are either giants or Population II objects of unknown evolutionary status. All these variables lie in the low luminosity extension of the Cepheid instability strip. However, most of the stars in this region of the H-R diagram appear to be nonvariable (*Breger*, 1979, 1982). Since the driving mechanism in δ Scuti stars is the same as in Cepheids we should expect that it may be saturated at similar amplitudes. Nonlinear calculations made by *Stellingwerf* (1980) showed that the amplitudes in the former case should be even larger. This excludes the possibility that the saturation occurs due to the observed modes. I rejected also a possibility that this is due to a large number of high-l modes which cannot be seen in light variations arguing that such modes should be seen in a form of line broadening. This hypothesis may be, however, worth reexamination because my argument relied on the assumption of the general relevance of the Stellingwerf calculations.

There is no convincing evidence for amplitude and period variations in the δ Scuti stars. Those reported in the literature were never confirmed by subsequent investigations. The theory of resonant mode coupling, as we will see in Section 4, pre-

dicts that a periodic amplitude and period modulation should happen fairly frequently. Discovery of such changes would be very important for our understanding of nonlinear effects in these stars.

The group of rapidly oscillating Ap stars discovered by *Kurtz* (1982) poses many intriguing questions to the theory. The oscillations seen in these stars cannot be regarded as an analogue of the solar "five minute" modes in spite of period similarity because the amplitudes are higher by three orders of magnitude and they are constant over a few years. In such a situation it is most likely that the oscillations in Ap stars represent linearly unstable modes with amplitudes limited by some very efficient nonlinear effect. Works by *Dolez* and *Gough* (1982) and by *Dolez, Gough,* and *Vauclair* (1987) demonstrated that high-order acoustic modes may be driven by opacity mechanism in appropriate stellar models. There are, however, uncertainties connected with the treatment of the magnetic field and element segregation effects in these stars.

In power spectra for some of the Ap stars the first harmonics of the main frequencies have been found. This is surprising because the amplitudes of the principal modes are of the order of 1 mmag. *Dziembowski* and *Goode* (1986) suggested that this may be a manifestation of the 2:1 near resonance between a linearly driven mode and a higher order damped mode. They speculated that the resonant coupling between such modes might be the needed amplitude limiting effect. I explore this possibility further in Section 4. The results, however, are not very encouraging.

Oscillating white dwarfs of ZZ Ceti type were once considered as an excellent playground for the mode coupling theory. Observers reported amplitude changes in several objects of this type occurring on the time scale of days which was consistent with the theoretical prediction (*Dziembowski* 1979). In particular in GD 385 such changes appeared to be well documented (*Fontaine et al.* 1980; *Vauclair* and *Bonazzola* 1981). However, an analysis by *Kepler* (1984) of long-time data showed that all drastic variations in the light curve result from the beating between modes of closely spaced frequencies. At present, there is no evidence for genuine amplitude changes in any oscillating white dwarfs.

This does not mean that the resonant coupling is unimportant in white dwarf oscillations. The amplitudes in these stars are closer to those found among δ Scuti-type than Cepheid-type variables, but differences in the kind of modes and in the driving mechanism means that the argument based on the size of amplitudes cannot be convincing. For a similar reason it is difficult to decide whether harmonics seen in the power spectra of many oscillating white dwarfs are abnormally enhanced which could be taken as evidence in favour of the mode coupling. In these instances where higher-order harmonics are seen the periodogram structure is very difficult to understand within the framework of the oscillation theory. Drs. Winget and Kepler called

my attention to three objects: GD154 (DAV), G191-16 (DAV), and PG131+489 (DBV) where such harmonics are seen. What is striking is that in all the cases the amplitude decreases with the order by a constant factor equal to 1/3. Since this behaviour concerns the light amplitudes in objects differing significantly in physical properties of their outer layers it seems inexplicable in terms of resonant coupling and saturation effects.

3.Formalism for the treatment of resonant mode coupling

3.1 The amplitude equations

We start by considering a simple case when only two or three modes take part in the interaction. We assume that the linear frequencies, σ, of the modes satisfy the relation

$$\sigma_a = \sigma_b + \sigma_c + \delta\sigma \quad ,$$

where subscripts *a, b, c* refer to the three modes, and $\delta\sigma$ is a small frequency mismatch. The case of two mode resonance corresponds to $b \equiv c$. Equations describing the evolution of the amplitudes of the involved modes may be written in the following form

$$dA_a/dt = \beta_a A_a - sHA_b A_c \exp(-i\delta\sigma t) \quad , \tag{1}$$

$$dA_b/dt = \beta_b A_b + HA_a A_c^* \exp(i\delta\sigma t) \quad , \tag{2}$$

where β is the linear growth rate, $s = 1$ and 1/2 for the three and two mode resonance, respectively, and H denotes the coupling coefficient, which is an integral involving products of eigenfunctions for the three modes. The amplitudes, A's, are understood as complex factors multiplying linear eigenvectors, $\mathbf{h}$'s, normalized in the following way

$$J = 2\sigma \int |\mathbf{h}|^2 dM_r = 1 \quad , \tag{3}$$

Since modes *b* and *c* appear in a symmetric way the equation for dA_c/dt may be obtained from equation (2) by interchange of *b* and *c* subscripts.

It will be assumed in this paper that H may be calculated with the use of the adiabatic eigenfunctions and therefore it is a real quantity. An explicit form of H valid in such a case may be found in my earlier paper (*Dziembowski* 1982). A formalism taking into account large departure from adiabaticity in the outer stellar layers, as well as nonlinearities in the driving rate was developed by *Buchler* and *Goupil* (1984). The equations retain then their form given by equations (1) and (2), but the expressions for β and H have to be modified.

Validity of our approximation regarding H depends on the relative contribution of the outer layers to its value. This contribution is certainly smaller than that to the value of β , and therefore it is reasonable to use fully nonadiabatic calculations to evaluate β while still using adiabatic approximation for H. The nonlinear modification of the driving rates is formally a higher order effect, but it may be important at relatively low amplitudes due to strong nonlinearities in the opacity formula, and it is indeed the dominant amplitude limiting effect in Cepheid-type variables.

Since H involves as a factor the integral of the three spherical harmonics, Y_l^m, the conditions for nonzero coupling may be written as follows

$$m_a = m_b + m_c, \quad l_3 = l_2 + l_1 - 2j, \quad j = 0, 1, \ldots < l_1/2 + 1 \tag{4}$$

where the subscripts 1, 2, 3 correspond in an arbitrary way to the different subscripts a, b, c. No such rigorous requirement exists for the radial orders except for asymptotic cases.

3.2 Onset of the resonant interaction

Suppose that only one of the lower frequency modes is linearly unstable, say $\beta_b > 0$, and $\beta_a < 0$. If the condition for the 2:1 resonance is fulfilled, $\sigma_a \approx 2\sigma_b$, then the growth of the mode will occur at any finite $|A_b|$. However, only if this amplitude is sufficiently large is the growth of mode b affected by the presence of mode a. The value B_{be} given below in equation (6) may be used for a rough estimate of this critical amplitude.

If mode a is the only linearly driven mode then an excitation of modes b and c may occur as a result of a parametric instability. If one may ignore the growth of mode a , then there is a simple criterion for the instability to occur which requires that $|A_a|$ exceeds a certain critical value, B_{ac}. The expression for B_{ac} is the same as for B_{ae} (see equation 5) except that β_a should be set to zero in q.

These are two clearly different situations. Consider, for instance, an unstable radial mode. Then, as follows from equation (4), the 2:1 resonant coupling may occur only with another radial mode while the parametric coupling is possible with any pair satifying the conditions $l_b = l_c$, $m_b = -m_c$. For all low degree modes the number of candidates for the former coupling is small and, therefore, we expect that this form of resonant interaction is less important. There are other important differences between these two types of resonances and we will discuss them later.

If any two modes are linearly unstable then the resonant excitation of the third one occurs in the same way as in the case of 2:1 resonance. We will see, however, that in such a situation the resonant mode coupling does not lead to constant amplitude oscillations.

3.3 Constant amplitude solutions

If one substitutes in equations (1) and (2) $A = B\ exp(i\alpha)$ then the problem is reduced to a real system of equations for B's and the common phase $\Phi = \delta\sigma t + \alpha_a - \alpha_b - \alpha_c$. When it is solved the individual phases may be found by means of a quadrature. The system has the following constant amplitude solution

$$B_a = B_{ae} = [\beta_b \beta_c\ (1+q^2)/H^2]^{1/2} , \tag{5}$$

$$B_b = B_{be} = B_{ae}(-\beta_a/\beta_b\ s)^{1/2} , \tag{6}$$

$$\text{ctan}\ \Phi = q = \delta\sigma/(\beta_a + \beta_b + \beta_c) . \tag{7}$$

These equations describe the solution of our problem only if all B's are real and therefore if β_b and β_c are of the same sign and of the opposite sign than β_a.

The constancy of B's and Φ implies that α's vary linearly with time in such a way that the observable frequencies satisfy exactly the resonance condition. This means that the presence of modes excited due to a resonance manifests itself in a similar form as a nonresonant nonlinear distortion of light and radial velocity curves.

3.4 Time-dependent solutions

A physical validity of the constant amplitude solutions is restricted by stability requirements. In general, there are three parameters determining the stability domain for the solutions described by equations (5) and (6). Here we choose $\mu_b = -\beta_b/\beta_a$, $\mu_c = -\beta_c/\beta_a$, and q. The results of stability analysis (*Wersinger et al.* 1980; *Dziembowski* 1982) may be summarized as follows. If $\beta_a < 0$ the constant amplitude solution is unstable unless $b \equiv c$ and $\mu_b < 1/2$. Thus, such a solution is valid only for the two-resonance provided that the damping is sufficiently strong. If $\beta_a > 0$, *i.e.* in the case of the parametric resonance, the explicit form of the stability criterion is somewhat more complicated and I will reproduce it here in the form valid if $\mu_b \approx \mu_c = \mu$

$$\mu > (1+\sqrt{3})/2 , \quad q^2 > (2\mu^2 - 2\mu + 1)/(2\mu^2 - 2\mu - 1). \tag{8}$$

Like in the previous case the first condition requires that the damping rate exceeds the driving rate in a certain way. The second condition requires that the frequency mismatch is not too small. Qualitatively, the general criterion is similar.

Numerical experiments by *Wersinger et al.* (1980) and by *Moskalik* (1985) have shown that in the stability domain the constant amplitude solutions are only asymptotic solutions of the problem, but outside this domain there is a large number of possibilities. In some range outside the stability boundary the asymptotic solution has the form of a simple periodic limit cycle, characterized by occurrence of single maximum and minimum within each period. Moving away from the boundary the solu-

tion goes through a series of bifurcations leading to an occurrence of increasing number of extrema, chaotic behaviour and finally to an unlimited amplitude growth.

Moskalik (1985) made a survey of simple periodic limit cycles arising in the case $\mu b = \mu c \gg 1$ which is of special interest in application to the δ Scuti stars. The period is then of the order of $1/\beta$ meaning 10^3-10^4 years if a is the lowest radial mode. Throughout most of the cycle an exponential growth of A_a occurs as described by the linear equation. *Moskalik* (1988) studied also the stability of such solutions.

3.5 Resonant coupling involving larger number of modes

Up to this point we have assumed that only at most three modes take part in the resonant interaction. We will see, however, in the following sections that an excitation of new modes or mode pairs is unavoidable in some cases. Generalization of the amplitude equations is easy, but very little is known about properties of their solutions.

Any of the modes involved in the three-mode interaction may be subject to the parametric instability leading to excitation of a new low-frequency pair. In particular for given unstable mode a there are always many (b, c) pairs characterized by similar values of $\delta\sigma$, H, and β. It is, thus, important to consider the possibility that many such parallel pairs exist in the asymptotic solution. The amplitude equations in this case are

$$dA_a/dt = \beta_a A_a - \Sigma s_k H_k A_{bk} A_{ck} \exp(-i\delta_k \sigma t) \quad , \tag{1a}$$

$$dA_{bk}/dt = \beta_{bk} A_{bk} + H_k A_a A_{ck}^* \exp(i\delta_k \sigma t) \quad , \tag{2a}$$

where $k = 1, \ldots, K$, and K is the total number of (b, c) pairs included. It may be shown that only for $K = 1$ and 2 has the domain of constant amplitude solutions a nonzero measure in the parameter space. The case of $K = 2$ was studied by Moskalik (to be published) who found that stable solutions exist in a very restricted domain and that the amplitude of mode a is then close to that obtained for $K = 1$.

In order to describe interaction with modes generated in a cascade-type instability of modes b and c we have to add new nonlinear terms in equation (2) or (2a) and supplement the system with equations for amplitudes of the new modes. It is likely, however, that a statistical approach analogous to the "random phase" approximation will be developed to treat this complicated problem.

There may also be a need to consider simultaneous interaction of a given unstable mode with few higher frequency damped modes. In particular, in the case of high-order acoustic mode instability the 2:1 resonance condition may be fulfilled for few such modes. Required modification of equations (1) and (2) consists in allow-

ing for larger number of modes b. In this case there is no restriction on the number of such modes in the constant amplitude solutions.

4. Parametric instability in Delta Scuti oscillation

The modes observed in this type of variables are acoustic modes of low orders and degrees. The linear stability analysis shows that such modes are indeed driven by the opacity mechanism. Here we will discuss how the development of the instability may be affected by a parametric excitation of gravity-mode pairs. This discussion is largely based on the already published results by *Dziembowski* and *Królikowska* (1985, DK).

Equation (5) may be used to evaluate the surface amplitude of a linearly unstable mode, a, corresponding to onset of the parametric instability to the growth of modes b and c. This critical amplitude may be given in the following form

$$Q_a = \{\beta_b\beta_c\ [1+(\delta\sigma)^2/(\beta_b+\beta_c)^2]/F_a^2\}^{1/2} \quad , \tag{9}$$

where Q denotes the surface average value of the relative radius amplitude, and $F_a = H/\sqrt{J_a}$ is calculated with the more standard normalization of the eigenvectors – $h_r(R) = RY_l^m$. The corresponding light amplitude may be evaluated with the help of linear nonadiabatic eigenfunction upon integrating over the disk. For nonradial modes, however, this amplitude is aspect-dependent. In this formula and throughout the whole paper we use $\sqrt{(4\pi G<\rho>)}$, where $<\rho>$ is the mean stellar density, as the frequency unit.

In the considered case modes b and c must necessarily be gravity modes. Bearing in mind the freedom in the choice of their l-degrees we must expect that for a given mode a there are many (b, c) pairs leading to small values of $\delta\sigma$. The critical amplitude of mode a, Q, should be, thus, understood as the minimum value in the whole set calculated for various pairs. Modes of relatively high degree and therefore invisible in the light and radial velocity measurements are most likely to be excited. There are more of them and they have denser frequency spectra. An upper limit for the l-values that need to be considered is determined by the linear damping effect which increases with the gravity mode degrees.

Properties of gravity modes are determined primarily by the behaviour of the Brunt-Väisälä frequency, N, in the star interior. In our units this frequency is given by the following expression

$$N^2 = m\ u\ /\ [n_p-(n_p+1)/\Gamma]\ /\ 3x^3 \quad , \tag{10}$$

where m is the fractional mass, $u = -d\ ln(p/\rho)\ /\ d\ ln\ (r)$, n_p is the local polytropic index, Γ is the adiabatic exponent, and x is the fractional radius. Through most of the outer envelopes of stellar models appropriate for the δ Scuti stars we have $m \approx 1$,

$\Gamma \approx 5/3$, $n_p \approx 3.5$, and $u \approx 1/(1-x)$. This implies that N reaches a minimum value of about 1.6 at $x = 0.75$. This is a general property of the models. The behaviour of N below the minimum changes, however, with the evolution. In ZAMS stars the inward increase of N is terminated at $x \approx 0.3$. Higher mass concentration in evolved stars implies that this termination occurs deeper and that the maximum values of N are higher.

A gravity mode with frequency σ may be trapped only in the region where $N > \sigma$. The existence of the minimum in N causes that modes with frequencies above this minimum value may be trapped in two separate cavities. This gives rise to two sets of modes of vastly different properties – "the outer" and "the inner" g-modes. The former ones are much stronger coupled (larger F-values) to the acoustic modes but they are also much more nonadiabatic. In the model used by us (DK) the role of these two types of modes turned out to be comparable.

Frequencies of the g-modes leading to small values of Q should satisfy the following approximate relations

$$l_b \approx l_c, \quad \sigma_b \approx \sigma_c \approx \sigma_a/2 \quad .$$

The first of them follows from equation (4) if we assume $l_a > l_b$, the second from considering the behaviour of F for high order g-modes. Since the dimensionless frequencies of radial modes are essentially constant for all δ Scuti star models, we may now specify that the interaction with the two sets of gravity modes begins with p_4-mode (here we assume a more standard classification of radial modes implying $f \equiv p_1$ rather than $f \equiv p_0$ used in DK).

In DK we gave results of the critical amplitude estimates for all unstable acoustic modes of $l \leq 2$ in a 1.4 $M_\odot$ star on ZAMS. We did not calculate actual values of Q because they would be too sensitive to the precise frequency values. Instead we assumed some uncertainty in the frequencies and calculated probability distributions. We found the following mean values of the critical light amplitudes for p_1 to p_5 radial modes: 13.4, 6.3, 3.6, 4.9, and 2.6 mmag. For $l = 1$ modes we got somewhat larger and for $l = 2$ modes somewhat smaller values than those.

For the first three modes the critical amplitudes are very close to the equilibrium amplitudes because in this case $|\beta_b + \beta_c| \gg \beta_a$. The interacting gravity modes propagate in nearly the whole interior, but virtually all the dissipation arises in the outermost layers. The most probable l-values are in the range 20–50. The constant amplitude solutions are in more than 80 percent cases stable. We found these results very encouraging for the hypothesis that the parametric resonance controls the nonlinear development of pulsation instability in these stars. The amplitudes were perhaps somewhat too large, but in the subsequent investigation (*Dziembowski et al.* 1988; *Królikowska* and *Dziembowski* 1988) it was shown that inclusion of the effects of rotation leads to their further lowering. The theory explains in a natural way the

frequent domination of the fundamental mode in spite of its very low excitation rate, and it accounts for coincidence of pulsating and nonpulsating stars in the same domain of the H-R diagram.

The situation is more complicated in the case of the higher order p-modes. The coupling to the inner gravity modes virtually never leads to a stable constant amplitude solution because these modes are very adiabatic and the first of the stability conditions given in equation (8) is not fulfilled. Taking into account the coupling to the outer *g*-modes we still find that the instability should occur in a predominant number of cases. The other complicating factor is a likely excitation of new *g*-mode pair as a result of the parametric instability of the three modes present in the original interaction. There is also a problem with the validity of the adiabatic approximation in the treatment of the interaction with the outer *g*-modes.

All δ Scuti stars with relatively large amplitude and therefore best studied are evolved objects. It is, thus, very important to see how the resonant interaction changes with the star's evolution. The effect of an increase of the mass concentration on the radial modes is small and consists in some increase of the driving rates. There is an opposite effect on nonradial *p*-modes of low degree, because they may penetrate the deep interior where they behave like gravity modes. The resonant *g*-modes except for the outer ones are subject to large modification. Their energies become more concentrated in the inner region, and this leads initially to a decrease in the damping rates. Shortly before the hydrogen exhaustion in the centre this tendency is reversed because the dissipation in the interior begins to dominate.

A consequence of the changes in the energy distribution for various modes is an increasing difference between the coupling coefficient calculated for radial and nonradial acoustic modes. A stronger coupling of the latter with the linearly damped gravity modes may help us in understanding why nonradial modes are not seen in some more evolved objects. However, as found by Królikowska (personal communication) even radial modes have smaller critical amplitudes than in ZAMS star models, because the effect of F decrease is overcompensated by a decrease of β and an increase of the density of the *g*-mode frequency spectra. Thus, the theory postulating an excitation of a single *g*-mode pair cannot account for the basic observational fact that there is a strong tendency for pulsation amplitudes to increase with the evolution.

The calculations made by Królikowska revealed, in fact, that the constant amplitude solution in evolved star models is likely to be unstable according to the criteria given in equation (8). Moreover, Moskalik (personal communication) found that an excitation of new *g*-mode pairs is inevitable because the coupling between *g*-modes is very much stronger than that involving one radial mode. Thus, we should expect that each of the unstable modes is coupled to a large number of gravity modes.

It should be stressed that even in the case of ZAMS stars where the constant amplitude solutions are most often stable it is possible that actually the amplitudes are limited as a result of a multimodal interaction. Therefore progress in the theory of such interactions is essential for our understanding of the observed properties in the whole type of δ Scuti variables. Studies of a long-term amplitude behaviour should provide important constraints for the theory.

5. The 2:1 resonance

The resonant coupling of an unstable mode to a higher order stable mode may result in an amplitude limitation in various forms, but we consider here only the most likely case of time-independent solutions. A convenient expression for the surface amplitude, Q , of mode b may be obtatined from equations (5)–(7). Using the same normalization as in the previous section we get

$$Q = \{-\beta_a \beta_b \ [1 + (\delta\sigma)^2/(2\beta_b + \beta_a)^2]/F_b\}^{1/2} \quad , \qquad (11)$$

where $F_b = H/\sqrt{(2I_b)}$. It is worth noting that if the damping rate is much larger than the driving rate then $Q_b \sim \sqrt{\beta_b}$ in the present case while in the case of parametric resonance the amplitude of the unstable mode is independent of the driving rate.

In Table 1 we give values of the parameters appearing in equation (11) for the resonant pairs of acoustic modes in the same stellar model as used in DK. We give also there the period of the lower frequency mode, P_b, radial orders, n, and factor f converting Q-amplitude into the light amplitude. In the list all resonant pairs in the vicinity of $\delta\sigma = 0$ involving $l_b = 0$ and 1 modes are included.

Table 1. The 2:1 resonances between p-modes in a ZAMS δ Scuti star model.

P_b (min)	σ_b	l_b	l_a	n_b	n_a	$\delta\sigma$	F	β_b	β_a	f_b
41.0	2.58	0	0	2	5	-0.062	0.02	2.0E-7	-2.1E-5	13
33.4	3.17	0	0	3	8	0.127	0.19	1.4E-6	-6.4E-4	15
14.8	7.14	0	0	9	19	-0.045	8.8	-1.8E-3	-3.7E-2	54
13.6	7.82	0	0	10	21	0.042	16.3	-3.6E-3	-4.5E-2	63
15.6	6.79	1	0	8	18	-0.070	14.2	-1.1E-3	-3.3E-2	61
14.2	7.46	1	0	9	20	0.037	23.4	-2.6E-3	-4.1E-2	72
14.2	7.46	1	2	9	19	-0.051	25.0	-2.6E-3	-4.1E-2	72
13.0	8.14	1	2	10	21	0.034	32.1	-4.7E-3	-4.7E-2	81

The resonance between p_2 and p_5 radial modes was of interest as a possible explanation of the conspicuous absence of the former one in two δ Scuti-type stars. Using the data from Table 1 in equation (11) we find 4 mmag for the light amplitude of this mode. Having in mind the fact that the model is not really appropriate

for these two objects we should allow for some parameter variations. The most important is uncertainty in the frequency mismatch. Assuming, for instance, an exact resonance we get 3 mmag for the amplitude. This means a significant amplitude limitation, but requires a very unlikely coincidence. The primary reason for this disappointing result is the low value of F in this case. The resonance between p_3 and p_8 modes does not lead to interesting values for the amplitude, either.

In our model all higher order modes are damped and therefore we cannot apply equation (11) to evaluate the amplitudes. It is, however, of interest to ask what should be the order of magnitude of the driving rates to imply the light amplitudes of the order of 1 mmag as observed in the rapidly oscillating Ap stars. The answer is that they should be by a factor of 10^{-4} to 10^{-3} smaller than the listed damping rates. Models proposed for the A_p stars are somewhat evolved and more massive than our model, but it cannot be expected that modifications in f-values and other parameters may reverse this conclusion. Thus, also in the present case we require an unlikely event which is now an essentially exact compensation of driving and damping effects. Moreover, if this is indeed the case we should expect that the nonlinear saturation of the driving mechanism is important at the observed amplitudes.

6. Conclusions

We are far from understanding the observed properties of the low amplitude variables. There are still considerable uncertainties on the level of the linear nonadiabatic theory. In certain types of stars we do not even know the driving mechanism. In those cases like δ Scuti or ZZ Ceti types where we think we understand the instability mechanism the question which of the nonlinear effects controls the amplitude limitation must be regarded as open. Except of the work by *Stellingwerf* (1980) concerning selected δ Scuti star models we do not have nonlinear calculations which would allow us to reject conclusively a collective saturation of the driving mechanism as the cause of the amplitude limitation.

The hypothesis that the resonant mode coupling is the dominant nonlinear effect has several attractive features. We have seen that the parametric excitation of gravity modes in δ Scuti stars occurs at the amplitudes of the unstable modes less than observed and, in most cases, less than the detection limit. The calculated amplitudes are sensitive to the model properties but they are not directly related to the linear growth rates; this feature appears consistent with observations. Furthermore, the importance of the g-modes is suggested by the observational evidence that the evolutionary status rather than the effective temperature determines pulsational properties in the δ Scuti variables, because these modes are primarily affected by the evolution.

There are also problems with this hypothesis. Consequences of the resonant mode coupling are easy to predict only if an unstable acoustic mode is coupled to a single gravity-mode pair, but this remains as a possibility only in the case of the lowest order *p*-modes in unevolved stars. In the remaining cases an excitation of a large number of the pairs must occur.We know that constant amplitude solutions do not exist in such cases, but there is no theory to handle the complicated time-dependent problem. Moreover, it is not clear how the apparent constancy of amplitude may then be explained.

We have seen that the 2:1 resonance cannot account for a systematic amplitude limitation, although it remains a viable explanation of an abnormal enhancement of the harmonics in power spectra. The problem why all known Ap stars have so small amplitude must, thus, be approached in a different way. The possibility that the parametric resonance is also important in this case deserves an investigation.

References

Buchler, J.R., and Goupil, M.J. 1984, *Ap. J.*, **279**, 394.

Breger, M. 1979, *Publ. A. S. P.*, **91**, 5.

Breger, M. 1982, *Publ. A. S. P.*, **94**, 845.

Dolez, N., and Gough, D.O. 1982, in *Pulsations in Classical and Cataclysmic Variables*, eds. J.P. Cox and C.J. Hansen, (JILA: Boulder), p. 441.

Dolez, N., Gough, D.O., and Vauclair, S. 1987 in *Advances in Helio- and Asteroseismology*, IAU Symp. No. 123, p. 291.

Dziembowski, W. 1979, in "White Dwarfs and Variable Degenerate Stars", eds. H. Van Horn and V. Weidemann, IAU Coll. No. 53, p. 392.

Dziembowski, W. 1980, in *Nonradial and Nonlinear Stellar Pulsation*, eds. H. Hill and W. Dziembowski, Springer: Berlin, p.22.

Dziembowski, W., 1982, *Acta Astr.*, **27**, 95.

Dziembowski, W., and Goode, P.R. 1986, in *Seismology of the Sun and Distant Stars*, ed. D.O. Gough, Reidel: Dordrecht, p. 441.

Dziembowski, W., and Królikowska, M. 1985, *Acta Astr.*, **35**, 5. (DK)

Dziembowski, W., Królikowska, M., and Kosovichev, A., 1988, *Acta Astron.*, **38** (in press).

Fontaine, G., McGraw, J.T., Coleman, L., Lacombe, P., Patterson, J., and Vauclair, G. 1980, *Ap. J.*, **239**, 898.

Kepler, S.O. 1984, *Ap. J.*, **278**, 754.

Królikowska, M., and Dziembowski, W. 1988, in these proceedings.

Kurtz, D.W. 1982, *M. N. R. A. S.*, **200**, 807.

Kurtz, D.W. 1988a, in these proceedings.
Kurtz, D.W. 1988b, in these proceedings.
Moskalik, P. 1985, *Acta Astr.*, **35**, 229.
Moskalik, P. 1988, in these proceedings.
Stellingwerf, R.F. 1980, in *Nonradial and Nonlinear Stellar Pulsation*, eds. H. Hill and W. Dziembowski, Springer: Berlin, p. 50.
Vauclair, G., and Bonazzola, S. 1981, *Ap. J.*, **246**, 947.
Wersinger, I.M., Finn, I.M., and Ott, E. 1980, *Phys. of Fluids*, **23**, 1142.
Winget, D.E. 1988, in these proceedings.

LIMITING AMPLITUDE EFFECT OF THE PARAMETRIC RESONANCE IN ROTATING MAIN SEQUENCE STARS

M. Królikowska and W. Dziembowski
Copernicus Astronomical Center, Warsaw, Poland

Abstract

We give limits for amplitudes of pulsations imposed by parametric resonance in rotating δ Scuti type stars. Calculations were performed for $M = 1.4\ M_\odot$ and a chemical composition $X = 0.7$, $Z = 0.02$. We consider the three lowest radial excited acoustic modes. It is shown that rotation above ≈ 20 km/s significantly reduces pulsational amplitudes.

1. Introduction

It is very difficult to separate influence of rotation, metallicity and evolution on pulsational behaviour of δ Scuti type stars. It seems, however, that there exist two known and distinctly visible observational facts which show that pulsational amplitude decreases due to rotation.

First, *Breger* (1969, 1979) showed, that in luminosity classes III and IV rotational velocities are significantly lower for pulsating stars than for the constant ones. However, among main sequence stars this tendency is reversed. This is because there are many slowly rotating (so called Am) stars which do not pulsate as a result of gravitational helium settling. After removal of metallic stars from the sample the rotational velocities of variables become slightly smaller than nonvariable.

Second (*Breger* 1982; *McNamara* 1985), the δ Scuti stars with rotational velocities $V_{rot} < 40$ km/s have much larger amplitudes than variables with higher rotation.

The aim of this paper is to show that the parametric resonance in rotating stars explains in a natural way both observational relationships.

2. Probability of parametric resonance in rotating stars

In this case parametric resonance results from interaction of an excited acoustic mode with two damped gravity modes.

We have generalized the formalism for the treatment of the parametric resonance in nonradially oscillating stars to include effect of rotation (*Dziembowski, Królikowska* and *Kosovitchev* 1988).

Using as a basis the linear displacement eigenfunctions for the three involved modes we obtain the amplitude equation in the same form as in the case of no rotation (*Dziembowski* and *Królikowska* 1985). A slow uniform rotation has a negligible effect on the coupling coefficient, ν, but this is not generally true if the rotation is nonuniform. In our investigation we allowed for variation of the angular velocity Ω with the radius r, but we restricted the form of this dependence which made possible to ignore modification of the coupling coefficient.

Thus, we assume that the rotation is only weakly nonuniform in the sense that:

$$m\ \Delta\Omega(r)/\bar{\omega} \ll 1 \quad , \tag{1}$$

where m is the azimuthal number, $\bar{\omega}=\omega+m\Omega_0$, Ω_0 is the average value of Ω, and $\Delta\Omega(r)$ describes deviations from uniform rotation. Furthermore, if we assume that in the propagation zone the Brunt-Väisälä frequency is much larger than $\bar{\omega}$ we obtain

$$\bar{\omega}_{n,l,m} = \bar{\omega}_{n,l,o} + m^2 <\Delta\Omega>^2/\bar{\omega}_{n,l,o} \quad , \tag{2}$$

where $\bar{\omega}_{n,l,o}$ denotes eigenfrequency without rotation, subscripts n, l, m identify the mode.

In the case of uniform rotation it is easy to show that

$$\bar{\omega}_{n,l,m} = \bar{\omega}_{n,l,o} + [m\Omega - m^2\Omega^2/\bar{\omega}_{n,l,o}] / l^2 \quad , \tag{3}$$

When we neglect the temporal variation of the amplitude of acoustic excited mode ("1") the criterion for the parametric excitation of two gravity damped modes ("2" and "3") may be written in the form

$$Q_1 > 2\ [\ \gamma_2\gamma_3\ (1+\Delta\omega/(\gamma_2+\gamma_3))\ ]^{1/2}/\nu \quad , \tag{4}$$

where Q_1 is understood as mean value of $\Delta R/R$ in $(4\pi G<\rho>)^{1/2}$ units, and ν is the normalized coupling coefficient, γ_2, γ_3 are the linear driving rates (for damped modes are negative), $\Delta\omega=\omega_a-\omega_{bo}-\omega_{co}-2m^2\varkappa$ is the frequency mismatch,

$$\varkappa = (\Omega^2/\omega_a)\ /\ l^2 \qquad \text{if } \Omega = \text{const.},$$

$$\varkappa = (\Omega^2/\omega_a)<\Delta\Omega^2>/<\Omega>^2 \qquad \text{if } \Omega = \Omega(r) \quad .$$

In order to determine the critical amplitude of acoustic excited mode we have to consider all the mode pairs ("2" and "3") satisfying the following relation

$$l_3 = l_2 + l_1 - 2k \quad , \quad \text{where} \quad k \leq l_1 \quad ,$$

which is implied by the $\nu \neq 0$ condition. For selected numbers l_2, l_3 we have few mode pairs identified by their radial numbers n which contribute to the resonance probability.

The most important effect of rotation lies in frequency splitting of modes differing by azimuthal number m. Larger number of pairs as compared to the non-rotating case satisfying $m_3 = -m_2 + m_1$ relation ($m_2 = -l_2, \ldots, 0, \ldots, l_2$) facilitates more precise frequency fitting.

In the following we consider only radial acoustic mode (ν is m-independent) and assume $\gamma_2 = \gamma_3$. From relation (4) we can find that for given pair the instability occurs for the mode amplitude "1" larger than Q. After some calculation one can show that

$$p_{l,j}(Q) = \begin{cases} - \quad 0 & \text{if } \lambda \leq \kappa \,, \\ (l+1)\lambda/\delta_n\omega - (\lambda^2 - \kappa^2)/(4\kappa\delta_n\omega) & \text{if } \kappa \leq \lambda \leq (2l-1)\kappa \,, \\ - \quad (l\lambda - \kappa l^2)/\delta_n\omega & \text{if } \lambda \geq (2l-1)\kappa \,, \end{cases} \qquad (5)$$

where $p_{l,j}(Q)$ is the summed over m probability of resonance at amplitude Q for given l, subscript j describes different combination of radial numbers n for given l, $\lambda = (Q^2\nu_j^2 - 4\gamma_l^2)^{1/2}$ and $\delta_n\omega = \omega_{n+1,l,0} - \omega_{n,l,0}$. To calculate the total probability of resonance we replace the sum over l by an integral. Since $p_{l,j}(Q) \ll 1$ we can write

$$P(Q) = 1 - \exp[\, -\textstyle\int l \sum_j p_{l,j}(Q)\mathrm{d}l \,] \quad . \qquad (6)$$

Equation (6) can be written in explicit form.

We give numerical results corresponding to the same ZAMS star model as in *Dziembowski* and *Królikowska* (1985). This model is characterized by $M = 1.4M_\odot$, $X = 0.7$, $Z = 0.02$.

In Figures 1 and 2 we show $P(Q)$ for the fundamental radial mode in the case of uniform and nonuniform rotation, respectively. Qualitatively the behaviour is the same for the first and the second overtones. The lowest curves in both figures are indistinguishable from the curves in the non-rotating case. One can see, an appreciable effect of rotation begins at $v_{rot} \approx 20$ km/s.

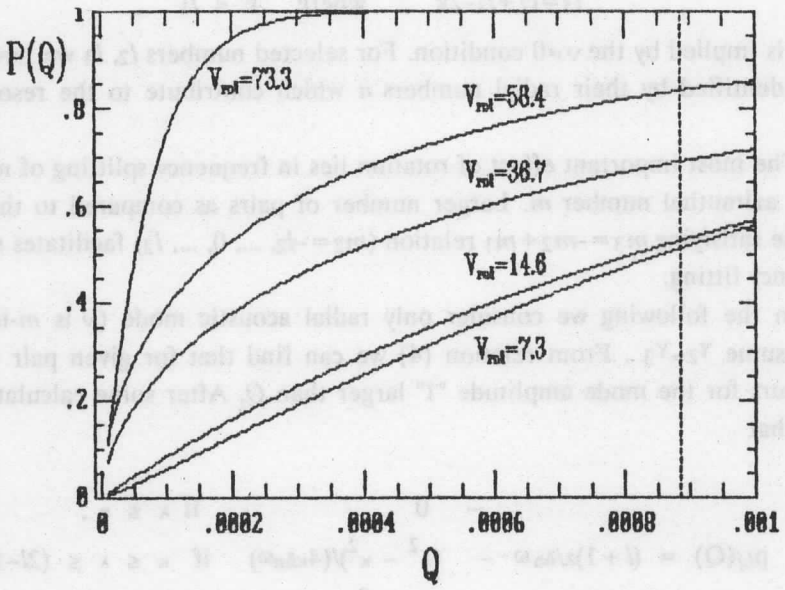

Fig. 1. Probability that the parametric instability of the fundamental radial mode occurs at the amplitude $\Delta R/R$ less than Q for various equatorial velocities of rotation, $v_{rot} = \Omega R$. The model represents $M = 1.4 M_\odot$ star on Population I ZAMS. Uniform rotation is assumed. The vertical line corresponds to A_V amplitude of 0.01 mag.

The r-dependence in $\Omega(r)$ is important if η exceeds 0.1 . We argue that it is plausible that the nonlinear interaction between a linearly unstable acoustic mode and two linearly damped gravity modes leads to the constant amplitude pulsation. The acoustic mode amplitude is then close to the critical value. Using the results of our calculation we may convert Q-amplitude to the light amplitude, A_V and evaluate-probability that the acoustic mode amplitude is larger than an observable value. Figures 3 and 4 show results of such calculation for the fundamental and the first overtone, respectively.

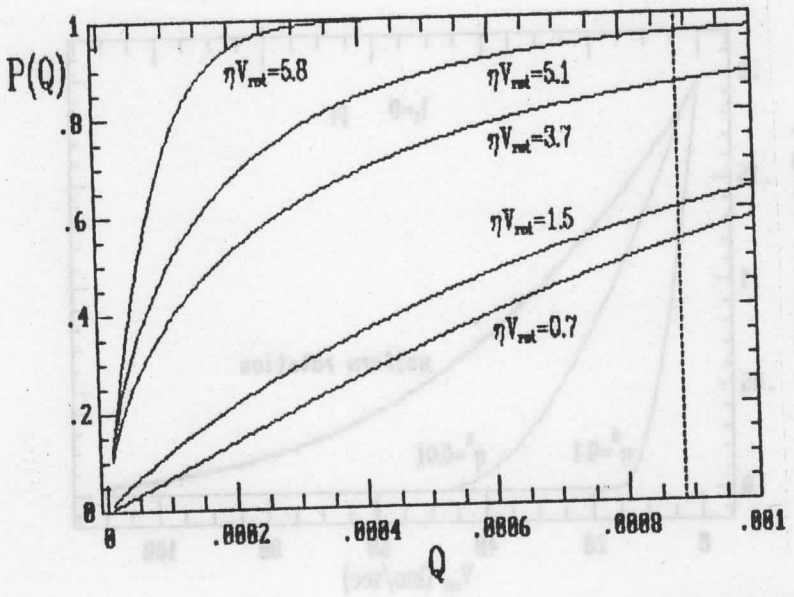

Fig. 2. Same as Figure 1 for nonuniform rotation, where $\eta = (<\Delta\Omega(r)^2>)^{1/2}/<\Omega>$.

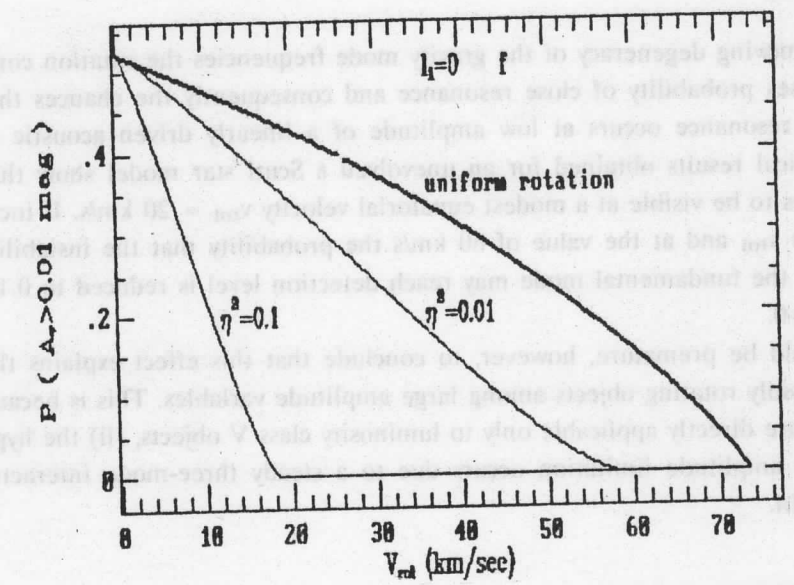

Fig. 3. Probability that the fundamental mode amplitude is larger than 0.01 mag as function of the equatorial velocity for uniform and nonuniform rotation.

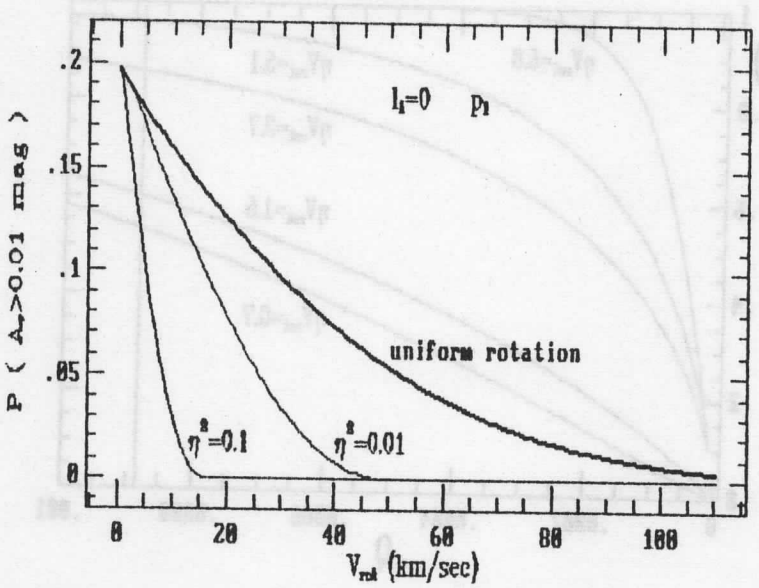

Fig. 4. Same as Figure 3 for the first radial mode.

3. Conclusions

By removing degeneracy of the gravity mode frequencies the rotation considerably increases probability of close resonance and consequently the chances that the parametric resonance occurs at low amplitude of a linearly driven acoustic mode. Our numerical results obtained for an unevolved δ Scuti star model show that the effect begins to be visible at a modest equatorial velocity $v_{rot} \approx 20$ km/s. It increases rapidly with v_{rot} and at the value of 60 km/s the probability that the instability occurs before the fundamental mode may reach detection level is reduced to 0.1 from 0.5 at $v_{rot} = 0$.

It would be premature, however, to conclude that this effect explains the absence of rapidly rotating objects among large amplitude variables. This is because (i) our results are directly applicable only to luminosity class V objects, (ii) the hypothesis that the amplitude limitation occurs due to a steady three-mode interaction is still uncertain.

References

Breger, M. 1969, *Ap. J. Suppl.* **19**, 79.
Breger, M. 1979, *Publ. A.S.P.*, **91**, 5.
Breger, M. 1982, *Publ. A.S.P.*, **94**, 845.
Dziembowski, W., and Królikowska, M. 1985, *Acta Astr.* **35**, 5.
Dziembowski, W., Królikowska, M., and Kosovitchev, A. 1988, *Acta Astr.*, submitted.
McNamara, D.H. 1985, *Publ. A.S.P.*, **97**, 715.

STABILITY OF THE THREE-MODE LIMIT CYCLES IN THE MULTIMODE PARAMETRIC RESONANCE CASE

P. Moskalik
Copernicus Astronomical Center, Warsaw, Poland

Abstract

The stability of a three-mode limit cycle against the decay into a pair of damped modes is studied. It is shown, that stability criteria for the limit cycle and for a constant amplitude solution are quite similar, although a few noticeable differences among them are also present.

Resonant mode coupling is very important in stellar pulsations, especially in dwarf-type variables. As it was argued by *Dziembowski* (1980), it is probably the main amplitude limiting effect in such stars. This suggestion was later confirmed by detailed numerical calculations carried out for a δ Scuti star model by *Dziembowski* and *Krolikówska* (1985). They have shown, that each linearly unstable *p*-mode with a frequency of ω_0 can excite easily a certain pair of damped gravitational modes (referred as 1 and 1') satisfying a near-resonance condition $\omega_0 \approx \omega_1 + \omega_{1'}$. This effect is called a parametric resonance instability and, at least for *f*-, p_1- and p_2 - modes in ZAMS variables, it leads to the limitation of the visual pulsation amplitudes at a level as low as it is actually observed. The limitation usually occurs in the form of oscillations with a constant amplitude (about 80% of all cases), but more complicated forms are also possible. The most probable one in the latter case is a limit cycle behaviour corresponding to slow, periodic amplitude modulation (*Moskalik* 1985).

All these solutions were obtained under the assumption that a given *p*-mode interacts with only one *g*-mode pair. This assumption, however, does not have to be true in general, because there are many g-mode pairs coupled to the same acoustic mode and all of them can in principle interact with the *p*-mode simultaneously. The aim of a present work was to study the stability of a three-mode limit cycle in such complicated situation.

The limit cycles I want to discuss were found numerically as asymptotic solutions of the familiar resonant amplitude equations

$$\frac{dQ_0}{dt} = \gamma_0 Q_0 - C_0 Q_1 Q_{1'} \exp(-i\delta_1 t) \quad , \tag{1a}$$

$$\frac{dQ_1}{dt} = -\gamma_1 Q_1 + C_1 Q_0 Q_{1'}^* \exp(i\delta_1 t) \quad , \tag{1b}$$

$$\frac{dQ_{1'}}{dt} = -\gamma_{1'} Q_{1'} + C_{1'} Q_0 Q_1^* \exp(i\delta_1 t) \quad , \tag{1c}$$

where $\gamma_j > 0$ are linear stability coefficients and $\delta_1 = \omega_0 - \omega_1 - \omega_{1'}$. These solutions may be written in the form

$$Q_j(t) = z_j(t) \exp(i(\Psi_j(t) + \varkappa_j t)) = B_j(t) \exp(i\varkappa_j t) \quad , \tag{2}$$

where functions $B_j(t)$ are strictly periodic and constants $\varkappa_j$ represent small nonlinear frequency shifts. All calculations reported here were done in the case $\gamma_1 = \gamma_{1'} \gg \gamma_0$, which case is the most important one in δ Scuti-type stars. Nonadiabatic effects in coupling coefficients were neglected, what was equivalent to the assumption, that C_j were purely real and positive (*Dziembowski* 1982). For the purpose of the present work only the simplest limit cycles possible were considered, namely the cycles having one minimum and one maximum in each amplitude during the modulation period. The detailed discussion of these solutions and their properties was given by *Moskalik* (1985).

The problem of the limit cycle stability against the decay of mode 0 to another *g*- mode pair (with parameters γ_2, $\gamma_{2'}$ and $\delta_2 = \omega_0 - \omega_2 - \omega_{2'}$) is equivalent to the problem of the excitation of this pair by *p*- mode oscillations with periodically variable amplitude and phase. Such excitation is described by differential equations similar to equations (1b) and (1c), but now Q_0 is not an independent variable, but is given by equation (2). Substituting into these equations $Q_j = S_j \exp(i(\delta_2 + \varkappa_0)t/2)$ we obtain a linear system with periodically variable coefficients for two unknown functions S_2 and $S_{2'}^*$

$$\frac{dS_2}{dt} = -(\gamma_2 + i(\delta_2 + \varkappa_0)/2) S_2 + C_2 B_0(t) S_{2'}^* \quad , \tag{3a}$$

$$\frac{dS_{2'}^*}{dt} = -(\gamma_{2'} - i(\delta_2 + \varkappa_0)/2) S_{2'}^* + C_{2'} B_0^*(t) S_2 \quad . \tag{3b}$$

According to the Floquet theorem its general solution can be written as

$$\begin{pmatrix} S_2 \\ S_{2'}^* \end{pmatrix} = \underline{v}_1(t) \exp(m_1 t) + \underline{v}_2(t) \exp(m_2 t) \quad , \tag{4}$$

where m_1, m_2 are characteristic exponents of the system and $\underline{v}_1(t)$, $\underline{v}_2(t)$ are periodic functions of time. Thus, the limit cycle $Q_0(t)$ is stable if the real parts of both m_1 and m_2 are negative and is unstable if at least one of them is positive.

In practice, characteristic exponents of equations (3) can be found only numerically with the standard method described for example by *Moulton* (1958). Typical results of this procedure in the case $\gamma_2 = \gamma_{2'}$, are shown in Figure 1. The solid line

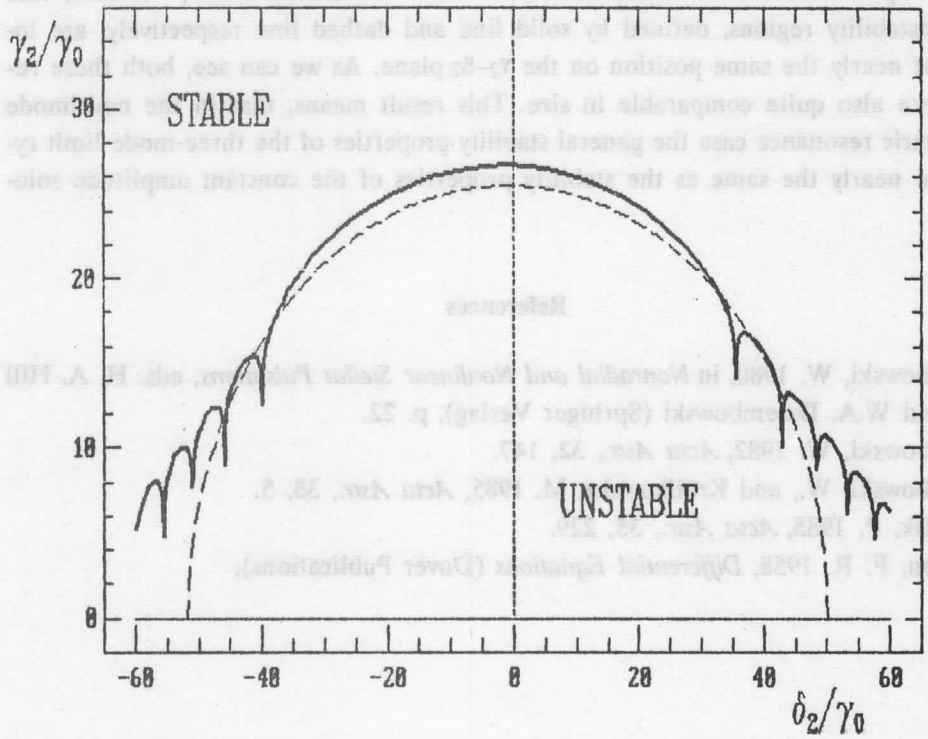

Fig. 1. The stability of the three-mode limit cycle with parameters $\gamma_1 = \gamma_{1'} = 10\gamma_0$, $\delta_1 = 15\gamma_0$ against the excitation of a second g-mode pair for the relative coupling strength coefficient $\Lambda = \sqrt{(C_2C_{2'}/C_1C_{1'})} = 2$. The dashed line represents the stability criterion valid in the case of a constant amplitude solution, calculated for given γ_1 and δ_1 from equation (4.5) of *Dziembowski* (1982).

represents the stability criterion obtained for the limit cycle with parameters $\gamma_1 = \gamma_{1'} = 10\gamma_0$, $\delta_1 = 15\gamma_0$ and for relative coupling strength coefficient $\Lambda = (C_2C_{2'}/C_1C_{1'})^{1/2} = 2$. The considered cycle is unstable to excitation of g-mode pairs with parameters (γ_2, δ_2) lying below this line, while it is stable to excitation of pairs with (γ_2, δ_2) lying above it. For comparison, the criterion valid in the case of a constant amplitude solution is also shown (dashed line). As one can see these criteria are different in two important respects. First, for constant amplitude solution a certain maximum value of $|\delta_2|$ always exists, above which all g-mode pairs are stable,

independently of their damping rates γ_2. No such limit for the frequency mismatch δ_2 can be found in the case of a limit cycle. Second, the dashed line is completely featureless, whereas characteristic narrow dips are present in the solid line. In other words, in the case of a limit cycle there are some specific values of δ_2 for which extremely low damping rates γ_2 are sufficient to stabilize the *g*-mode pair. In fact, additional calculations with higher resolution in δ_2 indicate, that the very narrow, flat bottoms of all the dips are located exactly at $\gamma_2 = 0$.

In spite of the differences mentioned above we should notice, however, that both instability regions, defined by solid line and dashed line respectively, are located at nearly the same position on the γ_2–δ_2 plane. As we can see, both these regions are also quite comparable in size. This result means, that in the multimode parametric resonance case the general stability properties of the three-mode limit cycles are nearly the same as the stability properties of the constant amplitude solutions.

References

Dziembowski, W. 1980, in *Nonradial and Nonlinear Stellar Pulsations*, eds. H. A. Hill and W.A. Dziembowski (Springer Verlag), p. 22.

Dziembowski, W. 1982, *Acta Astr.*, **32**, 147.

Dziembowski, W., and Królikowska, M. 1985, *Acta Astr.*, **35**, 5.

Moskalik, P. 1985, *Acta Astr.*, **35**, 229.

Moulton, F. R. 1958, *Differential Equations* (Dover Publications).

THE EXCITATION OF SOLAR OSCILLATIONS – OBSERVATIONAL RESULTS AND THEORETICAL SPECULATIONS

J. Christensen-Dalsgaard
Astronomisk Institut, Aarhus Universitet,
Aarhus C, Denmark

Abstract

Two different possible mechanisms have been proposed as responsible for the solar five minute oscillations: self-excitation and stochastic excitation by the turbulent convection. In the former case, a mechanism is also required to limit the growth of the oscillations, hence determining their final amplitudes. In principle it should be possible to distinguish between these possibilities from observations of the observed amplitudes of solar oscillation, and their variation with time. Additional information about the linear damping of the modes may be obtained from the observed line widths, as well as from observations of the phase variation with altitude in the solar atmosphere.

1. Introduction

The Sun is an extreme multi-mode oscillator. Currently of the order of several thousand modes have been identified (*e.g. Duvall et al.* 1988; *Libbrecht* and *Kaufman* 1988; *Pallé et al.* 1987a). Future observations, from the Global Oscillation Network Group and from the SOHO spacecraft (*e.g. Harvey, Kennedy,* and *Leibacher* 1987; *Noyes* 1987) should lead to the identification of essentially all modes in the five-minute region with degrees l up to 100-200, that is of the order of 10^5 modes.* Thus it is not unreasonable to predict that in the next decade more than 50 per cent of the modes of oscillation identified in *all* stars will belong to the Sun.

---

* At higher degree the phase propagation time around the Sun for the mode probably exceeds the mode life time, and so the oscillation loses its global modal structure in θ and ϕ. Here the individual modes merge into ridges, each corresponding to a given radial order n, as a function of the radial wave number k_h which must now be regarded as a continuous variable.

The principal interest of the solar oscillations lies in their use for helioseismic studies of the solar interior. This requires accurate determination, and careful analysis, of the oscillation frequencies, whereas the causes of the oscillations are, in a first approximation, largely irrelevant. Nevertheless, the mechanisms responsible for maintaining and determining the amplitudes of the oscillations are of considerable interest and importance. More specifically, the following aspects may be mentioned:

– *Interpretation of frequencies.* The excitation mechanisms may have effects on the oscillation frequencies which, given the high precision attainable in the observational determination of the frequencies, need to be taken into account when they are used for helioseismology.

– *The physics of multimode pulsation.* Because of the large number of modes present, the Sun provides a laboratory for the study of multimode pulsation, including possibly interaction between the modes, or between the oscillations and the turbulent convection.

– *Diagnostics of convection.* It seems likely that convection plays a major role in determining the properties of solar oscillations. If the physics of the interaction between convection and pulsation were to be understood, it might be possible to use the observed mode amplitudes to get information about the properties of convection beneath the solar photosphere.

– *Prediction of solar-like oscillations in other stars.* Given an understanding of the causes of solar oscillations, it may be possible to predict the amplitudes of similar oscillations in other stars. This might aid the detection and interpretation of such oscillations.

Here I only consider modes in the five-minute region. Observation of oscillations has also been reported at longer periods, corresponding to g modes of solar models. However, their identification is as yet tentative, and no definite assignment of modes to the observed oscillation has been possible. Hence speculation about their causes is somewhat premature.

The paper is only concerned with the excitation of solar oscillations, and the observable properties that may be relevant to understanding it. More detailed descriptions of solar oscillations and their use for helioseismology may be found, *e.g.*, in *Deubner* and *Gough* (1984) and *Christensen-Dalsgaard, Gough* and *Toomre* (1985a). A review of the excitation of solar and stellar oscillations was given by *Chitre* (1987), whereas *Frandsen* (1987) reviewed the diagnostic potentials of solar oscillations for the study of the solar atmosphere.

2. Observation of solar oscillations

2.1 The modal description

For a single, linearly damped or excited mode of oscillation, the velocity field can be written as

$$V_{n\ell m} = V_{n\ell m}\mathrm{Re}\left[\xi_r(r)Y_\ell^m(\theta,\varphi)e^{-i\omega_c t}\right]\mathbf{a}_r + \text{tangential part}, \tag{2.1}$$

where r is the distance to the centre, θ and φ are co-latitude and longitude, and t is time; $\mathbf{a}_r$ is a unit vector in the r-direction. Y_l^m is a spherical harmonic of degree l and azimuthal order m, and $\xi_r(r)$ is the radial eigenfunction. The tangential part may be neglected for the five-minute modes, except at high degree. The complex frequency ω_c is written as $\omega_c = \omega + i\eta$, where ω and η are real.

For a given observation scheme, the observed velocity may be written as

$$V(t) = A\cos(\omega t + \delta)e^{\eta t}, \tag{2.2}$$

where the amplitude A is related to V_{nlm} by the spatial filtering applied to the surface velocity (*e.g. Dziembowski* 1977, *Christensen-Dalsgaard* and *Gough* 1982, *Christensen-Dalsgaard* 1984), and δ is the phase at $t=0$. Thus ω determines the observed frequency, often specified in terms of the cyclic frequency $\nu = \omega/2\pi$, and η is the growth rate. Fourier transform of a time series lasting from $t=0$ to $t=T$ gives

$$\bar{V}(\omega') = \int_0^T V(t)e^{-i\omega' t}dt = \frac{1}{2}\frac{A^2}{i(\omega' - \omega) + \eta}\left\{e^{[i(\omega' - \omega) + \eta]T} - 1\right\}, \tag{2.3}$$

neglecting (for $\omega' > 0$) a similar term in $\omega' + \omega$. Hence the power spectrum is

$$P(\omega') = |\bar{V}(\omega')|^2 = \frac{e^{\eta T}\sin^2[(\omega' - \omega)\frac{T}{2}] + \frac{1}{4}(e^{\eta T} - 1)^2}{(\omega' - \omega)^2 + \eta^2}A^2. \tag{2.4}$$

The behaviour of $P(\omega')$ depends on the relative magnitude of the mode life time $|\eta|^{-1}$ and the observing time T. To be definite, we assume a damped oscillation, *i.e.* $\eta < 0$. For $|\eta T| \ll 1$,

$$P(\omega') = A^2T^2\mathrm{sinc}^2\left[\frac{(\omega'-\omega)T}{2}\right], \qquad (2.5)$$

where *sinc* x = *(sin* x*)/*x ; here the full width at half maximum (FWHM) in ω of the observed peak is given by 5.77 T^{-1}. For $|\eta T| \gg 1$, on the other hand, the line profile is Lorentzian,

$$P(\omega') = \frac{A^2}{(\omega' - \omega)^2 + \eta^2}, \qquad (2.6)$$

with a FWHM of 2η. The transition between these two cases is illustrated in Figure 1. Notice that when $|\eta T| \geq 3$, the damping makes a substantial contribution to the line width, and hence the damping rate may be measured from observed line profiles. For $|\eta T| > 5$ the line profile is essentially purely Lorentzian.

These results only strictly apply to an isolated oscillator that is neither forced nor interacts with other modes. However, as discussed in Section 3.3 below, a similar behaviour is obtained for damped modes that are excited stochastically by a forcing function whose spectrum is nearly white. Thus in this case, also, the measured line widths can be used to estimate the linear damping rates.

In practice, the observed spectral peaks are unlikely to display a smooth behaviour. Discrete sampling, effects of noise, and mode beating introduce fine structure, with a typical frequency spacing of T^{-1}, with an envelope given approximately by equation (2.4) *(Scherrer* 1984; *Isaak* 1986). Additional fluctuations may arise from the possibly stochastic nature of the excitation. The fluctuations introduce a scatter, of order $|\eta|$ in the frequency determination. By averaging separate spectra, each based on observations of sufficient duration, the fine structure can be suppressed; in this way it should be possible to determine the frequency with an accuracy considerably exceeding the natural width of the spectral peak.

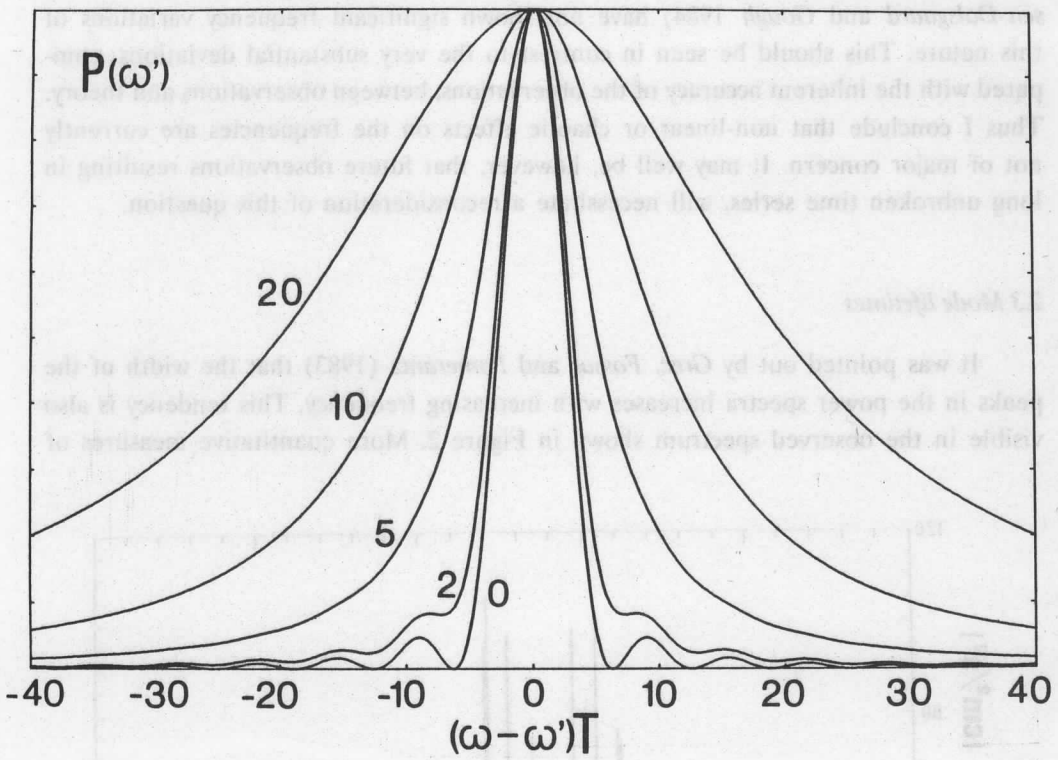

Fig. 1. Idealized power spectrum (see equation (2.4)) illustrating the combined effects of damping and finite observing time. The abscissa is frequency separation, in units of 1/T, where T is the duration of the time series. The ordinate has been normalized to a maximum value of 1. Curves are shown for different values of $|\eta T|$, indicated in the Figure, where η is the damping rate.

2.2 The oscillation frequencies

Evidence may be sought in the observed oscillation frequencies for non-linear effects (such as phase-locking caused by resonant mode interaction; see *Dziembowski,* 1988), or for "chaos" caused by deformation of the Sun (*Perdang,* 1988). This might lead to irregular variations in the frequencies, as functions of l and n. To search for such variations, one may consider the deviations from smooth fits to the frequencies, or from computed frequencies which in general depend smoothly on l and n. It must be born in mind, however, that the finite observing time and mode life time, as well as noise, may cause purely observational scatter in the frequencies. Additional complications may arise from beating between insufficiently resolved, closely spaced modes (*Christensen-Dalsgaard* and *Gough* 1982).

So far, comparisons between observed and computed frequencies (*e.g. Christensen-Dalsgaard* and *Gough* 1984) have not shown significant frequency variations of this nature. This should be seen in contrast to the very substantial deviations, compared with the inherent accuracy of the observations, between observations and theory. Thus I conclude that non-linear or chaotic effects on the frequencies are currently not of major concern. It may well be, however, that future observations resulting in long unbroken time series, will necessitate a reconsideration of this question.

2.3 Mode lifetimes

It was pointed out by *Grec, Fossat* and *Pomerantz* (1983) that the width of the peaks in the power spectra increases with increasing frequency. This tendency is also visible in the observed spectrum shown in Figure 2. More quantitative measures of

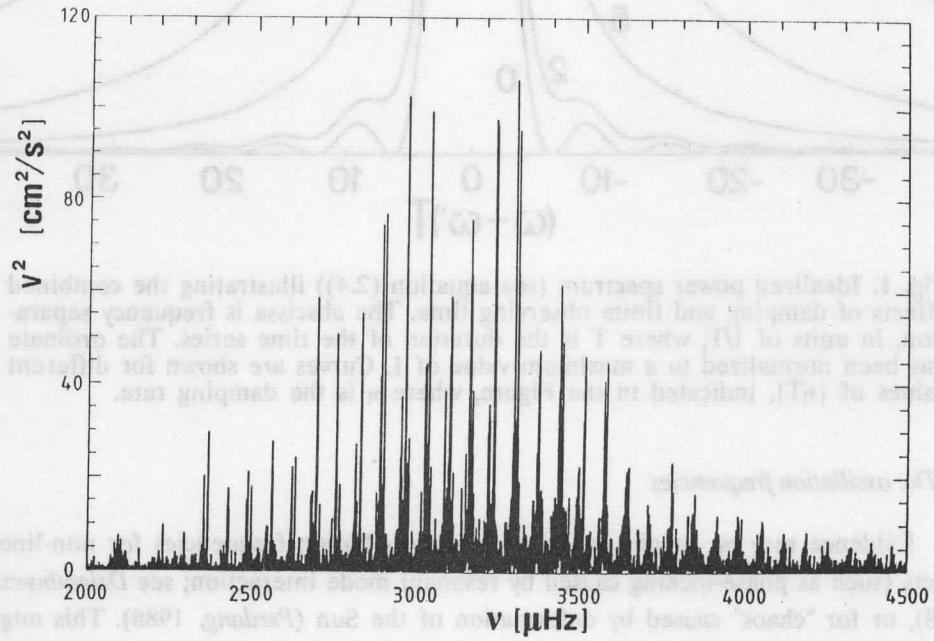

Fig. 2. Power spectrum of solar oscillations, from Doppler observations in light integrated over the disk of the Sun. The ordinate is normalized to show velocity power per frequency bin. (See *Claverie et al.* 1984).

line widths were obtained by *Isaak* (1986) from two-station observations over 88 days, and by *Libbrecht* and *Zirin* (1986) and *Libbrecht* (private communication; see also *Christensen-Dalsgaard, Gough* and *Libbrecht* 1988), who fitted Lorentzian profiles to

the peaks in power spectra. The resulting line widths are shown in Figure 7 below. There is a very substantial increase in the width with frequency; observationally this means that low-frequency modes are advantageous for very precise frequency determination, or for separation of closely-spaced peaks caused by, *e.g.*, rotational splitting. The theoretical interpretation of the line width measurements is discussed in Section 3.

2.4 Mode amplitudes

As is evident from Figure 2, the amplitude of the five-minute oscillations depends strongly on frequency, with a pronounced maximum at $\nu = 3000$ μHz and very small values for frequencies below 2000 and above 4000 μHz. While the spectrum in Figure 2 only contains low-degree modes, the same general behaviour is found at all l (*Grec* and *Fossat* 1977; *Libbrecht et al.* 1986). Figure 3, from *Libbrecht et al.*, shows velocity power averaged over several ranges in l, as a function of frequency. It is evident that the frequency dependence of power is virtually independent of l, even at high degree. *Libbrecht et al.* also showed that the average over ν of the energy per mode (*i.e.* individual set (n, l, m)) does not depend significantly on l, at least for $l \leq 200$; a similar, though less well-established, result was obtained by *Christensen-Dalsgaard* and *Gough* (1982) on the basis of observations by *Grec* and *Fossat* (1977). Finally *Libbrecht et al.* showed that, when averaged over frequency and degree, the energy of modes with $5 \leq l \leq 20$ is independent of m. Thus the available evidence indicates that the average mode energy is a function of frequency alone.

Figure 2 also shows that there are substantial variations in the amplitudes between adjacent modes. Part of this variation can be attributed to the variation in the observing sensitivity with l, or to mode beating; however there is strong evidence that the amplitude variations, which are found also at higher degrees, are significant. The distribution of mode amplitudes must carry information about the mechanisms determining them. Similar information may be sought from temporal variation of the mode amplitudes; the currently available information (*Grec et al.* 1983; *Gelly* 1987; *Pallé et al.* 1987b), however, is not conclusive, largely because of the difficulties of mode beating.

2.5 Phase relations

For adiabatic oscillations the maximum temperature perturbation occurs at maximum compression. Hence the velocity and temperature perturbation are 90° out of phase. Non-adiabatic effects change this phase relation. They also introduce changes

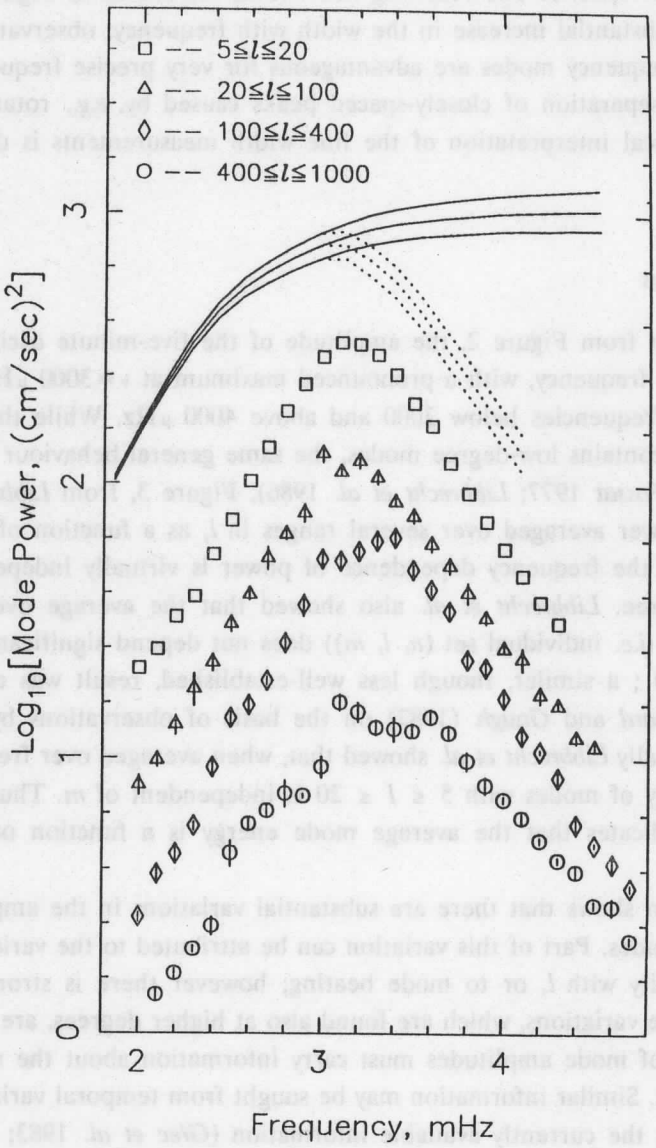

Fig. 3. Velocity power as a function of frequency, from *Libbrecht et al.* (1986). The data points show the power averaged over l for four different ranges in l, as indicated. The points for the lowest range in l are shown on the proper scale, the others have been shifted. The curves are discussed in the text.

in phase with height in the solar atmosphere. Thus by measuring phase differences between different types of observations, information can be obtained about the processes in the solar atmosphere that contribute to the damping or driving of the

oscillations. There now exist fairly extensive observations of phase relations between intensity and velocity in spectral lines (*e.g. Lites* and *Chipman* 1979; *Lites, Chipman* and *White* 1982; *Staiger et al.* 1984; *Staiger* 1987; *Stebbins* and *Goode* 1987), and a few measurements of phase relations in the continuum (*Fröhlich* and *van der Raay* 1984). The interpretation of such data is complicated by the non-local nature of the radiation field, but can, at least in principle, be accomplished by appropriate modelling of the behaviour of the oscillations in the solar atmosphere.

2.6 Solar-like oscillations in other stars

Just as a firm understanding of the causes of the solar oscillations would aid the detection of similar oscillations in other stars, it is evident that by observing them one would obtain important information about the excitation mechanisms, and their dependence on the parameters characterizing the star. So far only tentative evidence has been found for such oscillations in α Cen and Procyon (*Gelly, Grec* and *Fossat* 1986), with an amplitude distribution that may bear some resemblance to that of the Sun, as well as in ε Eri (*Noyes et al.* 1984). In addition *Christensen-Dalsgaard* and *Frandsen* (1983a) speculated that the luminosity fluctuations seen in cool giants and supergiants (*Maeder* 1980) might at least in some cases be caused by mechanisms similar to those that excite the solar oscillations. Much more definite observations are needed, however, before data of this kind can be applied to the study of the excitation mechanisms.

3. The theory of mode excitation

3.1 The behaviour of the eigenfunctions

The theoretical description of the excitation and damping processes depends on the details of the interactions between the oscillations on the one hand, and the radiation field and turbulent convection on the other. These interactions, which are to a large extent not understood, will be discussed in subsequent sections. However certain aspects of the results, in particular the rapid decrease in the excitation or damping rate with decreasing frequency, depend largely on simple properties of the oscillation eigenfunctions. These are discussed here.

We introduce the quantity

$$X(r) = c^2 \rho^{1/2} div \delta \mathbf{r} \quad , \tag{3.1}$$

where c is the adiabatic sound speed, ρ is density, and $\delta\mathbf{r}$ is the displacement field, so that $\mathbf{V} = \partial\delta\mathbf{r}/\partial t$. For adiabatic oscillations, and neglecting the perturbation in the gravitational potential, X approximately satisfies

$$\frac{d^2X}{dr^2} + \frac{1}{c^2}\left[\omega^2 - \omega_{co}^2 - \frac{L^2c^2}{r^2}\left[1 - \frac{N^2}{\omega^2}\right]\right]X = 0 \qquad (3.2)$$

(*Deubner* and *Gough* 1984); here ω_{CO} is a generalization of *Lamb's* (1909) acoustical cut-off frequency, $L = [l(l+1)]^{1/2}$, and N is the Brunt-Väisälä frequency. A mode is an oscillating function of r in the region where

$$\omega^2 > \omega_{co}^2 + \frac{L^2c^2}{r^2}\left[1 - \frac{N^2}{\omega^2}\right] \qquad (3.3)$$

and generally decreases approximately exponentially outside it. The region where equation (3.3) is satisfied is known as the *trapping region* for the mode.

For the solar five-minute modes, $|N| \ll \omega$ except in a very thin region just beneath the photosphere which can be neglected for the present purpose. The quantity Lc/r decreases rapidly with increasing r, whereas ω_{CO}, which is illustrated in Figure 4, is large only near the surface. The rapid variation in ω_{CO} very close to $r/R = 1$ is associated with the region where convection is substantially super-adiabatic. In the solar atmosphere, $\nu_{CO} = \omega_{CO}/2\pi$ varies relatively little, around a value of about 5300 μHz.

From this discussion of the characteristic frequencies it follows that a given mode is trapped between an inner turning point at radius r_t, given by $c(r_t)/r_t \approx \omega/L$, and an outer turning point r_o satisfying $\omega_{CO}(r_o) \approx \omega$. For low l, r_t is very near the solar centre; with increasing l the modes get confined closer and closer to the solar surface. As discussed, *e.g.*, by *Christensen-Dalsgaard et al.* (1985b) this variation of r_t enables the helioseismic inversion of the five-minute oscillation frequencies to study details of solar structure.

Here we are chiefly concerned with the behaviour of the eigenfunctions near the surface. At frequencies higher than about 5300 μHz, the value of ν_{CO} in the atmosphere, an acoustic wave can propagate out through the solar atmosphere. Therefore, in this simple approximation, one cannot even speak of trapped modes at these frequencies. In more detailed, nonadiabatic calculations (*e.g. Christensen-Dalsgaard* and *Frandsen* 1983b) this shows up as a very strong damping, which may well be

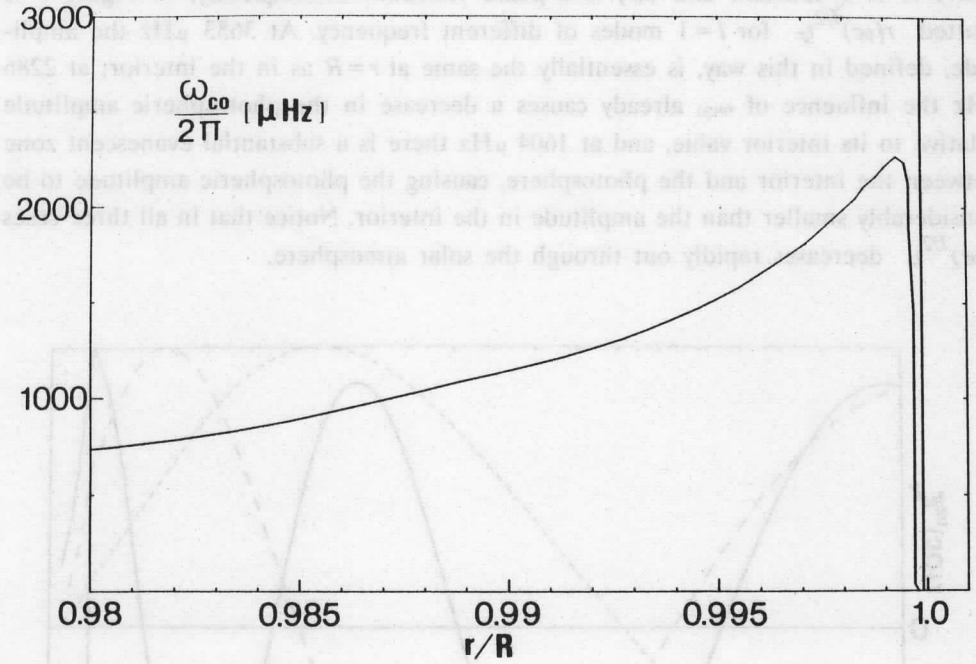

Fig. 4. The acoustical cut-off frequency, as defined by *Deubner* and *Gough* (1984), plotted against fractional radius r/R in the outermost parts of the Sun. In the atmosphere, for $r > R$, $\omega_{co}/2\pi$ exceeds 5000 μHz.

responsible for the cut-off at high frequency of the five-minute spectrum. Modes with frequencies below 5000 μHz are evanescent in the solar atmosphere. An important factor controlling their behaviour beneath the photosphere is the local maximum in ν_{co} at about 2260 μHz. For $\nu > 2260$ μHz, r_o is essentially at the photosphere, $r = R$. In this case the interior amplitude is, in a sense to be defined below, roughly equal to the amplitude at the photosphere, whereas the amplitude decreases in the atmosphere. For $\nu < 2260$ μHz, the mode penetrates an evanescent region beneath the photosphere, whose width increases with decreasing frequency, leading to an increase in the interior amplitude relative to the photospheric value.

The computed eigenfunctions follow the behaviour expected from the preceding discussion of the mode trapping. Asymptotic analysis of equation (3.1) shows that in the trapping region the amplitude ξ_r of the radial component of velocity (*cf.* eq. (2.1)) is approximately given by

$$\xi_r(r) \approx A(\rho c)^{-1/2} r^{-1} \cos[\Psi(r)], \tag{3.4}$$

where A is a constant and $\psi(r)$ is a phase function. Consequently, in Figure 5 is plotted $r(\rho c)^{1/2}\xi_r$ for $l=1$ modes of different frequency. At 3653 μHz the amplitude, defined in this way, is essentially the same at $r=R$ as in the interior; at 2286 μHz the influence of ω_{co} already causes a decrease in the photospheric amplitude relative to its interior value, and at 1604 μHz there is a substantial evanescent zone between the interior and the photosphere, causing the photospheric amplitude to be considerably smaller than the amplitude in the interior. Notice that in all three cases $r(\rho c)^{1/2}\xi_r$ decreases rapidly out through the solar atmosphere.

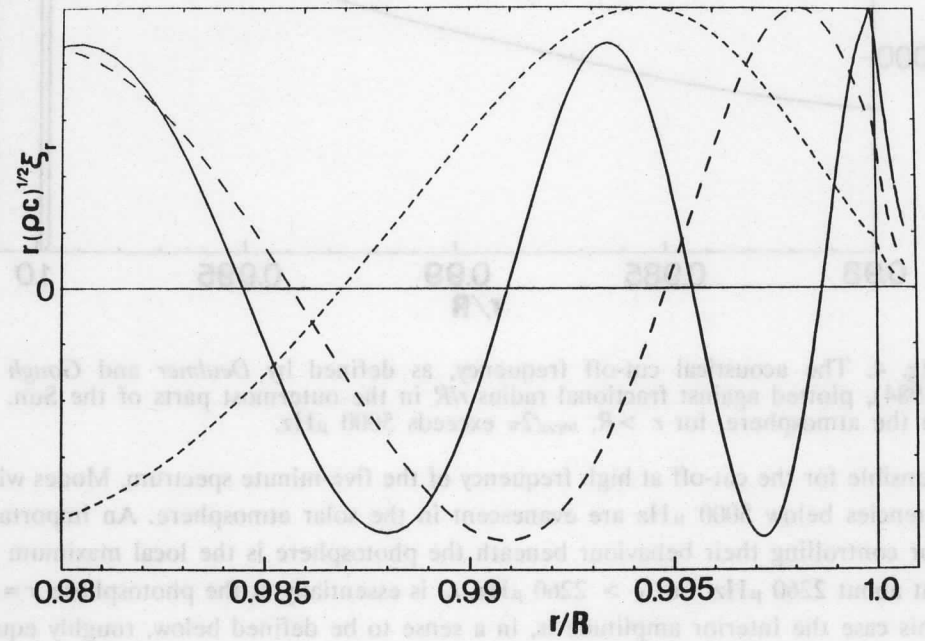

Fig. 5. Eigenfunctions of p modes with $l=1$, plotted against fractional radius r/R in the outermost parts of the Sun. The quantity shown is $r\xi_r\sqrt{(\rho c)}$, where ξ_r is the amplitude of vertical velocity. The cases shown are: ---- : $\nu=1604\mu$Hz, – – – – –: $\nu=2286\mu$Hz, ———— : $\nu=3653\mu$Hz.

The properties of the eigenfunctions are also reflected in the normalized mode energy, which I define by

$$E = \frac{\int_0^R [\xi_r^2(r) + \ell(\ell+1)\xi_h^2(r)]\rho r^2 dr}{4\pi M[\xi_r^2(R) + \ell(\ell+1)\xi_h^2(R)]}, \tag{3.5}$$

where M is the mass of the Sun. It is shown in Figure 6, for selected values of l. At a given l, E is roughly constant for $\nu \geq 3000$ μHz, whereas at lower frequencies, where the modes are increasingly confined by the evanescent region where $\omega < \omega_{co}$, E increases rapidly with decreasing frequency. E decreases with increasing l due to the decrease in the extent of the trapping region, as the inner turning point r_t moves outwards.

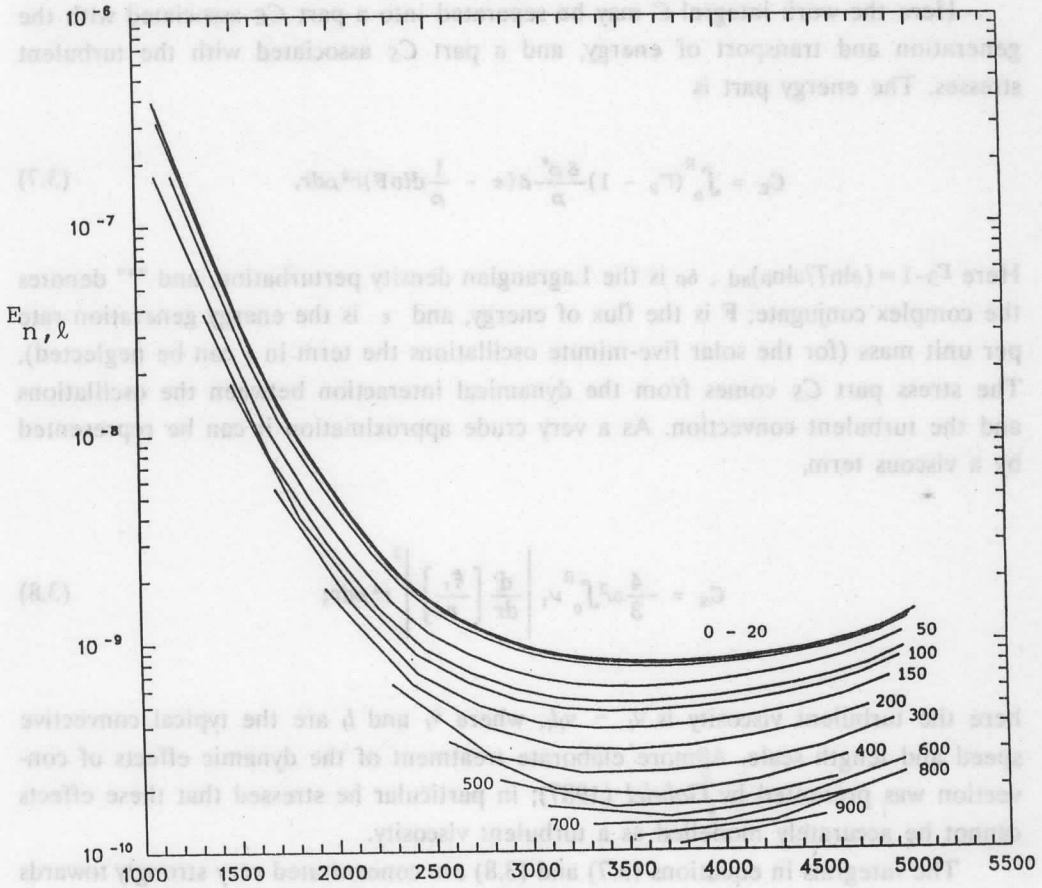

Fig. 6. Normalized energy $E_{n,l}$ (*cf.* eq. (3.5)) for p modes of the present Sun, as function of the cyclic frequency ν. For clarity points corresponding to modes with a given degree l have been connected. The curves are labelled with l.

3.2 Linear damping and excitation

It follows from the theory of nonadiabatic oscillations (*e.g. Ledoux* and *Walraven* 1958; *Unno et al.* 1979) that the growth rate can be written as

$$\eta = \frac{\mathrm{Re}(C)}{8\pi M \omega^2 \xi_r(R)^2 E} \quad . \tag{3.6}$$

Here the work integral C may be separated into a part C_E associated with the generation and transport of energy, and a part C_S associated with the turbulent stresses. The energy part is

$$C_E = \int_0^R (\Gamma_3 - 1)\frac{\delta\rho^*}{\rho}\delta(\varepsilon - \frac{1}{\rho} div \mathbf{F}) r^2 \rho dr. \tag{3.7}$$

Here $\Gamma_3 - 1 = (\partial \ln T/\partial \ln \rho)_{ad}$, $\delta\rho$ is the Lagrangian density perturbation, and "*" denotes the complex conjugate; **F** is the flux of energy, and ε is the energy generation rate per unit mass (for the solar five-minute oscillations the term in ε can be neglected). The stress part C_S comes from the dynamical interaction between the oscillations and the turbulent convection. As a very crude approximation it can be represented by a viscous term,

$$C_S = -\frac{4}{3}\omega^2 \int_0^R \nu_t \left| \frac{d}{dr}\left[\frac{\xi_r}{r}\right] \right|^2 r^4 \rho dr; \tag{3.8}$$

here the turbulent viscosity is $\nu_t \sim v_t l_t$, where v_t and l_t are the typical convective speed and length scale. A more elaborate treatment of the dynamic effects of convection was presented by *Gabriel* (1987); in particular he stressed that these effects cannot be accurately modelled as a turbulent viscosity.

The integrals in equations (3.7) and (3.8) are concentrated very strongly towards the solar surface. Thus, apart from the detailed physics, they are roughly proportional to $\xi_r(R)^2$. It follows from equation (3.6) that, equally roughly, $\eta \sim E^{-1}$. In particular, we may expect a rapid decrease of $|\eta|$ with decreasing frequency below 2500 μHz. This is confirmed by detailed calculations; the same trend is visible in the observed line widths (*cf.* Figure 7).

To compute η, we need an expression for $\delta(div\mathbf{F})$. The flux may be written as the sum of a radiative and a convective part,

$$\mathbf{F} = \mathbf{F}_R + \mathbf{F}_C \quad . \tag{3.9}$$

Additional contributions from mechanical energy transport in the solar atmosphere should possibly be included; however these contributions are highly uncertain, even in the non-pulsating case, and so their effect on the oscillations has been neglected up to now.

Given the uncertainty in the treatment of the convective flux in the equilibrium model, it is evident that the calculation of the convective flux perturbation must be very uncertain also. With a precise physical description of mixing length theory it is possible to perform a consistent linearization. This approach was used by, *e.g. Unno* (1967) and *Gough* (1977) under different assumptions, and consequently with somewhat different results. Much simpler, essentially phenomenological, approximations were suggested by, *e.g., Cox et al.* (1966). Furthermore, several calculations have neglected the perturbation in the convective flux entirely. It should be noticed that even this is not a precise proposition; thus there is a difference between neglecting, say, $\delta\mathbf{F}_C$ and neglecting $\delta(div\mathbf{F}_C)$. The choice of the neglected quantity is probably in general determined by computational convenience.

The calculation of the radiative flux perturbation is, in contrast, relatively straightforward. It was shown by *Christensen-Dalsgaard* and *Frandsen* (1983b) that for the purpose of calculating oscillation frequencies and growth rates the grey Eddington approximation was adequate. A more accurate treatment of radiative transfer, including effects of line blanketing, may be required for computation of the detailed behaviour of the oscillations in the solar atmosphere (*Christensen-Dalsgaard* and *Frandsen* 1984). This is needed to interpret observations of phase differences between different types of oscillation observations (*Frandsen* 1986).

A problem remains, however, in most of the calculations which employ the Eddington approximation. It follows from the equation of transfer, neglecting effects of sphericity, that the divergence of the radiative flux is given by

$$div\mathbf{F}_R = 4\pi\rho\kappa(B - J), \tag{3.10}$$

where κ is opacity, B is the integrated Planck function and J is the mean intensity. In the case of radiative equilibrium, $div\mathbf{F}_R = 0$ and so $B = J$. This is *not* the case, *e.g.,* in the upper part of the convection zone, where there is a transition from convective to radiative energy transport. By perturbing equation (3.10) we obtain

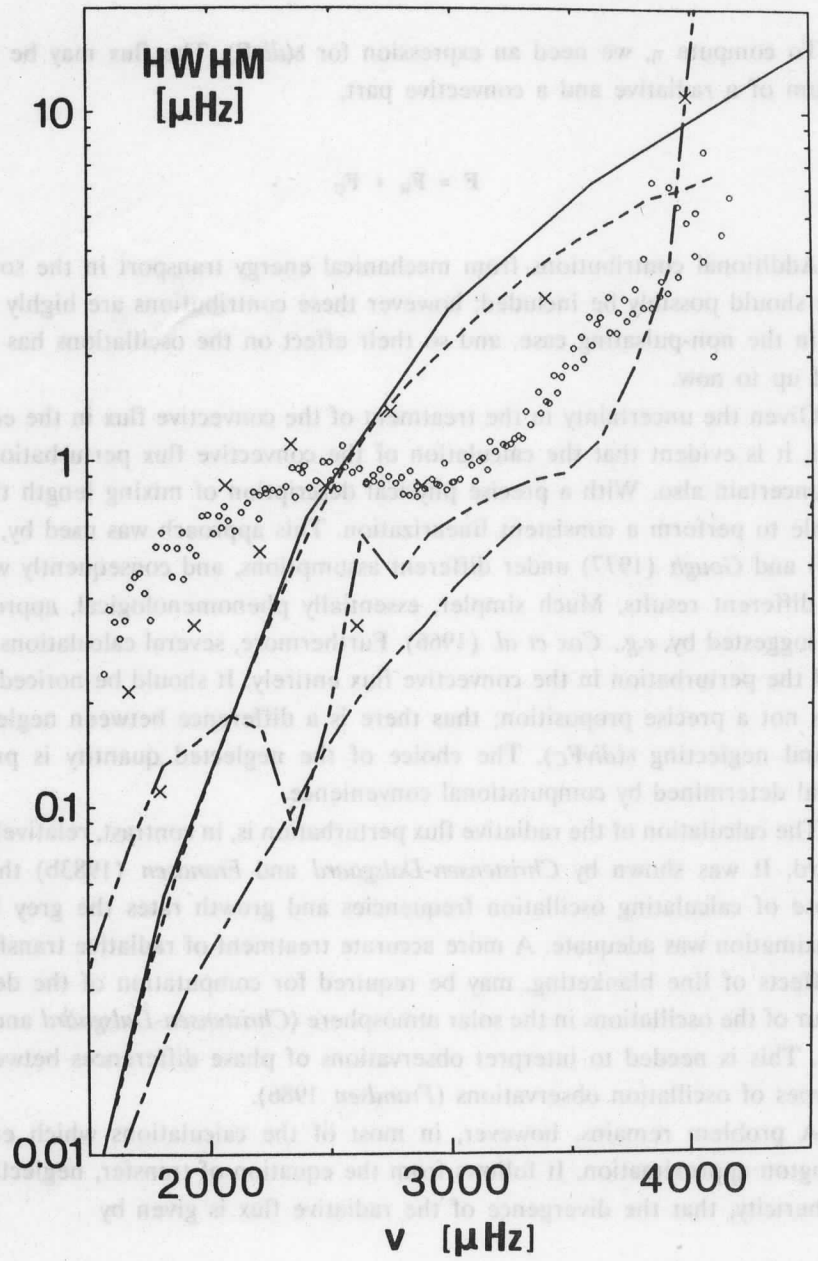

Fig. 7. Half width at half maximum for low-degree p modes. For a simple damped oscillator this corresponds to the damping rate η, in units of cyclic frequency (*cf.* equation (2.6)). The crosses are observations from Isaak (1986), and the circles are unpublished observations by Libbrecht. The curves show the following theoretical results: ——— : Christensen-Dalsgaard and Frandsen (1983b), - - - - - - - - - - : Kidman and Cox (1984), —·—·—·—·— : Goldreich and Keeley (1977a), —··—··—··—··— : Gough (1980).

$$\delta\left[\frac{1}{\rho}div\mathbf{F}_R\right] = 4\pi\kappa_0\left[\delta B - \delta J + \frac{\delta\kappa}{\kappa_0}(B_0 - J_0)\right], \tag{3.11}$$

where the subscript "0" denotes equilibrium quantities. The last term in this equation, corresponding to departures from radiative equilibrium in the mean state, has been neglected in most stability calculations utilizing the Eddington approximation. Yet *Christensen-Dalsgaard* and *Frandsen* (1983b) found that this term makes a strong contribution to the damping of the oscillations. This can be understood, at least partly, from the work integral in equation (3.7). The term makes the contribution

$$-\int_0^R(\Gamma_3 - 1)\frac{\delta\rho^*}{\rho}\frac{\delta\kappa}{\kappa}div\mathbf{F}_R r^2dr \approx$$
$$-\int_0^R(\Gamma_3 - 1)\left|\frac{\delta\rho}{\rho}\right|^2[\kappa_\rho + (\Gamma_3 - 1)\kappa_T]div\mathbf{F}_R r^2dr \tag{3.12}$$

to C_E ; here

$$\kappa_\rho = \left[\frac{\partial\log\kappa}{\partial\log\rho}\right]_T; \qquad \kappa_T = \left[\frac{\partial\log\kappa}{\partial\log T}\right]_\rho, \tag{3.13}$$

and we assumed the oscillations to be approximately adiabatic, so that the Lagrangian temperature perturbation δT is given by $\delta T/T \approx (\Gamma_3-1)\delta\rho/\rho$. In the outer part of the convection zone $\mathbf{F}_R$ increases with increasing r, so that $div\mathbf{F}_R > 0$; also $\varkappa_\rho$ and $\varkappa_T$ are positive, $\varkappa_T$ being as large as about 8. Accordingly, the term contributes to the damping of the oscillation.

Given the uncertainties in the calculation of η, it is not surprising that there is no general agreement about its magnitude, or even its sign. *Ando* and *Osaki* (1975, 1977) used the Eddington approximation, but neglected the term in B_0–J_0 ; they also neglected the perturbation in the convective flux. They found instability for a range of modes corresponding roughly to the observed five-minute oscillations. Using the same approximations for the radiative flux, but computing the perturbation in the convective flux from the prescription suggested by *Cox et al.* (1966), *Goldreich* and *Keeley* (1977a) obtained similar results; they also showed that the inclusion of turbulent viscosity, essentially as described in equation (3.8), stabilized all modes considered. *Antia, Chitre* and *Narasimha* (1982), employing the same treatment of radiation, but using a more elaborate description of convection, also found instability, as did *Antia, Chitre* and *Gough* (1987) who treated the perturbation in the convective flux in a manner similar to that described by *Unno* (1967) and *Gough* (1977).

The previous calculations all suffered from the neglect of B_0–J_0 . *Christensen-Dalsgaard* and *Frandsen* (1983b) used the grey Eddington approximation, neglecting $\delta(div \mathbf{F}_c)$, but with the option of neglecting or including B_0–J_0 . They found results roughly similar to those of *Ando* and *Osaki* (1975, 1977) when the term was neglected, whereas all modes were stable when the term was included. They also showed that a more accurate treatment of the radiative transfer, using variable Eddington factors, had little effect on the frequencies or the damping rates. Similarly, *Christensen-Dalsgaard* and *Frandsen* (1984) found that the inclusion of the dependence of the radiation field on the radiative frequency caused no significant changes in the damping rates, except possibly at high frequencies. Thus it appears that the grey Eddington approximation, when used correctly, is adequate for treating radiative transfer in calculations of the stability of solar oscillations.

Kidman and *Cox* (1984) used the diffusion approximation for radiation and neglected the perturbation in the convective flux. They obtained damping rates that were quite close to those found by *Christensen-Dalsgaard* and *Frandsen* (1983b); this is illustrated in Figure 7, where the corresponding line widths are plotted, together with those obtained by *Goldreich* and *Keeley* (1977a), when turbulent viscosity was included. Also shown are line widths obtained by *Gough* (1980) for radial modes; he used the diffusion approximation for radiation, but described the effects of convection according to the time-dependent mixing length theory developed by *Gough* (1977); with the exception of two modes, at frequencies of 4188 and 4340 μHz, all modes were found to be stable. Using the same technique, *Berthomieu et al.* (1980) found that five-minute modes of high degree were stable as well.

It is of great interest to compare the computed line widths with those observed (see also *Christensen-Dalsgaard, Gough* and *Libbrecht* 1988). Particularly striking is the similarity in shape, and actual values, between the observations of Libbrecht and the computations of Gough, at frequencies exceeding 3000 μHz. At lower frequencies the observed width is substantially higher than any of the computed values. This feature may also be visible in the line widths obtained by *Isaak* (1986), although the larger scatter makes a comparison more difficult. It is evident that the observations now have a precision which permits meaningful comparison with theory; and it is striking that the treatment of convection used by Gough appears to be favoured.

3.3 Stochastic excitation of solar oscillations

Although far from conclusive, the results discussed in the preceding section may be taken to indicate that the five-minute modes are stable in a linear stability analysis. In that case external sources must be sought for their excitation. *Lighthill* (1952) demonstrated that fluctuations in a fluid, caused for example by turbulence, may

generate sound waves. If the fluid is in a resonant cavity, the normal modes of the cavity would be excited. This is the mechanism responsible for sound generation in, *e.g.*, a recorder or a flute. Thus it is *a priori* plausible that the turbulence in the solar convection zone may excite the five-minute oscillations.

Before discussing this mechanism in more detail it is instructive to analyze the case of a simple, damped harmonic oscillator excited by random forcing (*e.g. Batchelor* 1956, section 4.1). Thus we consider a function $A(t)$ satisfying

$$\frac{d^2A}{dt^2} + 2\eta\frac{dA}{dt} + \omega_0^2 A = f(t), \tag{3.14}$$

where $f(t)$ is the forcing. In the absence of forcing the solution to equation (3.14) is of the same form as in equation (2.2), with a frequency $\omega = (\omega_0^2 - \eta^2)^{1/2}$. To solve the equation in the presence of forcing, we take the Fourier transform. Letting $\bar{A}(\omega')$ and $\bar{f}(\omega')$ be the transforms of $A(t)$ and $f(t)$ respectively, we obtain

$$\bar{A}(\omega') = \frac{\bar{f}(\omega')}{\omega_0^2 - \omega'^2 + 2i\eta\omega'}, \tag{3.15}$$

if terms arising from the initial conditions on A are neglected. Hence the average power spectrum $P_A(\omega') = \langle |\bar{A}(\omega')|^2 \rangle$ is

$$P_A(\omega') = \frac{P_f(\omega')}{(\omega_0^2 - \omega'^2)^2 + 4\eta^2\omega'^2} \approx \frac{1}{4\omega_0^2}\frac{P_f(\omega')}{(\omega_0 - \omega')^2 + \eta^2}, \tag{3.16}$$

if the average power spectrum $P_f(\omega') = \langle |\bar{f}(\omega')|^2 \rangle$ of the forcing varies slowly, and $|\eta| \ll \omega_0$. Thus the spectrum is approximately Lorentzian, as for the free, damped oscillator, with a width determined by the linear damping rate. Notice also that the integrated power is

$$\int_0^\infty P_A(\omega')d\omega' \approx \frac{1}{|\eta|}\frac{\pi}{4}\frac{P_f(\omega_0)}{\omega_0^2}. \tag{3.17}$$

Thus the power in the oscillation is proportional to the power of the forcing at the oscillation frequency, and inversely proportional to the linear damping rate.

The excitation of solar acoustic oscillations by turbulent convection was analyzed more carefully by *Goldreich* and *Keeley* (1977b). They considered the different non-linear terms introduced by the interaction between convection and pulsation, and identified as most important the term coming from the Reynolds stress. By expanding the motion on the linear eigenfunctions they obtained a set of amplitude equations, the solution of which is at least qualitatively similar to the solution discussed above. In particular, the total power in a mode of oscillation is analogous to equation (3.17), but with the forcing power replaced by an integral over the star involving the Reynolds stress, appropriately weighted by the eigenfunction. *Goldreich* and *Keeley* assumed that the viscous term in equation (3.8) dominated the damping. Both forcing and damping were then determined by the convection, and so, consequently, was the resulting mode amplitude. By approximating the integrals for the forcing and damping, they obtained the very simple, and intuitively appealing, result that the mode energy was given roughly by the energy in the convective eddy whose time scale matched the pulsation period.

It is instructive to consider *Goldreich* and *Keeley's* result in a somewhat simplified form, which, it is hoped, still captures the most essential features. The energy in a mode can be written as

$$\mathcal{E} = \frac{\pi^{1/2}}{16|\eta|} \frac{\int_0^R \left[\frac{d\xi_r}{dr}\right]^2 v_t^4 m_t \tau_t \exp\left[-(\tfrac{1}{2}\omega\tau_t)^2\right] r^2 \rho dr}{\int_0^R \xi_r^2 r^2 \rho dr} \,. \tag{3.18}$$

Here v_t, m_t and τ_t are the typical velocity, mass and time scale of a convective eddy at the given point in the Sun. Using also equation (3.5) to relate the integrated energy to the surface velocity V, and equation (3.6) for η, we finally obtain that

$$V^2 = \frac{\omega^2}{32\pi^{1/2} ME} \frac{\int_0^R \left[\frac{d\xi_r}{dr}\right]^2 v_t^4 m_t \tau_t \exp\left[-(\tfrac{1}{2}\omega\tau_t)^2\right] r^2 \rho dr}{|\mathrm{Re}(C)|} \,. \tag{3.19}$$

To estimate V^2 we require an expression for C. Following *Goldreich* and *Keeley*, I use equation (3.8) for the stress part. However, in contrast to them I also include the energy part, which I approximate, quite roughly, by the term coming from the departure of the mean state from radiative equilibrium, given by equation (3.13). Note also, in this term, that from the equation of continuity $\delta\rho/\rho \approx -d\xi_r/dr$.

The dominant contributions to the integrals in equation (3.19) come from a region whose thickness is only about 10^{-4} R. From Figure 5 it follows that it is then not unreasonable to assume $d\xi_r/dr$ to be constant. In equation (3.13) I also assume that $(\Gamma_3-1)\bar{\varkappa}_T$, where $\bar{\varkappa}_T \equiv \varkappa_\rho + (\Gamma_3-1)\varkappa_T$, is constant. Then this term can be written as

$$-(\Gamma_3 - 1)\bar{\kappa}_T \left[\frac{d\xi_r}{dr}\right]^2 \int_{r_F}^{R} div F_R r^2 dr \approx -(\Gamma_3 - 1)\bar{\kappa}_T \left[\frac{d\xi_r}{dr}\right]^2 \frac{L}{4\pi}, \tag{3.20}$$

if we assume that the lower limit r_F of the integral is at a point where energy is carried entirely by convection; here L is the surface luminosity of the Sun. Similarly, v_t, m_t and τ_t are replaced by constant average values; also, in accordance with equation (3.17), "resonant" eddies are selected whose time scale is the same as the pulsation period. We then obtain, *e.g.*, for the numerator in equation (3.19)

$$\left[\frac{d\xi_r}{dr}\right]^2 v_t^4 m_t \tau_t \int_{r_C}^{R} r^2 \rho dr \approx \left[\frac{d\xi_r}{dr}\right]^2 v_t^3 m_t l_t \frac{\Delta m}{4\pi}, \tag{3.21}$$

where we also neglected the exponential factor and used $\tau_t \sim l_t/v_t$; here Δm is the mass contained in the region contributing to the convective integral. For the integral in equation (3.8) a similar approximation is made. By combining equations (3.19)-(3.21), we finally obtain

$$V^2 = \frac{3}{128\pi^{1/2} ME} m_t v_t^2 \left[1 + \frac{3}{4}(\Gamma_3 - 1)\bar{\kappa}_T \frac{L}{v_t l_t \Delta m}\omega^{-2}\right]^{-1}. \tag{3.22}$$

In equation (3.22) $m_t v_t^2/2$ is the kinetic energy of a convective eddy. Thus when the second term in the square brackets is neglected, we obtain a result very similar to that of *Goldreich* and *Keeley*, viz. that the energy in a mode is similar to the energy in a convective eddy. To estimate the size of the term coming from radia-

tive damping, we take $\Delta m = 5\times10^{-10}M$, which includes most of the region contributing to the convective integrals, and evaluate the remaining quantities at the maximum of the superadiabatic gradient. The result is

$$V^2 \sim \frac{m_t v_t^2}{ME}\left[1 + 4\left[\frac{\nu}{3\text{mHz}}\right]^{-2}\right]^{-1}. \qquad (3.23)$$

This result evidently only provides an order-of-magnitude estimate. Thus *Goldreich* and *Keeley* (1977b) suggest that "resonant" eddies dominate the turbulent viscosity and show that this leads to the inclusion of a factor proportional to ω^{-2} in the turbulent viscosity, thus eliminating the frequency dependence in equation (3.23); furthermore, the notion of a turbulent viscosity is clearly only at best a rough approximation to the actual interactions between convection and oscillations. Also the treatment of radiative damping only includes one of the contributions of radiation to the damping or excitation of the oscillations. Nevertheless the result suggests that radiative damping makes a substantial contribution in reducing the amplitude. Notice that this is not inconsistent with the line widths shown in Figure 7.

An attractive feature of the stochastic excitation model, in the form discussed here, is that the predicted mode energy is essentially only a function of frequency; thus the "resonance" condition on the convective eddies only concerns their timescales, not their spatial scales. This is in agreement with the observations of *Libbrecht et al.* (1986). Without radiative damping, *Goldreich* and *Keeley* (1977b) obtained pulsation amplitudes that appeared inconsistent with early observations of oscillations in the apparent solar diameter. However *Gough* (1980) and *Christensen-Dalsgaard* and *Frandsen* (1983a) showed that amplitudes based on the simple energy equipartition results were in rough agreement with the observed values, if suitable choices were made of various undetermined constants in the theory (*e.g.* in the relation between eddy timescale and oscillation period). Also the factor E^{-1} in equation (3.22) causes a decrease in the amplitudes with decreasing frequency, although apparently not as rapidly as observed. On the basis of equation (3.23) it might be expected that the inclusion of the radiative damping would tend to decrease the amplitudes preferentially at low frequencies, hence improving the agreement in shape between the predicted and observed spectrum. However the predicted values of the amplitudes are also decreased, and it may therefore be difficult to reproduce the observed values.

Very recently *Goldreich* and *Kumar* (1988) found that dipolar terms, neglected by *Goldreich* and *Keeley* (1977b), dominate in the generation of acoustic waves by turbulent convection. As a result, very roughly, $m_t v_t^2$ should be replaced by $m_t c^2$ in the expression for the mode amplitude, c being the sound speed. Since the maxi-

mum Mach number in the solar convection zone, assuming mixing length theory, is of order 0.3, this might increase the predicted amplitudes by at least a factor 10. As far as I am aware this result has yet to be applied in detail to the prediction of the amplitudes of the solar five-minute oscillations. However, taken together with an adequate treatment of radiative damping, it offers some hope that it will become possible to understand the observed amplitude distribution.

Libbrecht et al. (1986) made an essentially phenomenological interpretation of their observed amplitudes, based on the excitation model discussed above. In Figure 3 they show with solid lines a quantity similar to E^{-1}, obtained from computed eigenfunctions. The dashed lines show $(\eta E)^{-1}$, where η was determined from the observed line widths of *Libbrecht* and *Zirin* (1986) for $\nu > 3000$ μHz, and supposed to be constant for smaller frequencies; thus for $\nu < 3000$ μHz the dashed and solid lines coincide. The latter quantity clearly bears a striking resemblance to the observed power. On this basis they suggested a phenomenological model for the mode excitation, where the modes are in equilibrium with convection at low frequencies, leading essentially to a constant mode energy, whereas the mode energy is decreased by additional sources of damping at higher frequencies. This description clearly finds some, although not complete, confirmation in the excitation model described above.

3.4 Phase relations for solar oscillations

Fairly detailed observations now exist of amplitude ratios and phase differences between different types of oscillation measurements. Since these quantities depend on the behaviour of the oscillations just beneath and in the solar atmosphere, they provide information about the damping and excitation processes going on here. Interpreting this information constitutes what B.W. Mihalas has called a Non-BOTE* problem. The observed quantities are based on measurements of radiative intensity, typically in a narrow part of a spectral line; hence they represent complicated integrals over the solar atmosphere of the behaviour of the oscillations. Nevertheless, given computation of the oscillation eigenfunctions in the atmosphere, it is in principle possible to compute the response of the intensity to the oscillation, and hence the observable quantity.

In Figure 8 are illustrated results of such a calculation, carried out by *Frandsen* (1986) on the basis of eigenfunctions computed by *Christensen-Dalsgaard* and *Frandsen* (1984). The solid line shows the local phase difference between temperature and

---

* Back Of The Envelope

velocity, whereas the squares give the computed, observable quantities corresponding to different positions in the spectral line, and hence to different levels in the atmosphere. The substantial difference between the local and the observable quantities at large optical depths indicates the significance of the non-local nature of the radiation field. At small optical depths, corresponding to the central parts of the line, the local and the observable quantities are in closer agreement. Even more striking, however, is the comparison between the computed and the observed quantities, indicated as circles with error bars. The agreement is reasonable at small optical depths, whereas there are very substantial discrepancies deep in the atmosphere. This indicates a serious deficiency in the computed eigenfunctions. Indeed an obvious source of error is the neglect by *Christensen-Dalsgaard* and *Frandsen* of the perturbation in the convective flux.

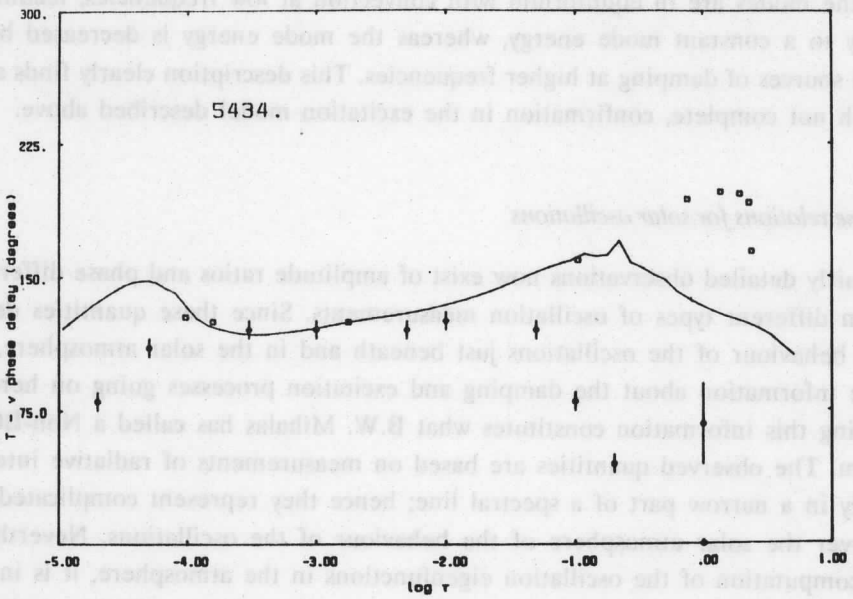

Fig. 8. Phase delay between temperature and velocity. The solid line shows the phase difference between the temperature and velocity eigenfunctions (positive values corresponding to temperature leading velocity), as a function of optical depth τ. The squares give computed phase delays between an intensity and a velocity signal, at various positions in the 5434 Å Fe I spectral line, and the circles with error bars give the corresponding observed values, largely from *Staiger et al.* (1984). The wavelength distance from the line core has been converted to an optical depth by means of suitable contribution functions. From *Frandsen* (1986).

That this may be the principal source of the error is indicated by the results obtained by *Gough* (1985). He compared phase differences, based on the calculations by *Gough* (1980) using the diffusion approximation but including the perturbation in the convective flux, with observations. The results were in reasonable agreement with the observed data of *Fröhlich* and *van der Raay* (1984), where velocity was compared with continuum intensity oscillations.

These results suggest that there are excellent possibilities for learning about the excitation of solar oscillations from phase measurements. Since the diffusion approximation for radiation fails in the solar atmosphere, a more detailed analysis requires the combination of the Eddington approximation for radiative transfer with a treatment of the convective flux perturbation. This has yet to be carried out.

4. Conclusion

We are still far from understanding the causes of the solar five-minute oscillations. Thus even the fundamental question of their stability or instability is undecided. On the basis of the evidence presented in Section 3, my personal preference is for assuming that the modes are stable and excited by convection. To the extent that this excitation mechanism has been studied (which is quite rudimentary), it appears to give results that are roughly, although not in detail, consistent with the observations. The alternative, *viz.* that the modes are unstable, has so far not been developed to the same extent. Thus, apart from the questions about the instability, the mechanisms that limit the growth of the modes and hence determine their amplitudes have not been identified.

The development of helioseismology has up to now concentrated on the measurement and interpretation of oscillation frequencies. However there is now an increasing amount of observational data relating to the processes causing the oscillations. Thus the study of these processes should undergo a rapid evolution in coming years.

A striking property of the results discussed in this paper is that the treatment of convection can now be tested observationally. Thus both the computed line widths, and the phase relations, seem to be sensitive to the inclusion of the convective flux perturbation in the calculations, with the formulation suggested by *Gough* (1977) giving results in reasonable agreement with the observations. More detailed investigations are required to establish the extent to which the observations can distinguish between the finer details in the description of time-dependent convection. Since convection is probably the most significant uncertainty in the theory of most types of pulsating stars, the information that may be obtained from studying solar oscillations is evidently of the greatest importance.

Acknowledgements. I am grateful to K.G. Libbrecht for permission to use his unpublished line widths, and to him, D.O. Gough and S. Frandsen for useful correspondence or conversations. M.J. Thompson is thanked for commenting on an earlier version of the manuscript. My participation in the workshop was financed through a grant from the Danish Natural Science Research Council.

References

Ando, H., and Osaki, Y. 1975, *Pub. A. S. J.*, **27**, 581.

Ando, H., and Osaki, Y. 1977, *Pub. A. S. J.*, **29**, 221.

Antia, H.M., Chitre, S.M., and Narasimha, D. 1982, *Solar Phys.*, **77**, 303.

Antia, H.M., Chitre, S.M., and Gough, D.O. 1987, in *Proc. IAU Symposium* No. 123, p. 371, Christensen-Dalsgaard, J. and Frandsen, S. (Eds.), D. Reidel Publ. Co.

Batchelor, G.K. 1956, *The Theory of Homogeneous Turbulence,* Cambridge University Press.

Berthomieu, G., Cooper, A.J., Gough, D.O., Osaki, Y., Provost, J., and Rocca, A., 1980, in *Lecture Notes in Physics*, **125**, 307, Hill, H.A. and Dziembowski, W. (Eds.), Springer-Verlag.

Chitre, S.M. 1987, in *Proc. IAU Symposium No. 123,* p. 345, Christensen-Dalsgaard, J. and Frandsen, S. (Eds.), D. Reidel Publ. Co.

Christensen-Dalsgaard, J. 1984, in *Solar Seismology from Space*, p. 219, Ulrich, R.K. *et al.* (Eds.), NASA, JPL Publ. 84-84.

Christensen-Dalsgaard, J., and Frandsen, S. 1983a, *Solar Phys.*, **82**, 469.

Christensen-Dalsgaard, J., and Frandsen, S. 1983b, *Solar Phys.*, **82**, 165.

Christensen-Dalsgaard, J., and Frandsen, S. 1984, *Mem. Soc. Astr. Ital.*, **55**, 285.

Christensen-Dalsgaard, J., and Gough, D.O. 1982, *M. N. R. A. S.*, **198**, 141.

Christensen-Dalsgaard, J., and Gough, D.O. 1984, in *Solar Seismology from Space*, Ulrich, R.K. *et al.* (Eds.), NASA, JPL Publ. 84-84, p. 79.

Christensen-Dalsgaard, J., Gough, D.O., and Toomre, J. 1985a, *Science*, **229**, 923.

Christensen-Dalsgaard, J., Duvall, T.J., Gough, D.O., Harvey, J.W., and Rhodes, E.J. 1985b, *Nature*, **315**, 378.

Christensen-Dalsgaard, J., Gough, D.O., and Libbrecht, K.G. 1988, *Nature*, submitted.

Claverie, A., Isaak, G.R., McLeod, C.P., van der Raay, H.B., Palle, P.L., and Roca Cortes, T. 1984, *Mem. Soc. Astr. Ital.*, **55**, 63.

Cox, J.P., Cox, A.N., Olsen, K.H., King, D.S., and Eilers, D.D. 1966, *Ap. J.*, **144**, 108.

Deubner, F.-L., and Gough, D.O. 1984, *Ann. Rev. Astr. Ap.*, **22**, 593.

Duvall, T.L., Harvey, J.W., Libbrecht, K.G., Popp, B.D., and Pomerantz, M.A. 1988, *Ap. J.*, in press.

Dziembowski, W.A. 1977, *Acta Astr.*, **27**, 203.

Dziembowski, W.A. 1988, these Proceedings.

Frandsen, S. 1986, in *Seismology of the Sun and the Distant Stars*, p. 73, Gough, D.O. (Ed.), D. Reidel Publ. Co.

Frandsen,S. 1987, in *Proc. IAU Symposium* No. 123, p. 405, Christensen-Dalsgaard, J. and Frandsen, S. (Eds.), D. Reidel Publ. Co.

Fröhlich, C., and van der Raay, H.B. 1984, in *The Hydromagnetics of the Sun*, p. 17, ESA SP-220, ESTEC.

Gabriel, M. 1987, *Astr. Ap.*, **175**, 125.

Gelly, B. 1987, *Sismologie du soleil et d'etoiles de type solaire*, Thesis, Université de Nice.

Gelly, B., Grec, G., and Fossat, F., 1986, *Astr. Ap.*, **164**, 383.

Goldreich, P., and Keeley, D.A. 1977a, *Ap. J.*, **211**, 934.

Goldreich, P., and Keeley, D.A. 1977b, *Ap. J.*, **212**, 243.

Goldreich, P., and Kumar, P. 1988, *Ap. J.*, **326**, in press.

Gough, D.O. 1977, *Ap. J.*, **214**, 196.

Gough, D.O. 1980, in *Lecture Notes in Physics*, **125**, 274, Hill, H.A. and Dziembowski, W. (Eds.), Springer-Verlag.

Gough, D.O. 1985, in *Future Missions in Solar, Heliospheric and Space Plasma Physics*, p. 183, Rolfe, E. and Battrick, B. (Eds.), ESA SP-235, ESTEC.

Grec, G., and Fossat, E. 1977, *Astr. Ap.*, **55**, 411.

Grec, G., Fossat, E., and Pomerantz, M.A. 1983, *Solar Phys.*, **82**, 55.

Harvey, J.W., Kennedy, J.R., and Leibacher, J.W. 1987, *Sky and Telescope*, **74**, 470.

Isaak, G.R. 1986, in *Seismology of the Sun and the Distant Stars*, p. 223, Gough, D.O. (Ed.), D. Reidel Publ. Co.

Kidman, R.B., and Cox, A.N. 1984, in *Solar Seismology from Space*, p. 335, Ulrich, R.K. *et al.* (Eds.), NASA, JPL Publ. 84-84.

Lamb, H. 1909, *Proc. London Math. Soc.*, **7**, 122.

Ledoux, P., and Walraven, T. 1958, *Handbuch der Physik*, Vol. 51, chapter IV; Springer-Verlag.

Libbrecht, K.G., and Kaufman, J.M. 1988, *Ap. J.*, in press.

Libbrecht, K.G., and Zirin, H. 1986, *Ap. J.*, **308**, 413.

Libbrecht, K.G., Popp, B.D., Kaufman, J.M., and Penn, M.J. 1986, *Nature*, **323**, 235.

Lighthill, M.J. 1952, *Proc. Roy, Soc. London,* **211A**, 564.

Lites, B.W., and Chipman, E.G. 1979, *Ap. J.*, **231**, 570.

Lites, B.W., Chipman, E. G., and White, O.R. 1982, *Ap. J.*, **253**, 367.

Maeder, A. 1980, *Astr. Ap.*, **90**, 311.

Noyes, R.W. 1987, in *Proc. IAU Symposium* No. 123, p. 527, Christensen-Dalsgaard, J. and Frandsen, S. (Eds.), D. Reidel Publ. Co.

Noyes, R.W., Baliunas, S.L., Belserene, E., Duncan, D.K., Horne, J., and Widrow, L. 1984, *Ap. J. (Letters)*, **285**, L23.

Pallé, P.L., Perez, J.C., Régulo, C., Roca Cortés, T., Isaak, G.R., McLeod, C.P., and van der Raay, H.B. 1987a, *Astr. Ap.*, **170**, 114.

Pallé, P.L., Perez, J.C., Régulo, C., Roca Cortés, T., Isaak, G.R., McLeod, C.P., and van der Raay, H.B. 1987b, *Astr. Ap.*, **169**, 313.

Perdang, J. 1988, these Proceedings.

Scherrer, P. 1984, in *Solar Seismology from Space*, p. 173, Ulrich, R.K. *et al.* (Eds.), NASA, JPL Publ. 84-84.

Staiger, J. 1987, *Astr. Ap.*, **175**, 263.

Staiger, J., Schmieder, B., Deubner, F.-L., and Mattig, W. 1984, *Mem. Soc. Astr. Ital.*, **55**, 147.

Stebbins, R., and Goode, P.R. 1987, *Solar Phys.*, **110**, 237.

Unno, W. 1967, *Pub. A. S. J.*, **19**, 140.

Unno, W., Osaki, Y., Ando, H., and Shibahashi, H. 1979, *Nonradial Oscillations of Stars*, University of Tokyo Press.

THEORY AND OBSERVATIONS OF PULSATING WHITE DWARF STARS

D.E. Winget*
Department of Astronomy and McDonald Observatory
University of Texas, USA

Abstract

The pulsating white dwarf stars are among the simplest of all stars undergoing nonradial pulsations; this is a reflection of the simplicity in the structure of the equilibrium star. This simplicity provides the hope for understanding these stars and using them to unravel the physics of the structure and evolution of white dwarf stars, and to achieve a better understanding of the general phenomenon of nonradial stellar pulsation. In this review we will discuss the status of the field, and identify the major problem areas that remain.

1. Motivation for studying white dwarf pulsators

The pulsating white dwarf stars are astrophysical laboratories tailored to the study of nonradial stellar pulsations and the physics of compact objects. In this review we summarize the progress made in exploiting these laboratories, and examine the problems at the frontiers of the field.

In the study of nonradial stellar pulsations you have to say that the buck stops here, with the pulsating white dwarf stars. By this I mean that if we cannot understand the nonradial pulsations in white dwarfs, it is probably hopeless to try and understand other nonradial pulsators. This extreme position is defended by four basic considerations. First, the underlying structure of the white dwarf stars is arguably the simplest of all stars. Second, the amplitudes of the pulsations are large enough to be observable, yet small enough (in many cases) to allow a linear treatment. Third, there is a veritable wealth of pulsation periods observed in many of the pulsators – each period providing independent clues about the underlying structure of the star. Fourth, and finally, the pulsation periods are extremely short (100-1000 s), so that many cycles can be recorded in a single observation. Fortunately, as the rest of this review will indicate, we have been able to reach some level of understanding of

* Alfred P. Sloan Research Fellow

the pulsations in the white dwarf stars. Thus we have the prospect of applying much that we have learned, and will learn in the future, to other nonradially pulsating stars.

These multi-frequency pulsations probe the deep interiors of the compact objects, allowing us to explore the physics of hot, high-density matter, studying the equation-of-state for conditions otherwise inaccessible. Additionally, we can use the pulsations to map out the compositional structure of the star from the photosphere to the center. Knowledge of the composition of the central regions tests our understanding of pre-white dwarf evolution, and nuclear reaction rates. Determination of the compositional structure of the outer layers will develop our knowledge of chemical diffusion in the presence of strong gravitational fields. Thus we can use the pulsations to refine our basic understanding of the structure and evolution of the white dwarf stars.

2. Basic properties of white dwarf stars

The first part of the white dwarf moniker is misleading – these stars have surface temperatures ranging from in excess of 150,000 K (white) down to about 3,000K (red). The corresponding range in luminosities is $4 \geq log(L/L_{\odot}) \geq -4.5$, indicating that they occupy the lower left half of the H-R diagram as shown in Figure 1. In spite of the enormous range they occupy in the H-R diagram, the white dwarf stars are a remarkably homogeneous class of objects.

Plotting the isolated, or non-interacting binary white dwarf stars in the theoretical H-R diagram, we find a more or less narrow distribution about an evolutionary sequence for a $0.6M_{\odot}$ planetary nebula nucleus (see the solid line in Figure 1). Indeed, observational determinations of the mass function for white dwarfs yield a sharply peaked distribution with about $0.6M_{\odot}$ for the mean mass and $\sigma \sim 0.1$ (*cf.* *Weidemann* and *Koester* 1984 and references therein). Except for the hottest white dwarf stars, the evolution is at nearly constant radius, with the primary pressure support for the star coming from degenerate electrons. The weak temperature sensitivity of this source of pressure support insures an approximate separation of mechanical and thermal properties – greatly simplifying the study of the evolution of the white dwarf stars.

Post-Main Sequence evolutionary calculations suggest that the cores are composed of a mixture of carbon and oxygen; there is little agreement at present, however, on the relative abundances of the two elements due to uncertainties in both reaction rates and pre-white dwarf evolution (*cf.* *Winget* and *Van Horn* 1988, and *Mazzitelli* and *D'Antona* 1988). Observations imply that most of these cores are coated with either a thin veneer of nearly pure hydrogen (white dwarfs of spectroscopic type

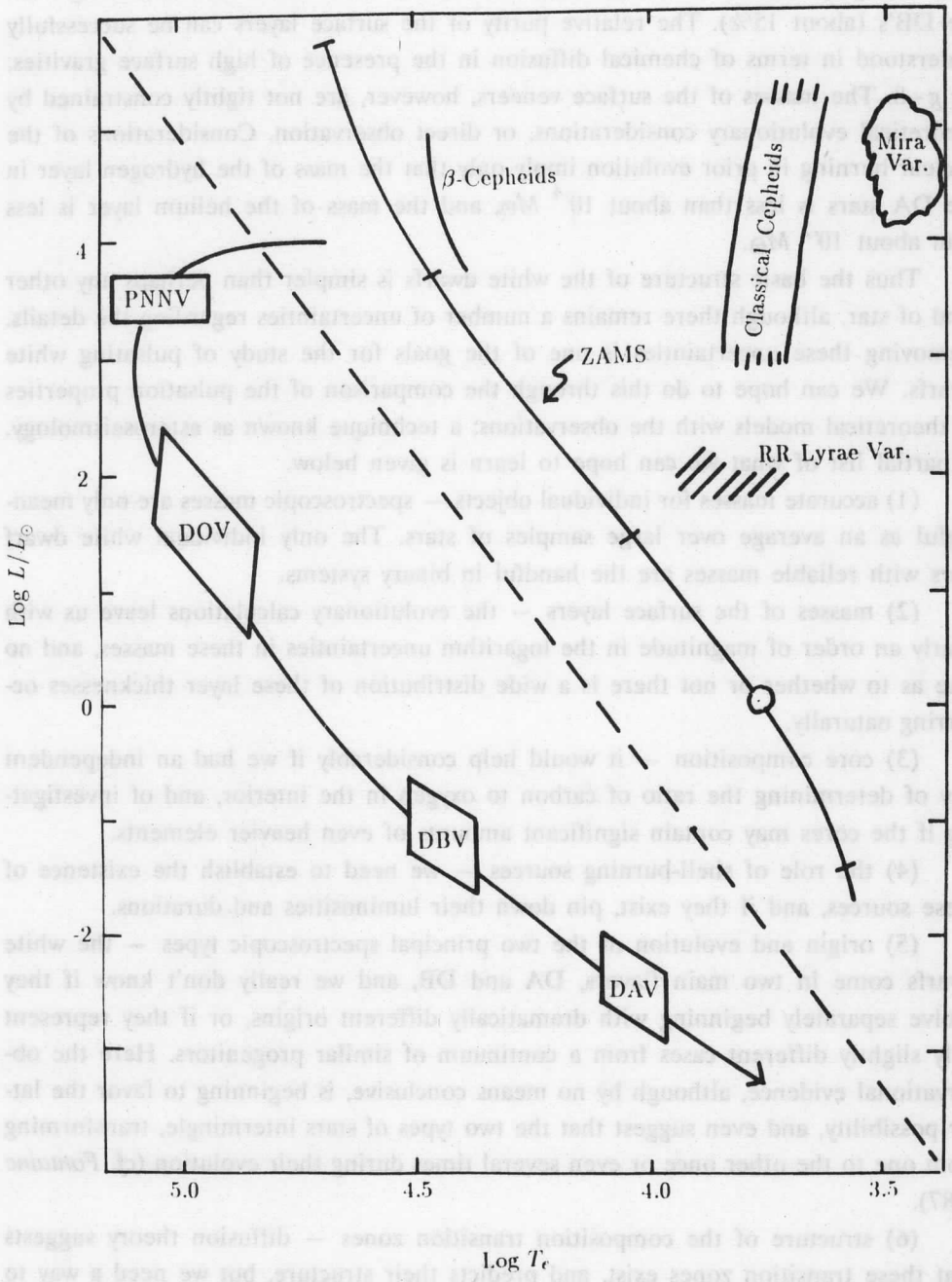

Fig. 1. A sketch of the location of the pulsating white dwarf stars in the H-R diagram

DA) or a thin veneer of essentially pure helium (white dwarfs of spectroscopic type DB): Roughly 80% of the white dwarfs are DA's, and most of the remaining stars are DB's (about 15%). The relative purity of the surface layers can be successfully understood in terms of chemical diffusion in the presence of high surface gravities, $\log g \sim 8$. The masses of the surface veneers, however, are not tightly constrained by theoretical evolutionary considerations, or direct observation. Considerations of the nuclear burning in prior evolution imply only that the mass of the hydrogen layer in the DA stars is less than about $10^{-4}\ M_{\odot}$, and the mass of the helium layer is less than about $10^{-2}\ M_{\odot}$.

Thus the basic structure of the white dwarfs is simpler than perhaps any other kind of star, although there remains a number of uncertainties regarding the details. Removing these uncertainties is one of the goals for the study of pulsating white dwarfs. We can hope to do this through the comparison of the pulsation properties of theoretical models with the observations: a technique known as asteroseismology. A partial list of what we can hope to learn is given below.

(1) accurate masses for individual objects – spectroscopic masses are only meaningful as an average over large samples of stars. The only individual white dwarf stars with reliable masses are the handful in binary systems.

(2) masses of the surface layers – the evolutionary calculations leave us with nearly an order of magnitude in the logarithm uncertainties in these masses, and no clue as to whether or not there is a wide distribution of these layer thicknesses occurring naturally.

(3) core composition – it would help considerably if we had an independent way of determining the ratio of carbon to oxygen in the interior, and of investigating if the cores may contain significant amounts of even heavier elements.

(4) the role of shell-burning sources – we need to establish the existence of these sources, and if they exist, pin down their luminosities and durations.

(5) origin and evolution of the two principal spectroscopic types – the white dwarfs come in two main flavors, DA and DB, and we really don't know if they evolve separately beginning with dramatically different origins, or if they represent only slightly different cases from a continuum of similar progenitors. Here the observational evidence, although by no means conclusive, is beginning to favor the latter possibility, and even suggest that the two types of stars intermingle, transforming from one to the other once or even several times during their evolution (*cf. Fontaine* 1987).

(6) structure of the composition transition zones – diffusion theory suggests that these transition zones exist, and predicts their structure, but we need a way to test these ideas.

(7) ages as a function of temperature – the age of the white dwarf stars as a function of temperature, or equivalently luminosity can be calculated theoretically, but again, this needs to be calibrated by observation – particularly since the age of the coolest white dwarfs is an important measure of the age of the disk.

3. General properties of the pulsating white dwarf stars

I will make no attempt here to deal with the historical development of the field of pulsating white dwarfs – even though this contains considerable lessons for workers in other areas of nonradial stellar pulsations – for this the reader is referred to *Winget* (1987). After summarizing the pulsation properties, I will discuss only the important developments since that review; other recent reviews have been published by *Kawaler* (1987), *Starrfield* (1987), *Cox* (1986), and *Winget* (1986).

The pulsating white dwarf stars, or more accurately the compact pulsators, divide into at least three, and possibly four, distinct classes of pulsating variable stars, named according to the classification scheme of *Sion et al.* (1983). If we lump the two hottest classes together, then the three remaining classes are almost uniformly distributed in $\log T_e$, and lay along white dwarf evolutionary tracks in the H-R diagram (see the sketch of the instability regions in Figure 1). In Figure 1, note that I have subdivided the hottest class, the DOV stars, into two classes, the DOV and the PNNV stars. I have treated the star K1-16 as distinct from the DOV stars for three fundamental reasons: unlike the four DOV's it is embedded in a nebula, its pulsation periods are a factor of three longer than those in the DOV stars, and finally its luminosity is considerably higher than that of the DOV stars. For these reasons we must be cautious with this star; it is tempting to lump it with the DOV's but this implies that the driving mechanism and the mode selection mechanism are the same – clearly a dangerous assumption at this time.

Representative light curves of stars in the hotter classes can be found in *Winget* (1987), and light curves of the DAV, or ZZ Ceti stars, can be found in *Robinson* (1979), and references therein.

In spite of the wide separation of the classes in the H-R diagram, they share remarkably similar pulsation properties. These properties are summarized in Table 1. All are multi-periodic, with periods in the range from about 100 s to 2,000 s (although this upper limit may be an observational selection effect imposed by limits of the observing technique). All are low-amplitude pulsators in the optical, with typical semi-amplitudes of individual modes of one percent or less.

We can show that the similarity of the underlying structure of these objects can account for much of the similarities in the observed properties. Let's begin by noting that the high mean densities of these objects imply that the radial pulsation timescales

for even the lowest density PNNV and DOV stars is considerably less than 100 s, and for the DBV and DAV stars it is less than 10 s. This suggests that we concentrate on the nonradial modes.

Table 1. Observed properties of pulsating white dwarf stars

Class	Spectra	log g	$\log L/L_\odot$	T_e(K)	P(s) (range) typical	Fract. Amp. (range) typical
PNNV	HeII, CIV nebula	>6	3-4	>100,000	(>1000) 1500	0.01
DOV	HeII, CIV, OVI abs. w/nar. em. core	7	2	>100,000	(300-850) 500	(<.001-.04) 0.01
DBV	HeI pure He abs.	8	-1.2	25,000	(140-1000) 500	(<.001-.04) 0.02
DAV	H pure abs.	8	-2.8	12,000	(100-1200)	(<.001-.1) 0.01

We can look at these with the aid of a diagram: the run of the square of the Brunt-Väisälä frequency, N^2, and the square of the acoustic, or Lamb, frequency, S_l^2 through a typical star. Figure 2 is such a diagram (for $l=2$) of a typical model representing a DAV with $M=0.6M_\odot$, $M_H/M_\odot = 10^{-10}$, and $M_{He}/M_\odot = 10^{-3}$. Local analysis of the asymptotic dispersion relation for nonradial oscillations shows that pressure modes, or p-modes, propagate only when the mode frequency is greater than both N^2, and S_l^2. The reverse is true for the gravity modes, or g-modes: they propagate locally only when the mode frequency is less than both N^2 and S_l^2 (for an elementary discussion of propagation zones and local analysis see *Cox* 1980, and *Unno et al.* 1979). From this diagram it is clear that modes which have frequencies corresponding to those observed are the nonradial g-modes.

The dramatic drop in N^2 as we go towards the interior (the bulk of the star – note the logarithmic scale of the horizontal axis) is caused by strong electron degeneracy. In contrast, the stiff equation-of-state associated with the strong degeneracy implies that the central condensation is low, and so the acoustic frequency rises only very gradually as we approach the interior. Thus the p-modes have a rather wide propagation zone and hence significant amplitudes even in the interior, while the g-modes are concentrated much more towards the surface. Note that these circumstances are reversed over stars in the upper right half of the H-R diagram (*cf. Cox* 1980), where because of the high central condensation we are used to thinking of p-modes as envelope modes and g-modes as core modes.

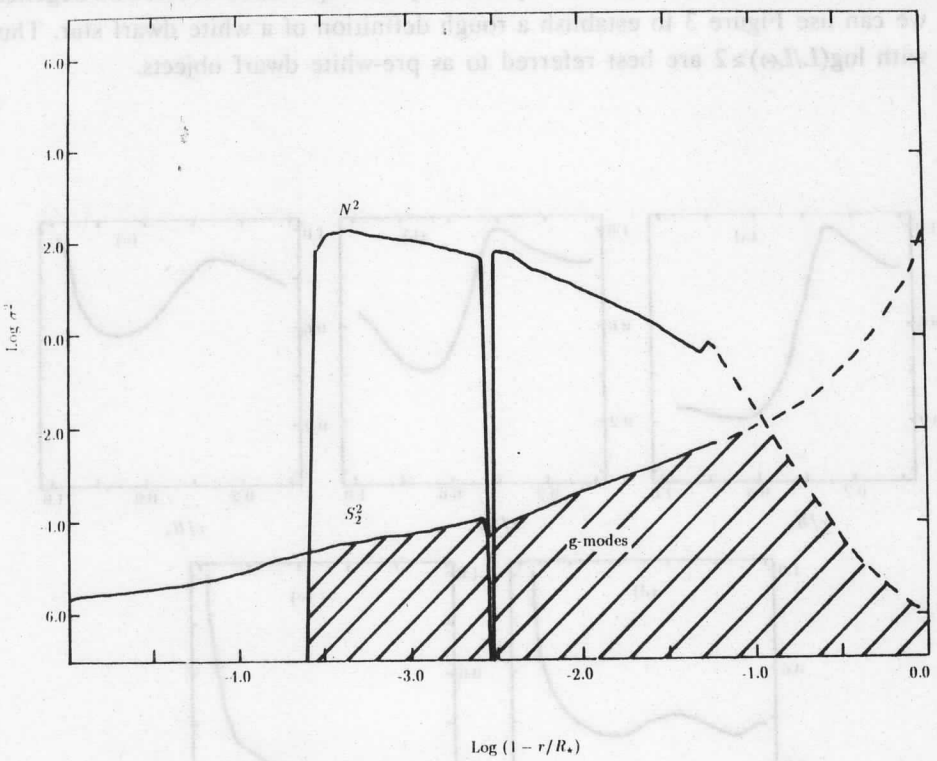

Fig. 2. A propagation diagram for a DAV model from a $0.6M_\odot$ evolutionary sequence with $log\ M_H/M_{star} = -10$, and $log\ M_{He}/M_{star} = -3$. Note that the center is on the right and the surface is on the left. The shaded regions indicate where g-modes are locally propagating.

The transition of the g-modes from core-dominated modes to envelope-dominated modes can be traced qualitatively with the aid of evolutionary calculations following the contraction and cooling of a model planetary nebula nuclei. Figure 3 (adapted from *Kawaler, Hansen,* and *Winget* 1985) shows the region of period formation for an $l = 1$, $k = 25$ mode in evolutionary models with luminosities ranging from $3 \geq log(L/L_\odot) \geq 1$. The plotted line in each figure is the envelope of the arbitrarily normalized Epstein weight function, regions where it is large represent regions of highest weight in determining the period. We can see that the increasing degeneracy in the interior gradually squeezes the mode to the surface. This plot shows that the transition to white dwarf-like envelope-dominated modes occurs around $\log(L/L_\odot) \sim 2$, about the luminosity of the DOV stars. Because we are measuring the degree of

central concentration in the object (or equivalently the importance of electron degeneracy), we can use Figure 3 to establish a rough definition of a white dwarf star. Thus stars with $\log(L/L_\odot) \geq 2$ are best referred to as pre-white dwarf objects.

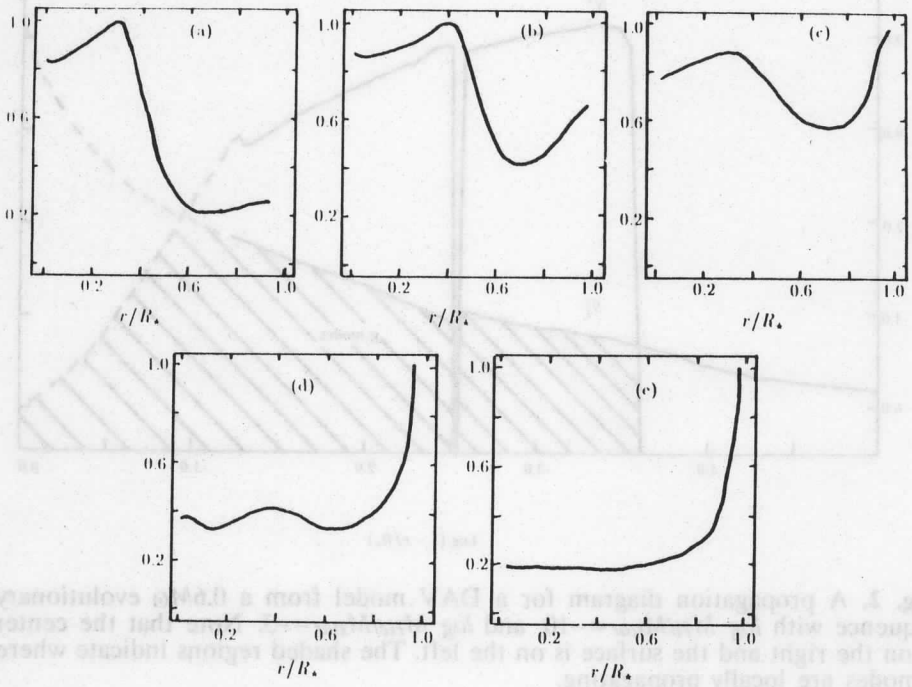

Fig. 3. The envelope of the Epstein weighting function, arbitrarily normalized to unity at the highest point in the curve, for a $k=25$, $l=1$, mode in five models from a $0.6M_\odot$ evolutionary sequence. This indicates the relative contribution of each region to the period formation. The effective temperatures and luminosities of the models are (a) $\log T_e = 171{,}000$K , $\log L/L_\odot = 3.0$, $\log T_e = 146{,}000$K, $\log L/L_\odot = 2.5$, (c) $\log T_e = 123{,}000$K, $\log L/L_\odot = 2.0$, (d) $\log T_e = 100{,}000$K, $\log L/L_\odot = 1.5$, (e) $\log T_e = 81{,}000$K, $\log L/L_\odot = 1.0$.

This transition seems to underscore our earlier point about the danger of lumping K1-16 (with $\log(L/L_\odot) > 3$) in with the DOV stars. Figure 3 suggests that interior properties may be much more important than envelope properties both for destabilizing the pulsations, and for producing the filter mechanism which determines what modes are observed. On the other hand, the surface concentration also increases rapidly with increasing k, and as indicated in Table 2 the values of k needed to account for the observed periods in K1-16 are a factor of 2 higher than those needed

for the DOV stars. Thus the envelope may still be the most important region, even for K1-16, for destabilizing the oscillations and for selecting the specific modes. Clearly this point needs to be looked at very carefully in the future.

Table 2. Theoretical summary of pulsating white dwarf stars

Class	Driving Mechanism	l	k (l=1)
PNNV	C, O p.i.?, nuclear?	1-4	50-100
DOV	C, O p.i.?, nuclear?	1-4	20-40
DBV	He p.i.	1-4	10-20
DAV	H p.i.	1-4	1-10

Table 3. Observational limits on rates of period change

Object	Type	P (s)	log P/(dP/dt) (yr)	Theoretical Expectation
PG1159-035	DOV	516	5.83	6
PG1351+489	DBV	489	>7	7-8
R 548	DAV	213	>8	9.6
L 19-2	DAV	114	>8	9.6
G 117-B15A	DAV	215	>9	9.6

Indeed, Table 3 indicates while all the pulsating white dwarf (and pre-white dwarf) stars seem to be pulsating in nonradial gravity-modes with very low spherical harmonic index, there is about a factor of 2 change in the values of k between each class. What is most interesting is the way in which this change occurs. As these objects evolve they become less centrally condensed, and the Brunt-Väisälä frequency decreases so that following an evolutionary track, as we come to each class we can drop down to smaller values of k and the modes corresponding to the observed periods remain envelope-dominated.

The exact significance of this class-to-class behavior of the pulsating variables has probably not been fully appreciated by us yet, but does, again, provide a hint that to a large extent the envelopes control the pulsations. This is born out in that the driving mechanism for the DAV and DBV stars has been conclusively established as resulting from the surface H and He ionization zones, respectively, in each class (*cf.* reviews by *Winget* and *Fontaine* 1982, *Van Horn* 1985, *Kawaler* 1987, and *Starrfield* 1987). Further, the most viable mechanisms which have been proposed for ex-

citing the observed oscillations in the PNNV and DOV stars are partial ionization of oxygen and possibly carbon in layers just below the surface, and nuclear burning of He in a thin shell near the surface. Both these mechanisms have serious problems, however, as we will discuss in Section 4.

The envelope also provides a possible filter mechanism for these stars. The need for this arises when we consider any of the partial ionization zone excitation mechanisms (although nuclear burning seems to carry its own sharp filter, see Section 4 and *Kawaler* 1987). These excite a very broad, roughly Gaussian distribution of modes with the peak near the thermal timescale at the base of the partial ionization zone. This would indicate that modes of consecutive k, for at least the lowest values of l, should all be observed. This is not the case, at least not for most of these stars. While the spectra of observed modes are dense, they are almost never observed to be as dense as the possible oscillation spectra. Hence, there is some filter mechanism at work which enhances some modes and suppresses others.

One possible selection mechanism is resonant mode-trapping. This refers to the lower kinetic energies associated with modes whose eigenfunctions resonate with the stratified surface layer thicknesses. This selectively enhances the excitation rate of the trapped mode (within the Gaussian distribution of unstable modes) over its neighboring modes, and may lead to saturation of the driving mechanism by the most unstable modes. Unfortunately all the calculations that have been done to date necessarily have been linear, and it is an inherently nonlinear problem. This selection mechanism has been described in detail elsewhere for DAV and DBV stars (*Winget, Van Horn* and *Hansen* 1981, *Dolez* and *Vauclair* 1981, and particularly *Winget* and *Fontaine* 1982). Most recently the consequences of these surface layer resonances are being investigated in the context of their effects on rates of period change by Wood (*cf. Wood* and *Winget*, these proceedings).

This sort of selection mechanism has also been discussed with application to the DOV and PNNV stars by *Kawaler* (1987) and *Cox* (1987). Here gravitational settling has not yet had time to produce a sharp chemical stratification, but nuclear shell burning may have done just that. In this case concentration gradient effects may initially cause chemical diffusion to work at blurring the composition transition zone with time – and we will speculate that this idea may help in understanding PG1159-035's recent behavior (see below). If the studies of mode-trapping are successful it is reasonable to hope that we can begin to map out surface layer thicknesses in individual stars.

We have discussed the nonradial g-mode pulsations as envelope-dominated modes in white dwarfs, temporarily ignoring the fact that they are global pulsations probing the entire star. It is this global nature which makes them interesting in another context: they provide an exciting opportunity to measure evolutionary timescales directly

– as *Kawaler* (1986) aptly put it, "turning stellar evolution into a spectator sport". This is possible because we have developed techniques to measure rates of period change through changes in phase. For white dwarf stars this period change translates in a very straightforward way, at least to order of magnitude, to an evolutionary timescale.

This can be seen, dimensionally, by differentiating the asymptotic (in k) expression for the period of nonradial g-modes, and substituting the expression for N^2 in a degenerate interior. The result is an expression for $\dot{P}/P$ which is the sum of two terms, one proportional to $\dot{R}_{star}/R_{star}$, and the other proportional to $\dot{T}_{core}/T_{core}$ (*cf. Kawaler* 1987, and *Winget* 1987). For our purposes we can take $\dot{R}_{star} \sim 0$, and see that $\dot{P}/P$ is proportional to e-folding timescale for the core temperature, *i.e.* the evolutionary timescale. (The observational technique, as well as the theory is discussed in considerable detail elsewhere, *cf. Robinson* and *Kepler* 1980, *Winget et al.* 1985, *Winget* 1987, *Kawaler* 1987).

Because of the fortuitous locations of the instability strips we have 3 well-separated temperature domains in which we can hope to measure evolutionary timescales. Thus we can hope to obtain a very accurate calibration of the white dwarf cooling sequence using the pulsating white dwarfs. Observational calibration will be indispensable in accurately determining the age of the coolest white dwarfs, and thereby the age of the galactic disk (*cf. Winget, Nather,* and *Hill* 1987).

Having taken a look at the overall picture for the pulsating white dwarfs, let's go ahead and look class by class at some of the recent developments, and especially some of the problems, that have arisen.

4. A class by class glance at the pulsating white dwarf stars: what we know and what we know we don't know

4.a The DOV and PNNV stars

The hottest groups, the DOV stars and PNNV stars, have effective temperatures in excess of 100,000 K. The total number of known pulsators in these groups has risen to five with the discovery of pulsations in the DO star PG0122+200 by *Grauer et al.* (1987a).

Surveys for additional pulsating DOV and PNNV stars have also turned up 15 null results (*Grauer et al.* 1988a). These candidates were selected because of their similarity to the other DOV and PNNV stars: 3 were spectroscopically identical with PG1159-035 and 4 were similar to K1-16. The absence of pulsations in these objects presents a serious challenge to our understanding of the driving mechanism in these stars.

Another class of problem exists with the proposed driving mechanisms for these stars. First consider the possibility of driving due to partial ionization of an abundant element near the surface. The only elements which could reasonably fill the bill are carbon and oxygen – hydrogen and helium would be completely ionized at these temperatures. The problem arises when we consider how to get the carbon/oxygen close enough to the surface to develop partial ionization zones.

While we do see C and O absorption features in most of these stars, we also see very strong He II absorption features. Also, the DOV's are a large fraction of the objects in this part of the H-R diagram; they must be supposed to be progenitors of a significant fraction of white dwarf stars, say the DB's (the problem will only get worse if we assume they are progenitors of DA stars). Thus we can explain all of the above if we assume the DOV's have a thin layer of He overlaying the C/O partial ionization zone, and further assume that the radiative He layer does not mix with the underlying convective C/O layer (*cf. Starrfield* 1987 and references therein). However, once the He becomes ionized, near $T_e \sim 30{,}000$ K, the whole surface mixes (*Fontaine* 1987) and we are left with no DB's, just C/O stars – which are not observed.

Thus we, full of hope, turn our attention towards the possibility of driving the oscillations with nuclear shell burning sources, particularly He-burning shells. Unfortunately there are serious problems here too. *Kawaler* (1987) has investigated this possibility extensively with evolutionary models of PNNV and DOV stars incorporating active He-shell burning sources. This mechanism does produce unstable g-modes in the models, but none with periods longer than about 200s. Not only do we not observe any periods this short in any of the pulsators, but an extensive survey of planetary nebula nuclei – where the shell burning sources should be most active – by *Hine* (1987) has produced only null results. So we are still at a loss to explain why the DOV and PNNV stars pulsate, in spite of nature's obvious ease in producing them.

The work on shell-burning sources has produced interesting results, however. It suggests that planetary nebula nuclei do not have active shell-burning sources at all, indicating that the mass loss in the planetary and pre-planetary nebula stages must extinguish the shell sources. This result can be combined with diffusion theory to produce a self-consistent picture of the spectral evolution of white dwarfs, wherein the DO stars – including the DOV stars – are the progenitors of both the DA and DB white dwarf stars (see *Fontaine* 1987 for a complete discussion of this idea).

Although the amplitude of the DOV pulsation modes is relatively small in the optical, the high effective temperatures of the DOV stars suggest that it is very interesting to look at shorter wavelength. Indeed, *Barstow et al.* (1986) have reported

the first observation of pulsations in the X-ray band. Their observations in the soft X-ray (44-150 Å) demonstrated large amplitude pulsations (up to 17% for individual mode semi-amplitudes) at the same frequencies detected in the optical.

The power spectra of the light curves of these stars separate into distinct bands of power, with most bands exhibiting some fine structure. In a series of recent papers Kawaler (*cf. Kawaler* 1987 and references therein) has shown, using the observations of PG 1159-035, that the period spacing between these bands can be used to determine the mass of the DOV to two significant figures, as well as to determine the l values of the observed modes. Observations of the new DOV, PG 0122+200, by *Hill, Winget,* and *Nather* (1987), have resolved the period bands present in it. They find the same sort of regular period spacing expected by Kawaler – thereby demonstrating the usefulness of this new technique to extract seismological information from the DOV stars. For this reason the resolution of the band structure in the other DOV stars should be of highest priority.

Recent re-observations of PG1159-035 (*Koupelis* and *Winget* 1987), have revealed that at least four new bands of power were present in the 1987 data which was not present above the noise in the considerable body of archival data from 1979-1984. Most puzzling is that the eight bands of power previously reported in the star (*Winget et al.* 1985) are still present at amplitudes consistent with the previous data – indicating that the new period bands grew in leaving the old unchanged. This view is lent further support by the analysis of the 1987 data for the phase of the 516 s peak (a single isolated peak) by *Winget* and *Kepler* (1988). The new data are consistent with the ephemeris of Winget *et al.*, and suggest that the 516 s peak has not only maintained its amplitude and frequency but its phase as well (including the slow secular evolutionary change), even as the new bands appeared. These observations will severely challenge models for the mode-selection mechanism in these stars, and also possibly provide unprecedented information about their nonlinear behavior.

It is interesting that the new bands appearing in PG1159-035 have periods consistent with Kawaler's model, providing further evidence that it is correct.

4.b The DBV stars

The pulsating compact stars of intermediate temperature are the DBV stars. Since the review of *Winget* (1987), a new DBV star, PG 1456+103, has been found by *Grauer et al.* (1988b), bringing the known total to 5. Studies of the temperature range of these stars indicate that all the variables fall into a very narrow range near the highest temperatures of the DB stars. The exact values of this temperature range remain somewhat uncertain due to difficulties in reconciling optical and IUE temperature estimates (*cf. Liebert et al.* 1986). The IUE results (*Liebert et al.* 1986) imply a

blue edge of 28,000 K ± 2,000 K, and a red edge of 24,000 ± 2,000 K. However, if the optical temperature scale is adopted the blue edge may be up to 3,500 degrees cooler, and the red edge about 2,000 K cooler.

The work of Liebert et al. serves to define an empirical instability strip, and suggests that most or all of the stars in the temperature strip pulsate and those outside do not. Indeed, Grauer *et al.* selected PG 1456 + 103 as a candidate because its temperature lays between known variables on the IUE temperature scale of *Liebert et al.* (1986). This suggests that similar to the DAV stars the pulsations are strictly an evolutionary effect, and that the DBV stars are otherwise normal DB stars. These conclusions must be regarded as tentative however, because the sample of stars, variable and nonvariable, upon which they are based is perilously small.

Only the light curve of PG1351 + 489 can be considered resolved, and its simplicity and similarity to some DAV light curves suggest that it may be a special case (*cf. Winget* 1987). Like the DAV stars G191-16, and GD 154, the light curve of PG1351 + 489 is very nonlinear in appearance. All three stars are dominated by a single frequency and its harmonics, with additional power at 3/2 the frequency of the main peak. The striking similarity of objects in two different classes remains unexplained, and probably must await nonlinear calculations.

Attempts to resolve the light curve of GD 358 by *Hill* (1987) succeeded in demonstrating, surprisingly, that the pattern of sets of five regularly spaced modes is not stable. The spacing appears to change, and on occasion the star appears to be nearly a mono-periodic pulsator. Hill points out that this sort of behavior casts serious doubt on the rotational splitting explanation for the equally spaced modes, and also indicates that the pulsations are not stable, since beating is not a plausible explanation for the dramatic changes in the character of the light curve.

4.c The DAV or ZZ Ceti stars

Rotational splitting still seems to be the explanation of choice for at least one of the coolest class of compact pulsators, the DAV stars. The work of *O'Donoghue* and *Warner* (1987) on L19-2, has demonstrated that rotational splitting is very successful in explaining not only the generally equally-spaced structure of the power spectrum, but also that the slight deviations from equal spacing can be accounted for by the next highest order terms due to rotational splitting.

O'Donoghue and Warner are also monitoring the phase of the pulsations in this star attempting to measure a rate of period change in this star. The same is being done for R548 (*Tomaney* 1987), and for G117-B15A (*Kepler et al.* 1987). Currently, the limits on all three stars are rapidly approaching the values expected from

theoretical evolutionary calculations (see Table 3, and *Wood* and *Winget 1988),* and the best limit comes from G117-B15A: $|dP/dt| \leq 7.7 \times 10^{-15}$, at the 68% confidence level.

Observations of PG2303+243 by *Vauclair et al.* (1987), indicate that it is the 20th DAV, and the only new one discovered since the review of *Winget* (1987). New variables may be found at a somewhat higher rate in the future, however, after the work of *Fontaine et al.* (1985). They showed that the well defined temperature instability strip for the DAV stars based on G-R colors can be almost as sharply defined using the much more readily available Strömgren colors. This result should increase the ease of identification of candidate stars.

Our discussion of the pulsating white dwarfs is not complete without noting that there may also be a class of hot DAV's, in addition to the ZZ Ceti stars, with surface temperatures similar to the DBV stars, and driving provided by He partial ionization at the top of the He-layer (*cf. Winget* and *Fontaine* 1982). Finally it is also possible that the coolest white dwarf stars may pulsate. Driving may occur from the κ-mechanism operating due to the large observed surface opacities – or if they are cool enough that the crystallization boundary is close to the surface, driving may result from the difference in heat capacities across the crystal/fluid transition region. The prospect of observing oscillations in the oldest white dwarfs, and thereby measuring their ages and probing the physics of crystallization, makes the search for cool pulsating white dwarfs a very high priority observational task.

Before closing this review, there are several points I would like to stress. We have a very good basic understanding of white dwarf stars and their pulsations. The field has matured to the point that we can begin to consider the prospect of seismological investigations of *individual* pulsators: we can measure pulsation frequencies to better than a part in 10^9, and we can actually measure evolutionary timescales in these stars. On the other hand, there are glaring gaps in our understanding which we will need to turn our attention in to the future: we still don't know why the hot stars pulsate; we don't have any real handle on the interaction of pulsations with convection, or how this affects the driving, or the mode selection; in general we have no real understanding of any nonlinear phenomena in these stars, in spite of the evidence of its importance.

References

Barstow, M.A., Holberg, J.B., Grauer, A.D., and Winget, D.E. 1986, *Ap. J., (Letters)*, **306**, L25.

Cox, J.P. 1980, *Theory of Stellar Pulsation* (Princeton, New Jersey: Princeton University Press).

Cox, A.N. 1986, *Highlights of Astron.*, ed. J.P. Swings (Dordrecht, D. Reidel) p. 229.

Cox, A.N. 1987, in IAU Colloq. No.95, *The Second Conference on Faint Blue Stars*, ed. A.G.D. Philip (Schenectady; Davis Press), in press.

Dolez, N., and Vauclair, G. 1981, *Astr. Ap.*, **102**, 375.

Fontaine, G. 1987, in IAU Colloq. No.95, *The Second Conference on Faint Blue Stars*, ed. A.G.D. Philip (Schenectady; Davis Press), in press.

Fontaine, G., Bergeron, P., Lacombe, P., Lamontange, R., and Talon, A. 1985, *A. J.*, **90**, 1094.

Grauer, A.D., Bond, H.E., Liebert, J., and Green, R.F. 1987a, *Ap. J.*, in press.

Grauer, A.D., Bond, H.E., Liebert, J., Fleming, T.A., and Green, R.F. 1988a, *Ap. J.*, in press.

Grauer, A.D., Bond, H.E., Liebert, J., and Green, R.F. 1988b, *A. J.*, in press.

Hill, J.A. 1987, in IAU Colloq. No.95, *The Second Conference on Faint Blue Stars*, ed. A.G.D. Philip (Schenectady; Davis Press), in press.

Hill, J.A., Winget, D.E., and Nather, R.E. 1987, in IAU Colloq. No.95, *The Second Conference on Faint Blue Stars*, ed. A.G.D. Philip (Schenectady; Davis Press), in press.

Hine, B.P. 1987, in IAU Colloq. No.95, *The Second Conference on Faint Blue Stars*, ed. A.G.D. Philip(Schenectady; David Press), in press.

Kawaler, S.D. 1986, *Ph. D. thesis,* University of Texas.

Kawaler, S.D. 1987, in IAU Colloq. No.95, *The Second Conference on Faint BlueStars,* ed. A.G.D. Philip (Schenectady; Davis Press), in press.

Kawaler, S.D., Hansen, C.J. and Winget, D.E. 1985, *Ap. J.*, **295**, 547.

Kepler, S.O., and Winget, D.E., Robinson, E.L., and Nather, R.E. 1987, in IAU Symposium No.123, *Advances in Helio- and Asteroseismology*, ed. J. Christensen-Dalsgaard (Dordrecht: Reidel), p. 325.

Koupelis, T., and Winget, D.E. 1987, in IAU Colloq. No.95, *The Second Conference on Faint Blue Stars,* ed. A.G.D. Philip (Schenectady; Davis Press), in press.

Liebert, J., Wesemael, F., Hansen, C.J., Fontaine, G., Shipman, H.L., Sion, E.M., Winget, D.E., and Green, R.F., 1986, *Ap. J.*, **309**, 291.

Mazitelli, I., and D'Antona, F. 1988, in IAU Colloq. No.95, *The Second Conference on Faint Blue Stars*, ed. A.G.D. Philip (Schenectady; Davis Press), in press.

O'Donoghue, D., and Warner, B. 1987, *M.N.R.A.S.*, **228**, 949.

Robinson, E.L. 1979, in Proceedings of IAU Colloquium No.53: *White Dwarfs and Variable Degenerate Stars*, eds. H.M. Van Horn and V. Weidemann (Rochester, N.Y.: University of Rochester Press), p. 343.

Robinson, E.L., and Kepler, S.O. 1980, *Space Sci. Rev.*, **27**, 613.

Sion, E.M., Greenstein, J.L., Landstreet, J.D., Liebert, J., and Shipman, H.L. 1983, *Ap. J.*, **269**, 253.

Starrfield, S. 1987, in IAU Colloq. No.95, *The Second Conference on Faint Blue Stars*, ed. A.G.D. Philip (Schenectady; Davis Press), in press.

Tomaney, A. 1987, in IAU Colloq. No.95, *The Second Conference on Faint Blue Stars*, ed. A.G.D. Philip (Schenectady; David Press), in press.

Unno, W., Osaki, Y., Ando, H., and Shibahashi, H. 1979, *Nonradial Oscillations of Stars* (Tokyo: Tokyo University Press).

Van Horn, H.M. 1985, in *Theoretical Problems in Stellar Stability and Oscillations*, ed. A. Noels and M. Gabriel (Cointe-Ougree, Belgium: Universitè de Liège), p. 307.

Vauclair, G., Chevreton, M., and Dolez, N. 1987, *Astr. Ap.*, **175**, L13.

Weidemann, V., and Koester, D. 1984, *Astr. Ap.*, **132**, 195.

Winget, D.E., 1986, in *Highlights of Astron.*, ed. J.-P. Swings, 221.

Winget, D.E. 1987, in IAU Symposium No.123, *Advances in Helio- and Asteroseismology*, ed. J. Christensen-Dalsgaard (Dordrecht: Reidel), p. 305.

Winget, D.E., and Fontaine, G. 1982, in *Pulsations in Classical and Cataclysmic Variable* Stars (Boulder: University of Colorado Press), p.46.

Winget, D.E., and Kepler, S.O. 1988, these proceedings.

Winget, D.E., and Van Horn, H.M. 1988, in IAU Colloq. No.95, *The Second Conference on Faint Blue Stars*, ed. A.G.D. Philip (Schenectady; Davis Press), in press.

Winget, D.E., Van Horn, H.M., and Hansen, C.J. 1981, *Ap. J., (Letters)*, **245**, L33.

Winget, D.E., Kepler, S.O., Robinson, E.L., Nather, R.E., and O'Donoghue, D. 1985, *Ap. J.*, **292**, 606.

Winget, D.E., Nather, R.E., and Hill, J.A. 1987, *Ap. J.*, **316**, 305.

Wood, M.A., and Winget, D.E. 1988, these proceedings.

ZZ CETI MODE TRAPPING REVISITED

M. A. Wood and D. E. Winget
The University of Texas at Austin and McDonald Observatory, USA

Abstract

We discuss the effects of compositional stratification on the evolution of the oscillation spectrum of a representative model sequence evolving through the ZZ Ceti instability strip. We find that the stratification has a dramatic effect on the period spacing, although the effect on the time-rate-of-change of the periods is P/(dP/dt) minimal – roughly equal for all. Thus the transformation of observed rates of period change into evolutionary timescales is straightforward: observed rates of period change provide direct calibration of theoretical white dwarf evolutionary calculations.

1. Introduction

All the DA white dwarf between the effective temperatures of 13,000 K and 11,000 K vary photometrically on timescales of 100-1000 s. The objects are multiperiodic, and in the objects whose period spectra have been resolved, the Q $(\equiv 1/|\dot{P}|)$ of the component periods is $\geq 10^{14}$. *Warner* and *Robinson* (1972) demonstrated these periods are consistent with the periods expected for high radial-order non-radial g-mode oscillations. For a more complete discussion of the properties of the ZZ Ceti stars, see the review by Winget (this volume, and references therein).

Although ZZ Ceti stars are among the most complicated pulsators observed, the observed period spectra are sparse when compared with the rich theoretical period spectra. The asymptotic expression for the spacing of the modes in a non-rotating model is:

$$P^2 \approx \frac{4\pi^2}{N^2} \frac{\ell(\ell+1)/r^2 + k^2}{\ell(\ell+1)/r^2},$$

where N^2 is the Brunt-Väisälä frequency. Note that for fixed l, and $k^2 \gg l(l+1)/r^2$, modes of consecutive k should be roughly equally spaced in period. For homogeneous models, this is indeed what we find for $k \geq 4$. When *Winget, Van Horn* and *Hansen* (1981) included H and He layers in their models, however, the oscillation spectrum changed drastically – the periods of the modes were no longer equally spaced in

k. Further, certain modes resonated with the H and/or He layer thicknesses, and had kinetic energies orders of magnitude lower than adjacent modes. These low kinetic energies imply large growth rates, which suggests that these resonant (or "trapped") modes may be the first to saturate the driving mechanism.

The purpose of these calculations is to extend the investigation of the effects of compositional stratification to the time-rate-of-change of the oscillation spectrum. Because the rate of period change of a given period is a function of the evolutionary timescale in the region of period formation, we can in principle merge our observations with our theoretical results to form a coherent seismological picture of the interiors of these stars. Because these stars are relatively simple, there is hope that this in fact may eventually be possible. As a first step towards this goal, we report the results of detailed calculations of the time evolution of the period spectrum of a representative ZZ Ceti model sequence, focusing on the effects of the compositional stratification.

2. The Models

We generated the evolutionary models with a modified version of the pure-carbon-white-dwarf evolution code described in *Lamb* and *Van Horn* (1975). In the modified code, H and He layers were included in the envelope as described by *Winget, Van Horn* and *Hansen* (1981). The composition-transition zones were idealized as discontinuities even though they are expected to be finite in extent because (i) the composition transitions can be handled in a physically-self-consistent manner in both the evolution and pulsation calculations, and (ii) as a good limiting case, the behavior should be qualitatively similar to that expected from the full solution including diffusive equilibrium. For example, in an evolutionary, diffusive-equilibrium model reported by *Winget et al.* (1982), the H layer ($M_H/M_* = 10^{-10}$) spans 17 pressure scale heights while the H/He transition layer spans only 3. Because the transition zones between regions of different composition are much thinner than the layers themselves, the condition of resonance should be relatively independent of the detailed structure of the transition zone until the mode wavelength is comparable to the transition zone thickness. This does not occur until beyond $k \geq 20$.

The He layer mass is constrained to be $10^{-3} \geq M_{He}/M_* \geq 10^{-4}$ by the carbon pollution problem (*Pelletier et al.* 1986), and the H layer is only loosely constrained to be $10^{-8} \geq M_H/M_* \geq 10^{-12}$ (see *Winget et al.* 1982). The sequence we evolved consisted of models of 0.6 $M_\odot$, whose carbon cores were surrounded by helium layers of mass $M_{He}/M_* = 10^{-3}$ and hydrogen layers of mass $M_H/M_* = 10^{-10}$. We evolved 26 models covering the effective temperature range $13{,}000\,K \geq T_{eff} \geq 11{,}000\,K$.

The pulsation calculations were all carried out in the quasi-adiabatic Cowling approximation. We report the results for $l=2$, $k=1$, 16 in this preliminary study.

3. Discussion of Results

As a white dwarf star cools, the Brunt-Väisälä frequency decreases, squeezing the eigenfunctions out into the envelope, and so forcing the eigenfrequencies down. It is generally true that because modes of differing k sample slightly different regions in the star with correspondingly different evolutionary timescales, we expect each mode to have a different rate of period change. If we plot the behavior of the periods of all of the modes k *versus* decreasing effective temperature across the instability strip, we expect to see bumping and avoided crossings of the sort described by *Aizenman, Smeyers* and *Weigert* (1977). Briefly, when a mode bumps another mode, it displaces the bumped mode to another frequency, and settles at approximately the frequency of the displaced mode. Further, the eigenfunctions exchange some characteristics.

Figure 1 shows the results of our calculations. There are several features of this figure that are worth mention. Perhaps the first feature apparent to the eye is the presence of small kinks in $P(k,T_{eff})$. These kinks are relatively larger for larger k, and appear to manifest themselves in several modes of differing k simultaneously. We looked into this problem, and found that either our envelope C equation of state table is too coarse, or our interpolation algorithm is less than ideal, or the evolution code was having trouble stitching together the core and envelope (or some combination of the three). In short, these kinks reflect the numerical noise in our calculations. Because the troubles are in the outer 0.1% of the star (by mass), it is not surprising that higher harmonics are more strongly affected. Happily, previous calculations of a sequence whose noise level was more than 10 times higher than here lead to essentially the same conclusions – which is to say that our results are insensitive to the numerical noise.

The second feature of note in the figure is the evidence for bumping and avoided crossings. A particularly clean example of this is the behavior displayed by modes $k=5$ and 6. To understand the exchange, it also helps to look at Figure 2, which shows the logs of the kinetic energies of the modes for all k up to at least 15, for all the models. At the hot end of the sequence (top of the figure), $k=6$ is the mode whose kinetic energy occupies the local minimum. As the models evolve, the kinetic energies and periods of the modes $k=5$ and 6 pull together. Between models 22 and 23, the two trade relative kinetic energies, and as the models continue to evolve, the $k=5$ mode retains its new status as the trapped mode.

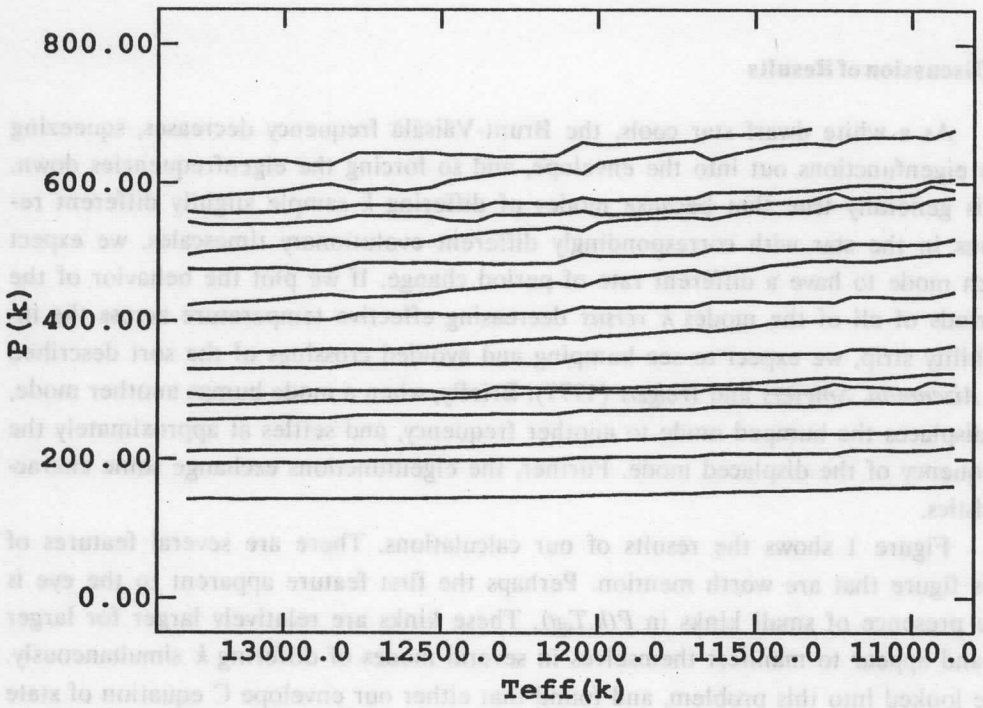

Fig. 1. Plot of the evolution of the oscillation spectrum from our model calculations. Note that the slopes of the lines increase as k increases (this is most easily seen by viewing the plot near-edge-on).

Another local minimum in Figure 2 occurs near 600 s, modes $k = 12$ to 15. Although the noise in the calculations makes the analysis of this period group less straightforward, the basic behavior is unchanged. At the hot end of the sequence, modes $k = 13$ and 14 are trapped. As the model cools through the instability strip, the $k = 12$ mode pulls closer. Before leaving the instability strip, the $k = 12$ mode takes over as occupant of the local minimum.

The final feature we draw your attention to in Figure 1 is the increase in the slopes of the lines $P(k, T_{eff})$ for increasing k. Although $\dot{P}$ increases with k, the measured quantity is in fact $P/\dot{P}$, which for these models varies by less than a factor of two with a centroid of $\sim 7 \times 10^{16}$s.

What do these results say about the observations? They say that within the instability strip the change in the trapped modes may have some observable consequences, although nonlinear calculations are required to confirm this. For example, the behavior of modes $k = 5$ and 6 suggests the following picture. A star may enter

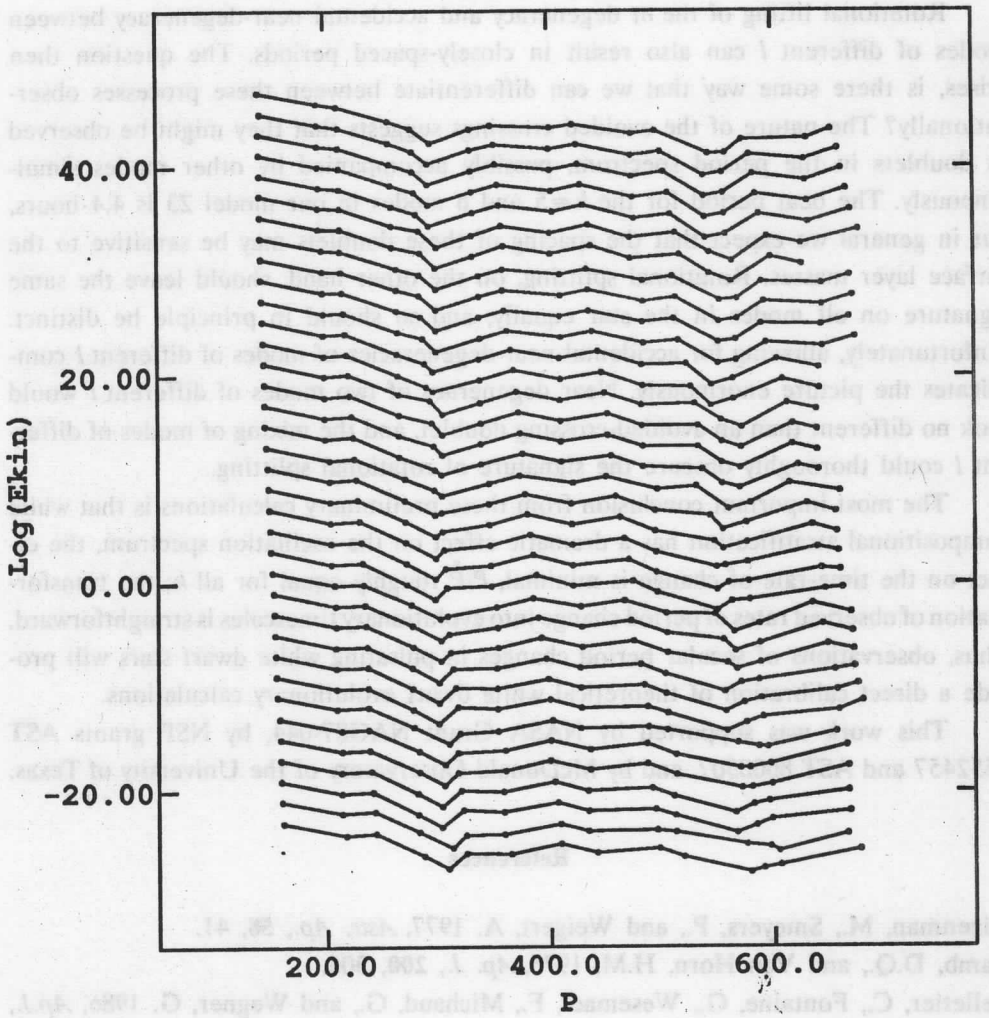

Fig. 2. Log of the kinetic energies of all the models. The top curve is on the scale at the left, and the others have been offset for clarity of presentation. At the hot end (top) of the sequence, the mode $k=6$ is the mode with the lowest local kinetic energy. As the models evolve, modes $k=5$ and 6 gradually pull together in period and smoothly exchange relative kinetic energies. As they cool out of the instability strip, the mode $k=5$ is the mode with the lowest local kinetic energy.

the instability strip pulsating in a mode of given k, and as the star evolves, another mode may bump the first – in doing so its physical properties will approach those of the first. When the physical properties of two modes become the same or nearly so, they should become indistinguishable to the driving mechanism, and both may be

driven simultaneously. This is consistent with the observations, where we commonly observe closely-spaced modes beating with each other.

Rotational lifting of the m degeneracy and accidental near-degeneracy between modes of different l can also result in closely-spaced periods. The question then arises, is there some way that we can differentiate between these processes observationally? The nature of the avoided crossings suggests that they might be observed as doublets in the period spectrum, possibly accompanied by other modes simultaneously. The beat period for the $k=5$ and 6 modes in our model 23 is 4.4 hours, but in general we expect that the spacing of these doublets may be sensitive to the surface layer masses. Rotational splitting, on the other hand, should leave the same signature on all modes in the star equally, and so should in principle be distinct. Unfortunately, allowing for accidental near-degeneracies of modes of different l complicates the picture enormously. Near degeneracy of two modes of different l would look no different than an avoided-crossing doublet, and the mixing of modes of different l could thoroughly obscure the signature of rotational splitting.

The most important conclusion from these preliminary calculations is that while compositional stratification has a dramatic effect on the oscillation spectrum, the effect on the time-rate-of change is minimal, $P/\dot{P}$ roughly equal for all k; the transformation of observed rates of period change into evolutionary timescales is straightforward. Thus, observations of secular period changes in pulsating white dwarf stars will provide a direct calibration of theoretical white dwarf evolutionary calculations.

This work was supported by NASA Grant NAG87-044, by NSF grants AST 8552457 and AST 8600507, and by McDonald Observatory of the University of Texas.

References

Aizenman, M., Smeyers, P., and Weigert, A. 1977, *Astr. Ap.*, **58**, 41.

Lamb, D.Q., and Van Horn, H.M. 1975, *Ap. J.*, **200**, 306.

Pelletier, C., Fontaine, G., Wesemael, F., Michaud, G., and Wegner, G. 1986, *Ap.J.*, **307**, 242.

Warner, B., and Robinson, E.L. 1972, *Nature Phys. Sci.*, **234**, 2.

Winget, D.E., Van Horn, H.M., and Hansen, C.J. 1981, *Ap. J. (Letters)*, **245**, L33.

Winget, D.E., Van Horn, H.M., Tassoul, M., Hansen, C.J., Fontaine, G., and Carroll, B.W. 1982, *Ap. J. (Letters)*, **252**, L65.

SECULAR EVOLUTION OF THE 516 s PERIOD IN THE PRESENCE OF NEW MODES IN PG 1159-035

D. E. Winget*
Department of Astronomy and McDonald Observatory University of Texas, USA
and
S. O. Kepler**
Instituto de Fisica Universidade Federal do Rio Grande do Sul, Brazil

Abstract

We report the analysis of the time rate of change of the 516 s period in the DOV star PG 1159-035. At least 5 new period bands have been detected in 1987, adding to the 8 bands previously present in the extensive archival data base on the star. Our analysis of the phase of the 516 s period in the 1987 data is consistent with no change relative to the previously reported ephemeris. Thus the period change due to secular evolution appears to be unaffected by the appearance of the new frequencies. This result provides very strong constraints on any model for the origin of the new frequencies.

1. The Star and the Old Data

McGraw's star, PG 1159-035, is a multi-periodic variable DO white dwarf and the proto-type of the class of DOV stars. The multi-periodic variations are thought to be the result of nonradial *g*-mode pulsations. At the time of the initial discovery of variability in the object, *McGraw et al.* (1979) pointed out that its location in the upper left-hand corner of the H-R diagram implied that, if the pulsations were stable, secular evolutionary period changes would be measurable with an observational baseline of only a few years.

As a result of this, archival data on this object was accumulated at the University of Texas and the University of Cape Town over the period from 1979-1984. The analysis of this data demonstrated that the star had eight separate groups of periods (or bands) which seemed to be stable, but only one period, at 516 s, which was an isolated peak suitable for secular stability analysis. With the 1984 data, there

---

* Alfred P. Sloan Research Fellow
** CNPq-Brazil Research Fellow

was sufficient data to demonstrate an unambiguous secular change in the 516 s mode (*Winget et al.* 1985). The rate of change of this period was completely consistent with the evolutionary timescale expected from theoretical evolutionary calculations.

2. The New Data and the New Results

Barstow et al. (1986), using EXOSAT to observe McGraw's star, demonstrated that the largest amplitude periods present in the optical were also present in the soft x-ray, although with an amplitude an order of magnitude larger than the optical. In addition, however, they indicated the presence of a new peak at about 524s, not present in the archival data, although there was some evidence of a corresponding period in the optical data taken in 1985. There was not enough data obtained in 1985 to obtain a meaningful phase for the 516 s period, especially with the complicating presence of a nearby period at 524 s.

In 1987 we obtained 49 hrs of high-speed optical photometry which unambiguously demonstrated not only the existence of the new peak at 525 s, but at least four additional bands, or sets of peaks, not present in the 1979-1985 data. The amount of data in the 1979-1985 data set, as well as the fact that a significant fraction of it was nearly continuous data from multiple longitudes, precludes the possibility that the new peaks were present at the time but did not appear because of an accident of the phase of the beat of the different frequencies in the new bands. Further, there is no measureable change in the amplitudes of the modes which were present previously, indicating that the new frequencies are not the result of some transfer of power between the old modes (mode-switching) (*Koupelis* and *Winget* 1987).

We have examined the new data for the phase of the 516 s to compare with the ephemeris of *Winget et al.* (1985). As in our 1985 analysis we have computed dP/dt using two independent techniques: fitting a parabola to the (O-C) diagram, and a direct nonlinear least squares fit to the entire data set of a sine curve incorporating a term linear in $d\omega/dt$. These techniques are described in *Winget et al.* (1985), and in even greater detail in *Kepler et al.* (1988).

Here we define our dP/dt using the dP/dt term arising in the 2nd order Taylor series expansion of the usual (O-C) relation — resulting in a difference of exactly a factor of two from *Winget et al.* (1985), so those results (and associated errors) must be multiplied by a factor of two for comparison with the numbers presented here. The new definition is consistent with treating the phase as ω integrated over the time of observation, and inserting a Taylor series expansion of ω in the integral expression. Previously, we treated the phase as given by ω times t, so the factor of two comes about because of the integration of the $d\omega/dt$ term in the new definition. These two methods are examined in some detail in *Kepler et al.* (1988), and although

the choice of definition is formally arbitrary (within multiplicative constants of order unity) as long as it is applied consistently – the conclusion is that the definition adopted here is the one which is physically self-consistent for use in comparison with theoretical calculations of *dP/dt*.

Using both the (O-C) technique and the nonlinear least squares technique, the results for the 1979-1984 data set, which we have completely re-analyzed, are

$$dP/dt(O\text{-}C) = (-2.36 \pm 0.4) \times 10^{-11},$$

$$dP/dt(nls) = (-2.44 \pm 0.06) \times 10^{-11},$$

where we note that the formal error quoted for the nonlinear least squares (nls) value is probably an underestimate of the true error. These results are completely self-consistent and consistent with those found previously (*Winget et al.* 1985). Both methods give the same nominal period, 516.025s, and ephemeris time of zero, $E_0 = 244{,}5346.873583$ *HJDD* ± 1.9s.

The results for the 1979-1987 data set, using the two techniques are:

$$dP/dt(O\text{-}C) = (-2.32 \pm 0.08) \times 10^{-11},$$

$$dP/dt(nls) = (-2.35 \pm 0.02) \times 10^{-11}.$$

Again, both methods are completely self-consistent, and give the same nominal period, 516.025s, and ephemeris time of zero, $E_0 = 244{,}5346.873583$ *HJDD* ± 1.9s. Also, and perhaps surprisingly in light of the presence of the new frequencies, the new values are completely consistent with the values from the 1979-1984 data set alone.

Thus our conclusion is that the secular change in the 516s period of PG 1159-035 has continued, unaffected by the appearance of the new modes. Whatever happened to the star that caused the new modes to grow-in, if that is indeed what happened, was subtle enough not only to leave no measurable effect on the amplitudes and basic frequencies of the original bands, but to leave no measurable effect on the phase of the 516 s mode either. This will place a severe constraint on any model for the way in which the new frequencies have arisen.

We speculate that what may have happened is that the effective band-pass of the filter mechanism responsible for the mode selection has gradually broadened allowing more modes to reach observable amplitudes. If the filter mechanism is associated with compositional stratification leftover from nuclear shell burning, as has been suggested by *Kawaler* (1987), then this may be comprehensible. Initially, after shell burning shuts down, concentration gradient effects will be at work broadening the composition transition zone and therefore its band-pass. This change would take place on diffusion timescales, as opposed to evolutionary timescales, thereby helping to explain how we can observe this over a period of several years. If this is the case perhaps we will see additional modes appearing in subsequent years. Clearly, we need

to investigate this idea quantitatively by examining the pulsation properties of evolutionary models incorporating the effects of diffusion (a calculation which can be done given current techniques). In any case, it will be extremely important to continue to monitor this star in the future.

This work was supported in part by NSF grants AST-8600507, and AST-8552457, and by McDonald Observatory of the University of Texas.

References

Barstow, M.A., Holberg, J.B., Grauer, A.D., and Winget, D.E. 1986, *Ap. J.* (Letters), **306**, L25.

Kawaler, S.D. 1987, in IAU Colloq. No.95, *The Second Conference on Faint Blue Stars,* ed. A.G.D. Philip (Schenectady: Davis Press), in press.

Kepler, S.O., Koupelis, T., Winget, D.E., Clemens, J.C., Hill, J.A., Hine, B.P., Wood, M.A., Nather, R.E., Warner, B., O'Donoghue, D., Cropper, M., Grauer, A.D., Hansen, C.J., Kawaler, S.D., Barstow, M.A., and Holberg, J.B. 1988, in preparation.

Koupelis, T., and Winget, D.E. 1987 in IAU Colloq. No.95, *The Second Conference on Faint BlueStars,* ed. A.G.D. Philip (Schenectady: Davis Press), in press.

McGraw, J.T., Starrfield, S.G., Liebert, J., and Green R.F. 1979 in IAU Colloq. No.53, eds. H.M. Van Horn and V. Weidemann (Rochester, N.Y.: University of Rochester), p.377.

Winget, D.E., Kepler, S.O., Robinson, E.L., Nather, R.E., and O'Donoghue, D. 1985, *Ap. J.*, **292**, 606.

THE STRUCTURE OF STELLAR QUANTUM CHAOS

J. Perdang
Institute of Astronomy, Cambridge, UK
and
Institut d'Astrophysique, Cointe-Ougrée, Belgium*

Abstract

We analyse the distribution of the acoustic frequencies of stars whose geometrical equilibrium structure is smoothly deformed. We show both by asymptotic analysis and by numerical experiments that the acoustic spectrum exhibits 'quantum chaotic' ranges of frequencies. Within these ranges the individual frequency levels shifted under the effect of the geometrical distortion are distributed irregularly around the frequency levels of the nonperturbed star of spherical symmetry. We study analytically how and where these quantum chaotic ranges are likely to be generated. We also briefly comment on the main differences between acoustic 'quantum chaos' and the formally similar problem of spectral, or 'quantum chaos' as encountered in quantum mechanical systems.

1. Introduction

According to the now canonical interpretation, the solar 5-minute oscillations are linear acoustic normal modes of a spherically symmetric hydrostatic equilibrium model. Perhaps the most persuasive argument in favour of linear modes comes from the equatorial observations of the solar disk. First carried out by *Deubner* (1975), these observations resolved the frequencies ν of the surface oscillations with respect to their horizontal wavenumber k_h (or the degree l, since $k_h \equiv (l+1/2)/R_\odot$, $R_\odot$ radius of the sun); when plotted against the wavenumber k_h the observed frequencies match the (asymptotic) theoretical $\nu - k_h$ patterns in a remarkable way, both for intermediate ($l \approx 4$–100) and for high degrees ($l \approx 100$–1000). The interpretation in terms of linear modes also accounts for the full-disk frequency observations initiated by Fossat and coworkers (*Grec et al.* 1983) at the South Pole and continued by satellite observations. These observations are reasonably reproduced by the acoustic frequencies of low degree ($l = 0$–4) of conventional solar models.

---

* Permanent Address

The high precision of the solar frequency measurements has made it clear, however, that the agreement with the acoustic frequencies of the currently best solar models is not fully satisfying. The differences between observation and theory are twofold. In the first place, plots of the observed frequencies $\nu_{obs}(n,l)$, identified by their degree l and radial order n, against n and for different values of l show a global regular pattern which does not fully coincide with the regular pattern traced out by the families of model frequencies $\nu_{mod}(n,l)$. The discrepancy is made quite obvious in the popular echelle diagrams (*cf. Toomre* 1986). In the second place, the observed frequencies $\nu_{obs}(n,l)$ do not all exactly fall on perfectly smooth $\nu - n$ curves as theory predicts. Only when averaged over a range of n values, $< \nu_{obs}(n,l) >$, does the observational curve show a smooth behaviour in n.

It has been claimed that the first difficulty can be overcome by implementing improved physics in the computation of the solar models (for instance, through a sophisticated equation of state, *cf. Ulrich* and *Rhodes* (1984). So far, however, a convincing proof of the relevance of this effect is wanting. The second difficulty, unless a result of observational noise, is hard to get rid of in the framework of solar model of high geometric symmetry. This latter point will be substantiated in the present paper.

Our work was originally motivated by the interpretation of the solar frequency discrepancies. It became obvious, however, as soon as the first analytical and numerical results became available, that the most exciting potential application of the particular theoretical framework we have concentrated on, namely the role of *smooth large scale geometric deformations* of a star, lies in the interpretation of the acoustic frequency spectrum of strongly deformed stars (close binaries, rapid rotators). Although at the moment observational information on an extended range of acoustic frequencies of such objects is still lacking, the rapid expansion of the relevant technology is indicative that this information will become available in the near future.

The following theoretical questions have been investigated.

(a) A precise definition of the phenomenon of *quantum regularity* of a spectrum of frequencies is given, using the formalism of nonstandard analysis; by the same token *quantum chaos* is defined as a phenomenon complementary to regularity. Our definitions apply to the very large acoustic frequency eigenvalues only. In our view the asymptotic part of the spectrum alone – a concept we shall also precisely define in the framework of nonstandard analysis – lends itself to a clear-cut theoretical treatment, since generically it is not contaminated by the inherent physical complexities of the full realistic stellar wave equation. Besides the neatness of a mathematically precise characterisation of quantum chaos, our definition also has the advantage of leading to a practical test of regularity or chaos of a fragment of the acoustic spectrum. We note in passing a duality between quantum regularity and

chaos of the oscillation eigenstates on the one hand, and the ordered crystal-like structure and the disordered liquid structure of matter on the other.

(b) We develop a systematic and general procedure for the actual computation of the frequencies of stars lacking spherical symmetry. Our procedure makes use of a mapping of the nonspherical stellar configuration in the actual physical space onto a spherical configuration in a fictitious space. This trick enables us to use the (complete set of) eigenfunctions of the spherical configuration as a basis for the expansion of the eigenfunctions of the deformed star. Thereby the virtually intractable partial differential eigenvalue problem is reduced to a conventional algebraic eigenvalue problem.

(c) We introduce an ideal many-parameter family of nonspherical stellar configurations whose specific geometry is characterised by a collection of free parameters $\{\lambda_i\}$, and whose physics reduces to a bare minimum. The parameters are chosen such that for $\{\lambda_i = 0\}$, the model becomes spherically symmetric. We have theoretical reasons to believe that just like the idealised Heisenberg or Ising models of statistical physics – which in spite of their rudimentary nature, reproduce adequately the behaviour of the most significant physical factors in the vicinity of the phase transitions – the family of models proposed here is appropriate to exhibit the main structural features of generic asymptotic acoustic spectra of deformed stars. We also believe that it is adequate to characterise the transition from regularity to chaos in the spectrum, although this point has not been investigated directly here.

A few preliminary numerical results on the behaviour of the spectrum under changes of the parameters $\{\lambda_i\}$ are presented. Our model makes it clear that the chaotic spectral ranges arise as the result of a coupling of almost radial ($l/n \leq 1$) with nonradial ($l/n \geq 1$) basis eigenfunctions, the natural choice for the latter being the set of eigenfunctions of the spherically symmetric model. In more physical terms, quantum chaos in a deformed star arises out of an avoided mode crossing –or resonance– between lower-l modes and higher-l modes of the nondeformed, spherically symmetric reference equilibrium configuration.

Barring the abstract group-theoretical conclusions on the structure of the oscillation modes of stars of arbitrary symmetry (*Perdang* 1968), the results presented here are, to the best of my knowledge, the only general results so far available on the acoustic frequency spectra of nonspherical stars.

I should point out at this stage that large scale deformations away from the spherically symmetric equilibrium may not be the most relevant symmetry breaking factors leading to observationally detectable effects in the structure of the acoustic spectrum. As stressed elsewhere (*Perdang* 1986), small scale deformations – breaking the original symmetry only locally, while globally, and on a large scale the spherical symmetry of the star survives – are likely to affect the asymptotic spectrum and to generate quantum chaos as well. The precise way how this is achieved remains

to be investigated. We mention here only that our mapping procedure breaks down for local deformations, as a result of a violation of the one-to-one correspondence between the old and new variables. This may suggest a basic change in the structure of the spectrum. Local geometric distortions, unavoidable for instance in convective zones, are presumably more relevant than global deformations in modifying the structure of the asymptotic acoustic frequencies of 'simple' stars, and in particular of the sun. Alternatively, even a globally spherical symmetry may not be a correct picture for the majority of 'simple' stars. It could well be that underneath a roughly spherical surface symmetry of the star conceals a complicated 3-dimensional sound speed pattern. In fact, I just wish to remind the reader that geophysical tomography has recently revealed – against common sense expectation – that the terrestrial sound speeds in the earth mantle show systematic changes of an amplitude of as much as 10% over horizontal scales of 1000 km, even though the geometrical surface of the earth is spherical to a remarkable degree.

Finally, I should like to sound a warning. The actually observed solar oscillations, even though interpreted as *linear* and essentially *adiabatic* oscillations, are intrinsically *nonlinear dissipative* phenomena. Indeed, the very occurrence of an oscillation requires an excitation, *i.e.* a dissipative mechanism; and any physical excitation of the modes necessarily involves nonlinear effects, otherwise the amplitudes would grow indefinitely. The stochastic excitation mechanism, as advocated by various authors (*cf. Christensen-Dalsgaard* 1987), is merely a 'model of ignorance' in which all nonlinear effects (mode-couplings, dissipative interactions) are mimicked by an unknown 'stochastic' forcing term. The resulting set of Langevin equations (or their discrete-time counterparts, the autoregressive schemes, and in particular the Yule scheme) define then by construction an entirely unpredictable time signal. In the context of such a model the solar oscillations are then strongly *chaotic* (in the sense of algorithmic complexity theory). In fact, this brand of chaos is not just *deterministic chaos*, the variety arising in nonlinear systems of a few effective degrees of freedom, as a result of instabilities in their deterministic equations of evolution; it is what should conveniently be called *indeterministic chaos*, namely an unpredictability in the oscillations due to the nondeterministic, probabilistic character of the evolution equation itself. We have commented elsewhere on the connection of the oscillation equations with autoregressive schemes, and on the definition of chaos in terms of algorithmic complexity (*Perdang* 1985).

The concept of *quantum chaos* of the *linear* oscillation spectrum as understood here, in contrast to the above varieties of deterministic and indeterministic chaos, does not relate to the time behaviour of the oscillations. It characterises the structure of the spectrum of linear eigenfrequencies and the distribution of the spacings of the frequency levels. In principle, the spectrum of linear acoustic eigenfrequencies is rigorously accessible observationally, provided that the framework of the stoch-

astic excitation mechanism is adequate (*cf. Christensen-Dalsgaard* 1987). However, in the framework of a refined excitation theory we have no guarantee that this conclusion continues to hold. The peaks in the power spectrum are indeed likely to be displaced by the nonlinearities. Therefore, the analysis of an observational spectrum of stellar frequencies, interpreted as linear eigenfrequencies, always involves an element of uncertainty. The observed spectrum may well be distorted by nonlinear effects. What we interpret as a geometric deformation – or, for that matter, as the manifestation of complicated new physical mechanism – may in reality just be a nonlinear component.

2. Geometric acoustics

The formal correspondence between the equations describing the linear adiabatic acoustic stellar oscillations and the quantum mechanical Schrödinger eigenvalue equation entitles us to carry over general results from one of these fields to the other virtually *verbatim*. In the early seventies, the Schrödinger eigenvalue problem was shown to give rise, under certain well defined conditions, to a phenomenon later referred to as 'quantum chaos' (*Percival* 1973, 1974). A precise definition of quantum chaos was not formulated; instead, it was characterised in terms of the qualitative properties of the spectrum (irregular spacings of the eigenvalues) and of the eigenfunctions (irregular pattern of the nodal lines, *etc.*; *cf. Percival* 1973, 1974; *Berry* 1977, 1983; *Zaslavsky* 1981).

We have made use of the above formal correspondence to point out the existence of a stellar counterpart of the phenomenon of 'quantum chaos' and its companion phenomenon, 'quantum regularity', in the spectrum of the adiabatic oscillation frequencies (*Perdang* 1984, 1986).

Consider a general Schrödinger eigenvalue problem

$$H(\mathbf{q},\mathbf{p})\ \psi(\mathbf{q}) = E\ \psi(\mathbf{q}) \quad , \tag{2.1}$$

defined in an f-dimensional configuration space of coordinates

$$\mathbf{q} = (q_1, q_2, \ldots , q_f) \quad , \tag{2.2}$$

the linear partial differential operator $H(\mathbf{q},\mathbf{p})$ is a function of the coordinates $\mathbf{q}$ as well as of the array of space derivatives

$$\mathbf{p} \equiv i\partial/\partial\mathbf{q} = (i\partial/\partial q_1, i\partial/\partial q_2, \ldots , i\partial/\partial q_f) \quad ; \tag{2.3}$$

the function $\psi(\mathbf{q})$ defined over the configuration space, is the eigenfunction associated with the energy eigenvalue E. (We have assumed that a system of units is chosen in which Planck's normalised constant is 1).

The classical limit of equation (2.1) is generated by the substitution of an ordinary f-dimensional vector to the vector operator (2.3),

$$\mathbf{p} \rightarrow (p_1, p_2, \ldots, p_f) \quad , \tag{2.4}$$

where the components p_j, $j = 1, 2, \ldots, f$ are interpreted as the classical generalised momenta. Under the substitution (2.4) the original partial differential equation collapses into a scalar equation

$$H(\mathbf{q},\mathbf{p}) = E \quad . \tag{2.5}$$

In other words, the energy state E now becomes a function of the generalised coordinates and momenta. The function $H(\mathbf{q},\mathbf{p})$ is the classical Hamiltonian. If $\mathbf{q}(t)$, $\mathbf{p}(t)$ is a solution of the Hamiltonian equations

$$d/dt\ \mathbf{q} = \partial/\partial\mathbf{p}\ H(\mathbf{q},\mathbf{p}) \quad \text{and} \quad d/dt\ \mathbf{p} = -\partial/\partial\mathbf{q}\ H(\mathbf{q},\mathbf{p}) \quad , \tag{2.6}$$

of initial conditions $\mathbf{q}(0) = \mathbf{q}_0$, $\mathbf{p}(0) = \mathbf{p}_0$, then the orbit $[\mathbf{q}(t),\mathbf{p}(t)]$ in the 2f-dimensional phase space is carried by the 2f–1 dimensional subspace specified by $H(\mathbf{q}(t),\mathbf{p}(t)) = H(\mathbf{q}_0,\mathbf{p}_0) = E$.

Consider on the other hand the *asymptotic* equation of the stellar acoustic oscillations. By 'asymptotic' we mean here the limiting form of the acoustic eigenvalue problem for arbitrarily large frequencies, keeping the leading order terms only. A precise definition will be postponed to Section 6. In this limit the equation reduces to the conventional standing wave equation

$$\Omega(\mathbf{r},\mathbf{k})^2\ \psi(\mathbf{r}) = \omega^2\psi(\mathbf{r}) \quad . \tag{2.7}$$

In this expression $\mathbf{r}$ is the f-dimensional position vector of components x_j, $j = 1, 2, \ldots, f$ in the configuration space; f may be equal 1, 2 or 3, depending on whether we consider 1-dimensional (for instance radial waves in a spherically symmetric star), 2-dimensional (for instance waves in the presence of a rotational symmetry), or genuine 3-dimensional wave propagation. $\Omega(\mathbf{r},\mathbf{k})^2$ is a linear partial differential operator depending on the position vector and on the array of differential operators

$$\mathbf{k} = (i\partial/\partial x_1, i\partial/\partial x_2, \ldots, i\partial/\partial x_f) \quad ; \tag{2.8}$$

explicitly

$$\Omega(\mathbf{r},\mathbf{k})^2 = |\mathbf{k}|^2 c(\mathbf{r})^2 \quad , \tag{2.9}$$

$c(\mathbf{r})$ being the adiabatic sound speed at position $\mathbf{r}$ in the star. The eigenfunction $\psi(\mathbf{r})$, defined over the accessible configuration space (the volume of the star), is physically interpreted as the pressure perturbation; the associated eigenvalue is ω^2, ω being an oscillation eigenfrequency. In principle, the partial differential equation (2.7) is to be supplemented by the surface boundary condition. The surface singularity in the differential system, in the case of a sound velocity vanishing at the surface, substitutes the regularity requirement for the eigenfunction to an extra boundary condition.

The manifest formal analogy between the acoustic mode equation (2.7) and the Schrödinger equation (2.1) suggests that we can associate a 'classical limit' with the acoustic equation, by the formal substitution

$$\mathbf{k} \rightarrow (k_1, k_2, \ldots, k_f) \quad , \tag{2.10}$$

i.e. $\mathbf{k}$ is now regarded as an f-dimensional vector. We are then left with an algebraic equation for the frequencies

$$\Omega(\mathbf{r},\mathbf{k})^2 = \omega^2 \quad \text{or} \quad \pm\Omega(\mathbf{r},\mathbf{k}) \equiv \nu(\mathbf{r},\mathbf{k}) = \omega \quad . \tag{2.11}$$

The vector $\mathbf{k}$ is seen to have the physical interpretation of a wavevector. Again, by analogy with the quantum mechanical problem, we are led to view the function $\nu(\mathbf{r},\mathbf{k}) \equiv \pm\Omega(\mathbf{r},\mathbf{k})$ – here a local frequency – as a Hamiltonian depending on the generalised coordinates $\mathbf{r}$ and the generalised momenta $\mathbf{k}$. Associated with this Hamiltonian we then have 'equations of motion'

$$\mathrm{d}/\mathrm{d}t\ \mathbf{r} = \partial/\partial\mathbf{k}\ \nu(\mathbf{r},\mathbf{k}) \quad \text{and} \quad \mathrm{d}/\mathrm{d}t\ \mathbf{k} = -\partial/\partial\mathbf{r}\ \nu(\mathbf{r},\mathbf{k}) \quad . \tag{2.12}$$

The latter, generated here in a strictly formal way, are seen to have a simple physical interpretation. They describe the asymptotic approximation of *geometric acoustics*, *i.e.* the propagation of narrow directed beams of acoustic energy – the acoustic rays – in the limit of short wavelengths.

In this brief and unconventional derivation of geometric acoustics we have so far not insisted on the basic differences which arise between our oscillation eigenvalue problem and Schrödinger eigenvalue problem. I mention here in the first place that the selection of $\pm\Omega(\mathbf{r},\mathbf{k})$ as the relevant Hamiltonian $\nu(\mathbf{r},\mathbf{k})$ is not unambiguously imposed. We could as well have chosen for instance $\Omega(\mathbf{r},\mathbf{k})^2$ as the classical Hamiltonian. The formal lack of uniqueness of the assignment of a Hamiltonian mirrors a similar lack of uniqueness in the ray equations as derived by the more conventional procedures (*cf.* *Eckart* 1960, *Jeffrey* and *Taniuti* 1964, *Tolstoy* 1973). Moreover, with our choice, which has the advantage of having a direct physical interpretation as the local acoustic frequency, the Hamiltonian of geometric acoustics acquires a peculiar mathematical feature not encountered in mechanics. We are dealing with a multivalued function of $\mathbf{r}$ and $\mathbf{k}$, since both $+\Omega(\mathbf{r},\mathbf{k})$ and $-\Omega(\mathbf{r},\mathbf{k})$ *simultaneously* define our Hamiltonian $\nu(\mathbf{r},\mathbf{k})$ (eq. (2.11)). These two sheets are seen to join at the surface of the star where the sound speed vanishes. The sheet to be used in the ray equations is ruled by a continuity requirement. A ray initially described by the sheet $+\Omega(\mathbf{r},\mathbf{k})$ will be moving towards the stellar surface, it bounces off the surface following the ray equations containing sheet $-\Omega(\mathbf{r},\mathbf{k})$ of the Hamiltonian. An alternation of the sheets of the Hamiltonian occurs at every encounter of the ray with the surface. The double branch structure of the Hamiltonian thus handles directly the problem of the surface reflection of the rays without any need for an externally imposed reflection condition.

The fact that our Hamiltonian is double-valued, implies that each point of the (**r**,**k**)-space supports two orbits (namely one generated by the branch $+\Omega(\mathbf{r},\mathbf{k})$ and the other by the branch $-\Omega(\mathbf{r},\mathbf{k})$) instead of a single one in the case of conventional Hamiltonian mechanics. This multi-valuedness prevents us from directly applying the results of classical mechanics to our formulation of geometric acoustics. We manage to get rid of the multi-valuedness by simple geometrical trick used in the discussion of billiards and which consists essentially in changing the topology of the (**r**,**k**)-space (*Arnold* 1978). The configuration space of coordinates **r**, namely the region inside the star accessible to the rays (topologically an f-dimensional disc D^f) will be regarded as two-sheeted; these two sheets are then glued together at the boundary of the region (the surface of the star). As is obvious from Figure 1, the combined two-sheeted region acquires therefore the topology of an f-dimensional sphere S^f. An actual position in the star, of coordinates **r**, is regarded as lying either on the 'upper' sheet, in which case we denote its coordinates by $\mathbf{r}_+$, and the associated sheet of Hamiltonian $\nu(\mathbf{r},\mathbf{k})$ is $+\Omega(\mathbf{r},\mathbf{k})$; or it is viewed as lying on the 'lower' sheet, in which case we denote the coordinates by $\mathbf{r}_-$, and the associated sheet of the Hamiltonian is $-\Omega(\mathbf{r},\mathbf{k})$.

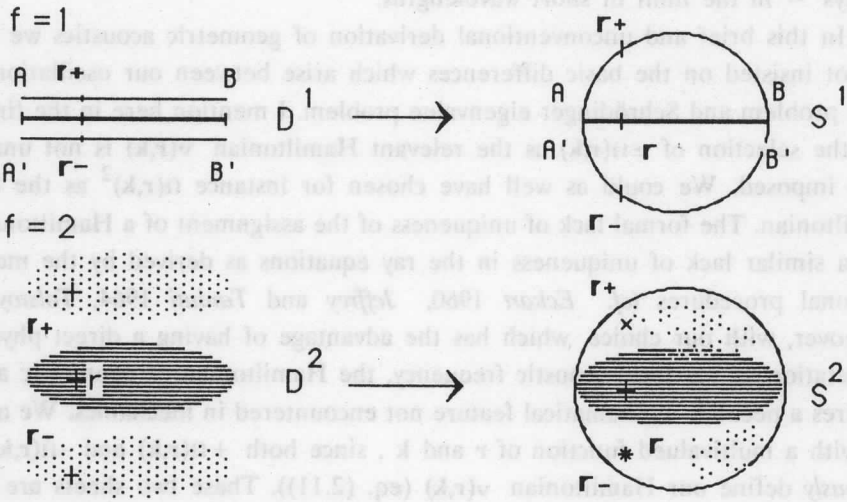

Fig. 1. The physical configuration space and the two-sheeted extended configuration space of the ray propagation problem if f = 1 and 2 dimensions; for f = 1 the combined upper and lower sheets, with A identified with A', and B identified with B', define a circle S^1; for f = 2 the combined upper and lower sheets with boundaries identified, define the surface of the sphere, S^2.

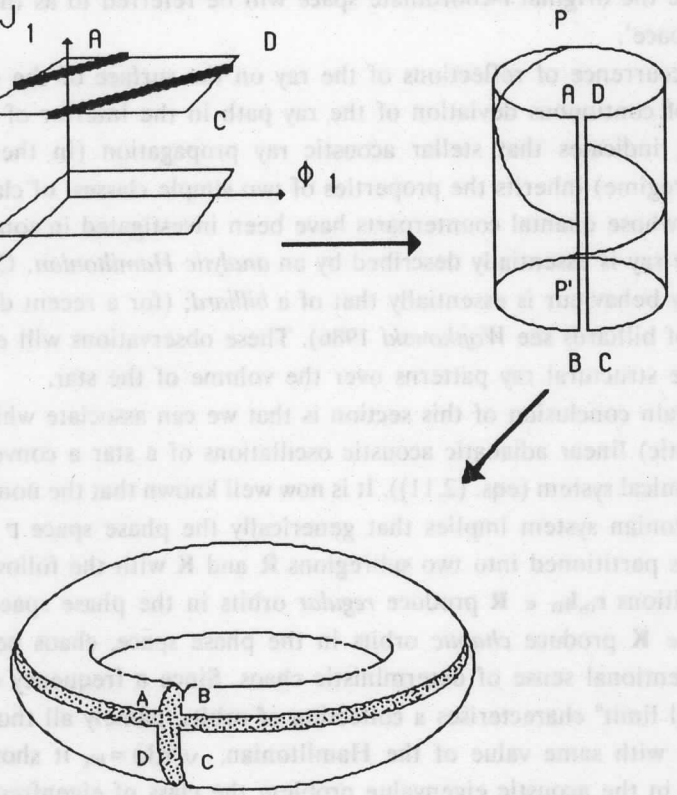

Fig. 2. Solution of an integrable system of ray equations displayed in the angle-action variables Φ, **J**, for $f=2$; the 'square' ABCD has its opposite sides identified, AB ≡ DC and BC ≡ AD ; By pasting successively BC and AD , and then AB and DC together, we produce a cylindrical surface and a torus; a ray then winds around this torus.

The a priori accessible space of wavevector **k** is the f-dimensional Euclidean space E^f. More precisely, for the typical sound velocity profile we shall adopt here (*cf.* eq. (5.4)), it transpires from the Hamiltonian equations of motion that the wavevector takes on infinite values at the surface of the star; therefore the actual wavevector space is $E^f \cup \{\infty\}$, where we denote by ∞ the point at infinity. This space has again the same topology as the f-sphere, S^f. With our extension of the configuration space (of topology S^f), and the topological specification of the wavevector space (also S^f), we obtain a conventional phase space $(\mathbf{r}_\pm, \mathbf{k})$, henceforth denoted by Γ, of topology $S^f \times S^f$. Our Hamiltonian system is specified by a conventional single-valued vector field (the RHS of eqs. (2.12)) defined over the phase space Γ. We shall refer to the two-sheeted configuration space as the 'extended configuration

space', while the original r-coordinate space will be referred to as the 'physical configuration space'.

The occurrence of reflections of the ray on the surface of the star on the one hand, and of continuous deviation of the ray path in the interior of the star on the other hand, indicates that stellar acoustic ray propagation (in the above defined asymptotic regime) inherits the properties of two simple classes of classical mechanical systems whose quantal counterparts have been investigated in some detail: Inside the star, the ray is essentially described by an *analytic Hamiltonian*. Close to the surface, the ray behaviour is essentially that of a *billiard*; (for a recent discussion of the properties of billiards see *Wojtkowski* 1986). These observations will enable us to understand the structural ray patterns over the volume of the star.

The main conclusion of this section is that we can associate whith the problem of (asymptotic) linear adiabatic acoustic oscillations of a star a conventional Hamiltonian dynamical system (eqs. (2.11)). It is now well known that the nonlinear character of a Hamiltonian system implies that generically the phase space Γ of the dynamical system is partitioned into two subregions **R** and **K** with the following properties. Initial conditions $\mathbf{r}_0,\mathbf{k}_0 \in \mathbf{R}$ produce *regular* orbits in the phase space; initial conditions $\mathbf{r}_0,\mathbf{k}_0 \in \mathbf{K}$ produce *chaotic* orbits in the phase space, chaos being understood in the conventional sense of deterministic chaos. Since a frequency eigenvalue ω in the "classical limit" characterises a collection of orbits, namely all those orbits in the phase space with same value of the Hamiltonian, $\nu(\mathbf{r},\mathbf{k})=\omega$, it should not be surprising that in the acoustic eigenvalue problem the class of eigenfrequencies related to regular families of orbits and the class related to chaotic orbits display basic differences.

3. Hamiltonian ray dynamics. The integrable case

A single-valued Hamiltonian is globally *integrable* if it admits of f independent contants of motion, *i.e.* f independent functions which are constant along an orbit in the phase space

$$\mathbf{J}(\mathbf{r},\mathbf{k}) = \mathbf{J}(\mathbf{r}_0,\mathbf{k}_0) = \mathbf{J}_0 \quad , \tag{3.1}$$

$\mathbf{J} = (J_1, J_2, \ldots, J_f)$;

$\mathbf{J}_0$ is here a constant f-dimensional vector; $\mathbf{r}_0,\mathbf{k}_0$ are the initial position and momentum (wavevector) of the orbit generated by the dynamical system (2.12) (*cf. Arnold* 1978 for the full definition of integrability). With the above formal extension of the configuration space, our Hamiltonian $\nu(\mathbf{r},\mathbf{k})$ is made single-valued in the $(\mathbf{r}\pm,\mathbf{k})$ - phase space Γ. The conventional definition of integrability is therefore applicable to our ray system.

We mention that each individual constant of motion $J_j(\mathbf{r},\mathbf{k}) = \text{constant}$, $j = 1, 2, \ldots, f$ confines the motion to a subspace Σ_j^{2f-1} of dimension $2f-1$. Accordingly the collection of the f independent constants of motion defines a region in phase space which is the intersection of the subspaces Σ_j^{f-1}, and therefore of dimension f

$$\Sigma_1^{f-1} \cap \Sigma_2^{f-1} \cap \ldots \cap \Sigma_j^{f-1} \equiv \Sigma^f \quad . \tag{3.1a}$$

We now select a collection of f variables $\boldsymbol{\phi}$ such that the transformation

$$T: \quad \mathbf{r}_\pm, \mathbf{k} \mid\!\rightarrow \boldsymbol{\phi}, \mathbf{J} \quad , \tag{3.2}$$

be a canonical transformation (for a proof of existence of such a transformation see *Arnold* 1978). Under this mapping the Hamiltonian $\nu(\mathbf{r},\mathbf{k})$ becomes

$$\nu(\mathbf{r}(\boldsymbol{\phi},\mathbf{J}), \mathbf{k}(\boldsymbol{\phi},\mathbf{J})) \equiv F(\boldsymbol{\phi},\mathbf{J}) \quad , \tag{3.3}$$

and therefore we have the following ray equations

$$d/dt\ \boldsymbol{\phi} = \partial/\partial \mathbf{J}\ F(\boldsymbol{\phi},\mathbf{J}) \quad \text{and} \quad d/dt\ \mathbf{J} = -\partial/\partial\boldsymbol{\phi}\ F(\boldsymbol{\phi},\mathbf{J}) \ . \tag{3.4}$$

The variables $\mathbf{J}$ being by construction constants of motion, their time derivatives vanish. This requires the Hamiltonian in the new canonical variables to be independent of $\boldsymbol{\phi}$ or $F(\boldsymbol{\phi},\mathbf{J}) \equiv F(\mathbf{J})$. Setting then

$$\mathbf{w}(\mathbf{J}) \equiv \partial/\partial \mathbf{J}\ F(\mathbf{J}) \quad , \tag{3.5}$$

we can explicitly write down the solution of the ray equations in the new variables $\boldsymbol{\phi}$, $\mathbf{J}$

$$\boldsymbol{\phi}(t) = \mathbf{w}(\mathbf{J})\ t + \boldsymbol{\phi}_o \quad \text{and} \quad \mathbf{J}(t) = \mathbf{J}_o \quad , \tag{3.6}$$

$\boldsymbol{\phi}_o$ and $\mathbf{J}_o$ being the initial conditions.

We shall now introduce a special requirement on the rays:
The rays as referred to the new canonical variables, are *bounded* in the phase space Γ. In other words, for any finite initial condition $\boldsymbol{\phi}_o$, $\mathbf{J}_o$ we postulate that there exists a finite positive constant A such that

$$\forall\ t: \ |\boldsymbol{\phi}(t)| \leq A \quad , \tag{3.7}$$

the norm being the Euclidean norm. Requirement (3.7), together with the explicit solution (3.6) implies that the variables $\boldsymbol{\phi}$ must be cyclic variables, *i.e.* each component ϕ_j, $j = 1, 2, \ldots, f$ is defined modulo a positive real number m_j. Without loss we can choose the real m_j all equal to 2π, so as to identify the variables $\boldsymbol{\phi}$ as *angles*. The constants of motion $\mathbf{J}$ are then referred to as *actions*. Each variable ϕ_j, being thus defined over a circle S^1, the collection of the f angular variables (eq. (3.6)) is defined over the direct product of f circles

$$S^1 \times S^1 \times \ldots \times S^1 \equiv T^f \quad , \tag{3.8}$$

which is an f-dimensional torus T^f (*cf.* Fig. 2), in the integrable case the region Σ^f (eq. (3.1a)) acquires the topological structure of a torus.

Let us introduce at this stage the following definition. A system of ordinary differential equations

$$\mathrm{d/dt}\ \mathbf{x} = \mathbf{f(x)} \quad , \tag{3.9}$$

with $\mathbf{x}$ defined in an n-dimensional phase space γ, and with R an invariant set in γ, will be said to be *simple* in R, if a smooth one-to-one transformation exists

$$\mathrm{T}: \mathbf{x} \mapsto \mathbf{y} \quad , \tag{3.10}$$

such that for any $\mathbf{x} \in R$ the differential equation reduces to

$$\mathrm{d/dt}\ \mathbf{y} = \mathbf{a} \quad , \tag{3.11}$$

with $\mathbf{a}$ constant; the new variables $\mathbf{y}$ are defined mod($\mathbf{b}$) (with $\mathbf{b}$ possibly $\to \infty$).

Conversely equation (3.9) is said to be *nonsimple* in an invariant set $K \subset \gamma$ if no transformation (3.10) exists leading to a differential equation (3.11).

We recall that *locally*, namely in the neighbourhood of any regular point of the vector field $\mathbf{f(x)}$, the original differential system can always be reduced to the form (3.11) (*cf. Arnold* 1980). The above definition of simplicity stipulates that the full orbit (for $-\infty \leq t \leq +\infty$) is described by system (3.11).

We see that for a system simple in R, the variables $\mathbf{y}$ define an orbit in $R \subset \gamma$ which traces out a deceptively regular pattern, namely *straight parallel lines* in a 'hypercube' (in which opposite sides are identified); a geometric regularity of this pattern is preserved under the inverse transformation of (3.10), so that in the variables $\mathbf{x}$ the orbit continues to define a regular pattern. Moreover, the projection of this regular pattern onto any subspace $V \subset \gamma$ cannot destroy the regularity of the pattern. We conclude therefore that the projection of the orbit into any subspace $V \subset \gamma$ produces a regular pattern in V. Alternatively, for a system which is nonsimple, any orbit in K, expressed in any set of new variables $\mathbf{y}$ we like (eq. (3.10)), keeps by definition a complicated analytic form. Accordingly, it generates a complicated irregular geometric orbit structure. Generically the projection of such an orbit onto some subspace V then remains irregular.

We have shown that if our ray Hamiltonian $\nu(\mathbf{r},\mathbf{k})$ is integrable, then the rays lie on an f-dimensional torus $T^f \subset \Gamma$. Moreover, as is seen from equation (3.6), our dynamical system is *simple* in the sense defined above, everywhere in our phase space Γ. The projection of the ray pattern from $(\mathbf{r}_\pm,\mathbf{k})$ - space onto the physical configuration space $(\mathbf{r})$ — namely onto the actual volume of the star — then displays a regular ray pattern. It transpires from this discussion that *all* rays of an integrable ray problem display a regular pattern in the configuration space $\mathbf{r}$. We shall refer to these rays as *regular rays*.

A further point is of relevance for our purposes. For generic initial conditions, the set of frequencies $\mathbf{w}(\mathbf{J})$ (eq. (3.5)) is typically rationally independent (except possibly for very special ray systems); this means that for any collection of f integers $\mathbf{n}=(n_1, n_2, \ldots, n_f)\neq 0$ we have

$$\mathbf{n}\,\mathbf{w}(\mathbf{J}) \neq 0 \quad . \tag{3.12}$$

It follows that the ray carrying torus T^f specified by the set of actions $\mathbf{J}$ is densely covered by the ray (*cf. Arnold* 1978). Such a torus is referred to as a *nonresonant torus*. Conversely if for some set of nonzero integers $\mathbf{n}$ we have

$$\mathbf{n}\,\mathbf{w}(\mathbf{J}) = 0 \quad , \tag{3.13}$$

then the torus defined by the actions $\mathbf{J}$ is said to be a *resonant torus*. The totality of resonant tori forms a subset in the phase space Γ of (Euclidean) 2f - dimensional measure zero. In spite of this sparseness, the resonant tori are dense in the phase space.

A subvariety of the resonant tori are the *periodic tori*. A torus is periodic if it supports closed, and therefore periodic orbits; such orbits arise if the values of the actions $\mathbf{J}$ are such as to secure that for any pair of components of the set of frequencies $\mathbf{w}$ (eq. (3.5)) we have

$$\forall\, i,j, \quad i,j = 1, 2, \ldots, f: \quad \omega_i / \omega_j = n_i / n_j \quad , \tag{3.14}$$

n_i, n_j being nonzero integers. A periodic torus actually carries a continuous infinity of periodic rays which cover the torus. Although the periodic tori are infinitely sparser than the resonant ones, they still cover the phase space Γ densely. Geometrically these properties mean that given an arbitrary initial condition $(\mathbf{r}_{\pm o}, \mathbf{k}_o)$ in phase space Γ, there is always an arbitrarily close point $(\mathbf{r}_{\pm op}, \mathbf{k}_{op})$ such that latter is an initial condition of a periodic ray.

We shall need one further result from mechanics for the calculation of asymptotic eigenvalues. Let $\mathbf{C}$ be a closed ray path in the phase space Γ. Let C be the projection of $\mathbf{C}$ onto the extended configuration space $(\mathbf{r}_{\pm})$. The integral

$$\Delta S \equiv \int_C d\mathbf{r}\ \mathbf{k}(\mathbf{r}) \quad , \tag{3.15}$$

where $\mathbf{k}(\mathbf{r})$ is the uniquely defined value of the wavevector of the periodic solution at the position $\mathbf{r}=\mathbf{r}_{\pm}$ is computed as follows. Introduce the angle-action variables (3.2), and rewrite the integral

$$\begin{aligned}(1/2\pi) \int_C d\mathbf{r}\ \mathbf{k} &= (1/2\pi) \int_{m_1C_2 + m_2C_2 + \ldots + m_fC_f} d\boldsymbol{\phi}\ \mathbf{J} \\ &= \Sigma_{i=1}^{f}\, (m_i/2\pi)\ \Delta S_i \quad ,\end{aligned} \tag{3.16}$$

with

$$\Delta S_i \equiv \int_{C_i} d\phi_i\ J_i = 2\pi\, J_i \quad , \tag{3.17}$$

In these expressions the closed path C in the phase space is decomposed into f "irreducible" circuits of the torus carrying C

$$\mathbf{C} = m_1\mathbf{C}_1 + m_2\mathbf{C}_2 + \ldots + m_f\mathbf{C}_f \quad , \tag{3.18}$$

the coefficients $m_1, m_2, \ldots, m_f$ being integers (*cf.* Fig. 3 for an illustration of this decomposition for f=2); the circuits C_j, j = 1, 2, ... , f are the projections of $\mathbf{C}_j$ into the configuration space.

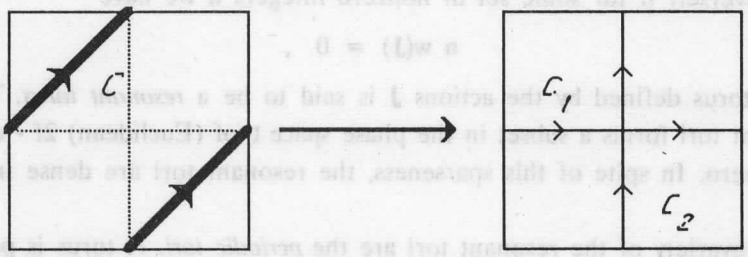

Fig. 3. A periodic orbit C on a 2-dimensional torus T^2 can be regarded as a linear combination with integer coefficients n_1 and n_2 of the 'irreducible' circles C_1 and C_2 of the torus (illustration for $C = C_1 + C_2$).

While it is known that integrability of Hamiltonian system is an exceptional property (*cf. Arnold* 1978), it has been proved that the acoustic ray Hamiltonian of a spherically symmetric star is always integrable, irrespective of the run of the sound speed c(**r**) throughout the star (*Perdang* 1986).

4. Hamiltonian ray dynamics. The nonintegrable case

The generic case of stellar ray dynamics in the presence of geometric deformations of the equilibrium state, is that the Hamiltonian $\nu(\mathbf{r},\mathbf{k})$ is not globally integrable. The following possibilities arise.

(A) For initial conditions $(\mathbf{r}_o \pm, \mathbf{k}_o)$ in a subset **R** of the phase space Γ we still can find f local integrals of motion **J** (eq. (3.1)).

(B) For initial conditions in the complementary subset of the phase space,

$$\Gamma \backslash \mathbf{R} \equiv \mathbf{K} \quad , \tag{4.1}$$

we have less than f local integrals of motion. Notice that even in this case we have at least one integral, namely the Hamiltonian itself, which remains a global integral.

The limiting case of **K** being an empty set corresponds to an integrable ray problem. The limiting case of **R** being of measure zero is encountered in billiards with non analytic boundaries (the stadium billiard for instance, *cf. Berry* 1983; *cf.* also

Wojtkowski 1986), since the equations of acoustic rays in an isothermal medium are equivalent to those of billiards, this latter limit should not be dismissed as entirely irrelevant under stellar conditions.

(A) In the region **R** of Γ we can *locally* apply the above theoretical analysis. For initial conditions in **R** the solutions of the Hamiltonian equations are then again fully represented in the form (3.6). The rays are supported by f-dimensional tori, T^f, covering **R**. The resonant tori, and in particular the periodic orbits, are dense in **R**. The region **R** is thus carrying the regular rays. We refer to it as the *regular region* of the phase space.

(B) To characterise the rays in the region **K** complementary to **R**, we consider in some detail the case of a single integral of motion

$$\mathbf{J(r,k)} = J_o \quad , \tag{4.2}$$

assuming that there are no other local integrals.

Again we can set up a canonical transformation

$$T': \quad \mathbf{r}, \mathbf{k} \mapsto \phi, \underline{q}, J, \underline{p} \quad , \tag{4.3}$$

where $\underline{q}$ and $\underline{p}$ are (f–1)-dimensional arrays of variables, such that the Hamiltonian in the transformed variables

$$\nu(\mathbf{r}(\phi,\underline{q},J,\underline{p}), \mathbf{k}(\phi,\underline{q},J,\underline{p})) \equiv G(\underline{q},\underline{p},J) \quad , \tag{4.4}$$

becomes independent of the unique angular-type variable ϕ. The equations of motion in the variables $(\underline{q},\underline{p})$ then become

$$d/dt\ \underline{q} = \partial/\partial\underline{p}\ G(\underline{q},\underline{p},J) \quad \text{and} \quad d/dt\ \underline{p} = -\partial/\partial\underline{q}\ G(\underline{q},\underline{p},J) \quad . \tag{4.5}$$

For a given initial action J_o, the variables $(\underline{q},\underline{p})$ can be solved separately. Let $\underline{q}(t)$, $\underline{p}(t)$ be the solution of system (4.5) for given initial conditions $\underline{q}_o$, $\underline{p}_o$, J_o. Then the angular-type variable is obtained by a quadrature

$$\phi(t) = \int_o^t dt\ \omega(\underline{q}(t),\underline{p}(t),J_o) + \phi_o \quad ; \tag{4.6}$$

here ϕ_o is the angle at time 0, and

$$\omega(\underline{q},\underline{p},J) \equiv \partial/\partial J\ G(\underline{q},\underline{p},J) \quad . \tag{4.7}$$

The main point which transpires from this transformation is that the vector field of the RHS of system (4.5) cannot be reduced to a constant vector field, or our differential system is *nonsimple* in **K**. In fact, we could carry out a reduction to a simple differential system, then our Hamiltonian system would again be locally integrable, which contradicts our hypothesis. Notice that even the angular-type variable $\phi(t)$ (eq. (4.6)) obeys here a complicated time behaviour.

The solutions of Hamiltonian systems which are *nonsimple* are referred in the literature as *chaotic solutions*. The region in phase space **K** occupied by chaotic orbits is the *chaotic region*.

The existence of a single integral of motion (4.2) confines the ray to a (2f-1)-dimensional subspace, $\Sigma^{2f-1} \subset \Gamma$, which is invariant under the solutions of our Hamiltonian ray system. This invariant subspace Σ^{2f-1} in turn may decompose into invariant subsets, $M_k^{2f-1} \subset \Sigma^{2f-1}$, of same dimension 2f–1, which themselves cannot be further decomposed into invariant sets of dimension 2f–1 (but possibly into lower dimensional sets). An example is provided in Figure 2 which we interpret here as showing the subspace $\Sigma^3 \subset \Gamma$ for a system of 2 degrees of freedom with at least one family of regular solutions (say for $J_1' \leq J_1 \leq J_1''$, J_1', J_1'' two constants); the latter are carried by a rectangular 'box' limited to two 'squares' (*cf.* Fig. 2); this box then divides the invariant subspace Σ^3 into two invariant subregions, an 'upper', M_+^3, and a 'lower' one, M_-^3; a chaotic solution of initial condition in M_+^3 then cannot penetrate into M_-^3, since the orbit is unable to cross the tori, the latter being themselves invariant sets of the Hamiltonian system. In the case of 3-dimensional rays and a single integral of motion there is no such general topological constraint requiring a partition of the chaotic region into invariant subregions.

The above discussion can be repeated for Hamiltonian ray systems with $r < f$ local constants of motion, where r may change from one part of the phase space to the other. Under those conditions we have local regions in phase space of dimension 2f–r, Σ^{2f-r}, which decompose again into invariant sets M_k^{2f-r} in **K**. The chaotic region **K** of the phase space is the union of all of these invariant sets M_k^{2f-r}. The invariant sets M_k^{2f-r} in **K** play the parts of the (invariant) tori T^f in **R**. They are the carriers of the chaotic solutions; and they are densely covered by the latter. Genealogically these sets are found to arise out of resonant tori; the latter 'explode' (*i.e.* they acquire a dimension higher than f) as a parameter in the differential system is varied. We mention here two properties of the chaotic region **K**.

On the one hand, it can be shown that the solutions in **K** have a *sensitive dependence on the initial conditions.* Intuitively this means that if $\mathbf{r}_{+a}$, $\mathbf{k}_a$ and $\mathbf{r}_{+b}$, $\mathbf{k}_b$ (or $\mathbf{r}_{-a}$, $\mathbf{k}_a$ and $\mathbf{r}_{-b}$, $\mathbf{k}_b$) define two arbitrarily close points in **K** playing the parts of initial conditions for two rays L_a and L_b, then these rays separate exponentially with time (for precise definition see *Devaney* 1986). In other words these rays are unstable. This property is often used as the definition of chaotic solutions.

On the other hand the closed rays are *dense* in **K**. The difference between closed rays (periodic solutions of the Hamiltonian ray equations) lying in the chaotic region and those in the regular region is that the former are stable while the latter are unstable. Together with the above-mentioned property of denseness of the periodic rays in **R**, we conclude that the whole phase space Γ is densely covered by periodic rays.

We shall see now a few illustrations of regular and chaotic rays in geometrically deformed stars.

5. Numerical integration of the ray equations

In order to analyse the nature of the ray patterns in stars we have solved numerically the ray equations (2.12), using the following representation for the run of the sound speed c(**r**) throughout the star

$$c(\mathbf{r})^2 \equiv C(R)^2 \quad , \tag{5.1}$$

where R is defined by

$$R^2 = r^2 + \Sigma_{L=2}^{\infty} \lambda_L r^L \Sigma_{m=0,\pm1,\pm2,\ldots,\pm l} D_{lm}^{(L)} Y_l^m(\Theta,\phi) \quad . \tag{5.2}$$

$R^2 = constant$ thus represents a surface of constant sound speed. The surface of the star will be represented by $R = 1$. This choice fixes our unit of length.

In expression (5.2) (r,Θ,ϕ) are the spherical coordinates of a point **r** of the star, of Cartesian coordinates (x_1, x_2, x_3),

$$\begin{aligned} x_1 &= r \cos\Theta \quad , \\ x_2 &= r \sin\Theta \sin\phi \quad , \\ x_3 &= r \sin\Theta \cos\phi \quad . \end{aligned} \tag{5.3}$$

The coefficients λ_L indicate the *order of magnitude* of the deformations of the surface of constant sound speed. We require the latter to be small enough so that the individual surfaces of constant sound speed all remain *convex*. The integer L denotes the algebraic degree of the deformation in the radial coordinate; the numerical factors $D_{lm}^{(L)}$ (of order 1) measure the precise values of this deformation for an algebraic degree L, a spherical degree l, and an azimuthal number m; the notation $Y_l^m(\Theta,\phi)$ stands as usual for the spherical harmonics. Expression (5.2) shows that R is an average radius of the surface of constant sound speed.

For the function C(R) we have chosen

$$C(R)^2 = 1 - R^2 \quad , \tag{5.4}$$

which reflects the overall trend of the sound speed in a realistic star, although it does not reproduce the fine structure of the latter. The unit of speed is selected such as to have a central sound speed equal to 1.

We have investigated stellar configurations whose surfaces of constant sound speed preserve rotational symmetry $C_{\infty v}$. The symmetry axis is chosen to be the Ox_1 axis, O being the centre of mass of the configuration. Such a symmetry of the ray Hamiltonian implies that any initial condition $\mathbf{r}_0$, $\mathbf{k}_0$ such that $\mathbf{k}_0$ is directed towards the symmetry axis, generates a ray which is confined to the symmetry plane Π going through the symmetry axis and the initial position $\mathbf{r}_0$.

We have studied so far only those families of rays which lie in the symmetry planes Π, since those rays are easily displayed graphically. In the absence of symmetry planes we have, in general, no families of planar rays. On the other hand, a systematic investigation of non-planar rays would require special plotting devices of the ray system (for instance stereoscopic plots).

With our attention focused on planar rays only, the effective Hamiltonian ray equations we are working with have $f=2$ degrees of freedom. The physical configuration space is a meridian plane Π of the star, and the extended configuration space has topology S^2. The initial conditions for the rays are parametrised as follows. We first observe that the monotonic structure of the sound speed as a function of the average radius R of the surfaces of constant sound speed implies that *any* ray in Π intersects the symmetry axis Ox_1; we shall refer to the latter as the polar axis NS (North-South). Any ray can therefore be generated by selecting an appropriate position $\mathbf{r}_0$ on the polar axis; let X denote the Cartesian coordinate of this position. The initial wavevector $\mathbf{k}_0$ is fixed by the angle w this vector makes with the positive polar axis Ox_1; the symmetry of the configuration implies that $0 \leq w \leq \pi$; notice also that $w=0$ and $w=\pi$ actually produces the same ray pattern, namely a ray remaining on the polar axis. We can convince ourselves that the modulus $|\mathbf{k}_0| = k$ of the initial wavevector does not influence the ray pattern. In fact, under the same transformation

$$\mathbf{k} \rightarrow K\,\mathbf{k} \tag{5.5}$$

K an arbitrary real constant, the Hamiltonian (*cf.* eqs. (2.9, 11)) is multiplied by K. The Hamiltonian equations (2.12) are seen to remain invariant. Accordingly we parametrise the initial conditions

$$(X,w) \in D^1 \times S^1 \quad . \tag{5.6}$$

Since as far as the ray pattern is concerned $w=0$ and $w=\pi$; are to be identified, we see that w is defined over a circle S^1; the position X is defined over a finite interval D^1; therefore the parameter space of the ray patterns in the meridian planes Π has the topology of a cylindrical surface $D^1 \times S^1$.

The following shapes of the surfaces of constant sound speed have been studied.
(A) If we set $\lambda_L = 0$ for $L \geq 2$, we have the trivial case of a deformation that preserves the *spherical symmetry*. We have mentioned that the corresponding ray equations remain integrable irrespectively of the precise functional form of C(R).

The rays belong to one of the following families.
(a) For initial conditions $w=0$ or π and X arbitrary, we generate a *Polar Ray* (PR) *i.e.* a closed ray coinciding with the polar diameter of the star.
(b) For initial conditions $X=0$ (centre of the star) and $0<w<\pi$, we generate a *Radial Ray* (RR) *i.e.* a closed ray coinciding with an arbitrary diameter of the star.

The admittedly artificial distinction between radial rays and the polar ray, related to our choice of the parameter space (5.6) of the initial conditions, may appear as misleading; actually, it will turn out to be relevant in the case of the deformed configurations.

(c) For initial conditions $X \neq 0$ and $w \neq 0$ and π we generate a *Surface Ray* (SR); the surface ray remains confined to an outer ring in the star; due to the spherical symmetry of the configuration the ring has a circular inner boundary or *caustic (Perdang* 1986); the outer boundary is the surface of the star. In the extended configuration space of topology S^2 the image of this ring is a spherical annulus A_S; the latter is either *densely* covered by the projection of the orbit, or it carries a closed (periodic) orbit; the two boundaries of the annulus (which coincide with the inner boundary of the ring in the physical configuration space) are the *caustics* of the ray family. As the initial condition X approaches the origin, the annular region A_S tends to cover the whole extended configuration space; the circular caustic then degenerates into a single point of the physical configuration space (the image of two points of the extended configuration space). Denote by $F(PR)$, $F(RR)$ and $F(SR)$ the sets of polar rays, radial rays and surface rays respectively. Then the definition of these families implies that the closure of the set of SR, $cl\ F(SR)$, is given by

$$cl\ F(SR) = F(SR) \cup F(RR) \cup F(PR) \quad . \tag{5.7}$$

The set of radial and polar rays can therefore be written

$$F(RR) \cup F(PR) = cl\ F(SR) \setminus F(SR) \equiv \partial\ F(SR) \quad , \tag{5.7a}$$

where $\partial\ F(SR)$ stands for the derived set (or set of limit points) of the set of surface rays.

It is perhaps also interesting to observe that the closure of the radial rays as defined above obeys

$$cl\ F(RR) = F(RR) \cup F(PR) \quad , \tag{5.8}$$

or

$$F(PR) = cl\ F(RR) \setminus F(RR) \equiv \partial\ F(RR) \quad . \tag{5.8a}$$

In the 2-dimensional space of initial conditions (5.6) we notice that the families $F(PR)$ and $F(RR)$ are generated by 1-dimensional sets of points, which are therefore of measure zero; almost all points of the space (5.6) produce surface rays.

(B) If $\lambda_L = 0$ for $L \geq 3$, with $\lambda_2 \neq 0$, then the deformed surfaces of constant sound speed are *ellipsoids*, which, by our assumption are of revolution. We represent the latter in the parametric form

$$R^2 = r^2\ (a_p \cos^2\Theta + a_n \sin^2\Theta) \quad . \tag{5.9}$$

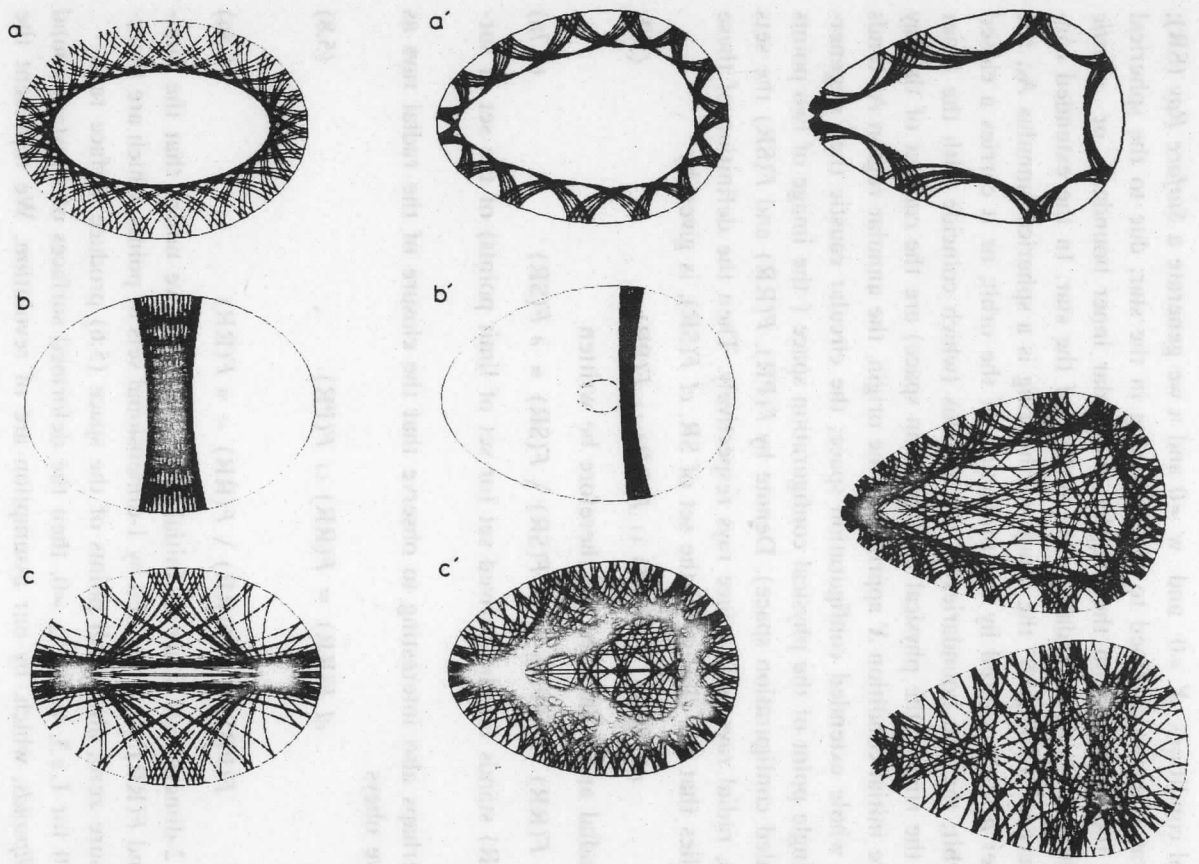

Fig. 4. The main families of acoustic rays of the elliptical configuration: (a) Surface Rays (SR); (b) Minor Axis Rays (MAR); and (c) Focal Rays (FR); corresponding families of rays of the pear-shaped configuration: (a') SR; (b') MAR; and (c') Chaotic Rays (CR).

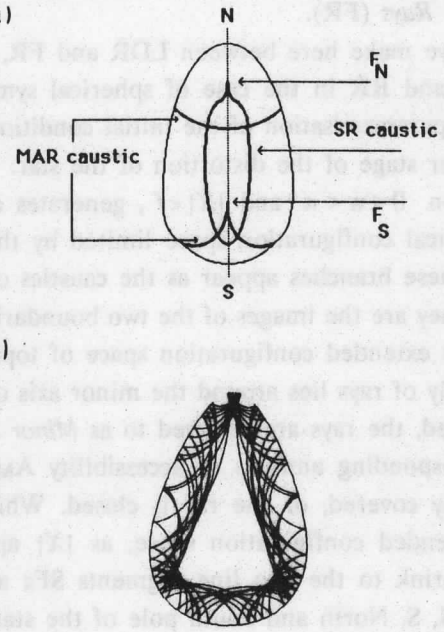

Fig. 5. Pseudo focal rays of the pear-shaped configuration: (a) schematic representation of the caustics and their singularities; (b) an illustration of a surface focal ray.

We shall choose

$$a_p\, a_n^2 = 1 \quad , \tag{5.9a}$$

in order to secure that the volume of the ellipsoid remains equal to the volume of the nondistorted sphere. The family of ellipsoidal cofigurations is then specified by a single independent parameter, which is taken as a_p. It can be shown that the ray equations remain *integrable* for the specific representation of the run of the sound speed (5.4). We shall consider only the case $a_p \leq 1$ corresponding to prolate ellipsoids; for oblate ellipsoids the classification of the ray families in the meridian planes is obtained *mutatis mutandis* as a result of a trivial duality of the meridian planes in both configurations.

The numerical integration of the ray equations in the meridian planes demonstrates the existence of the following families of planar rays.

(a) For initial conditions $w = 0$ or π and X arbitrary, we generate a ray propagating along the longest diameter (*Longest Diameter Ray*, LDR).

(b) For initial conditions w arbitrary and $X = \pm f$, where $\pm f$ are the Cartesian coordinates of two specific points F_N and F_S on the polar axis, we produce rays with the following property: a ray through F_S is reflected at the surface and sent through F_N

and *vice versa*. The points F_N and F_S thus play the parts of acoustic *foci*. We refer to these rays as *Focal Rays* (FR).

The distinction we make here between LDR and FR, just as the artificial distinction between PR and RR in the case of spherical symmetry, appears as being related to the special parametrisation of the initial conditions; its physical relevance will transpire at a later stage of the distortion of the star.

(c) An initial condition $0<w<\pi$ and $|X|<f$, generates a ray constrained to stay in a zone of the physical configuration space limited by the two branches of a hyperbola (*cf.* Fig. 4); these branches appear as the caustics of the ray in the physical configuration space; they are the images of the two boundaries of the ray in an annular region A_M of the extended configuration space of topology S^2. Since the zone accessible to this family of rays lies around the minor axis of the ellipsoidal surfaces of constant sound speed, the rays are referred to as *Minor Axis Rays* (MAR). For a given MAR the corresponding annulus of accessibility A_M in the extended phase space is either densely covered, or the ray is closed. While any MAR avoids the polar caps in the extended configuration space, as $|X|$ approaches f, the avoided zones progressively shrink to the two line segments SF_S and NF_N in the physical configuration space (N, S, North and South pole of the star respectively); the latter are degenerate caustics in the physical configuration space; the annulus A_M then tends to cover the whole of the extended configuration space.

(d) Any initial condition $0<w<\pi$ and $|X|>f$, produces a ray which, in the physical configuration space (of disk topology), is confined to a zone between the surface of the star and an ellipse (*cf.* Fig. 4); the latter plays the part of the caustic of this ray in the physical configuration space; the elliptical boundary is again the image of the two boundaries, or caustics of the ray in the extended configuration space, of an annular region A_S. In the physical configuration space the zone accessible to this class of rays lies near the surface of the star; therefore this family is referred to as the family of *Surface Rays* (SR). Notice that as $|X|$ approaches f, the avoided zone in the physical configuration space shrinks to the line segment F_SF_N which is also a degenerate caustic; the annulus A_S thus tends again to cover the full configuration space.

The mode of generation of these families of rays makes it clear that the families F(LDR) and F(FR) arise out of 1-dimensional sets of initial conditions in the 2-dimensional space of initial conditions (5.6), so that they are of measure zero among the totality of rays; the families F(MAR) and F(SR) have 2-dimensional sets of initial conditions in the space of initial conditions (5.6) .

The closure of the SR or the MAR obeys

$$cl\ F(\mathrm{SR}) = \mathrm{F(SR)} \cup F(\mathrm{FR}) \cup F(\mathrm{LDR}) \quad , \tag{5.10}$$

$$cl\ F(\mathrm{MAR}) = F(\mathrm{MAR}) \cup F(\mathrm{FR}) \cup F(\mathrm{LDR}) \quad ,$$

so that

$$F(\mathrm{FR}) \cup F(\mathrm{LDR}) = cl\, F(\mathrm{SR}) \setminus F(\mathrm{SR}) \equiv \partial F(\mathrm{SR}) \quad , \tag{5.10a}$$

$$= cl\, F(\mathrm{MAR}) \setminus F(\mathrm{MAR}) \equiv \partial F(\mathrm{MAR}) \quad ;$$

or alternatively

$$F(\mathrm{FR}) \cup F(\mathrm{LDR}) = cl\, F(\mathrm{SR}) \cap cl\, F(\mathrm{MAR}) \quad . \tag{5.10b}$$

Likewise

$$cl\, F(\mathrm{FR}) = F(\mathrm{FR}) \cup F(\mathrm{LDR}) \, , \tag{5.11}$$

or

$$F(\mathrm{LDRR}) = cl\, F(\mathrm{FR}) \setminus F(\mathrm{FR}) \equiv \partial F(\mathrm{FR}) \tag{5.11a}$$

As the ellipsoidal deformation parameter λ_2 vanishes (or $a_p \to 1$), the family of minor axis rays together with the family of focal rays degenerate into the class of radial rays of the sphere; the longest diameter ray becomes the polar ray of the sphere while the surface rays transform into surface rays of the sphere:

$$\lambda_2 \to 0 : \quad F(\mathrm{MAR}) \cup F(\mathrm{FR}) \to F(\mathrm{RR}) \quad ,$$

$$F(\mathrm{LDR}) \to F(\mathrm{PR}) \quad ,$$

$$F(\mathrm{SR}) \to F(\mathrm{SR}) \quad . \tag{5.12}$$

Or conversely, through the breaking of the spherical symmetry by an ellipsoidal distortion the degenerate radial rays "unfold" into minor axis rays and focal rays.

(c) By setting $\lambda_L = 0$ for $L \geq 4$, with λ_2 and $\lambda_3 \neq 0$, the deformed surfaces of constant sound speed become in principle arbitrary surfaces of third degree. By our above assumptions these surfaces are required to be closed, convex and of revolution about the polar axis. We shall actually restrict the class of surfaces further by adopting here the following parametric form

$$R^2 = r^2 (a_p \cos^2\Theta + a_n \sin^2\Theta)$$

$$+ \beta\, r^3 \cos\Theta (b_p \cos^2\Theta + b_n \sin^2\Theta) \tag{5.13}$$

in which we set

$$b_p = 1 \quad \text{and} \quad b_n = -3/2 \quad . \tag{5.13a}$$

Without loss we require again relation (5.9a) to hold, so that the configurations actually investigated depend on two parameters a_p and β; the latter parameter measures here the order of magnitude of the cubic deformation which confers the surfaces of constant sound speed a *pear-shaped* structure. We shall refer to the point of greatest curvature of the surface of the star as the North pole (N); the diametrically opposite point will be called the South pole (S).

The astrophysical relevance of such a family of surfaces of constant sound speed is that they are encountered in stars of homogeneous density whose equilibrium structure is deformed by a close companion, the effect of the tidal distortion is computed to third degree in the Cartesian coordinates of the star (*cf. Moray* 1986). Such configurations are direct extensions of the classical Jeans ellipsoids (*Chandrasekhar* 1969).

The formal reason why we have not analysed the most general type of cubic deformations (5.2) compatible with our symmetry requirement is that parametric representation (5.13) is already found to be flexible enough to produce nonintegrable ray Hamiltonians, and therefore also chaotic families of rays. In fact, the numerical results seemingly indicate that for *any* value $\beta \neq 0$ we have a nonintegrable ray Hamiltonian.

The rays we find belong to the following families.

(a) The initial conditions $w = 0$ or π and X arbitrary, produce again a ray propagating along the polar axis (*Longest Diameter Ray* LDR).

(b) For initial conditions $0 < w < \pi$ and $X = f_N$, where f_N is the Cartesian coordinate of a singular point F_N closest to the North pole on the polar axis, we notice that a ray going through F_N traverses F_N again and again. This ray displays a closed caustic having F_N as a cusp point (Fig. 5); the caustic intersects the polar axis at a second point Φ_S, of Cartesian coordinate ξ_S, close to the South pole. F_N is seen to play a part reminiscent of a focus of the ellipsoidal configuration. I shall refer to such a ray as a *Surface Focal Ray* (SFR).

(c) In a parallel fashion, initial conditions $0 < w < \pi$ and $X = f_S$, where f_S is the Cartesian coordinate of a singular point F_S on the polar axis closest to the South pole, give rise to a ray traversing F_S again and again. Such a ray is found to have a caustic consisting of two branches, one towards the South pole having F_S as a cusp point (Fig. 5); the other branch, closer to the North pole, is smooth and intersects the polar axis at a point Φ_N of coordinate ξ_N. Again F_S is reminiscent of a focus of the ellipsoidal configuration. I shall refer to such a ray as a *Minor Axis Focal Ray* (MFR).

(d) For an initial condition $0 < w < \pi$ and $f_S < X < \xi_N$, we generate a ray in the physical configuration space constrained to stay in a zone limited by the two branches of a distorted hyperbola (*cf.* Fig. 4); as in the ellipsoidal configuration, the latter branches are the caustics of this ray in the physical configuration space; again these branches are the 'projections' of the two boundaries of a region of annular topology A_M of the extended configuration space. Such rays are therefore *Minor Axis Rays* which either densely cover the annulus of accessibility A_M in the extended phase space, or they represent closed orbits. As X approaches the critical point F_S, the caustic tends towards the caustic of the minor axis focal rays.

(e) An initial condition $0<w<\pi$ and $X>f_N$ or $X<\xi_S$, leads to a ray which, in the physical configuration space, is confined to a zone between the surface of the star and a deformed ellipse (*cf.* Fig. 4); the inner boundary is the caustic of the ray pattern in the physical configuration space; this caustic in turn is the projection of the two caustics of the ray in the extended configuration space; the ray covers an annular region A_S in the latter configuration space, the covering being dense if the ray is not periodic. This family of rays are the *Surface Rays*. If we let X approach the singular point F_N, we notice that the caustic deforms into the caustic of the surface focal rays.

The ray families so far listed are all *regular* families of acoustic rays of the pear-shaped star. The patterns of these rays traced out in the physical configuration space are obtained by a regular deformation of the corresponding patterns of the ray families in ellipsoidal stars. As is seen in Figure 4, these ray patterns do indeed preserve a regular-looking geometry.

In addition to the regular rays, the numerical integration reveals the existence of a presumably chaotic ray family.

(f) If $0<w<\pi$, and $\xi_N<X<f_N$ or $f_s<X<\xi_S$, then we generate a ray which seemingly covers the whole physical configuration space densely; the coverage is not uniform, the orbits being apparently more concentrated in the neighbourhood of the degenerate caustics of the focal rays. We cannot disclose any regular geometric pattern in this ray system, so that we have good reasons to believe that we are dealing with a chaotic ray. We therefore refer to this family as the *Chaotic Rays* (CR). Figure 4 produces illustrations of these rays in pear-shaped configurations for different values of the parameters a_p and β.

I should point out that a detailed numerical demonstration of the chaotic nature of *all* of these latter rays – for instance by means of a surface of section analysis – is so far lacking. A word of caution is therefore in order. Although it seems very unlikely that the ray Hamiltonian of the pear-shaped configurations is integrable, it could well be that "in between" the surface and minor axis focal rays there exist other regular families, which then ought to display caustics. The caustics we are concerned with here are the boundaries of the projections onto a plane of 2-dimensional tori, embedded in a 4-dimensional space. It is quite obvious that the latter may develop singularities over some parameter range; intuitively, the boundary of the shadow cast by a tyre on a table, shows, for certain ranges of orientation of the tyre an angular point. From the general theory of caustics (see *Arnold* 1983, *Ozorio de Almeida* and *Hannay* 1982, *Nye* 1985) it is indeed known that under a change of p parameters catastrophes of codimension $(p+2)$ may occur on the caustics. In other words, beyond the range of our initial conditions which produce surface rays and then surface focal rays (with a singularity in their caustic), we have no a priori math-

ematical argument to exclude a family of rays with a caustic exhibiting stable singularities; a similar remark holds for the minor axis rays and minor axis focal rays. The presence of the caustic itself is a fingerprint of regularity of the ray.

Futhermore it is likely that the precise values of the parameters of the configuration influence the structure of the caustics. For strongly deformed pear-shaped stars ($\beta \sim 0.2$) we find that the caustic of the surface rays tends to develop two additional singular points off the polar axis; the chaotic ray pattern then shows a high concentration of rays in the neighbourhood of those points.

The above presented classification of the families of acoustic rays in a pear-shaped star, although more refined than the preliminary classification given in *Perdang* (1987), should therefore be considered as a tentative and incomplete one. In particular a closer examination of the different shapes of the caustics is needed, since, as will be indicated below, the nature of the configuration of the caustics influences the asymptotic oscillation frequencies.

The definition of the different families of rays implies that the families F(LDR), F(SFR), and F(MFR) are produced from initial conditions in 1-dimensional sets of the 2-dimensional space of initial conditions (5.6); therefore these families are of measure zero among the totality of rays; the families F(MAR) and F(SR), as well as the family of chaotic rays, F(CR), have 2-dimensional sets of initial conditions in the space of initial conditions (5.6). Randomly selected initial conditions in the space (5.6) thus generate surface rays, minor axis rays, or chaotic rays with probability 1; LDR, SFR and MFR have probability 0.

The closure of the SR or the MAR obeys

$$\begin{aligned} cl\ F(\mathrm{SR}) &= F(\mathrm{SR}) \cup F(\mathrm{SFR}) \cup F(\mathrm{LDR}) \quad , \\ cl\ F(\mathrm{MAR}) &= F(\mathrm{MAR}) \cup F(\mathrm{MFR}) \cup F(\mathrm{LDR}) \quad , \\ cl\ F(\mathrm{CR}) &= F(\mathrm{CR}) \cup F(\mathrm{SFR}) \cup F(\mathrm{MFR}) \cup F(\mathrm{LDR}) \, , \end{aligned} \tag{5.14}$$

so that

$$\begin{aligned} F(\mathrm{SFR}) \cup F(\mathrm{LDR}) &= cl\ F(\mathrm{SR}) \setminus F(\mathrm{SR}) \equiv \partial\ F(\mathrm{SR}) \, , \\ F(\mathrm{MFR}) \cup F(\mathrm{LDR}) &= cl\ F(\mathrm{MAR}) \setminus F(\mathrm{MAR}) \equiv \partial\ F(\mathrm{MAR}) \, , \\ F(\mathrm{SFR}) \cup F(\mathrm{MFR}) \cup F(\mathrm{LDR}) &= cl\ F(\mathrm{CR}) \setminus F(\mathrm{CR}) \equiv \partial\ F(\mathrm{CR}) \, ; \end{aligned} \tag{5.14a}$$

or alternatively

$$\begin{aligned} F(\mathrm{SFR}) \cup F(\mathrm{LDR}) &= cl\ F(\mathrm{SR}) \cap cl\ F(\mathrm{CR}) \quad , \\ F(\mathrm{MFR}) \cup F(\mathrm{LDR}) &= cl\ F(\mathrm{MAR}) \cap cl\ F(\mathrm{CR}) \quad . \end{aligned} \tag{5.14b}$$

As the cubic deformation parameter λ_3 vanishes we notice that the chaotic rays collapse onto the focal rays of the ellipsoidal configuration, the surface rays, minor axis rays and longest diameter rays deform into surface rays, or more precisely

$$\lambda_3 \to 0: \quad F(\mathrm{CR}) \cup F(\mathrm{SFR}) \cup F(\mathrm{MFR}) \to F(\mathrm{FR}) \ ,$$
$$F(\mathrm{LDR}) \to F(\mathrm{LDR}) \ ,$$
$$F(\mathrm{MAR}) \to F(\mathrm{MAR}) \ ,$$
$$F(\mathrm{SR}) \to F(\mathrm{SR}) \ . \qquad (5.15)$$

Conversely, the breaking of the ellipsoidal symmetry by a pear-shaped distortion unfolds the degenerate focal rays into chaotic rays together with their derived set. Since the focal rays form the 'boundary' between two distinct classes of regular rays, namely the SR and MAR, it should not come as a surprise that the 'explosion' of the latter under a change of a parameter of the star, leads to chaos; this kind of unfolding of a frontier between two families of regular orbits is in fact a traditional route to chaos in Hamiltonian systems. The classical illustration is the occurrence of chaos on the separatrix between the family of oscillatory motions and the rotations of the pendulum, when the latter is perturbed by a plane wave (*cf. Chernikov et al.* 1987).

Finally, the combination of relations (5.15) and (5.12) demonstrates that the *chaotic rays arise as the unfolding of the singular radial rays of the sphere*, the degeneracy being lifted by the terms of third degree ($\lambda_3 \neq 0$) of the deformation of the sphere. As we shall see, this observation is relevant for the location of quantum chaos in the oscillation spectrum of a pear-shaped star.

Before we bring this section on the numerical investigation of the rays to a close we wish to emphasise the following further points.

(1) We have discussed only deformed stellar models of $C_{\infty v}$ symmetry which therefore admit of *planar* ray systems in the physical configuration space. In addition to the latter these models also admit of *3-dimensional rays* which remain entirely to be investigated, the only information on these rays we have at the moment is that the axial symmetry implies the existence of a second integral.

(2) Our restriction to the $C_{\infty v}$ symmetry implies a mirror symmetry in the plane Π of the rays, with respect to the NS axis; this symmetry in turn secures the existence of a singular ray of one degree of freedom, namely the longest diameter ray. It has been argued on the basis of numerical experiments that 2-dimensional billiards lacking this mirror symmetry present a behaviour differing significantly from the behaviour of symmetric billiards (*Hayli* and *Dumont* 1986). Since ray propagation shares many geometric properties of its ray patterns with the patterns of billiard orbits, we expect that our problem develops likewise a more complicated type of behaviour under a symmetry breaking destroying the reflection axis. In fact, we can present a general intuitive argument in favour of the appearance of a further class of orbits: On the one hand the LDR is unstable , and this orbit is degenerate; on the other hand a slight generic symmetry breaking lifts the degeneracy of this orbit; the latter then 'explodes' into a family of orbits filling a certain volume of phase space; since

the LDR belongs to the frontier of two distinct regular families of rays, namely the surface and minor axis rays, the breaking up is again likely to produce a chaotic class of rays; furthermore, since the LDR also belongs to the derived set of the chaotic ray family, unfolding the degeneracy may produce a chaotic family prolongating the CR family we have traced above.

(3) For arbitrary convex surfaces of constant sound speed we have no geometric symmetry, so that all ray families are 3-dimensional ($f=3$). Generically the ray equations then admit of no integral besides the frequency integral $\Omega(\mathbf{r},\mathbf{k}) = \text{constant}$. The chaotic region $\mathbf{K}$ in the phase space Γ is then connected, forming what has been called a stochastic web (*Chernikov et al.* 1987); any chaotic ray diffuses all through the phase space. It is so far unknown whether this 'Arnold diffusion' manifests itself on the structure of the asymptotic frequency spectrum.

6. The nonstandard asymptotic wave equation

The above chapters were concerned with the 'classical' approximation to the wave equation. We shall now analyse how these ray properties materialise in the *asymptotic spectrum* of eigenvalues. A precise definition of what we mean by 'asymptotics' will be presented below.

Suppose we have at our disposal an ideal computer (or a measuring device) capable of solving the frequencies of the full standing wave equation (respectively capable of recording the frequencies) of oscillations of stars of arbitrary symmetry. Even though ideal, such a computer will be able to deal with numbers in some range only. The computer can find only those eigenfrequencies whose numerical values, when expressed in a given system of units, obey

$$\omega \in A \quad \text{with} \quad A = \{\omega | \mu < |\omega| < M\} \subset X \quad , \tag{6.1}$$

where μ and M are positive numbers of a given class X (for instance the rationals, or the reals, or the complex numbers); the set of 'accessibility' A is a subset of the number set X; the latter may be called the 'enlargement' of the set A. Typically, the 'resolution' of the computer, μ, is of the order of $1/M$.

Although capable of operating *precisely* with numbers of A alone, the computer can deal with numbers of the 'enlargement' of the set A , according to the following prescriptions: (1) A frequency less than μ appears as 'infinitesimal' to the computer, and is actually set equal to zero in the computations. (2) Two frequencies which differ by less than the resolution μ are regarded as equal by the computer. (3) A frequency exceeding M plays the part of an 'infinite' number, and is actually treated as such in the calculations (its inverse is set zero *etc.*).

As is known from the spherically symmetric case, the spectrum of the acoustic eigenfrequencies of a star is unbounded, and this property holds also for the case of stars lacking the spherical symmetry. Accordingly, the limitation (6.1) of the computer seemingly entails that most of the acoustic spectrum – and in fact almost all of it – will remain numerically inaccessible.

The relevant point is that by resorting to adequate *scalings* ($S(\rho)$) and *translations* ($T(\tau)$) of the frequencies.

$$S(\rho): \quad \omega \mapsto \rho\omega \quad , \tag{6.2}$$

$$T(\tau): \quad \omega \mapsto \omega + \tau \quad ,$$

ρ and τ being arbitrary positive numbers of X, *i.e.* not constrained to lie in the range (6.1), we can manifestly transform *any* set of frequencies not inside the range of accessibility into a set of frequencies belonging to this range. The scaling may produce an unwanted side effect; it may generate an overcrowding of the frequencies such as to have a spacing between successive discrete frequencies less than the computer resolution μ; the rescaled spectrum then appears to be continuous. The actual discreteness of the spectrum can however be restored by using a second magnifying scaling.

These remarks are meant to make it clear that through successive transformations (6.2) of the spectral equations we can investigate the eigenfrequencies indirectly, in any (arbitrarily large, or small) range of the frequency axis.

The mathematical framework capable of formalising and generalising the above ideas is provided by *nonstandard analysis*. We regard as the counterpart of the 'set of accessibility' A (eq. (6.1)) a set of real numbers R, more specifically called here the set of *standard reals*. The analogue of the 'enlargement' of the latter, denoted by *R, is referred to as the set of *nonstandard reals*. The (undefined) predicates 'standard' and 'nonstandard' are specified by 3 axioms due to *Nelson* (1977; *cf.* the short text by *Robert* 1985 for a simple introduction to Nelson's theory). For our purposes we shall make explicit use of two of them which will be stated informally.

(1) Given a set of numbers x obeying an 'internal' relation R with free variables (parameters), then there exists at least one number $^*x$ satisfying relation R, and in addition possessing certain attributes of Leibniz's infinite (or infinitesimal) numbers. By 'internal' we mean that the relation itself does not involve the labels 'standard' or 'nonstandard'; by 'free variables' in the relation it is understood that the relation itself does not contain quantifiers (for instance $R(x)$ is not allowed to stand for '*there is* an x such that $x > 100$', but it may stand for '$x > 100$'). We refer to this statement as the principle or *Axiom of Idealisation*. The set of all numbers x and $^*x$ is a nonstandard set *B.

(2) If a given 'internal' relation R with free variables x and t, t', ... , $t^{(n)}$ holds for 'standard' values of the variables, then it holds also for any value of the variable x. This is known as the principle or *Axiom of Transfer*. We illustrate the latter principle by an example. If x and t are conventional (standard) reals, then for any such pair we have the relation ($x<t$ or $x=t$ or $x>t$); in this form this relation transfers to *any* real $^*x$, *i.e.* any element of the set of nonstandard reals *R, with t remaining however standard, or ($^*x<t$ or $^*x=t$ or $^*x>t$). On the other hand, consider the conventional relation 'any conventional (standard) real x is finite, F(x)'; the relation F(x) is here an abbreviation for the explicit relation ($\exists$ t, t finite) ($x<t$); the variable t is not free here, therefore the relation cannot be transferred to the nonstandard reals.

The enlargement of the set of integers Z (the standard integers), *Z (the nonstandard integers), contains in fact, besides all the finite integers 0, ± 1, ± 2, ..., $\pm n$, $\pm (n+1)$, also a new class of integers $\pm {}^*J$, $\pm(^*J+1)$, ... , $^*J$ being one representative of the integers not in Z; such an integer is referred to as an 'infinite' integer. The existence of at least one such integer is secured by the principle of idealisation. The transfer principle then enables us to conclude that if $^*J \in {}^*Z$ then $\pm(^*J+1) \in {}^*Z$, since the counterpart of this relation exists in the standard set Z; continuing in this fashion one sees that there is an infinity of infinite integers. The enlargement of the set of reals R, the nonstandard reals *R, contains, by successive applications of the transfer principle, all of the infinite integers, as well as numbers of the form $\pm(a(^*J)^b + c)$, where a and b are arbitrary conventional reals; if $b>0$ these numbers are called 'infinite' reals (*L); if a is standard, $b<0$, and $c=0$, they are 'infinitesimal' numbers ($^*\varepsilon$).

As a final tool from nonstandard analysis we need the operation of extracting the standard component – if it exists – out of a nonstandard element. This *standard part*, or shadow, of a nonstandard element $^*x$ of the enlargement *X of a standard set X is the element $x \in$ X 'closest' to $^*x$; the latter requirement implies that we have endowed the set X with a distance. For instance, if $^*x$ is a nonstandard finite real, we can always decompose the latter in the form

$$^*x = x + {}^*\varepsilon \quad , \tag{6.3}$$

where $^*\varepsilon$ is an infinitesimal, and x a standard real; then

$$st(^*x) = x \quad , \tag{6.3a}$$

the natural distance between two reals (standard or nonstandard) x,y being the absolute value $|x-y|$.

We have explicitly mentioned so far only nonstandard sets of numbers. Nonstandard functions, manifolds *etc.* can then be introduced in a natural way. We shall

make a free use of these concepts for our investigation of the spectrum of the acoustic wave equation.

In our physical context the operation 'standard part' formalises the procedure of 'neglecting higher orders'; 'infinitesimals' model those contributions which are 'small', and which, at the same stage, will be discarded; 'infinites' represent what we mean in physical problems by 'large quantities' *cf. Harthong* 1981). The nonstandard setting thus offers a clean and systematic framework for dealing with what is known as 'asymptotics' in physical problems.

Consider the complete linearised adiabatic oscillation eigenvalue equations for a star of arbitrary symmetry, in the form of the linearised equation of continuity, the linearised equation of momentum, the gravitational field equation, and the constraint of adiabaticity. We are then dealing with a system of partial differential equations in space, involving as the highest space derivatives the Laplacian. We regard these equations as nonstandard equations defined over nonstandard configuration space *V (the nonstandard volume of the star) of (nonstandard) coordinates **r** ; the eigenfunctions themselves are thereby turned into nonstandard functions.

Without loss the latter will be represented in the following form

$$*\mathbf{O}(\mathbf{r}) = *\mathbf{A}(\mathbf{r}) \exp[i\ *\mathrm{L}\ \mathrm{S}'(\mathbf{r})] \quad , \tag{6.4}$$

with

$$*\mathbf{A}(\mathbf{r}) = *\mathbf{P}(\mathbf{r}) \exp[i\ *\Theta(\mathbf{r})] \quad ; \tag{6.4a}$$

all functions in this representation are nonstandard.

The starred parameter *L will now be set equal to an infinite positive real; this enables us to capture the spectrum of the asymptotic *i.e. infinite eigenvalues* of the acoustic spectrum. In fact, since we do know that the spectrum of the conventional acoustic frequencies is unbounded, the nonstandard spectrum of the nonstandard extension of the eigenvalue problem must contain infinite eigenvalues (idealisation).

The complex ansatz for the eigenfunction (6.4, 4a) singles out a pseudo amplitude factor, *A(**r**), and a phase factor *L S'(**r**). The pseudo amplitude itself is represented again in the form of a true amplitude (*P(**r**) real and nonnegative) and an extra phase *Θ(**r**). This representation is chosen by analogy with conventional asymptotic theory. The presence of the infinite factor *L causes the phase to oscillate infinitely rapidly over any finite length, while the function S'(**r**) is varying smoothly. Likewise the pseudo amplitude *A (**r**) changes smoothly over finite lengths, with the exception of the crossings of a critical region *U, where different kinds of accident may happen: On the one hand *A(**r**) may become *infinitesimal* and go through zero, changing its sign; this is taken care of by an extra phase shift of $(-\pi)$ introduced by *Θ(**r**). Or *A(**r**) may take on *infinite* values, again in general with an accompanying change of phase described by *Θ(**r**). Or finally, at the surface, where the wave suffers

a reflection, the function $^*\mathbf{A}(\mathbf{r})$ may undergo a phase shift. The extra phase factor $^*\Theta(\mathbf{r})$ thus enters in our representation to handle the explicitly nonstandard behaviour of the pseudo amplitude; by construction $^*\Theta(\mathbf{r})$ is constant over the remainder of the star $^*V \setminus {}^*U$.

Ideally the critical region $^*U$ should be found by fully solving tha eigenvalue problem without directly using the ansatz (6.4); $^*U$ is then the set of values $\mathbf{r} \in {}^*V$ over which the eigenfunction $^*\mathbf{O}(\mathbf{r})$ becomes infinitesimal or infinite when it is oscillating infinitely rapidly in space; the measure of infinity is fixed by the arbitrary parameter $^*L$. As a rule, and in all cases we are interested in, this definition implies that the surface of the star is included in $^*U$. In practice, of course, the search for $^*U$ has to be carried out by some approximation procedure. (For instance, by substituting the ansatz (6.4) into the wave equation and ordering the latter with respect to decreasing power in $^*L$, the solution for $^*\mathbf{A}(\mathbf{r})$ in the leading order shows that this amplitude diverges over certain regions – which turn out in fact to be the classical caustics – or at the singular points of the partial differential equations, such as at the surface of the star). It transpires from our very definition of the set $^*U$ that with $^*L$ infinite, this region has an infinitesimal 'thickness' $\propto (^*L)^{-b}$, b some positive number; therefore, although its topological dimension is equal to the dimension of the configuration space $^*V$ (f in our previous notation), the standard part $U = st(^*U)$ acquires a lower dimension – physically, because it coincides with the caustics and regions of singularities. If $f = 3$, the dimension of U will typically be 2. This implies that st $(^*\Theta(\mathbf{r}))$ changes in fact discontinuously as the wavefunction crosses U, while it takes on constant values in the standard region $V \setminus U$.

If we substitute ansatz (6.4) into the partial differential equations, we notice that any operation with $\partial/\partial\mathbf{r}$ on the eigenfunction produces a term proportional to $^*L$. The system thus takes the form

$$(^*L)^2 c(\mathbf{r})^2 |\mathbf{k}'|^2 {}^*\mathbf{O}(\mathbf{r}) + \ldots = (^*\omega)^2 \, {}^*\mathbf{O}(\mathbf{r}) + \ldots \,, \tag{6.5}$$

where the terms not explicited are of 'orders' $(^*L)$ or $(^*L)^0 = 1$, or $^*\omega$; $c(\mathbf{r})$ is the sound speed as above, and $\mathbf{k}'$ is defined as

$$^*L \, \mathbf{k}' = {}^*L \, \partial/\partial\mathbf{r} \, S'(\mathbf{r}) \equiv \partial/\partial\mathbf{r} \, S(\mathbf{r}) = \mathbf{k} \quad ; \tag{6.6}$$

a comparison with equations (2.7,9) shows that $\mathbf{k}'$ appears as a rescaled wavevector; $S'(\mathbf{r})$ in turn is interpreted as a rescaled Hamiltonian-Jacobi action function.

Let now $^*\omega_{ref} = {}^*L \, \omega_0$ be a reference *infinite eigenvalue*, ω_0 being a finite real frequency; we shall identify the latter with the fundamental acoustic frequency of the star. If we then divide equation (6.5) by $(^*L)^2$ and take the standard part, we are left with the equation

$$c(\mathbf{r})^2 |\mathbf{k}'|^2 \mathbf{O}(\mathbf{r}) = \sigma^2 \mathbf{O}(\mathbf{r}) \quad \text{in } V \setminus U \tag{6.7}$$

for **r** ranging over the standard part of the configuration space of the star, from which we exclude the standard part of the exceptional 'surface' U; the latter will require a special treatment.

All factors entering equation (6.7) are standard. We use the notation **O(r)** for $st(^*\mathbf{O}(\mathbf{r}))$. The parameter σ is defined as

$$\sigma = st\ (^*\omega\ /^*\omega_{ref}) \tag{6.8}$$

i.e. it represents the infinite eigenvalues of the spectrum, rescaled so as to become accessible to numerical calculations; we refer to this spectrum of eigenvalues σ as the *rescaled spectrum*. The (nonstandard) eigenfrequencies themselves near the reference frequency $^*\omega_{ref}$ will be labelled.

$$\ldots \leq \ldots \leq {}^*\omega_{ref-1} \leq {}^*\omega_{ref} \leq {}^*\omega_{ref+1} \leq {}^*\omega_{ref+2} \leq \ldots \leq {}^*\omega_{ref+q} \leq \ldots \tag{6.9}$$

The relative ordering parameter q (integer) with respect to the reference eigenvalue will be used as the identification label of the rescaled spectrum, whose eigenvalues will be denoted by σ_q.

It is known that the density function of the acoustic spectrum, $g(\omega)$ (number of frequencies per unit frequency interval) is a power law of the frequency ω for large enough frequencies (*Perdang* 1982), which we may write

$$g(\omega) = (g_0/\omega_0)(\omega/\omega_0)^{D-1} \quad ; \tag{6.10}$$

here g_0 is a dimensionless parameter (of order of magnitude 1), and D a numerical parameter which can be interpreted as a fractal spectral dimension; in a fictitious star in which the sound speed nowhere vanishes, D is equal to the dimension of the configuration space (D = 3); for conventional stellar models with vanishing surface sound speed D is close to 4.5 . The transfer principle enables us to extend this relation to the nonstandard infinite eigenvalues. From this relation it follows that the average (nonstandard) spacing between eigenvalues near the eigenvalue $^*\omega$ is

$$^*\Delta\omega \sim \omega_0(\omega_0/{}^*\omega)^{D-1} \quad , \tag{6.10a}$$

showing that this spacing is infinitesimal. Accordingly the standard part of the average spacing of the rescaled spectrum (6.8) vanishes, or the rescaled spectrum appears as a *continuum*, of density described by the formula (6.10). In order to preserve information on the actual discrete character of the infinite eigenvalues, we introduce a renormalised spacing parametrically depending on a standard coefficient d, as follows

$$s_d(q,ref) = st\ [(^*\omega_{ref})^d(\omega_{ref+q} - \omega_{ref})] \ , \quad 0 \leq d \leq D-1 \ . \tag{6.11}$$

We shall refer to this standard function as the *d-spacing function*. The interest of this measure of the spacing is that it enables us to pick those families of modes which have nonstandard spacings of order $^*\omega_{ref}^d$; families with spacings 'substan-

tially smaller' than ${}^*\omega_{\text{ref}}{}^d$ *i.e.* of the form ${}^*\omega_{\text{ref}}{}^{d-a}$, a a positive finite real, have infinitesimal renormalised spacings whose standard part is then zero; those whose spacings are of the form ${}^*\omega_{\text{ref}}{}^{d+a}$ have infinite renormalised spacings, and their standard part ceases to exist.

We next observe that if we introduce the ansatz (6.4) into the simple wave equation (2.7) interpreted as a nonstandard equation, and if we carry out the same manipulations as above, we again end up with the same standard equation (6.7).

This coincidence leads us to define the *asymptotic form* of the nonstandard acoustic oscillation eigenvalue equation as the analytically *simplest form* of the partial differential eigenvalue problem producing the rescaled spectrum of eigenvalues as well as the O-spacing function of the true acoustic eigenvalue problem. Barring contrived situations, we notice that this simplest form is generated by throwing away all but the highest space and time derivatives of the original wave equation in our case, the relevant asymptotic form of our acoustic equations is then equation (2.7) (to be regarded as nonstandard).

A word of physical justification of our admittedly lengthy procedure of introducing the 'asymptotic form' associated with our starting eigenvalue problem is in order. The actual spectrum of the acoustic eigenvalue problem is soiled by numerous physical phenomena, such as for instance the interaction with gravity modes, the effect of gravitational field fluctuations etc. This physical 'pollution' creates a local disorder in the structure of the spectrum, causing the spacings of the eigenvalues to vary nonsmoothly. As we proceed to larger acoustic eigenvalues, however, this local disorder becomes progressively less important. The interest of the nonstandard formulation is that in the range of the infinite eigenvalues the physical contamination is *practically* sifted out; the corrections due to the latter become infinitesimal, requiring for their examination an analysis of the d-spacing functions, with $d \geq 1$. The virtue of the introduction of the asymptotic form of the acoustic eigenvalue equations is that the latter *fully* eliminates the pollution effects at the outset.

As we shall demonstrate, this does not preclude the existence of disorder in the spectrum of the asymptotic form of the eigenvalue problem. Irregularities which reach into this asymptotic spectrum are more fundamental than the physical contamination effects; they are irreducibly linked to the geometrical nature of the partial differential equation. They conceal therefore information on the geometry of the stellar structure.

I believe that the approach outlined here for the study of the acoustic eigenvalue problem eliminates the kind of ambiguities surrounding the concept of quantum chaos as encountered in quantum chemistry. Various authors have indeed interpreted mere pollution effects as the signature of quantum chaos in the low-lying energy levels of various quantum mechanical systems.

7. Integrable and nonintegrable wave equations. Stellar quantum regularity and chaos

We shall analyse in this section the distribution of the asymptotic, *i.e.* infinite, eigenvalues of the *asymptotic* form of the acoustic eigenvalue problem. The latter will be said to be integrable or nonintegrable, depending on whether the associated Hamiltonian ray problem (eqs. (2.9, 11, 12)) is integrable or nonintegrable. There will be no difficulty in regarding the latter as a nonstandard Hamiltonian system.

(A) We consider first the integrable case.

By virtue of the denseness of the periodic tori in the phase space, arbitrarily close to any point of the (nonstandard) phase space $^*\Gamma$ there exists a closed nonstandard orbit $^*\mathbf{C}$ of our Hamiltonian ray equations, carried by a (nonstandard) f-dimensional torus $^*T^f$. Let $^*\Phi(\mathbf{r})$ be a stationary wave function defined along the projection $^*C$ of the path $^*\mathbf{C}$, onto the extended nonstandard configuration space. If $\mathbf{r}_0$ is an initial point of $^*C$, and if we describe the path $^*C$ in the direction $\mathbf{k}_0$, back to the initial point $\mathbf{r}_0$ then the hypothesis of stationarity of the wavefunction implies that the total change of phase of the latter is an integer multiple of 2π. Using the decomposition of the actual path into irreducible circuits of the torus (eq. (3.18)), the latter requirement amounts to the condition

$$\Delta^*\Theta + {}^*\mathrm{L}\ \Delta\mathrm{S}' = n_i\ 2\pi\ ,\ i = 1, 2, \ldots, \mathrm{f} \quad . \tag{7.1}$$

where n_i is an infinite integer, and $\Delta^*\Theta$ and $^*\mathrm{L}\ \Delta\mathrm{S}'$ are the changes of the two phase factors entering the wave function (6.4) as we follow the irreducible (nonstandard) circuit $^*C_i$. The change in S' is given by

$$\Delta\mathrm{S}' = \int_{^*C_i} \mathrm{dS}' = \int_{^*C_i} \mathbf{dr}\ \partial/\mathbf{dr}\ \mathrm{S}'(\mathbf{r}) = \int_{^*C_i} \mathbf{dr}\ \mathbf{k}' \tag{7.2}$$

with the notations of (6.6). But the latter expression is given, up to the factor $^*\mathrm{L}$, by equation (3.17), so that it is measured by an action J_i . The change in the extra phase factor $\Delta^*\Theta$ is just equal to the algebraic sum of the different changes this phase suffers at the passages of $^*C_i$, through the critical set $^*\mathrm{U}$. The change of $\Delta^*\Theta$ at an individual crossing c of $^*\mathrm{U}$ is denoted by $(\pi/2)\ ^*\mu_{ci}$; in the standard limit when U collapses to a surface, the factor μ is known in the literature as the *Maslov index* of the critical point (the intersection of the standard sets U and C_i being a point), the latter is a topological parameter (defined modulo 4), whose explicit computation on classical cautics is described in *Maslov* (1972; *cf.* also *Arnold* 1978). Denoting by $^*\mu_i$ the algebraic sum of the indices $^*\mu_{ci}$ over all crossing points of the circuit $^*C_i$, we finally see that the total phase change (7.1) of a stationary wave yields

$$\mathrm{J}_i \equiv \mathrm{J}_i(n_i) = n_i + (1/4)^*\mu_i \quad , i = 1, 2, \ldots, \mathrm{f} \quad . \tag{7.3}$$

Simple direct rules for estimating the standard value μ_{ci} on caustics and foci are given by *Keller* (1958); a procedure for reading off the resulting sum μ_i from the

pictures of classical Hamiltonian orbits in the configuration space, has been proposed in the chemical literature (*cf. Noid et al.* 1979).

The stationarity condition of the wavefunction then amounts to single out, among the continuum of tori, J_i = arbitrary constants, $i = 1, 2, \ldots, f$, a discrete subset, defined by the actions (7.3). The integers

$$\mathbf{n} = (n_1, n_2, \ldots, n_f) \tag{7.4}$$

are the *quantum numbers* specifying the stationary state. In the context of our treatment *L is infinite, so that these numbers are *infinite* integers.

Recall now that integrable Hamiltonian when expressed in the angle-action variables depends on the actions alone (*cf.* eqs. (2.11), (3.3)). Therefore, from equations (7.3) we see the allowed frequencies of the asymptotic eigenvalue equation are given by

$$^*\omega(\mathbf{n}) = F(J_1(n_1), J_2(n_2)), \ldots, J_f(n_f)) \equiv F(\mathbf{J}(\mathbf{n})) \quad . \tag{7.5}$$

Since the value of $\mathbf{J}(\mathbf{n})$ (eq. (7.3)) depends on the encounters of the rays with the caustics, through the Maslov indices, it is important to have at our disposal a full survey of the structure of the caustics. Moreover, since different ray families have in general caustics of different structures, the Maslov corrections are different for the frequencies attached to different ray families. We may state therefore that each ray family has associated with it an asymptotic spectral branch. Or *in the presence of p families of rays there are p asymptotic spectral branches.*

Since by assumption the Hamiltonian is a smooth function of the actions, we may expand the latter expression with respect to the actions in the neighbourhood of a reference set of eigenvalues, $\mathbf{n}_{\mathrm{ref}}$. The *rescaled spectrum* (6.8) then becomes

$$\sigma = st\ (\omega(\mathbf{n})/\omega(\mathbf{n}_{\mathrm{ref}}))$$

$$= 1 + \mathbf{A}\,\mathbf{x} = 1 + A_1 x_1 + A_2 x_2 + \ldots + A_f x_f \quad , \tag{7.6}$$

with

$$A_i = st\ [\partial/\partial J_i\ F(\mathbf{J})]_{\mathbf{J}=\mathbf{J}(\mathbf{n}_{\mathrm{ref}})} \quad , \tag{7.6a}$$

$$x_i = st\ [(n_i - n_{i\mathrm{ref}}) / {}^*\omega(\mathbf{n}_{\mathrm{ref}})] \quad . \tag{7.6b}$$

These expressions show that in the space of the normalised quantum numbers x_i and close to the origin $x_i = 0$, the rescaled eigenvalues define a *plane*. The values of the coordinates x_i themselves are continuous.

Alternatively, we can construct the *O-spacing function* (6.11)

$$S_O(\Delta\mathbf{n}, \mathbf{n}_{\mathrm{ref}}) = st\ [{}^*\omega(\mathbf{n}_{\mathrm{ref}} + \Delta\mathbf{n}) - {}^*\omega(\mathbf{n}_{\mathrm{ref}})]$$

$$= \mathbf{A}\Delta\mathbf{n} \quad , \tag{7.7}$$

with

$$\Delta \mathbf{n} = st\ (\mathbf{n} - \mathbf{n}_{\mathrm{ref}}) \quad . \tag{7.7a}$$

The latter expression requires that the differences between the quantum numbers $\mathbf{n}$ and $\mathbf{n}_{\mathrm{ref}}$, must be finite, even though the quantum numbers themselves are infinite integers. This spacing function shows that the eigenvalues are evenly spaced in each of the quantum numbers (in the neighbourhood of the reference quantum numbers). Or in other words, a magnification by the infinite factor ${}^*\omega(\mathbf{n}_{\mathrm{ref}})$ of the plane (7.6) continuously filled with eigenfrequencies actually resolves the latter *into a discrete regular planar lattice* of eigenfrequencies in a small region around the origin. No dislocations in this crystal-like structure are permitted. The 'physical impurities' of the complete wave equation can create 'dislocations' – *i.e.* localised accidents in the spacings – among the low lying levels only. If we fix all but one of the quantum numbers and let the remaining one vary near its reference value, then the (f–1)-parameter family of eigenvalues so defined is evenly spaced in the free quantum number.

The above treatment demonstrates that the asymptotic frequencies of integrable acoustic ray equations are not properties of individual rays; they are attributes of the ray carrying tori.

The general result we have obtained can be summarised as follows. In the integrable case, *all* infinite *i.e.* asymptotic eigenvalues are locally evenly spaced in all of their f quantum numbers. We shall refer to this characteristic feature as the *regular spacing* property. A collection of asymptotic eigenvalues obeying the regular spacing property is called *quantum regular.* Accordingly, the whole asymptotic spectrum of an integrable acoustic wave problem is quantum regular.

(B) Consider next a nonintegrable wave equation.

Just as for the acoustic ray propagation, we distinguish between two cases.

(a) In the *regular region* ${}^*\mathbf{R}$, which in general will be made up of disconnected parts of the phase space ${}^*\Gamma$, we have, just as for an integrable Hamiltonian, a dense coverage by resonant tori. We can therefore repeat the above discussion of the phase of the wave function to determine the stationarity of the latter (eqs. (7.1)-(7.5)). The only difference with the latter case is that the infinite quantum numbers $\mathbf{n}$ are defined over certain ranges only, namely those ranges which through equation (7.3) do produce tori of the regular region.

Again, associated with each regular ray we have a distinct asymptotic spectral branch, so that the existence of ρ regular families of rays implies the existence of ρ asymptotic spectral branches. In general, the latter now differ not only in their Maslov correction factor, but also in the actual functional dependence $F(\mathbf{J})$, since the 'local' integrals $\mathbf{J}$ now change from one family to the other.

We have again rescaled spectra of the form (7.6) and O-spacings obeying (7.7). Therefore the asymptotic spectrum attached to the regular region of the phase space

satisfies the regular spacing property. Hence this asymptotic spectrum is *quantum regular.*

(b) In the chaotic region $^*\mathbf{K}$ of the phase space $^*\Gamma$ we have no surviving tori. Since we have seen that asymptotic frequencies appear as attributes of the orbit carrying tori, there may be some doubt as to whether there are any asymptotic frequencies at all related with the chaotic orbits.

The following argument shows that the existence of continuous families of tori is not required for the existence of asymptotic eigenfrequencies. The density formula (6.10), wich is independent of the geometry of the oscillating medium, recudes indeed to Jeans's classical result for wave equations with a space independent sound speed; under the latter circumstance D is equal to the topological dimension f of the configuration. Take in particular the two-dimensional oval configuration of *Benettin* and *Strelcyn* (1978; *cf.* also *Wojtkowski* 1986); this 'billiard' is known to be ergodic, *i.e.* it possesses no regular families of rays. But since the frequency density formula continues to hold, the existence of eigenfrequencies is guaranteed; obviously, the latter cannot be attached with families of tori.

It is natural to conjecture that these frequencies are in fact connected with 'exploded' tori, namely the sets M_k^{2f-r} (*cf.* Section 4) carrying the rays in the chaotic region. We can immediately make a general statement about the distribution of the asymptotic frequencies of the wave equation related to chaotic rays:

The collections of infinite frequencies attached with the chaotic region $^*\mathbf{K} \subset {}^*\Gamma$ *are not quantum regular.*

In fact, if these frequencies were regular, they could, by definition be represented locally as functions of f integers $\mathbf{n}$ satisfying the spacing formula (7.7) and playing therefore the parts of local quantum numbers; the latter in turn could then be used to define classical action parameters via an equation of type (7.3) , namely by setting $\mathbf{n} = \mathbf{J} +$ constant (the constant being actually irrelevant in the ray problem). But this means that we are locally able to introduce a Hamiltonian depending on actions alone, which implies in turn that we are in a regular region $^*\mathbf{R}$ of the phase space. This contradicts our starting hypothesis.

The characteristic feature of these sets of frequencies is that their spacings are *uneven* and disordered; the previous crystal-like lattice structure (7.7) has collapsed into the disordered structure of a liquid. A collection of frequencies, which is not quantum regular, will be called *quantum chaotic.*

It transpires from this analysis that the frequency ranges connected with the chaotic rays are then quantum chaotic.

To indicate more explicitly how the irregularity in the spacing of the frequencies comes about we consider the case of an associated ray problem with a single integral J. We then take account of the fact that the chaotic region $^*\mathbf{K}$ is densely

filled with closed rays (not carried by f-dimensional tori). Let $^*\mathbf{C}$, $^*\mathbf{C}'$, ... then be closed rays going through the neighbourhood of $(\pm\mathbf{r},\mathbf{k})$, and $^*C$, $^*C'$, ... their projections onto the configuration space. A wave concentrated around $^*C$ and represented by the ansatz (6.4) will be stationary, if the change of phase, as we go around $^*C$, is again a multiple of 2 . As above, this requires that the integral of the motion (action) J is the form (7.3)

$$J = J(n) = n + {}^*\mu/4 \quad , \tag{7.8}$$

where $^*\mu$ is again a measure of the phase shifts of the extra phase factor $^*\Theta$. If for $n = m$, the value $J(m)$ is associated with the closed orbit $^*C$, and for the next integer $n = m+1$ the action $J(m+1)$ is attached to the closed orbit $^*C'$, then these two orbits, as a consequence of the instability of the chaotic region $^*\mathbf{K}$, are *entirely different* and uncorrelated; as a consequence, there is no reason to expect the corresponding $^*\mu$ values to remain equal; the eigenfunction traverses different singularities as it follows uncorrelated paths.

The explicit form of equation (7.8) is therefore

$$J(n) = n + {}^*\mu(n)/4 \quad ; \tag{7.8a}$$

the precise value $^*\mu(n)$ is practically 'unpredictable' , in the same sense and for the same reason that we are unable to predict in the ray context which actual path in the chaotic region will be followed, given initial conditions with a limited accuracy.

This situation is drastically different from the situation arising in the regular region in the phase space; two sets of quantum numbers $\mathbf{n}'$ and $\mathbf{n}''$ which are close define two orbit carrying tori which are close as well; it is therefore always possible to select corresponding irreducible circuits on the two tori which are sufficiently close; the Maslov correction factors $^*\mu$ – being topological family indices – remain therefore the same over both orbits. They can differ only if we start with two tori belonging to two different families.

For a given initial condition $\mathbf{r}_o,\mathbf{k}_o$ in the chaotic region $^*\mathbf{K} \subset {}^*\mathbf{\Gamma}$ carry out the canonical transformation (4.3); let ϕ_o, $\underline{q}_o$, J_o, $\underline{p}_o$ be the initial conditions of the new canonical variables. Let $^*\mathbf{C}$ be a closed orbit through this point (or passing arbitrarily close to this point). By equations (4.4) and (7.8a) we obtain a branch of the frequency spectrum

$$^*\omega(n) = G(\underline{q}_o, \underline{p}_o, n + {}^*\mu(n)/4) \quad . \tag{7.9}$$

As already mentioned, for $f > 2$ the chaotic region is connected. Any classical solution diffuses all through the region. Equation (7.9) therefore covers the full spectrum attached to the chaotic rays.

For $f = 2$ the regular families divide the chaotic region into disjoint chaotic zones $^*M_1$, $^*M_2$, ... , $^*M_x$; each of the latter is covered by a generic solution. Under the latter alternative, there are x branches of the spectrum attached to the chaotic so-

lutions; branch b corresponds to the choice of an initial point in a chaotic zone ${}^*M_b$, $b = 1, 2, \ldots, x$.

The d-spacing function (6.11) becomes

$$S_d(\Delta n, n_{ref}) = st\{{}^*\omega(n_{ref})^d[{}^*\omega(\Delta n + n_{ref}) - {}^*\omega(n_{ref})]\} = A_d\ \Delta n + f(\Delta n) \quad , (7.10)$$

with

$$A_d = st\{G^d\ \partial/\partial J\ G\} \quad , \tag{7.11a}$$

$$\Delta n = st\ (n - n_{ref}) \quad , \tag{7.11b}$$

$$f(\Delta n) = (1/4)\ st\ \{G^d\ \partial/\partial J\ G\ [{}^*\mu(n_{ref} + \Delta n) - {}^*\mu(n_{ref})]\} \quad . \tag{7.11c}$$

In these expressions G and $\partial/\partial J\ G$ are to be computed at a reference orbit corresponding to the asymptotic value n_{ref} of the quantum number. The exponent d is to be selected such as to secure the existence of expression (7.11a). The local spacing is then composed of an even spacing, $A_d\ \Delta n$, plus the contribution $f(\Delta n)$ which according to our previous discussion depends erratically on the finite integer Δn.

As is seen from these considerations, a single global quantum number n survives for *any* quantum chaotic collection of frequencies. This quantum number may be interpreted as an (absolute) ordering parameter of frequencies (*cf.* eq. (6.9)). Besides, additional exact quantum numbers may exist; if the ray Hamiltonian admits of r ($< f$) independent integrals, the number of quantum numbers is seen to be equal to r. We may say then that quantum chaos is the result of an insufficient number of quantum numbers specifying the frequency eigenvalues.

In spite of the fact that we do not possess a complete set of quantum numbers to characterise the eigenvalues in the quantum chaotic ranges, it is always possible to attach a complete set of f *pseudo quantum numbers* **p** to the actual eigenvalues. To this end it suffices to regard the actual acoustic eigenvalue problem as a perturbation of an integrable eigenvalue problem. In the stellar context, the natural reference configuration is the spherically symmetric star, which is indeed integrable. Identify, *i.e.* label, the eigenfrequencies of the distorted configuration under consideration by the quantum numbers (n, l, m) of the spherically symmetric comparison star via some operationally well defined rule. A natural way of doing so is through a homotopic deformation of the spherical structure, S_{sph}, into the deformed structure, S_{def}. Schematically

$$S(\eta) = \eta S_{def} + (1-\eta) S_{sph}, \qquad \eta \in [0,1] \quad . \tag{7.12}$$

For η ranging from 0 to 1, $S(\eta)$ represents a fictitious structure which goes continuously from the spherical ($\eta = 0$) to the actual structure ($\eta = 1$).

If $\omega(\mathbf{p})$ denotes the spectrum of eigenvalues of the integrable configuration, S_{sph}, these eigenvalues being identified by their quantum numbers **p**, then we write the eigenvalues of the formal structures $S(\eta)$ as $\omega(\mathbf{p},\eta)$; regarded as a function of

η , the latter symbol is understood as a smooth function (of class $C^1[0,1]$) (with $\omega(\mathbf{p},\eta=0) \equiv \omega(\mathbf{p})$). The quantum numbers of the spherical star, **p**, then serve the purpose of labels, or pseudo quantum numbers **p** of the distorted star. Notice that the assignment of pseudo quantum numbers to a non integrable wave problem depends on the precise choice of the homotopy (7.12); two different homotopies may produce different identifications of the eigenvalues of the deformed structure by means of the same pseudo quantum numbers.

Our discussion implies that the quantum chaotic branches of the asymptotic spectrum cannot obey the regular spacing property in the pseudo quantum numbers **p**. The spacings are irregular in the space of the pseudo quantum numbers $\Delta\mathbf{p} = \mathbf{p} - \mathbf{p}_{\text{ref}}$.

The converse of this property, namely that an irregular spacing in one pseudo quantum number – at fixed remaining pseudo quantum numbers – implies quantum chaos, requires a few specifications. If the free pseudo quantum number mixes up several branches of regular frequencies, an apparent disorder in the frequency distribution may be created, due to a switch over from regular family to another. A careful examination of the regular branches of frequencies is therefore needed before one can draw a conclusion on the existence of quantum chaos from a limited spectral sample. Only in the case of a very extended series of frequency data is a frequency versus free pseudo quantum number plot sufficient to reveal the individual frequency families directly.

Provided that one exercises a sufficient amount of care, an examination of the spacing of the frequency eigenvalues as a function of one pseudo quantum number does enable one to differentiate between quantum regularity and quantum chaos.

8. A few illustrations

Although the above theoretical considerations refer to ideal infinite eigenvalues only – which are beyond our reach – the real practical interest of the conclusions drawn from our nonstandard formulation, is, as stressed by *Harthong* (1981), that the latter remain applicable *approximately* to finite, sufficiently large, acoustic eigenvalues.

For instance the property of *uniform spacing* of the infinite frequencies of a given regular family (7.7) then translates into a property of *smooth spacing* in the large quantum numbers; this means that a spacing in one free quantum number q can be represented as

$$\begin{aligned} S_0(\Delta q, q_{\text{ref}}) &= \omega(q_{\text{ref}} + \Delta q) - \omega(q_{\text{ref}}) \\ &= a_0 + a_1 \Delta q + a_2 \Delta q^2 + \ldots \ , \end{aligned} \tag{8.1}$$

where $q = q_{ref} + \Delta q$ is the free quantum number, the remaining f–1 quantum numbers being held constant; the coefficients a_0, a_1, a_2, ... depend on the large reference value of the free quantum number q, as well as on the fixed values of the remaining quantum numbers. We have sketched elsewhere a graphical method exploiting the Moiré effect to exhibit the smoothness of the spacing (*Perdang* 1984). The validity of a formula of type (8.1) secures in turn the existence of a conventional 'asymptotic expansion' of the families of frequencies in one (or more generally f) quantum number(s).

The property of *uneven spacing* of a given quantum chaotic family of finite frequencies translates into the statement

$$S_0(\Delta p, p_{ref}) = \omega(p_{ref} + \Delta p) - \omega(p_{ref}) \quad \text{nowhere smooth in } \Delta p \ , \tag{8.2}$$

$p = p_{ref} + \Delta p$ being a free large pseudo quantum number, the other f–1 pseudo quantum numbers being held fixed; an expansion in a power series in Δp is then not allowed at the reference value p_{ref} .

We shall briefly consider a few applications of the tests embodied in the statements (8.1) and (8.2) to theoretically computed acoustic solar models on the one hand, and observed solar modes on the other hand.

The acoustic modes of a conventional solar model of spherical symmetry computed by *Scuflaire et al.* (1981) have been analysed for regularity of their spacings in the regular quantum number n. This spectrum is theoretically known to be quantum regular, irrespective of the physical ingredients of the model.

We discuss here only the results for the family of fixed quantum number $l = 1$ and for n in the range 16 to 27, which are displayed in Figure 6 in the following form.

(a) A linear interpolation of the computed frequencies $\nu(n)$ produces the expression

$$\nu(n)_{int1} = 229.31 + 136.33\ n \quad (\mu Hz) \quad ; \tag{8.3}$$

the residuals

$$\Delta\nu_1(n) = \nu_{int1}(n) - \nu(n) \tag{8.3a}$$

are seen to distribute on a parabola (Fig. (6.a)).

(b) The quadratic interpolation yields

$$\nu_{int2}(n) = 302.85 + 129.31\ n + 0.16\ n^2 \quad (\mu Hz) \quad , \tag{8.3b}$$

and produces indeed residuals $\Delta\nu_2(n)$ which apparently are random fluctuations, of the order of $0.1\mu Hz$. It seems clear that these fluctuations just represent numerical noise. Interpolations by polynomials of higher degrees fail to remain consistent with the polynomials of degree 1 and 2, leading to expansion coefficients a_0 and a_1,

which differ completely from those of expressions (8.3, 8.3b); the corresponding residuals remain basically of the same order as the residuals $\Delta\nu_2(n)$.

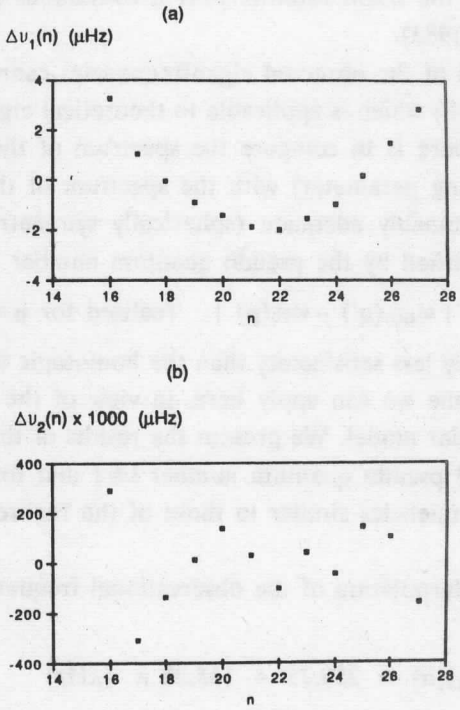

Fig. 6. Behaviour of a regular spectrum of acoustic modes: computed p modes of a conventional solar model at fixed spherical degree $l = 1$ and for radial orders $n = 16$–27 (*Scuflaire et al.* 1981); (a) residuals of a linear interpolation; (b) residuals of a quadratic interpolation.

Our experiment demonstrates how the presence of *noise* in the frequency spectrum, whether in the form of numerical errors or observational noise, manifests itself in an irregular spacing of the frequencies. We have argued elsewhere that noisy component might, in principle, be distinguished from an intrinsically irregular spacing (*Perdang* 1986).

We should of course keep in mind that the frequency range we are referring to must be regarded as a poor approximation to 'infinite' eigenvalues; it is surprising that in this range of low quantum numbers, where the frequencies might have been expected still to suffer contaminations by the complexities in the physics of the sun, the only obvious irregular effect is noise. The theoretical property of regularity of the infinite acoustic frequencies of spherical stellar models seemingly reaches down

into frequency range of relatively low radial quantum numbers n. In very simple models, such as the model of homogeneous density, it has been demonstrated to hold over the whole acoustic spectrum.

The same method has been applied to the analysis of the full disk solar oscillations as recorded by the SMM satellite over a continuous period of 280 days (*cf.* *Woodard* and *Hudson* 1983).

The identification of the observed eigenfrequencies cannot be made by the homotopic procedure (7.12) which is applicable to theoretical eigenvalue problems only. The method adopted here is to compare the spectrum of the observed frequencies $\omega_{obs(q)}$ (q, the ordering parameter) with the spectrum of the theoretical frequencies $\omega_{th}(\mathbf{p})$ of a presumably adequate (spherically symmetric) solar model. Then mode $\omega_{obs(q')}$ is identified by the pseudo quantum number $\mathbf{p}'$ provided that

$$\min_{[\mathbf{p}]} \mid \omega_{obs}(q') - \omega_{th}(\mathbf{p}) \mid \quad \text{realised for } \mathbf{p}=\mathbf{p}' \ . \tag{8.4}$$

While theoretically less satisfactory than the homotopic identification, this identification is the only one we can apply here, in view of the limited a priori information on the 'real' solar model. We present the results of the analysis of the family of frequencies of fixed pseudo quantum number $l=1$ and for n in the range 18 to 24, *i.e.* a branch of frequencies similar to those of the theoretical model mentioned above.

(a) The linear interpolation of the observational frequencies $\nu(n)$ leads to the expression

$$\nu_{int1}(n) = 259.75 + 135.20\ n \quad (\mu Hz) \quad ; \tag{8.5}$$

the residuals $\Delta\nu_1(n)$ are seen to deviate significantly from a parabola (Fig. 7a).

(b) The quadratic interpolation yields

$$\nu_{int2}(n) = 302.51 + 131.09n + 0.098\ n^2 \quad (\mu Hz) \quad , \tag{8.5a}$$

with residuals $\Delta\nu_2(n)$ which apparently show important fluctuations, of the order of several times $0.1\mu Hz$ at $n=19$ and $n=22$ (Fig. 7b); the standard deviation of the residuals is $0.21\mu Hz$; this value is significantly larger than the intrinsic precision of an individual frequency resulting from the finite run time of the observations ($\sim 0.05\mu Hz$).

According to our theoretical considerations of the previous section it is not impossible that the apparent disordered distribution of the residuals could be interpreted as quantum chaos, and therefore as the result of nonspherically symmetric effects in the equilibrium structure of the sun. But it cannot be ruled out either that the modes $n=19$ and $n=22$ belong to another regular branch. Both interpretations require a breaking of the conventional spherical symmetry ($\varepsilon \sim 10^{-5}$).

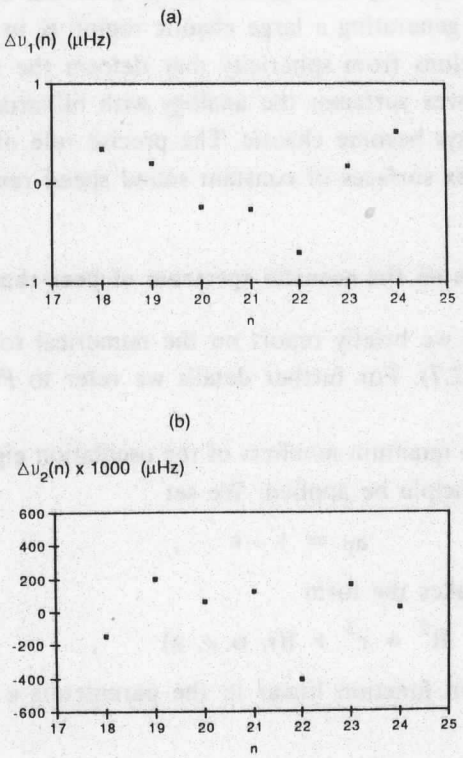

Fig. 7. Behaviour of the acoustic solar modes as observed by SMM satellite (*Woodard* and *Hudson* 1983); the modes plotted are identified as $l=1$ and $n=18$–24; (a) residuals of linear interpolation; (b) residuals of quadratic interpolation.

In principle, the latter may consist in large scale deformations of the surfaces of constant sound speed (for instance due to the solar rotation, and possibly an accompanying large scale circulation); we should keep in mind that even if the oblateness in the solar density distribution is estimated to be $<10^{-5}$ (*Gough* 1984) the temperature distribution, which enters more directly in the sound speed, might show a larger deviation from sphericity.

It does not seem likely, however, that this tiny geometrical effect can generate quantum chaos on an observable scale; our numerical experiments on ray propagation in globally deformed stars make it clear that ray chaos is produced over a significant range in the parameter space of initial condition only if the distortion of the star itself is large enough (ε and β of the order of 0.1); only then do we expect quantum chaos to arise over a noticeable fragment of the spectrum. Alternatively,

small deviations from spherical symmetry, such as the presence of a convection zone, could be responsible for generating a large chaotic region **K** in phase space.

In fact, local deviations from sphericity may deform the surfaces of constant sound speed into nonconvex surfaces; the analogy with billiards then suggests that the majority, if not all rays become chaotic. The precise role of ray propagation in the presence of nonconvex surfaces of constant sound speed remains to be studied.

9. Some numerical results on the acoustic spectrum of pear-shaped stars

In this final section we briefly report on the numerical solution of the acoustic eigenvalue problem (2.7). For further details we refer to *Perdang* and *Nejad* (1987).

To introduce pseudo quantum numbers of the oscillation eigenstates the following procedure can in principle be applied. We set

$$a_p = 1 - \varepsilon \quad , \tag{9.1}$$

so that equation (5.13) takes the form

$$R^2 = r^2 + f(r, \Theta, \varepsilon, \beta) \quad , \tag{9.2}$$

with $f(r, \Theta, \varepsilon, \beta)$ a known function linear in the parameters ε and β . Under the substitution

$$\varepsilon \to \eta\varepsilon \quad \text{and} \quad \beta \to \eta\beta \quad , \tag{9.3}$$

we therefore generate a relation defining a homotopy (7.2) in the form

$$R(\eta)^2 = r^2 + \eta f(r, \Theta, \varepsilon, \beta) \quad , \quad \eta \in [0,1] \quad . \tag{9.2a}$$

Pseudo quantum numbers for the eigenfrequencies of the pear-shaped configuration can then be introduced via this homotopy relation.

The method of solution proceeds as follows.

(a) For $\eta = 0$ the (spherically symmetric) eigenvalue problem can be solved analyticallly; the corresponding eigenvalues are

$$(\omega(\mathbf{p}))^2 \equiv (\omega(n, l, m))^2 = 4n(n + l + 1/2) \quad , \tag{9.4}$$

where $\mathbf{p} = (n, l, m)$ stands for the conventional quantum numbers of the sphere; the symmetry implies that these eigenvalues are m-independent and therefore $(2l + 1)$ times degenerate. Note that the density law (6.10) of this spectrum is characterised by a spectral dimension $D = 4.5$. We shall denote the eigenfunctions corresponding to the eigenvalues (9.4) by $\Phi_{\mathbf{p}}$. This set of eigenfunctions is complete.

(b) To study the deformed configurations ($\eta = 1$) we carry out the following mapping. We associate with the point P, of Cartesian coordinates (x_1, x_2, x_3) and spherical coordinates (r, Θ, ϕ) (eq. (5.3)) in the physical configuration space, a point

P' in a fictitious space, of Cartesian coordinates (x_1', x_2', x_3') and spherical coordinates (R, Θ', ϕ')

$$x_1' = R \cos \Theta' \quad ,$$
$$x_2' = R \sin \Theta' \sin \phi' \quad , \tag{9.5}$$
$$x_3' = R \sin \Theta' \cos \phi' \quad ,$$

with

$$\Theta' = \Theta \; ; \quad \phi' = \phi; \quad R = R(r, \Theta, \phi) \quad . \tag{9.5a}$$

The latter relation is explicitly given by the equation of the surfaces of constant sound speed (eqs. (5.2), (5.13)). The mapping

$$M: \quad P \mid\!\rightarrow P' \tag{9.6}$$

transforms any point P inside the star (of arbitrary geometry) in the original configuration space, into a *unique* image point P' in a fictitiuos space in which the surfaces of constant sound speed become concentric spheres; in particular the image of the surface of the star becomes a sphere (Fig. 8). The relevance of this mapping is that it transforms the original eigenvalue problem (2.7) over a star of arbitrary geometry into an eigenvalue problem over a spherical configuration. Of course, the price to be paid for the geometrical simplification of the configuration is an increased complexity of the transformed Hamiltonian

$$M: \quad \Omega(\mathbf{r},\mathbf{k})^2 \mid\!\rightarrow W(R, \Theta, \phi; \partial/\partial R, \partial/\partial\Theta, \partial/\partial\phi)^2 \tag{9.7}$$

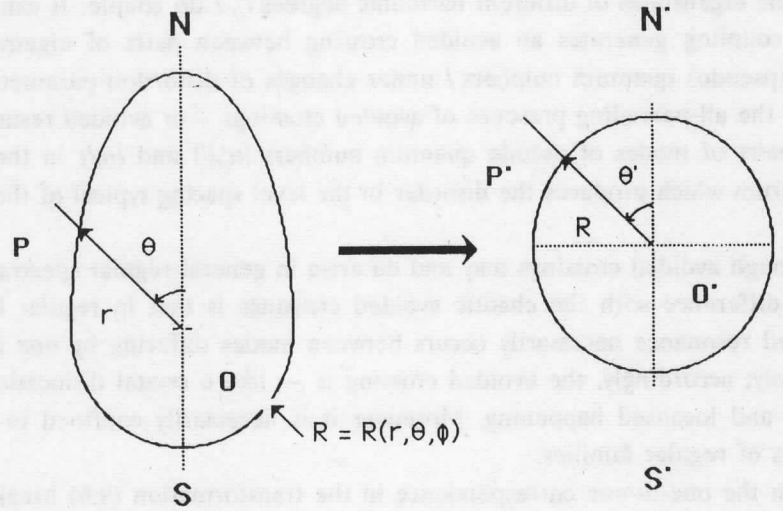

Fig. 8. Defining the mapping r, Θ, ϕ | → R, Θ', ϕ', from the physical configuration space of the star into a fictitious configuration space in which the surfaces of constant sound speed are concentric spheres; since $\phi' = \phi$, the transformation is shown in a symmetry plane only.

The one-to-one character of the transformation (9.6) breaks down when the surfaces of constant sound speed cease to be convex. Convexity is virtually unavoidably lost in localised deformations, which are relatively large over small fractions of the star.

In the new coordinates any eigenfunctions Ψ of the wave equation can be expanded in the set of eigenfunctions Φ_p of the spherical configuration

$$\Psi[R(r, \Theta, \phi), \Theta, \phi] = \Sigma_p \, a_p \, \Phi_p(R, \Theta, \phi) \quad , \tag{9.8}$$

where the summation extends over all values of the triplet of the quantum numbers. The coefficients a_p are the new unknowns of the problem. Substitution of the expansion (9.8) into the transformed eigenvalue equation, and operation by $\int_{V'} dV'/C(R)\Phi_{p'}$ where dV' and V' are the volume element and total volume in the fictitious space, produces a conventional matrix eigenvalue problem of the form

$$(M - \omega^2 E)\mathbf{a} = 0 \quad ; \tag{9.9}$$

here M denotes the matrix of elements $M_{p'p}$ describing the transformed LHS of the eigenvalue equation; E denotes the unit matrix; and $\mathbf{a}$ denotes the array of coefficients a_p of the expansion (9.8).

It is found that the eigenfunctions corresponding to different azimuthal quantum numbers m', m do not couple; accordingly the quantum number m of the sphere remains a genuine quantum number of the deformed configuration. This is a consequence of the preserved symmetry of revolution, which implies a conservation law (a second global integral), and therefore a second exact quantum number. In contrast, the eigenstates of different harmonic degrees l', l do couple. It can be seen that this coupling generates an avoided crossing between pairs of eigenvalues of different (pseudo) quantum numbers l under changes of distortion parameters. It is ultimately the all-pervading presence of avoided crossings —or avoided resonances— between pairs of modes of pseudo quantum numbers (n',l') and (n,l) in the asymptotic spectrum which produces the disorder in the level spacing typical of the chaotic spectrum.

Although avoided crossings may and do arise in general regular spectra as well, the main difference with the chaotic avoided crossings is that in regular branches the avoided resonance necessarily occurs between modes differing by one quantum number only; accordingly, the avoided crossing is – like a crystal dislocation – an accidental and localised happening. Moreover it is necessarily confined to the low lying levels of regular families.

When the one-to-one correspondence in the transformation (9.6) breaks down, the analogy with billiards suggests that ray chaos is turned into the dominant phenomenon; indeed the Hamiltonian ray equations may define a K-system. The algebraic representation (9.9) of the spectrum is expected to involve a matrix M whose

off-diagonal elements are essentially 'random'. Accordingly, the well known eigenvalue theory of random matrices should then become applicable.

The explicit calculation of the matrix elements requires a double numerical integration over R and Θ, and is therefore exceedingly time consuming. For this reason we have so far been constrained to work with small-sized matrices (18×18 or 25×25). Furthermore, we have carried out the calculations only for oscillation states of quantum number $m=0$. The latter are associated with the families of planar rays studied in Section 5.

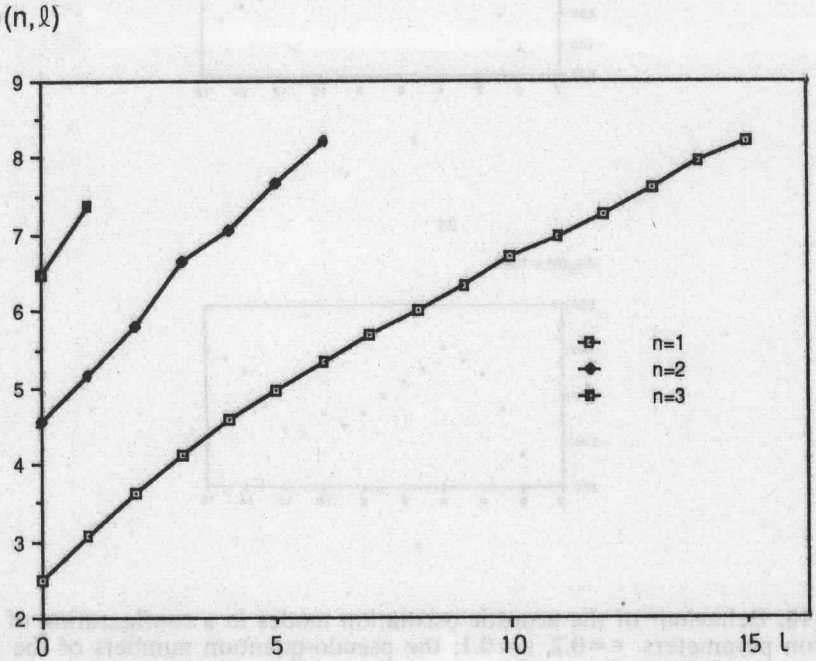

Fig. 9. Fan diagram of the acoustic modes of a nonspherical star of deformation parameters $\varepsilon=0.2$, $\beta=0.1$, for the pseudo quantum numbers $n=1, 2, 3$ and $l=0$–15. The diagram shows the same general shape as for spherical stars; the individual modes scatter around the frequencies of the nonperturbed spherical configuration.

The numerical results are summarised in Figures 9, 10, and 11. In Figure 9 we show a plot of the frequencies of pseudo quantum numbers $n=1, 2, 3$ and l in the range 0 to 11 for configuration of elliptic deformation parameter $\varepsilon=0.2$ (eq. (9.1)) and cubic deformation $\beta=0.1$. We mention the close similarity of this diagram with the solar frequency–horizontal wavenumber plots of the type first produced by *Deubner* (1975); notice that in contrast with the theoretical frequencies of spherically symmetric equilibrium models, the individual frequency values do not follow a precise

regular fanlike pattern; like the observed solar frequencies, the theoretical values found to scatter around an average regular pattern, namely the frequency pattern (9.4) of the symmetric model.

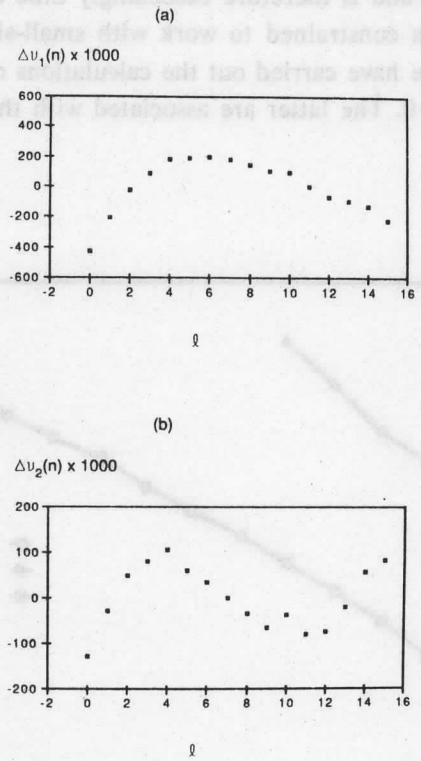

Fig. 10. Behaviour of the acoustic oscillation modes in a configuration of deformation parameters $\varepsilon = 0.2$, $\beta = 0.1$; the pseudo-quantum numbers of the modes are $n = 1$ and $l = 0$–15; (a) residuals of the linear interpolation; (b) residuals of the quadratic interpolation. Modes $l = 4$ and $l = 10$ are not smoothly connected to the neighbouring modes.

Figure 10 describes the regularity test of the collection of modes of pseudo quantum numbers $n = 1$ and l in the range 0 to 15, again for the deformed configuration $\varepsilon = 0.2$ and $\beta = 0.1$. Figure 10a shows the residuals of the linear interpolation, suggesting that modes $l = 4$ and 10 do not follow the regular pattern; Figure 10b showing the residuals of the quadratic interpolation confirms this result. A closer examination of the numerical results indicates that the mode ($n = 1$, $l = 4$) suffers an avoided crossing with the mode ($n = 2$, $l = 0$), while the mode ($n = 1$, $l = 10$) is likewise in approximate resonance with ($n = 2$, $l = 3$). It seems justified to regard these modes as belonging to a chaotic family of frequencies for the following reason. The ray propagation in ellipsoidal and pear-shaped stars discloses the existence of the SR

and MAR families, with the CR family arising out of their common boundary FR (*cf.* relations (5.10, 5.15)); the frequencies attached with the MAR family have manifestly relatively *lower* spherical degree l and *higher* radial radial order n; while those connected with SR have *higher* spherical degree l and *lower* radial order. Therefore quantum chaotic frequencies will arise as an interaction (materialising as an avoided crossing) between both types of modes. The two pairs we have traced seemingly obey this stipulation.

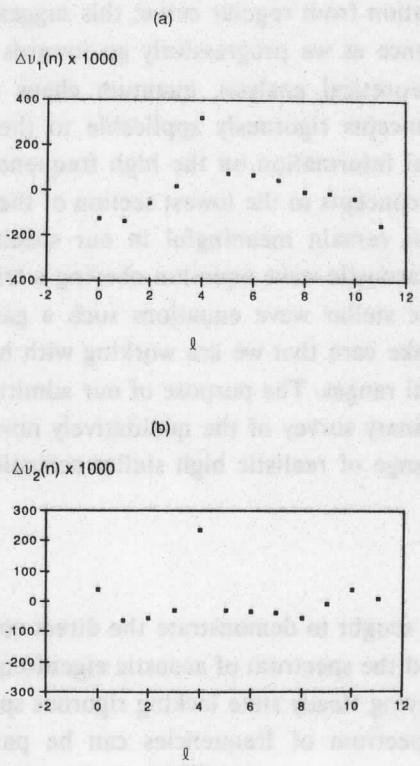

Fig. 11. Behaviour of the acoustic oscillation modes in a star of nonspherical equilibrium structure of deformation parameters $\varepsilon = 0.3$, $\beta = 0.2$; the pseudo quantum numbers of the modes are $n = 1$ and $l = 0$–11; (a) residuals of the linear interpolation; (b) residuals of the quadratic interpolation. Modes $l = 0$ and $l = 4$ are not smoothly connected to the neighbouring modes.

Figure 11 finally gives the result of the application of the regularity test to modes of pseudo quantum numbers $n = 1$, and $l = 0$ to 11, in a strongly deformed configuration ($\varepsilon = 0.3$ and $\beta = 0.2$). The residuals of the linear interpolation are displayed in Figure 11a, indicating that modes $l = 0$ and 4, as well as perhaps the higher end of the branch do not follow the regular pattern; the residuals of the quadratic interpolation given in Figure 11b are consistent with this conclusion. The

mode ($n=1$, $l=0$) does not interact with any other frequency, so that this mode cannot be interpreted as belonging to the quantum chaotic frequency branch; in fact, this mode must belong to a regular family, since we have found that its special behaviour survives in the integrable ellipsoidal case ($\beta=0$); we presume that it is to be regarded as a frequency attached to the regular MAR family. On the other hand, the mode ($n=1$, $l=4$), just as the mode of same identification in Figure 10, is resonant with ($n=2$, $l=0$), and is therefore to be interpreted as belonging to the quantum chaotic branch. The modes towards the higher l values of our diagrams show a more random looking deviation from regular curve; this suggests that quantum chaos is a more frequent occurrence as we progressively go towards higher frequencies.

According to our theoretical analysis, quantum chaos and regularity of the frequency spectrum are concepts rigorously applicable to the 'infinite' frequencies only. For want of numerical information on the high frequency range we have been forced to extrapolate these concepts to the lowest section of the spectrum. We believe that this extrapolation does remain meaningful in our specific case, since we are dealing with a very simple acoustic wave equation obeying a trivial scaling invariance (*cf.* eq. (5.5)). For realistic stellar wave equations such a game is not allowed; in genuine stars we have to take care that we are working with high enough oscillation states, and extended spectral ranges. The purpose of our admittedly academic illustration is to provide a preliminary survey of the qualitatively novel features we have to expect in the asymptotic range of realistic high stellar acoustic frequencies.

10. Epilogue

In this paper we have sought to demonstrate the direct correspondence between acoustic ray propagation and the spectrum of acoustic eigenfrequencies in stars, under the conditions of an underlying steady state lacking rigorous spherical symmetry. Our main result is that the spectrum of frequencies can be partitioned into distinct branches, each one being associated with a specific family of rays. Therefore we have been led to carry out a closer examination of the different ray families encountered in distorted stars. By the same token, we have made an attempt at understanding the genealogy of these families out of the trivial ray families of a spherical star.

The correspondence between ray and spectral families predicts a spectral branch whose properties differ radically from the properties of the familiar acoustic spectrum of spherical stars. This new branch – the quantum chaotic branch – is the spectral counterpart of the phenomenon of ray chaos. Perhaps the most surprising feature of the quantum chaotic frequencies is the fact that they cannot be captured by an asymptotic representation formula; the individual levels are highly sensitive to

the parameters characterising the geometry of the star, thus defying any smooth asymptotic ansatz.

A tentative first step only towards an understanding of the spectral families in nonspherical stars, our approach, instead of settling an astrophysical problem, actually raises a whole variety of questions: So far only planar ray families in configurations preserving a $C_{\infty v}$ symmetry have been studied. Even among the latter, our information on the structure of the allowed caustics remains fragmentary. A precise knowledge of the caustics is required to compute the Maslov correction factors in the asymptotic frequency representations of the regular families. The nontrivial problem of reexpressing the ray Hamiltonian in the 'local' integrals (F(J), eq. (3.3)), thereby producing a generalised Birkhoff normal form, has not been investigated either; such a form is needed for the explicit construction of the asymptotic frequency formulae.

A systematic study, both analytical and numerical, of the onset of quantum chaos is also lacking. We have found that for small deformations the measure of the chaotic zone in the parameter space of the initial conditions (5.6), although nonzero, remains small; it is not clear whether the occurrence – or the observability – of quantum chaos sets in at arbitrary small deformations, or whether it requires some finite threshold deformation. Perhaps the analogy between spectral regularity and crystal order, on the one hand, and spectral chaos and liquid disorder on the other could help clarify this point, possibly through a thermodynamic analysis of the (phase) transition from regularity to chaos in the frequency spectrum.

A detailed investigation of the structure of the eigenfunctions of the chaotic states is also missing. A knowledge of the shape of the eigenfunctions is vital for astroseismological purposes – and astroseismology is ultimately the practical justification for our interest in stellar oscillation spectra. In order to hammer out information from a set of measured frequency data, about the physical conditions prevailing say in the core of the star, the eigenfunctions associated with these frequencies must have significant amplitudes in the core. To some extent the ray patterns do already reflect the behaviour of the asymptotic eigenfunctions. Only those zones actually visited by the rays can have nonvanishing amplitudes; and the amplitude becomes large near points where we notice an accumulation of rays. These remarks are already indicative that the chaotic frequency branch, since it is associated with rays traversing the whole body of the star, should be especially relevant for exploring those regions which are not easily accessible to the regular acoustic rays.

At the moment nothing is known about the acoustic spectrum of stars devoid of any symmetry. We may conjecture, however, that spectral chaos then produces an even higher degree of disorder. In the algebraic formulation (9.9) interactions, *i.e.* avoided crossings, between oscillation states of different triplets of quantum numbers

(n, l, m) and (n', l', m') being now allowed, are obviously easier to materialise than avoided crossings between states of same azimuthal quantum number.

As a final point, I wish to emphasize that if we have an extended range of observed acoustic eigenfrequencies of a star at our disposal, and if we are able to distinguish different branches of frequencies, then we can make inferences on the possible geometries of the star; in this sense, spectral branches play a qualitative role similar to the classical mode splitting. On the quantitative level we can formulate an explicit inverse problem in the framework of the matrix eigenvalue problem (9.9). Without special effort the matrix formalism can be extended to the complete acoustic eigenvalue problem of deformed stars. Regarding the surfaces of constant sound speed as parametrised by equation (5.2), we observe that the algebraic formulation (9.9) implies that

$$\mathrm{dtm}\ \{M[\lambda_L\ ,\ D_{lm}^{(L)}] - \omega_{obs}(q)^2 E\} = 0 \qquad ,\ q = 1, 2, \ldots, N \qquad (10.1)$$

for each observed frequency $\omega_{obs(q)}$. Under the assumption that the physics of the star is fully known, and that N observed frequencies are available, equations (10.1) define a system of N constraints on the parameters λ_L , $D_{lm}^{(L)}$. Therefore we have the possibility of estimating a number N' $(\leq N)$ of independent parameters of the geometry of the star.

The author wishes to thank D.O. Gough for critical comments and L. Nejad for numerical assistance. He also thanks the members of the Institute of Astronomy, Cambridge, for the hospitality extended to him, as well as the Royal Society for the grant of a European Exchange Fellowship.

References

Arnold, V.I. 1978, *Mathematical Methods of Classical Dynamics*, Springer, New York.

Arnold, V.I. 1980, *Ordinary Differential Equations*, Mir, Moscow.

Arnold, V.I. 1983, *Uspekhi Mat. Nauk*, **38** (2), 77.

Benettin, G., and Strelcyn, J.M. 1978, *Phys. Rev.*, **A17**, 773.

Berry, M.V. 1977, *J. Phys.*, **A10**, 2061.

Berry, M.V. 1983, in *Chaotic Behaviour of Deterministic Systems*, Les Houches, eds.: Jooss G., Helleman, H.G., Stora, R., p. 171.

Chandrasekhar, S. 1969, *Ellipsoidal Figures of Equilibrium*, Yale University Press, New Haven.

Chernikov, A.A., Sagdeev, R.Z., Usikov, D.A., Zakharov, M.Yu., and Zaslavsky, G.M. 1987, *Nature*, **326**, 559.

Christensen-Dalsgaard, J. 1987, these Proceedings.

Deubner, F.L. 1975, *Astr. Ap.*, **44**, 371.

Devaney, R.L. 1986, *Chaotic Dynamical Systems*, Benjamin - Cummings, Menlo Park, California.

Eckart, C. 1960, *Hydrodynamics of Oceans and Atmospheres*, Pergamon, Oxford.

Gough, D.O. 1984, in *Solar Seismology from Space*, p. 49, Snowmass, Colorado, JPL Publication 84-84.

Grec, G., Fossat, E., and Pomerantz, M.A. 1983, *Solar Physics*, **82**, 55.

Harthong, J. 1981, *Advances in Appl. Math.*, **2**, 24.

Hayli, A., and Dumont, T. 1986, *Celestial Mechanics*, **38**, 23.

Jeffrey, A., and Taniuti, T. 1964, *Non-linear Wave Propagation*, Academic Press, New York.

Keller, J. 1958, *Ann. Physics*, **4**, 180.

Maslov, V.P. 1972, *Theorie des Perturbations et Methodes Asymptotiques*, Dunod, Paris.

Moray, F. 1986, Mémoire de Licence, Université de Liège.

Nelson, E. 1977, *Bull. American Math. Society*, **83**, 1165.

Noid, D.W., Koszykowski, M.L., and Marcus, R.A. 1979, *J. Chemical Physics*, **71**, 2864.

Nye, J.F. 1985, *Geophys. J.R. Astron. Soc.*, **83**, 477.

Ozorio de Almeida, A.M., and Hannay, J.H. 1982, *Annals of Physics*, **138**, 115.

Percival, I.C. 1973, *J. Phys.*, **B6**, L229.

Percival, I.C. 1974, *J. Phys.*, **A7**, 794.

Perdang, J. 1968, *Astr. Space Sci.*, **1**, 355.

Perdang, J. 1982, *Astr. Space Sci.*, **83**, 311.

Perdang, J. 1984, in Proceedings of the 25th Liège International Colloquium *Theoretical Problems in Stellar Stability and Oscillations*, Universite de Liège, p. 425.

Perdang, J. 1985, *Physicalia*, **7**, 239.

Perdang, J. 1986, in *Seismology of the Sun and the Distant Stars*, NATO ASI 169, Reidel, Dordrecht, p. 141.

Perdang, J. 1987, in *Proceedings of the IAU Symposium* No. 123, Aarhus, 1986. Eds.: J. Christensen-Dalsgaard and S. Frandsen, p. 125.

Perdang, J., and Nejad, L. 1987 (in preparation).

Robert, A. 1985, *Analyse Non Standard*, Presses Polytechniques Romandes, Lausanne.

Scuflaire, R., Gabriel, M., and Noels, A. 1981, *Astr. Ap.*, **99**, 39.

Toomre, J. 1986, in *Seismology of the Sun and the Distant Stars*, NATO ASI 169, Reidel, Dordrecht, p. 1.

Tolstoy, I. 1973, *Wave Propagation*, McGraw-Hill, New York.

Ulrich, R.K., and Rhodes, E.J. 1984, in *Solar Seismology from Space*, NASA JPL Publication 84-84, Pasadena, p. 371.

Wojtkowski, M. 1986, *Commun. Math. Phys.*, **105**, 391.

Woodard, M., and Hudson, H.S. 1983, *Nature*, **305**, 589.

Zaslavsky, G.M. 1981, *Phys. Rep.*, **80**, 157.

CHAOTIC PULSATIONS IN STELLAR MODELS

J. R. Buchler
University of Florida, Department of Physics, Florida, Gainesville, USA
G. Kovács
Konkoly Observatory, Budapest, Hungary
and
Marie-Jo Goupil
Observatoire de Nice, Nice, France

Abstract

Numerical hydrodynamical studies of sequences of Population II Cepheid models reveal two well-known types of universal routes from regular to chaotic pulsations as the effective temperature is lowered; these are the period-doubling bifurcation sequence and the tangent bifurcation. Depending on their behavior these models would be classified as W Virginis, RV Tauri or Semi-Regular. We wish to stress that the techniques used for the analysis of the numerically generated luminosities and radial velocities could also very fruitfully be applied to observational data of this type of stars if the latter were gathered in a more suitable fashion.

There are at least some superficial indications of period doublings and chaos as well as intermittency among the classical intrinsic variable stars. For example, period doubling seems to manifest itself as so-called RV Tauri behavior; this is an alternation of shallow and deep minima in the light curves of certain W Virginis and RV Tauri stars, alternations which can be regular or irregular (*e.g. Tsesevich* 1975). At the same time fluid experiments, chemical reactions and many other nonlinear phenomena have been found to undergo typical routes from regular, periodic to irregular chaotic temporal behavior. It seemed therefore natural to us to explore whether astrophysical fluids such as pulsating stars, would exhibit similar behavior. It should, however, be obvious that their physical complexity is far greater than that of the laboratory systems which have been studied or that of the usually studied low-dimensional systems of equations, such as the Lorenz attractor, in which similar behavior is found.

Irregular behavior is commonly classified as *noisy* or *chaotic* depending on the number of degrees of freedom which are involved. Chaos is said to occur when the latter is small, and its interest lies in the fact that we can hope to find a relatively simple physical mechanistic as opposed to stochastic model for the observed behavior and thence gain a deeper understanding of the underlying dynamic. Unfortunately most of the currently available observational data are not suitable for an analysis

with the modern techniques of nonlinear dynamics. At the present time we therefore have to resort to numerical hydrodynamical modelling to understand the temporal behavior of the pulsations of these stars. Because of the cost of the numerical hydrodynamical integrations we are necessarily limited in the parameter studies we can afford. In the interpretation of the behavior of the models we therefore heavily lean on the experience gained from the study of very simple systems and mappings.

A fairly extensive recent survey of luminous Population II Cepheids has shown that the pulsations of these models undergo two well-known universal routes from periodic to chaotic (aperiodic) behavior as a control parameter (in our case the effective temperature) is varied. In a lower luminosity sequence *Buchler* and *Kovács* (1987) found a typical Feigenbaum series of *period doubling bifurcations* followed by chaos. In another recent publication *Buchler, Goupil* and *Kovács* (1987) describe the pulsations of luminous Population II Cepheid models which exhibit intermittency, *i.e.* streches of regular behavior interrupted by erratic bursts; they identify a *tangent bifurcation* as being responsible for this behavior. The full survey of sequences of Population II Cepheids is discussed in *Kovács* and *Buchler* (1988). Since our discovery of period doubling and tangent bifurcation in stellar models *Aikawa* (1987) has independently found similar tangent bifurcation in a sequence of somewhat more massive Population II Cepheid models as well. (We refer the reader who is unfamiliar with the language of chaos to the beautiful introduction by *Bergé, Pomeau* and *Vidal* 1986; see also *Buchler, Perdang* and *Spiegel* 1985).

It is interesting to note that RV Tauri-like as well as irregular behavior in radiative W Vir models has sporadically reported in the literature, but that it has never received any systematic attention, perhaps for want of a theoretical framework within which to interpret and understand such behavior (*Christy* 1966; *Davis* 1972,1974; *Fadeyev* 1984; *Fadeyev* and *Fokin* 1985; *Bridger* 1984, 1985; *Takeuti, Nakata* and *Aikawa* 1985; *Nakata* 1987). It should be stressed that the two discovered universal routes to chaos are very common phenomenon in Population II Cepheid models and that their occurence is robust with respect to physical and numerical parameters. The survey of *Kovács* and *Buchler* (1988) shows the following systematical behavior of model sequences for a given mass, luminosity and composition as the control parameter, the effective temperature, is lowered:

(i) In the low-luminosity sequences the fundamental periodic pulsation remains stable down to very low effective temperatures. for more luminous sequences two qualitatively different types of behavior are observed:

(ii) for an intermediate luminosity range pulsations of increasing complexity arise which are due to period doubling bifurcations and end up as chaotic as the effective temperature is lowered; further on one observes typical noisy reverse period doubling bifurcations.

(iii) for the most luminous of the model-sequences the periodic oscillations are interrupted by irregular bursts which become increasingly frequent as the effective temperature is lowered until the motion is chaotic.

The hydrodynamical behavior of the models is studied with a slightly modified version of *Stellingwerf's* (1974, 1975) 1-D Lagrangean hydro-code. Heat transport is assumed to occur solely through radiative diffusion. For numerical purposes the models are discretized into N mass-shells (N = 60). Since each mass-shell is characterized by a radius, velocity and entropy (or any other thermal variable) the phase-space of our discretized approximation to the partial differential differential system of hydrodynamics has therefore a dimension of 3N (= 180). We use 200 equal time-steps per linear fundamental period.

We shall briefly describe here the dynamical behavior of two selected stellar models both of which behave chaotically, but which have entered the chaotic regime through the two different routes. The chosen stellar parameters, namely the masses, luminosities, compositions and effective temperatures are those of cool Population II Cepheids. They straddle what observers would classify as W Vir, RV Tauri or Semi-Regular stars.

Before embarking on a discussion of the interesting behavior of the two models, in some detail we shall give the reader a brief glimpse of one of the techniques which have been developed for the analysis of chaotic signals, especially since they should also be very useful for the analysis of observational data. One such technique which has by now become commonplace is *a phase- space reconstruction* (*Packard et al.* 1980; *cf. Berge et al.* 1986). Consider a given 'signal' $\{x_i = x(t_i)\}$, which can be any one of the dynamical variables of the system or any suitable function thereof and which is sampled at equally-spaced epochs t_i . From this sequence we construct the 'vectors' $\mathbf{X}_i = (x_i, x_{i+k}, x_{i+2k}, \ldots, x_{i+(m-1)k})$ which trace the trajectory in an *m-dimensional embedding* space. The quantity k is a delay which is necessary to spread the attractor away from the diagonal in a densely sampled signal. The interest of this study rests on the fact that the topological properties of the reconstructed attractor are the same as those of the original attractor. If the dimension of the chaotic attractor is d_a (noninteger), then it can be shown that the attractor can be embedded in a $(2d+1)$-dimensional space, where d is the integer part of d_a augmented by unity. It appears that for most real-life attractors it is sufficient to use an embedding space of dimension d. In practice one thus embeds the attractor in spaces of increasing dimension m until there is no longer an intersection of orbits. It is clear that if this dimension turns out to be very large then the procedure becomes not only very cumbersome, but there does not seem much point in studying such a complicated high-dimensional attractor as little physical insight can be gained from this study. Many observed attractors have been found to be low-dimensional (*e.g. Bergé et al.* 1986).

Model 1 has a mass of 0.6, a luminosity of 200, both in solar units, a composition of X = 0.745 and Z = 0.005 and an effective temperature of 4266 K. All the linear modes of the model are stable except the fundamental.

The temporal variation of the surface radius and of the radial velocity for this model are shown in Figure 1.

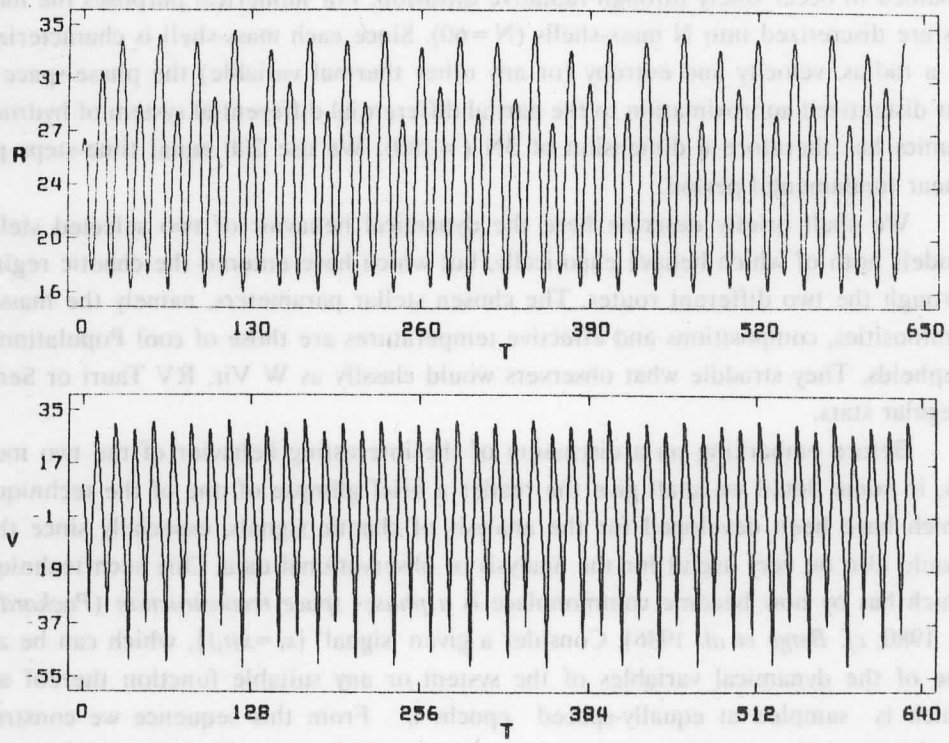

Fig. 1. Temporal variations (a) of the surface radius (in units of 10^{11} cm) and (b) of the (radial) surface velocity (in km/s) of Model 1. The time is in days.

The signal seems to have a well defined period but the amplitude is 'modulated' in a very erratic way with RV Tauri (alternating) characteristics. A Fourier amplitude spectrum, shown in Figure 2, confirms the fairly sharp periodicity (associated with the fundamental frequency of oscillation). It exhibits also the large first subharmonic and displays an additional second subharmonic structure. The harmonics, on the other hand, are very weak indicating rather weak nonlinearity. The peaks are not sharp. In fact, for a chaotic signal finer and finer resolution with a longer data-base would reveal more and more structure to the peaks, ad infinitum. A Fourier analysis is generally not a very appropriate tool for the analysis of irregular signals. We therefore turn to another technique of analysis mentioned above.

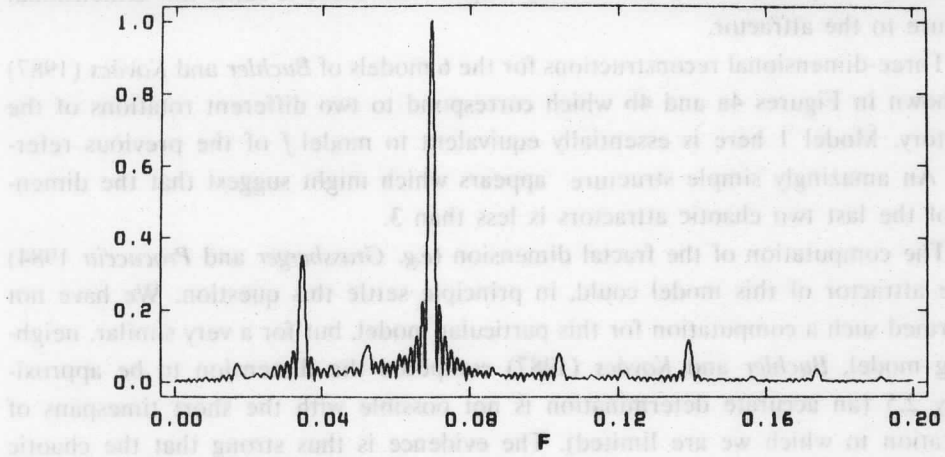

Fig. 2. Fourier amplitude spectrum of the radius variation of Model 1 (frequency in 1/day).

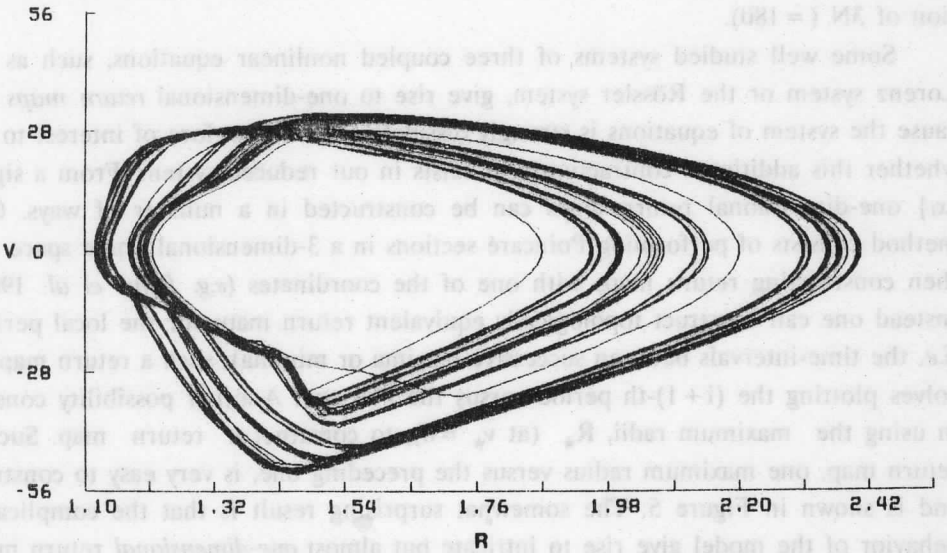

Fig. 3. Projection of the trajectory onto the surface radius – radial velocity plane.

We start with an analysis in 2-dimensional space. Instead of a 2-dimensional phase-space reconstruction, *i.e.*, a plot of X_i , constructed with the surface radius, we present in Figure 3 a topologically equivalent reconstruction, namely a plot of (x_i, dx_i/dt). As expected, the trajectories intersect in this 2-D plot (since a chaotic attractor cannot be embedded in a two-dimensional space). Since Figure 3 is not a totally

disordered mess, so that one can already suspect that there is some low-dimensional structure to the attractor.

Three-dimensional reconstructions for the 6 models of *Buchler* and *Kovács* (1987) are shown in Figures 4a and 4b which correspond to two different rotations of the trajectory. Model 1 here is essentially equivalent to model *f* of the previous reference. An amazingly simple structure appears which might suggest that the dimension of the last two chaotic attractors is less than 3.

The computation of the fractal dimension (*e.g. Grassberger* and *Procaccia* 1984) of the attractor of this model could, in principle settle this question. We have not performed such a computation for this particular model, but for a very similar, neighboring model, *Buchler* and *Kovács* (1987) computed the dimension to be approximately 2.5 (an accurate determination is not possible with the short timespans of integration to which we are limited). The evidence is thus strong that the chaotic attractor is indeed embeddable in 3 dimensions. The dynamic should thus be parametrizable with three generalized coordinates which have to satisfy three differential equations. This is a remarkable result since, we recall, our phase-space has a dimension of 3N (= 180).

Some well studied systems of three coupled nonlinear equations, such as the Lorenz system or the Rössler system, give rise to one-dimensional *return maps* because the system of equations is strongly dissipative. It is therefore of interest to see whether this additional contraction also exists in our reduced system. From a signal $\{x_i\}$ one-dimensional return maps can be constructed in a number of ways. One method consists of performing Poincaré sections in a 3-dimensional phase space and then constructing return maps with one of the coordinates (*e.g. Bergé et al.* 1986). Instead one can construct topologically equivalent return maps for the local periods (*i.e.* the time-intervals between successive maxima or minima); such a return map involves plotting the $(i+1)$-th period versus the i-th one. Another possibility consists in using the maximum radii, R_* (at $v_* = 0$), to construct a return map. Such a return map, one maximum radius versus the preceding one, is very easy to construct and is shown in Figure 5. The somewhat surprising result is that the complicated behavior of the model give rise to intricate but almost *one-dimensional* return maps with the same general properties as the quadratic Feigenbaum map.

Many astronomers are used to thinking that every time sequence can be fitted with multiperiodic sum (which, indeed, is mathematically true over a finite time-interval) and they may wonder what this chaotic fuzz is all about. From the Fourier analysis (Figure 3) one can see that it would be necessary to use many closely spaced frequencies (without a physical basis) to reproduce the irregular behavior of the time series. It also turns out that the return maps for a typical multi-periodic signal generally do not at all look like the type of return map shown above.

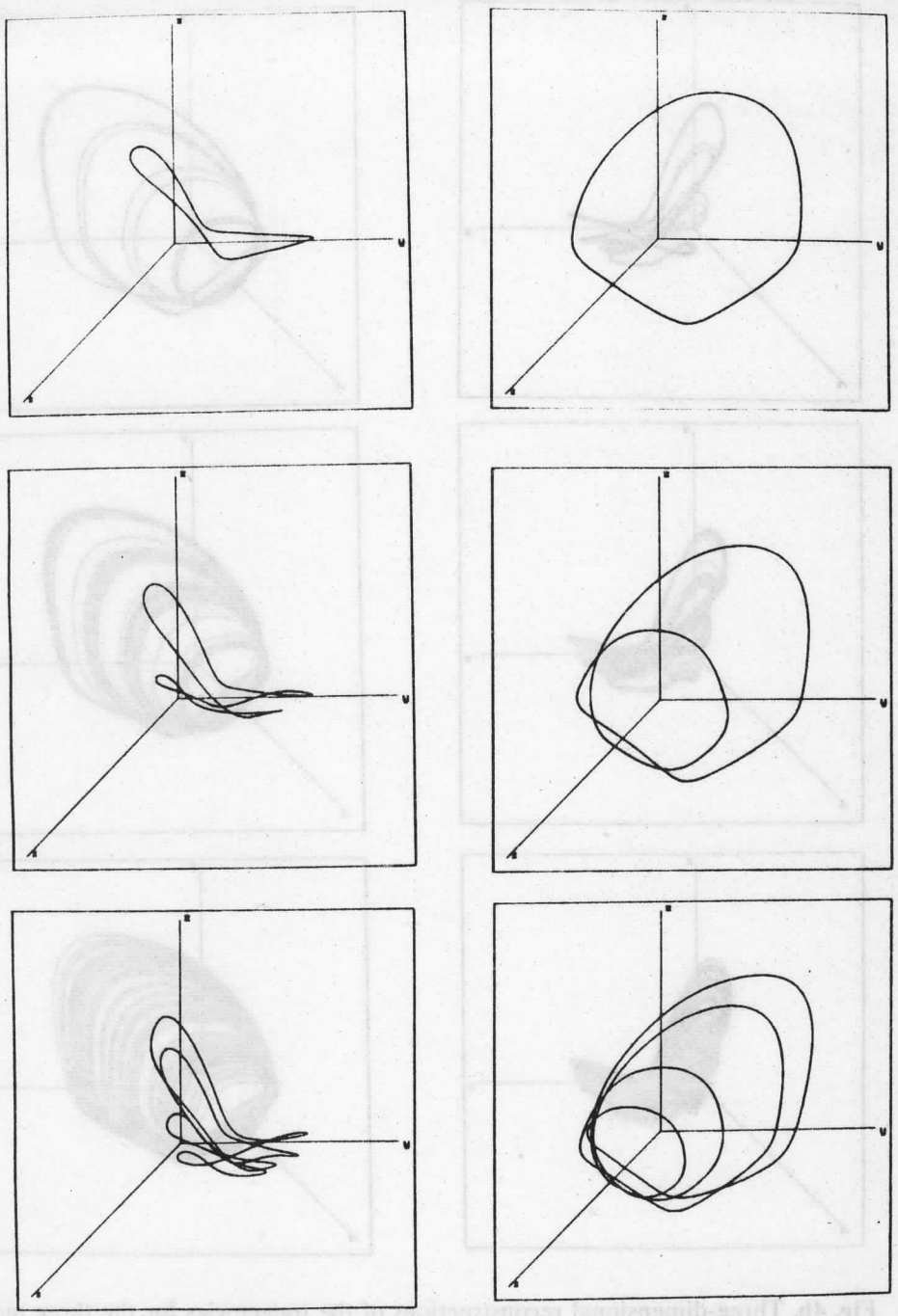

Fig. 4a. Three-dimensional reconstructions of the trajectories for the three models of *Buchler* and *Kovács* (1987) for two different aspects ($x = x_i$, $y = x_{i+k}$, $z = x_{i+2k}$).

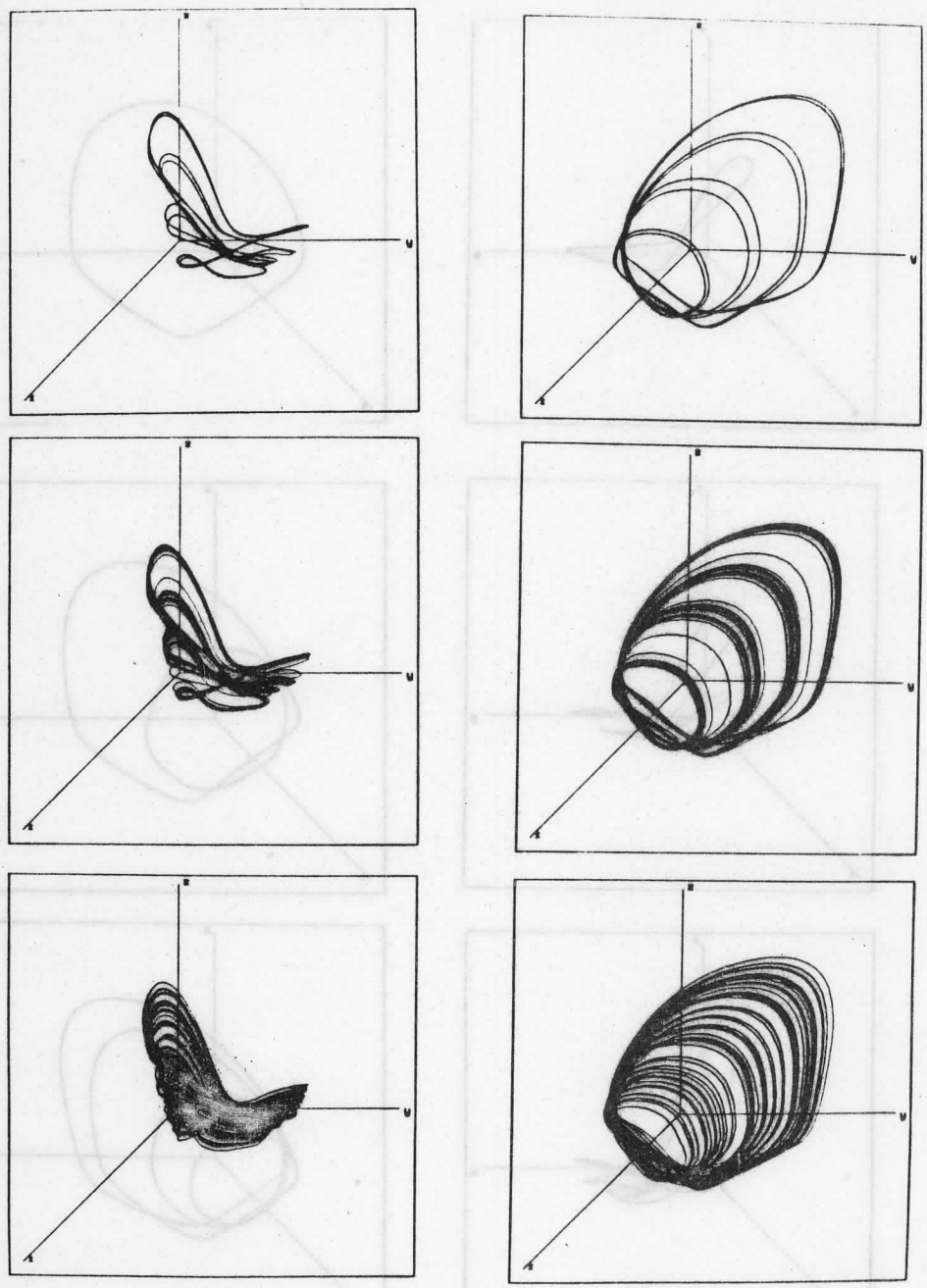

Fig. 4b. Three-dimensional reconstructions of the trajectories for the three models of *Buchler* and *Kovács* (1987) for two different aspects ($x = x_i$, $y = x_{i+k}$, $z = x_{i+2k}$).

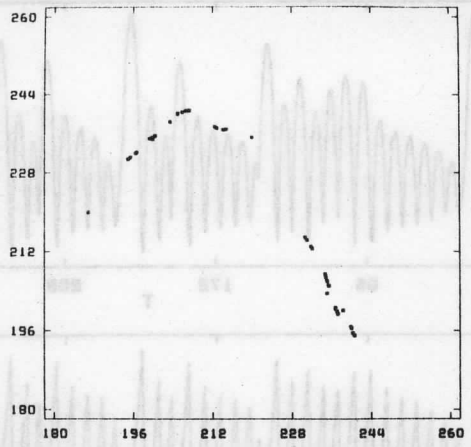

Fig. 5. Return map for the maximum radius.

Model 2 has a higher luminosity to mass ratio with a mass of 0.4, a luminosity of 400, both in solar units, a composition of $X = 0.745$ and $Z = 0.005$ and an effective temperature of 5870 K.

A typical temporal behavior of the surface radius and of the radial velocity are shown in Figure 6. The Fourier amplitude spectrum is shown in Figure 7. The large peak corresponds to the basic pulsation and the wild amplitude modulation gives rise to a very noisy subharmonic structure. There is very little harmonic structure which shows that nonlinear effects seem to be very weak. Again, otherwise very little knowledge can be gained from the Fourier analysis.

The type of behavior exhibited by this model and the whole sequence of models to its left in the HR diagram studied in *Buchler, Goupil* and *Kovács* (1987) was first explained by *Pomeau* and *Manneville* (1980) and they labelled it 'type I intermittency'. It is most clearly understood with a return map. Figure 8 shows the return map constructed from the Poincaré sections of the reconstructed orbits. The return map clearly does not appear one-dimensional. However if we plot a blow-up of the same return map for selected streches as in Figure 9 which shows the successive visitation number, it becomes very close to one-dimensional. One sees that the orbit gets temporarily trapped near a bottleneck which is the vestige of an intersection of the return map with a 45° line. The latter indicates the prior existence of a couple of fixed points (one stable and one unstable) in a model at higher effective temperature (*cf. Buchler, Goupil* and *Kovács* 1987). Once the bottleneck is passed the trajectory jumps around a strongly unstable fixed point on the upper right

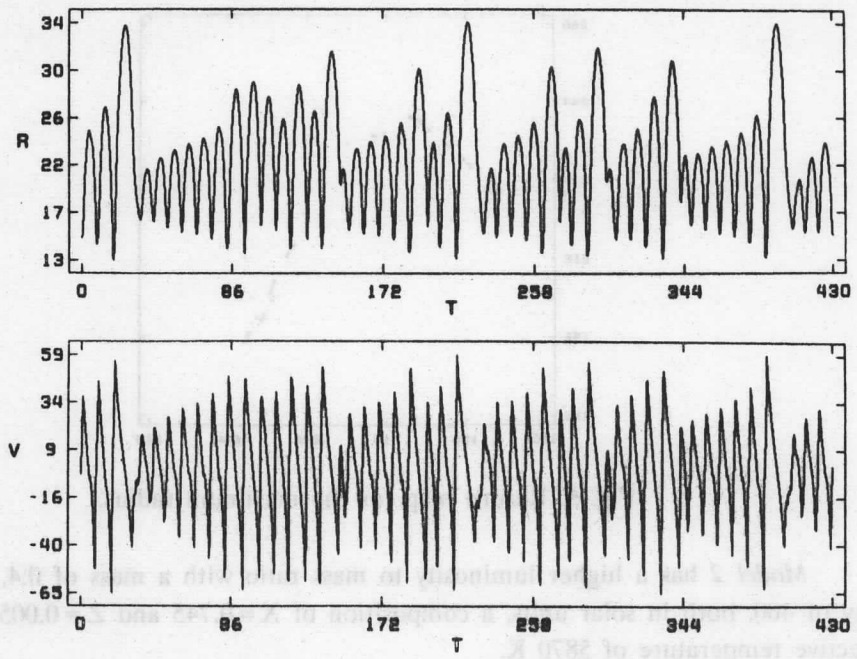

Fig. 6. Temporal variations (a) of the surface radius (in units of 10^{11} cm) and (b) of the (radial) surface velocity (in km/s) of Model 2 (time in days).

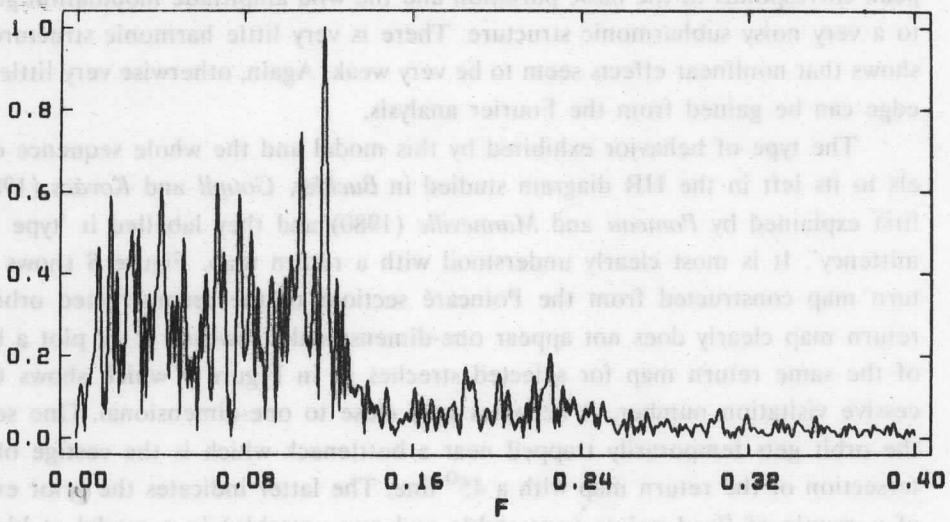

Fig. 7. Fourier amplitude spectrum of the radius variation of Model 2 (frequency in 1/day).

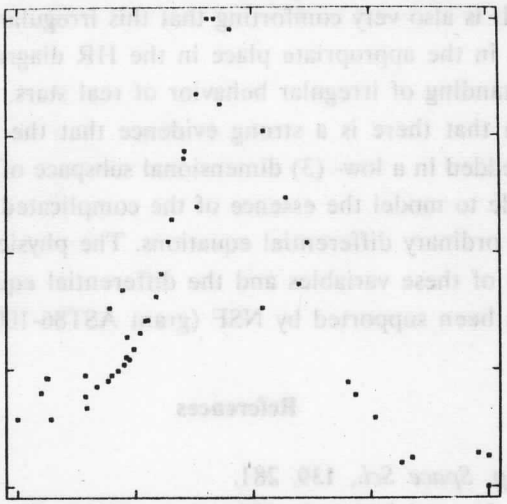

Fig. 8. Return map on a Poincaré section for Model 2.

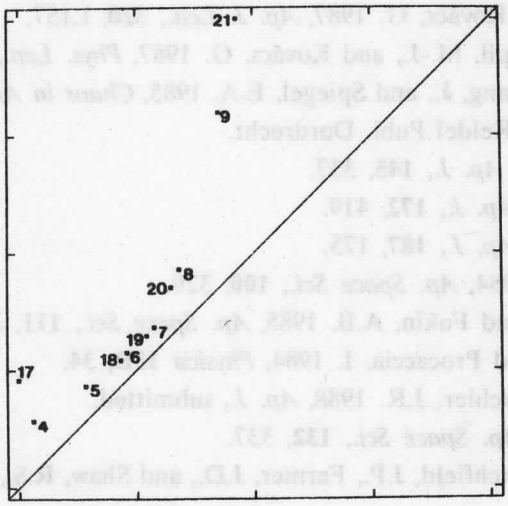

Fig. 9. Pieces of the previous return map with visitation number.

(located at the intersection of the return map function and the 45° line) until a sufficiently large pulsation reinjects it to the left of the tangency bifurcation.

The survey of *Kovács* and *Buchler* (1988) has demonstrated that a number of widely different sequences of cool radiative Population II Cepheid models show two typical, well understood, routes leading to chaotic pulsations as the effective tempera-

ture is lowered. This type of irregular behavior is not an oddity of a few models, but is very robust. It is also very comforting that this irregular behavior of the models should show up in the appropriate place in the HR diagram. This opens up the door to the understanding of irregular behavior of real stars.

We have seen that there is a strong evidence that the underlying chaotic attractor can be embedded in a low- (3) dimensional subspace of phase-space. It should therefore be possible to model the essence of the complicated behavior with a small number of coupled ordinary differential equations. The physical challenge now is to discover the nature of these variables and the differential equations they obey.

This work has been supported by NSF (grant AST86-10097).

References

Aikawa, T. 1987, *Ap. Space Sci.*, **139**, 281.

Bergé, P., Pomeau, Y., and Vidal, C. 1986, *Order Within Chaos, Wiley*, N.Y.

Bridger, A. 1984, *Ph. D. Thesis*, University of St. Andrews.

Bridger, A. 1985, in *Cepheids: Theory and Observations*, IAU Colloquium No. 82, ed. B.F. Madore, Cambridge Univ. Press, Cambridge, p. 246.

Buchler, J.R., and Kovács, G. 1987, *Ap. J. Lett.*, **320**, L157.

Buchler, J.R., Goupil, M.-J., and Kovács, G. 1987, *Phys. Lett.*, **A126**, 177.

Buchler, J.R., Perdang, J., and Spiegel, E.A. 1985, *Chaos in Astrophysics*, NATO ASI series, **C161**, Reidel Publ. Dordrecht.

Christy, R.F. 1966, *Ap. J.*, **145**, 337.

Davis, C.G. 1972, *Ap. J.*, **172**, 419.

Davis, C.G. 1974, *Ap. J.*, **187**, 175.

Fadeyev, Yu. A. 1984, *Ap. Space Sci.*, **100**, 329.

Fadeyev, Yu. A., and Fokin, A.B. 1985, *Ap. Space Sci.*, **111**, 355.

Grassberger, P., and Procaccia, I. 1984, *Physica* **13D**, 34.

Kovács, G., and Buchler, J.R. 1988, *Ap. J.*, submitted.

Nakata, M. 1987, *Ap. Space Sci.*, **132**, 337.

Packard, N.H., Crutchfield, J.P., Farmer, J.D., and Shaw, R.S., 1980, *Phys. Rev. Lett.*, **45**, 712.

Pomeau, Y., and Manneville, P. 1980, *Comm. Math. Phys.*, **74**, 189.

Stellingwerf, R.F. 1974, *Ap. J.*, **192**, 139.

Stellingwerf, R.F. 1975, *Ap. J.*, **195**, 441.

Takeuti, M., Nakata, M., and Aikawa, T. 1985, *Sendai Astronomiaj Raportoj*, Nr. 275.

Tsesevich, V.P. 1975, in *Pulsating Stars*, ed. Kukarkin, J., Wiley Publ., N.Y., p. 112.

A NONADIABATIC OSCILLATOR PRODUCING CHAOS

M. Takeuti
Astronomical Institute, Faculty of Science,
Tohoku University, Sendai, Japan

Abstract

An oscillator including simple nonadiabatic terms with phase delay is studied. The oscillator shows period doubling into chaos.

The aim of the present short paper is to show a simple oscillator, which may express the features of stellar pulsations. In the oscillator, the equation of motion is linear and the nonadiabatic term in the equation of state is nonlinear. The orbits of the oscillator indicate period-doubling developing into chaos with the changes of parameters.

The oscillator is proposed by *Tanaka* and *Takeuti* (1987a). It is written in the following form

$$dx/dt = y \quad , \tag{1}$$

$$dy/dt = \alpha x + \mu y + z \quad , \tag{2}$$

$$dz/dt = -3\gamma y - pz - qy + syz \quad , \tag{3}$$

where α, μ, γ, p, q, and s are contants. Equation (1) defines the velocity y as the derivative of displacement x by the time t. Equation (2) is the equation of motion where μ is the damping constant, which we may use to express the γ-mechanism in the deep quasi-adiabatic region or any other linear damping in the stellar envelopes. Equation (3) is the equation of state where γ is the adiabatic exponent. p and q express the nonadiabatic effect just around the equilibrium state. If the motion is linear adiabatic and oscillatory one, y is proportional to dz/dt. So the expression $-pz-qy+syz$ can be regarded as expression to show how the entropy changes on the z–dz/dt plane.

Compared with one-zone stellar models (for example *Baker* 1976), we have put α equal to 4. $\gamma = 5/3$ is chosen for simplicity. Then the model will be dynamically stable. The condition of secular stability is as follows:

$$\alpha p < 0 \quad . \tag{4}$$

When the condition

$$-\mu p^2 + (\mu^2 + 3\gamma + q)p + \mu(-1-q) < 0 \quad , \tag{5}$$

is satisfied, the singularity at the origin will be the unstable centre of spiral. This is nothing else than the pulsational instability.

Since we hope to reproduce various irregularity found in stellar variability by the oscillator, the parameters are chosen to melt into the conditions (4) and (5). From the inequality (4) we must put $p<0$. To increase the growth rate of oscillation with the decrease of p, we put $\mu<0$. Negative μ comes from the restricted form of the oscillator not from the physical assumption.

When we put $p<0$, $q<0$, the nonadiabaticity near the origin produces the pulsational instability. And then we put $s<0$. In this case, the nonadiabatic term shows the occurrence of strong nonlinear cooling a little later maximum compression. The cooling coincides with the observed luminosity maximum in Cepheid-type stars.

Another cooling in third quadrature of the y–z plane is the result of the simplicity of the expression. The cooling in this phase works to reduce the effect of the cooling just after the maximum compression.

In Figures 1 – 4, a part of the numerical results are indicated. The parameters μ, q and s are –0.5, –0.7 and –10, respectively. The parameter p is changed from –0.05 to –0.08. The decrease of p produces clearly the sequence of period-doubling into chaotic motion. The orbits show that the strong nonlinear damping in the first quadrant of the y-z plane is effective to make solutions chaotic. The detailed results will be published in *Tanaka* and *Takeuti* (1987a).

We point out here only the fact that the oscillator has a close similarity to the well-known Rössler equation (*Rössler* 1976) the original form of which is written as follows:

$$dX/dt = -Y - Z \quad , \tag{6}$$

$$dY/dt = X + aY \quad , \tag{7}$$

$$dZ/dt = b + Z(X - c) \quad , \tag{8}$$

where a, b, and c are constants. The similarity is clear when we arrange the original equation into the following form

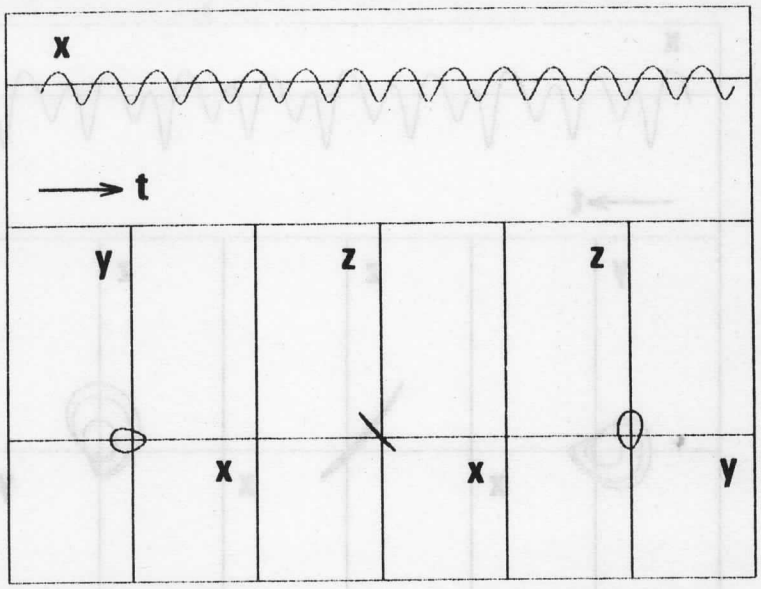

Fig. 1. Period 1 limit-cycle of the oscillator presented by *Tanaka* and *Takeuti* (1987a). The parameters are $\mu = -0.5$, $p = -0.05$, $q = -0.7$, $s = -10$, respectively. The upper diagram indicates the variation of x with the time t. The lower diagrams indicate the orbit in the x-y-z space. The scale of z is one fourth of others.

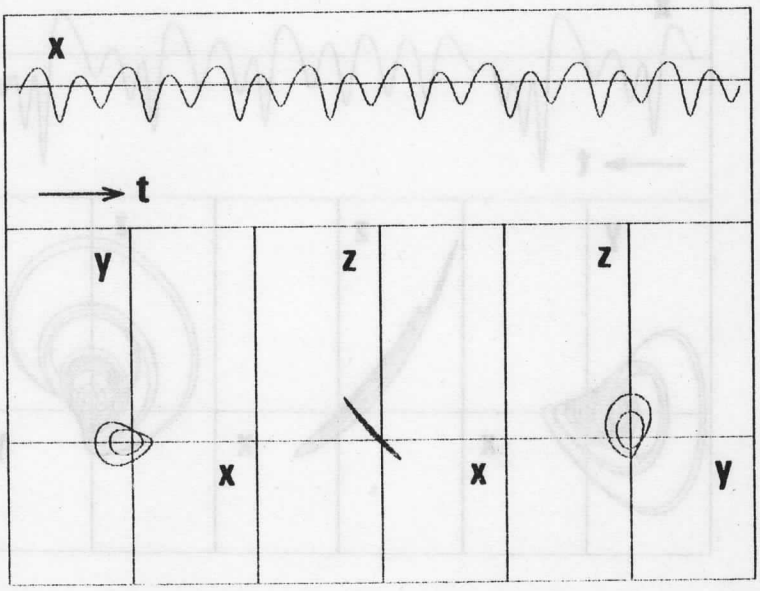

Fig. 2. The period 2 limit-cycle of the oscillator. The parameters are $\mu = -0.5$, $p = -0.06$, $q = -0.7$, $s = -10$, respectively.

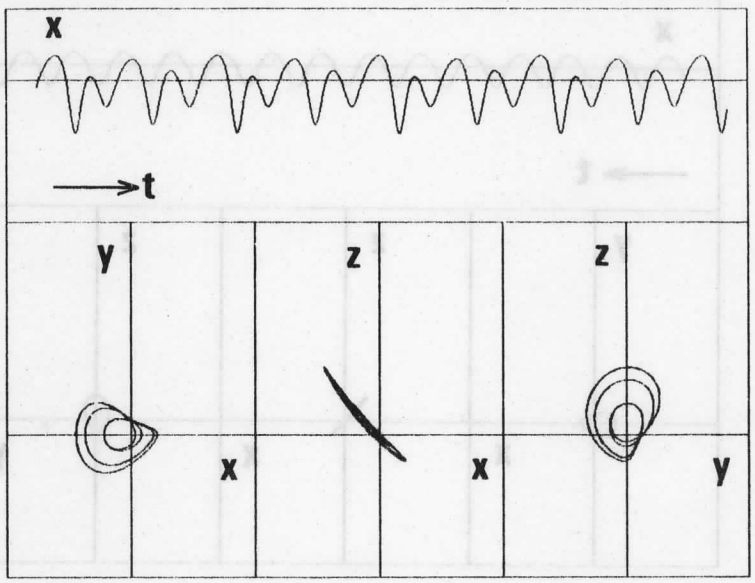

Fig. 3. The period 4 limit-cycle of the oscillator. The parameters are $\mu = -0.5$, $p = -0.07$, $q = -0.7$, $s = -10$, respectively.

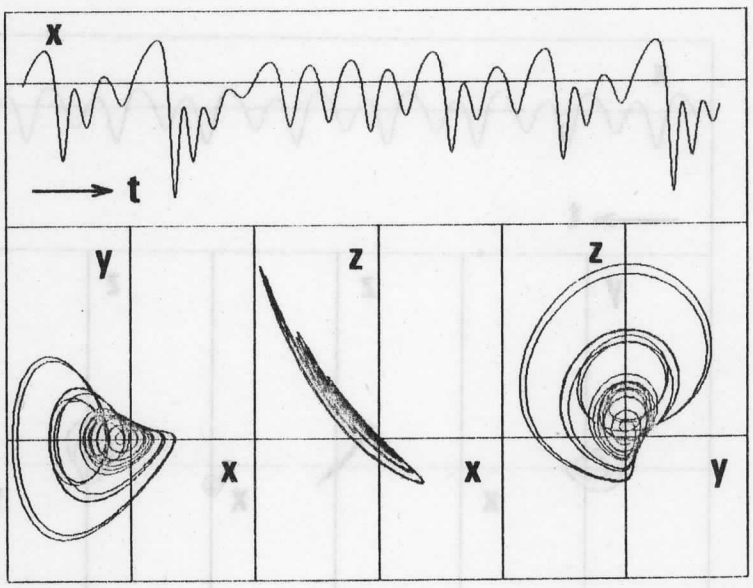

Fig. 4. Chaotic oscillations of the oscillator. The parameters are $\mu = -0.5$, $p = -0.08$, $q = -0.7$, $s = -10$, respectively.

$$dx/dt = y \quad , \tag{9}$$

$$dy/dt = -x + ry + z \quad , \tag{10}$$

$$dz/dt = (z - q)(-rx + y - rp) - pqr \quad , \tag{11}$$

where p, q, and r are constants. This form has been found in *Tanaka* and *Takeuti* (1987b).

We try to compare the oscillator with hydrodynamic stellar models. The development of period-doubling into chaotic oscillation is found in the model W Virginis stars (*Buchler* and *Kovács* 1987). Even though we have not known how is the feature of delayed luminosity maxima in their models, such a nonlinear strong damping may cause the period-doubling. Theirs are the first hydrodynamic models showing period-doubling, although the radiative models may not be adequate at the red side of the Cepheid instability strip. A characteristic sequence of pulsations found in less massive stellar models (see *Nakata* 1987; *Takeuti* 1987) is now understood as the consequence of the tangent-bifurcation (*Buchler, Goupil,* and *Kovács* 1987; *Aikawa* 1987). It is not yet clear that the oscillator shows this kind of bifurcation.

A lot of variable stars having small surface gravity show irregularity. The observations have not been indicated on the return maps except for the Mira stars (*Saijo* and *Watanabe* 1987). The return maps for Mira stars show stable fixed point likely found in the maps of period-doubling type nonlinear oscillations. Unfortunately, other stars have not been investigated in this way. It is not clear whether or not the tangent bifurcation is real in the variable stars. The difference in the return maps may be useful to investigate the hydrodynamical properties of stellar envelopes. It is very important to draw the return maps of irregular variables based on the sequence of observational materials.

We can see that the irregular oscillation is produced by the nonlinearity of non-adiabaticity, when the parameters of the oscillator melt into some conditions. It seems interesting to investigate one-zone stellar models much more precisely, by using the properties of our simple oscillator.

I wish to express my thanks to Professor Y. Tanaka, Dr. T. Aikawa for their useful comments and advice. I also thank to Professor Y. Sawada for his conversation.

References

Aikawa,T. 1987, *Ap. Space Sci.*, **139**, 281.

Baker, N.H. 1976, in *Stellar Evolution*, ed. R.F. Stein and A.G.F. Cameron, (Plenum Press), p. 333.

Buchler, J.R., and Kovács, G. 1987, *Ap. J.* (Letters), **320**, L57.

Buchler, J.R., Goupil, M.-J., and Kovács, G. 1987, *Phys. Lett.*, **126A**, 177.

Nakata, M. 1987, *Ap. Space Sci.*, **132**, 337.

Rössler, O.E. 1976, *Phys.Lett.*, **57A**, 397.

Saijo, K. and Watanabe, M. 1987, private communication.

Takeuti, M. 1987, *Ap. Space Sci.*, **136**, 129.

Tanaka, Y., and Takeuti, M. 1987a, in preparation.

Tanaka, Y., and Takeuti, M. 1987b, preprint.

TESTING FOR CHAOS IN LONG PERIOD VARIABLES

S. Blacher
Institut d'Astrophysique, Cointe-Ougrée, Belgium
and
J. Perdang
Institute of Astronomy, Cambridge, UK
and
Institut d'Astrophysique, Cointe-Ougrée, Belgium*

Abstract

The behaviour of the variance function σ_n^2 of the local cycles ($n=1$), double cycles ($n=2$), triple cycles ($n=3$), ... , of artificially generated time series is analysed and compared with the variance function of a collection of Long Period Variables. For strictly periodic and multiperiodic (F-periodic, with F small), noisy periodic and multiperiodic, strictly chaotic, and noisy chaotic time series the variance as a function of the cycle multiplicity n shows a characteristic shape. The variance function of the light curves of a broad sample of Long Period Variables is found, in many cases, to have a behaviour similar to the variance of a chaotic signal.

1. Introduction

Theoretical arguments that the variability of the less regular variables might be interpreted as *chaos*, in the sense of deterministic chaos arising from a few excited degrees of freedom only, were presented already in 1979 (*Perdang* 1979). The original mathematical analysis was later substantiated by numerical experiments (*Perdang* and *Blacher* 1982, 1984; *Däppen* and *Perdang* 1984; *Whitney* 1984) which explored as a possible factor generating chaos by the nonlinearities in the mechanical equations describing the stellar oscillations (*Hamiltonian chaos*). The relevance of nonlinearities in the thermodynamics of the oscillations as a mechanism generating chaos (*dissipative chaos*) was demonstrated by *Buchler* and *Regev* (1982) and by *Auvergne* and *Baglin* (1985) in the framework of one-zone models. The recent hydrocode experiment by *Buchler* and *Kovács* (1987), in which the full model complications of 'real-

* Permanent Address

istic' W Virginis type variables are implemented, and the full nonlinearities of the pulsations are taken into account, has perhaps most persuasively shown that deterministic chaos is indeed a likely mode of stellar variability.

While on the theoretical front the idea of chaos in the stellar oscillations has thus become a well-established paradigm, no direct observational evidence in favour of chaos in the actual light or velocity curves has been presented so far. Ruelle's phase space reconstruction technique – now the most popular method for detecting deterministic chaos in an empirically given signal (*Grassberger* and *Procaccia* 1983, *Ben-Mizrachi, Procaccia,* and *Grassberger* 1984) – has been applied to Cepheids and variable white dwarfs, without leading to a clear-cut conclusion. The observations are found to be too noisy to lend themselves to a proper phase space analysis (*Auvergne* 1987). As a further practical difficulty, significant phase space reconstructions require a continuous, extremely long time run, of length T ideally of the order of several thousand cycles. Observational light or velocity curves, however, typically present gaps; moreover, they are known over rather short time runs only.

The construction of return maps – another popular procedure for testing for deterministic chaos – is based on the same premises and requirements as the phase space reconstruction. Accordingly, it faces the same difficulties.

The construction of power spectra of the time series at different resolutions, a method in favour in chemistry (*cf. Blacher* and *Perdang* 1981), does not lend itself here to a satisfying test either. In order to be convincingly applicable, this method requires an a priori knowledge of the (effective) dimension of the phase space of the oscillating system producing the signal.

In this paper we have adopted an approach based on the behaviour of a variance function defined in terms of the easily observable maxima of the time series only. First introduced in the study of the Long Period Variables by *Eddington* and *Plakidis* in 1929, this function has the virtue of isolating the noise contributions – assuming that the latter is Gaussian. In principle, it also isolates, a regular signal (in the sense of a periodic or multiperiodic signal with a small number F of independent periods), provided that all of the basic periods of the latter lie in the range $(\Delta t, T)$, where Δt is the (constant) timestep between two successive data points. Non-regular behaviour in the signal is found to produce a variance function showing a specific average shape (*cf.* eq. (11)).

In contrast to the standard phase space reconstruction and the return maps, which practically presuppose that the time signal to be analysed is produced by a dynamical system whose effective phase space dimension D is low (say no higher than 4), the method we describe here does not rely on such a restrictive assumption. The possibility always remains that the actual stellar signal – which is undoubtedly more complex than a theoretically generated surface velocity curve or light

curve of a highly schematised n-zone model, even if $n = 1{,}000$ or $50{,}000$ – is so strongly distorted by the real structure and physical properties of the star as to make the idea of even deterministic chaos obsolete. The actually observed signal could well be intrinsically much more irregular than just deterministically chaotic. We wish to recall at this stage that even the simplest families of (deterministic) cellular automata exhibit a 'fourth class' of behaviour which is indeed notoriously more random than the third, or 'chaotic class' of behaviour (*Wolfram* 1984). Surely, what cellular automata can do should not be too difficult for a variable star. The variance function has, in principle, the potentiality of revealing also these classes of higher order randomness.

We have selected the Long Period Variables (Miras) as the objects of our analysis, for the following reasons. In the first place, the light amplitudes of Miras being at least 2–2.5 mag (*Hoffmeister, Richter,* and *Wenzel* 1984), strict observational errors in the determination of the maxima, and therefore in the time intervals between successive maxima are expected to be minimal. In the second place, the large amplitudes make it plausible that nonlinear effects do indeed directly influence the oscillations. Thirdly, being easily observable, these stars have been extensively and continuously surveyed. Fourthly, Miras do have a single conspicuous period, which seemingly undergoes changes over timescales of the order of the period itself as well as of the order of about 10 times the period; these changes could suggest the existence of a second, and perhaps a third period modulating the light curve.

Besides these points in favour of our choice of Mira variables, we are well aware of at least two unfavourable circumstances. On the one hand, since the periods are longer than ~90 d, the variability of Miras has never been followed continuously over a very large number of cycles. On the other hand, being Red Giants or Supergiants (of ~ $1 M_\odot$) surrounded by circumstellar envelopes in the process of losing mass, Miras undergo pulsations which may be strongly distorted by atmospheric and envelope phenomena; there exist at the present no simple theoretical models capable of accounting for the observed character of the pulsations of these objects.

2. The variance function of artificial signals

Let $f(t)$ be the light curve of a Mira star given over the time interval $0 \le t \le T$. Let t_i , $i = 0, 1, 2, \ldots , c$ be the epochs of c successive maxima. We define the local periods, or cycles, $P_i^{(1)}$, the local 2-periods $P_i^{(2)}$, ... , the local n-periods $P_i^{(n)}$ as follows

$$P_i^{(1)} = t_{i+1} - t_i \,, \quad i = 0, 1, \ldots, c-1 \,, \tag{1}$$
$$P_i^{(2)} = t_{i+2} - t_i \,, \quad i = 0, 1, \ldots, c-2 \,,$$
$$\ldots \qquad \ldots \qquad \ldots$$
$$P_i^{(n)} = t_{i+n} - t_i \,, \quad i = 0, 1, \ldots, c-n \,.$$

We next define the variance of the local n-periods, σ_n^2

$$\sigma_n^2 = (c-n+1)^{-1} \sum_{i=o}^{c-n} (P_i^{(n)} - \langle P^{(n)} \rangle)^2 \,, \tag{2}$$
$$n = 1, 2, 3, \ldots \,,$$

with

$$\langle P^{(n)} \rangle = (c-n+1)^{-1} \sum_{i=o}^{c-n} P_i^{(n)} \approx n \langle P^{(1)} \rangle \tag{3}$$

We have analysed the dependence of the variance σ_n^2 on the cycle multiplicity n under the following circumstances.

(1) If the star is *strictly periodic*, of period $P \equiv P_i^{(1)}$, $i = 1, 2, \ldots, c-1$, then the variance function vanishes for any cycle multiplicity n

$$\sigma_n^2 = 0 \,, \tag{4}$$

provided that the observations are error-free.

If the determination of the epochs of the maxima is subject to accidental *observational errors*, then we have

$$\sigma_n^2 = 2\, \sigma_{obs}^2 \,, \tag{5}$$

where σ_{obs}^2 is the variance of a single epoch measurement. The factor 2 accounts for the fact that a determination of an n-period requires two epoch measurements. The variance is thus independent of the cycle number n.

Relation (5) holds in the limit of a very large number of cycles only ($c \to \infty$). For a finite time run, the variance undergoes relative fluctuations of $\propto 1/\sqrt{c}$. This effect of a finite number of cycles c is illustrated in Figure 1, showing the slow convergence towards the constant value (5) with increasing number of cycles. The noise is produced using a Gaussian random number routine, with $\sigma_{obs}/\langle P \rangle = 0.1$. The two curves labelled $c = 100$ correspond to two different series of random numbers. All continuous curves are obtained using a spline interpolation.

Typical observational runs of Miras involve of the order of 100 cycles. Therefore, the effect of noise cannot be completely filtered out; it is, however, significantly reduced.

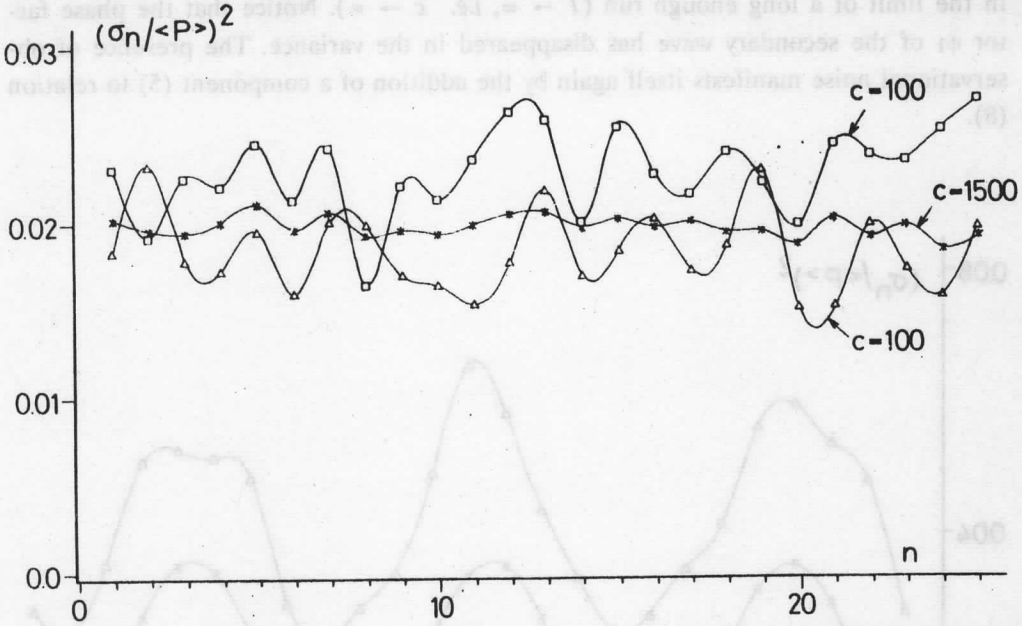

Fig. 1. The contribution of Gaussian noise to the variance function of a periodic signal, for different total numbers of cycles $c \approx 100$ (two experiments) and 1500.

(2) Consider next the case of a Long Period Variable which is intrinsically *double-periodic*. We assume that one amplitude is much smaller than the other (as is suggested by the well defined cycles of these variables). Then the corresponding variance function is a periodic function of the cycle number n. This is analytically seen for a light curve of the form

$$f(t) = A \sin \omega t + A_1 \sin (\omega_1 t + \phi_1) \quad , \tag{6}$$

in which the dominant signal, of amplitude A and frequency ω is contaminated by a secondary wave. Assuming that

$$\varepsilon_1 = (A_1 \omega_1 / A\omega) \ll 1 \text{ with } r_1 = \omega_1/\omega < 1 \quad , \tag{7}$$

we have for the variance, to lowest nonzero order in ε_1 ,

$$\sigma_n^2 = (\varepsilon_1/\omega)^2 [1 - \cos (2\pi r_1 n)] \quad , \tag{8}$$

in the limit of a long enough run ($T \to \infty$, *i.e.* $c \to \infty$). Notice that the phase factor ϕ_1 of the secondary wave has disappeared in the variance. The presence of observational noise manifests itself again by the addition of a component (5) to relation (8).

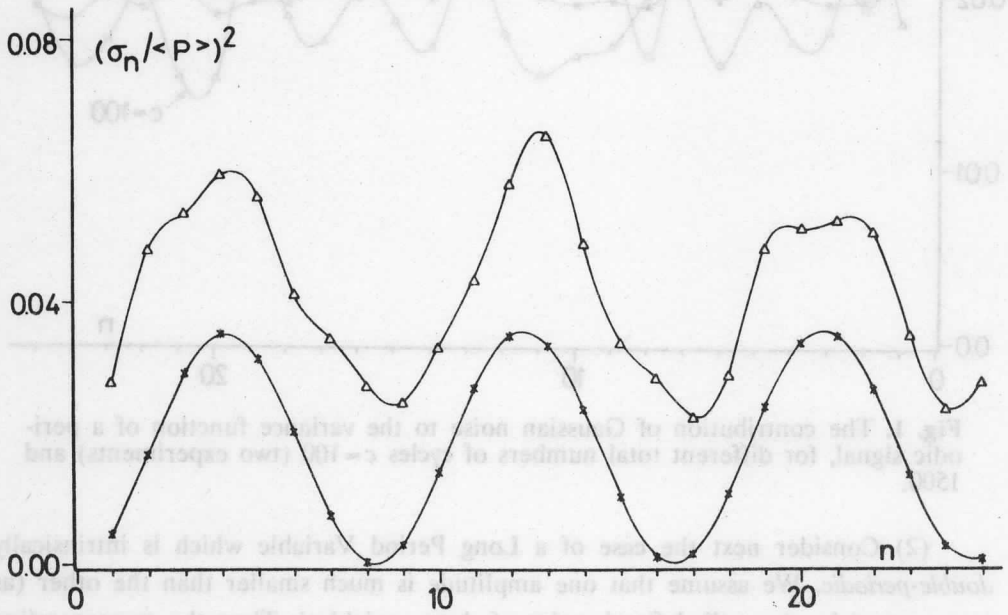

Fig. 2. The variance function σ_n^2 corresponding to a double periodic surface displacement of the standard polytrope in the absence and in the presence of Gaussian noise in the epoch measurements ($\sigma_{obs}/<P> = 0.1$; $c \approx 70$).

Figure 2 illustrates that these conclusions qualitatively hold for an arbitrary nonlinear double-periodic light or velocity curve. The lower curve in the figure corresponds to a double periodic surface oscillation involving the coupled modes 8 and 9 of the standard polytrope (*Perdang* and *Blacher* 1982). The addition of noise is seen to raise this curve on average by $2(\sigma_{obs}/<P>)^2$ (upper curve); but it introduces at the same time a slight deformation of the original strictly periodic curve; the deformation is the result of the fluctuations of the noise component due to the finite number of cycles (as in Fig. 1); we mention also that the finite number of cycles introduces a slight dependence on the phase ϕ_1 in the variance function.

(3) Suppose next that the star is intrinsically *multiperiodic*, ($F+1$ -periodic), one period being dominant, as is typically the case for Mira stars. Then the resulting variance function σ_n^2 is in principle an F-periodic function of n. One can show this property analytically using a representation of the signal similar to equation (6)

$$f(t) = A \sin \omega t + \Sigma_{i=1}^{F} A_i \sin(\omega_i t + \phi_i) \quad , \tag{9}$$

assuming that the components i are 'recessive', *i.e.* satisfy inequalities (7). The variance function in the limit of a large enough number of cycles ($c \to \infty$) is then a linear superposition of expressions of type (8) (neglecting cross-terms between pairs of the recessive modes i,j , $i,j = 1, 2, \ldots, F$)

$$\sigma_n^2 = \Sigma_{i=1}^{F} (\varepsilon_i / \omega)^2 [1 - \cos(2\pi r_i n)] \quad . \tag{10}$$

This approximation is sufficient to indicate that over times shorter than the shortest period ($P = 2\pi/\omega$) the variance function increases quadratically with n ($\sigma_n^2 \propto n^2$). Over long time intervals (sufficiently longer than the longest period P_F) it exhibits the multiperiodic, regular behaviour of the variance; moreover, when averaged over long times, say time intervals longer than the longest period (P_F), the oscillatory behaviour is sifted out and there remains just the constant component of the sum (10). Over time intervals between the shortest (P) and the longest period (P_F), the number of components effectively contributing to the sum (10) increases with time (n); therefore the variance function shows an average regular increase with n, the average rate of increase being essentially conditioned by the spacing of the frequencies.

The presence of noise again raises the σ_n^2–n curve by the constant factor $2\sigma_{obs}^2$, provided that the number of cycles is large enough. The actual finite value of c produces fluctuations in the noise term; as mentioned above, the latter show up as a slight distortion (of relative order $\propto 1/\sqrt{c}$) in the intrinsic variance function of the signal.

It can explicitly be shown that high frequency components in the signal (9), *i.e.* periods shorter than the spacing of the data points of the signal, will manifest themselves as a noisy, n-independent component in the variance function (*Perdang* and *Blacher* 1987).

(4) Besides the above examples of *regular* time series we have attempted to simulate *irregular* signals using an expansion of type (9) (but relaxing the conditions 7), and by progressively increasing the number of components ($F \to \infty$). It is indeed clear that any observational signal given over a finite time interval, $0 \le t \le T$, can be represented analytically by such a Fourier type representation (9), on condition we choose F large enough.

FIGURE 3A

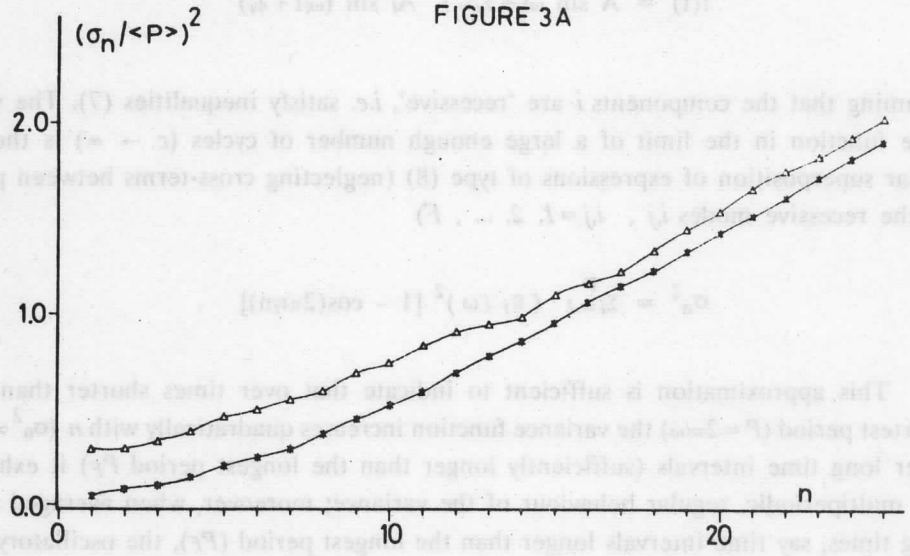

FIGURE 3B

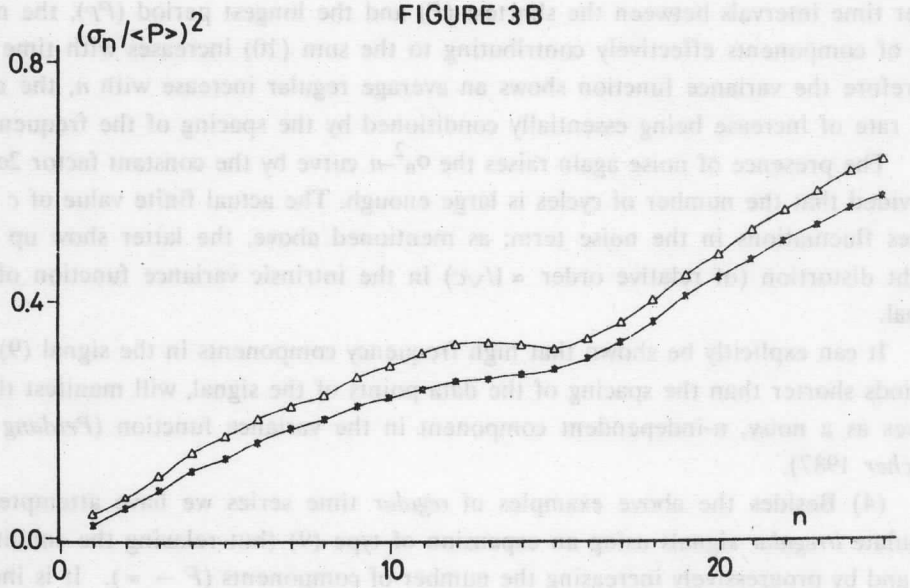

Fig. 3. The variance function σ_n^2 corresponding to a multi-periodic signal with frequencies coinciding with the 10 first frequencies of the standard polytrope, (a) for amplitudes chosen at random, with a uniform distribution in (0,1), in the absence (lower curve) and in the presence of noise (upper curve) respectively, with $\sigma_{obs}/<P> = 0.5$ and $c \approx 180$; (b) for amplitudes decreasing like a power of the order j^{-2}, $j = 1, \ldots, 9, 10$, in the presence and in the absence of Gaussian noise, with $\sigma_{obs}/<P> = 0.1$ and $c \approx 60$.

We find that the character of the variance function strongly depends on the statistical distribution of the frequencies and on the frequency dependence of the amplitudes. We discuss here only two cases (*cf. Perdang* and *Blacher* 1987 for further illustrations).

Figures 3a,b are dealing with the simulation of time series by Fourier-like representations. Instead of an actual Fourier series with frequencies $\omega_n = n\omega_0$, $n = 1,2, \ldots$, $\omega_0 = 2\pi/T$, we use a set of statistically uniformly distributed frequencies over a certain range, in particular those of the standard polytrope; as the normalisation of the fundamental frequency we choose 1 instead of $2\pi/T$; with this choice a small number of frequencies allows us to simulate a still wide variety of time signals (although the long-time behaviour of these signals is fixed by their short-time variations).

Figure 3a shows the case of amplitudes A randomly distributed in the interval $0 \leq A \leq 1$; the mean 1-period $<P>$ is then found to decrease with increasing F. We observe a regularly increasing variance, with a quadratic behaviour near the origin (as observed for $n \leq 3$), an approximately linear increase at higher cycle numbers, and finally a tendency towards a flattening at $n \approx 25$. We expect that for higher n values, the curve shows oscillations. The addition of even a very large amount of noise ($\sigma_{obs}/<P> = 0.5$) is seen to produce only a slight local deformation.

Figure 3b corresponds to the case of amplitudes A decreasing with the frequencies according to a power law, essentially as $A \propto \omega^{-a}$, $a = 2$. The diagram exhibits an increasing variance with a trend towards oscillation manifesting itself at lower n values. The addition of noise ($\sigma_{obs}/<P> = 0.1$) produces as expected, a vertical displacement and a slight deformation of the intrinsic variance.

For amplitudes decreasing exponentially with the frequencies, $A \propto exp(-a\omega)$, the behaviour of the variance depends strongly on a. For a very slow exponential decrease, we recover case (a); for $a \geq 1$ we reproduce the regular cases discussed above, and in particular the behaviour of Figure 2.

In these illustrations the intrinsic variance is fluctuating about a curve of positive and slowly varying slope; analytically we may describe this behaviour by

$$\sigma_n^2 = An^{\alpha} + P(n) \quad , \tag{11}$$

where A and α are positive constants and $P(n)$ is an oscillatory component. A best fit of (11) over the interval plotted, disregarding the fluctuating term, gives $\alpha > 1$. The overall increasing trend (An^{α}) holds over a finite n-interval only; it levels off and eventually fluctuates around a finite threshold.

FIGURE 4 A

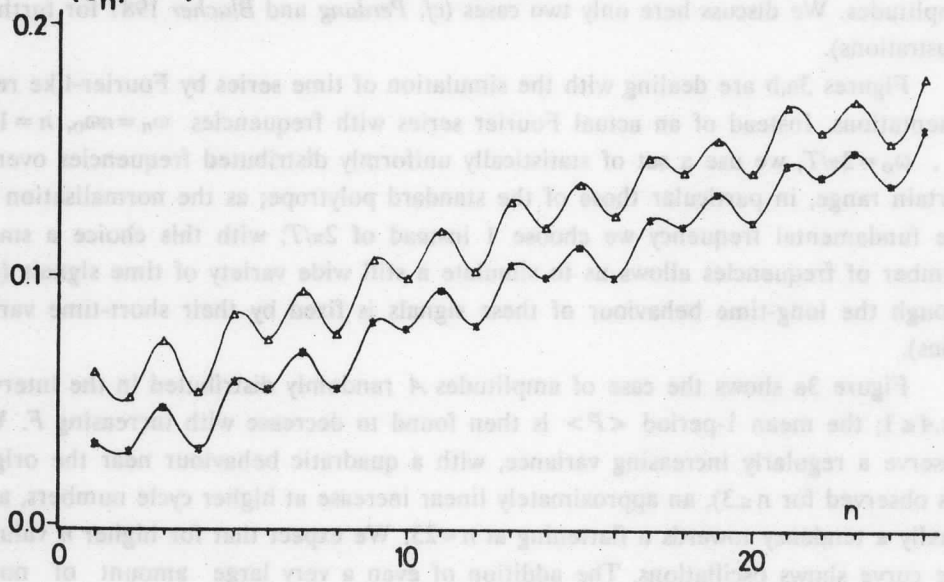

FIGURE 4 B

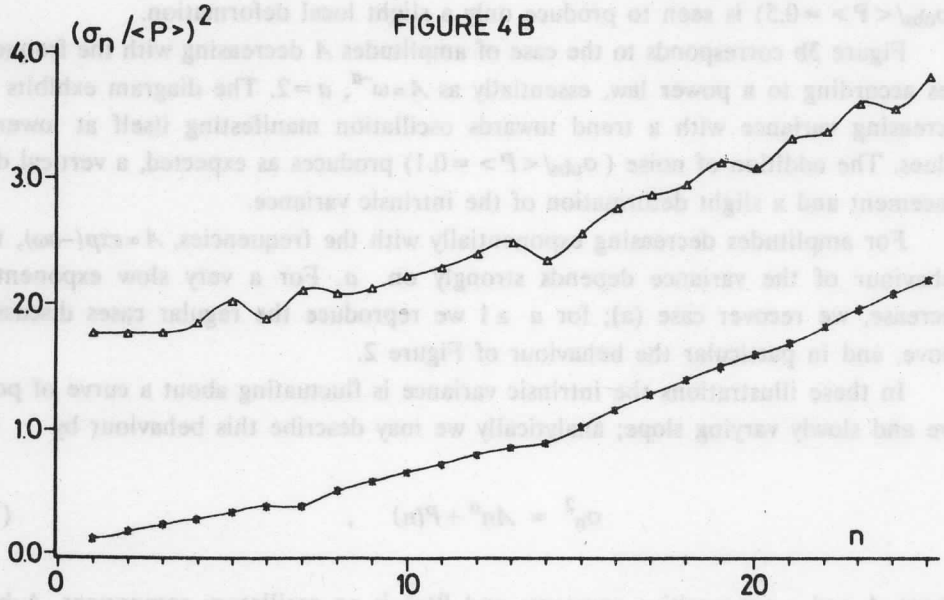

Fig. 4. The variance function σ_n^2 corresponding to a multi-periodic signal with frequencies proportional to $10x2^{-j}$, $j=1, \ldots, 9, 10$ (a) for amplitudes chosen at random, with a uniform distribution in (0,1), in the absence and in the presence of noise respectively, with $\sigma_{obs}/<P>=0.1$ and $c\approx 600$; (b) for amplitudes decreasing as $j^{-0.5}$, $j=1, \ldots, 9, 10$ again in the presence and in the absence of Gaussian noise; with $\sigma_{obs}/<P>=0.9$ and $c\approx 600$.

In our second series of simulations displayed in Figures 4a,b we let the frequencies accumulate towards the origin. The frequency distribution is represented by $\omega_j = 10x2^{-j}$, $j = 1,2, \ldots, 10$.

In Figure 4a the amplitudes are statistically uniformly distributed, $0 \leq A \leq 1$. The variance function shows again an increasing trend, with a superimposed oscillation. Representation (11), with $P(n)$ oscillatory is seen to be an excellent approximation to the actually computed variance function, with α practically 1. Noise ($\sigma_{obs}/<P> = 0.1$) produces here little deformation, since we are using a much larger number of cycles than in previous cases.

Figure 4b shows the variance function for amplitudes decreasing with order j, as j^{-a}, $a = 0.5$. Again representation (11) applies. The effect of even an enormous amount of noise ($\sigma_{obs}/<P> = 0.9$) does not change the trend of the intrinsic variance function.

Although the time series corresponding to the variance functions plotted in Figures 4a,b remain of course strictly *regular*, the fact that the amplitudes do not decrease at least exponentially with order is indicative that these signals conceal a latent chaotic-like character: genuine *chaos* would manifest itself in the limit $F \rightarrow \infty$. The species of 'incipient' chaos generated by the signal of Figure 4b is essentially deterministic chaos arising through a Feigenbaum sequence. The species of chaos created out of a signal of Figure 4a is seemingly more irregular than the variety of Figure 4b, since all amplitudes remain in the same order in the former case.

In the limit $F \rightarrow \infty$, the time behaviour underlying the variance shown in Figures 3a,b can likewise be considered as leading to chaos, provided that the amplitudes do not decrease exponentially with order, and provided that we include also longer and longer periods, (the longest periods being longer than the time interval T over which the signal is given). The lack of predictability in a chaotic signal – which is the fingerprint of chaos – is precisely the consequence of the existence of arbitrarily long periods within the signal.

(5) We have investigated also a signal modelled by expansion (9) with the frequencies showing a self-similar, hierarchical distribution at a reference frequency and at the origin. Such a representation simulates the kind of chaos encountered in Hamiltonian chaos. The behaviour of the variance function is then essentially the same as for an adiabatic chaotic oscillation of a stellar model. In Figure 5 we display the variance function for a genuine chaotic oscillation produced through the coupling of modes 8 and 9. The trend (11) is again obeyed, with $\alpha < 1$ with a fluctuating component of pseudo-period ~ 12 cycles. A similar result holds for the coupling of the fundamental mode and the first harmonic; the fluctuating term has a shorter pseudo-period.

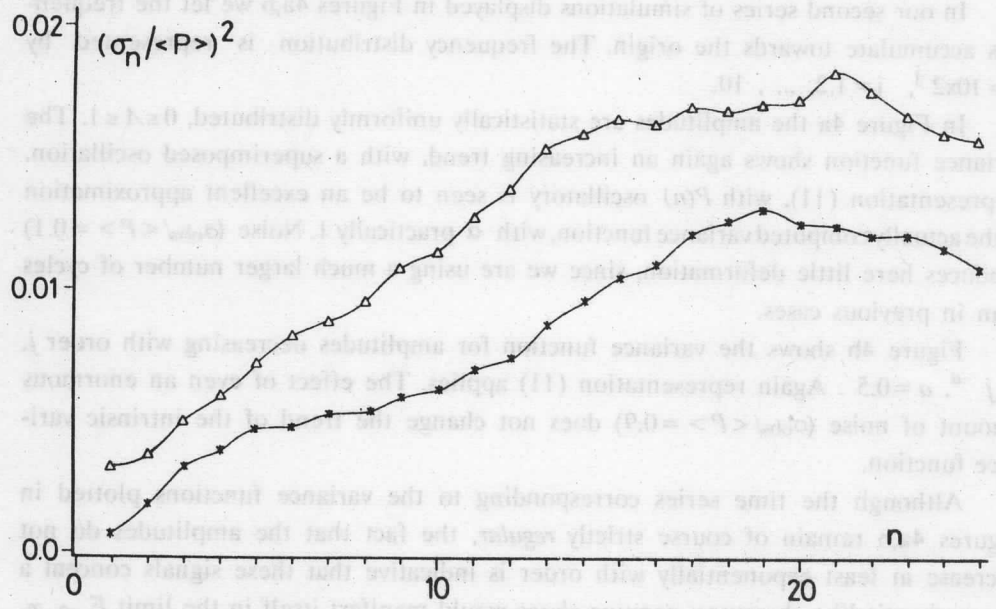

Fig. 5. The variance function σ_n^2 corresponding to a chaotic surface displacement of the standard polytrope (coupled modes 8–9) in the absence and in the presence of Gaussian noise, with $\sigma_{obs}/<P> = 0.03$ and $c \approx 40$.

Our numerical results demonstrate the well known fact that a chaotic signal of finite length T cannot be distinguished from a signal *en route* towards chaos, namely a regular signal with a large number of frequencies (including frequencies less than $2\pi/T$). Empirically any finite-length signal with a very large number of frequencies can either be viewed as regular or chaotic. If no further information is available – for instance the dimension of the phase space of the dynamical system which generated the signal, *etc.* – then manifestly *no* method can be devised to decide either way. However, provided that long enough time series are at our disposal, we can easily distinguish regular signals with a small number F of effective degrees of freedom (*cf.* Fig. 2) from chaotic signals with a small number of degrees of freedom *or* from regular signals with a very large number of effective degrees of freedom (Figs. 3–5). Noise, as our experiments demonstrate, does not seriously affect the shape of the variance function. Perhaps we should point out that in all experiments we have adopted a noise level which largely exceeds the realistically expected observational errors in the epoch determination of Miras.

Noise pollution of the variance function – provided that it is in the form of Gaussian noise – can be sifted out in a trivial way from genuine information. In the representation of the variance function noise just manifests itself as an additive positive factor (eq. 5) plus a slight deformation of the noiseless variance shape. This

is clearly borne out in all of our experiments (Figs. 1–5). As indicated above, however, the actual constant contribution in a variance function is, in general, only partially an observational noise effect; short period fluctuations do contribute a constant factor to the variance as well.

3. The variance function of Mira stars

The variance function σ_n^2 as a global characterisation of the variability of stars was introduced in connection with a study of the light curves of the Long Period Variables *o* Ceti and x Cygni by *Eddington* and *Plakidis* (1929). In their paper Eddington and Plakidis raised the question of the physical nature of the irregularities superimposed on the dominant periodic variability of these stars. In current terminology they actually asked whether the variability of Long Period Variables is regular or chaotic.

In fact, the type of chaos Eddington had in mind was of a more irregular nature than the mere deterministic variety. The idea Eddington suggested was that the local periods $P_i^{(1)}$ showed strictly stochastic fluctuations, without any correlation between the fluctuations of successive periods $P_i^{(1)}$ and $P_{i+1}^{(1)}$. It can be seen that under this hypothesis the variance function obeys

$$\sigma_n^2 = An \quad , \tag{12}$$

(the exponent α in eq. (11) being equal to 1 and the fluctuating component $P(n)$ being zero). The direct calculation of the variance function from the observational data led Eddington and Plakidis to conclude that 'the curves of *o* Ceti and x Cygni appear to be fairly concordant with the hypothesis...' [of uncorrelated fluctuations].

The attempt at characterising the lack of strict periodicity of Long Period Variables by means of a variance function of type (12) (plus a constant noise term) was followed up by several authors, but eventually abandoned in the sixties. Representation (12) plus noise was indeed found to lead to various observational inconsistencies (*cf.* the historical account in *Perdang* 1985).

We have computed the variance function σ_n^2 for a large sample of Mira stars whose light curves have been observed over about 100 successive cycles. The observational information, taken from Campbell's catalogue (*Campbell* 1955), refers to objects whose mean light curves are all symmetric, and virtually sinusoidal. It is therefore reasonable to conclude that there is no major exotic physical mechanism operating in these stars.

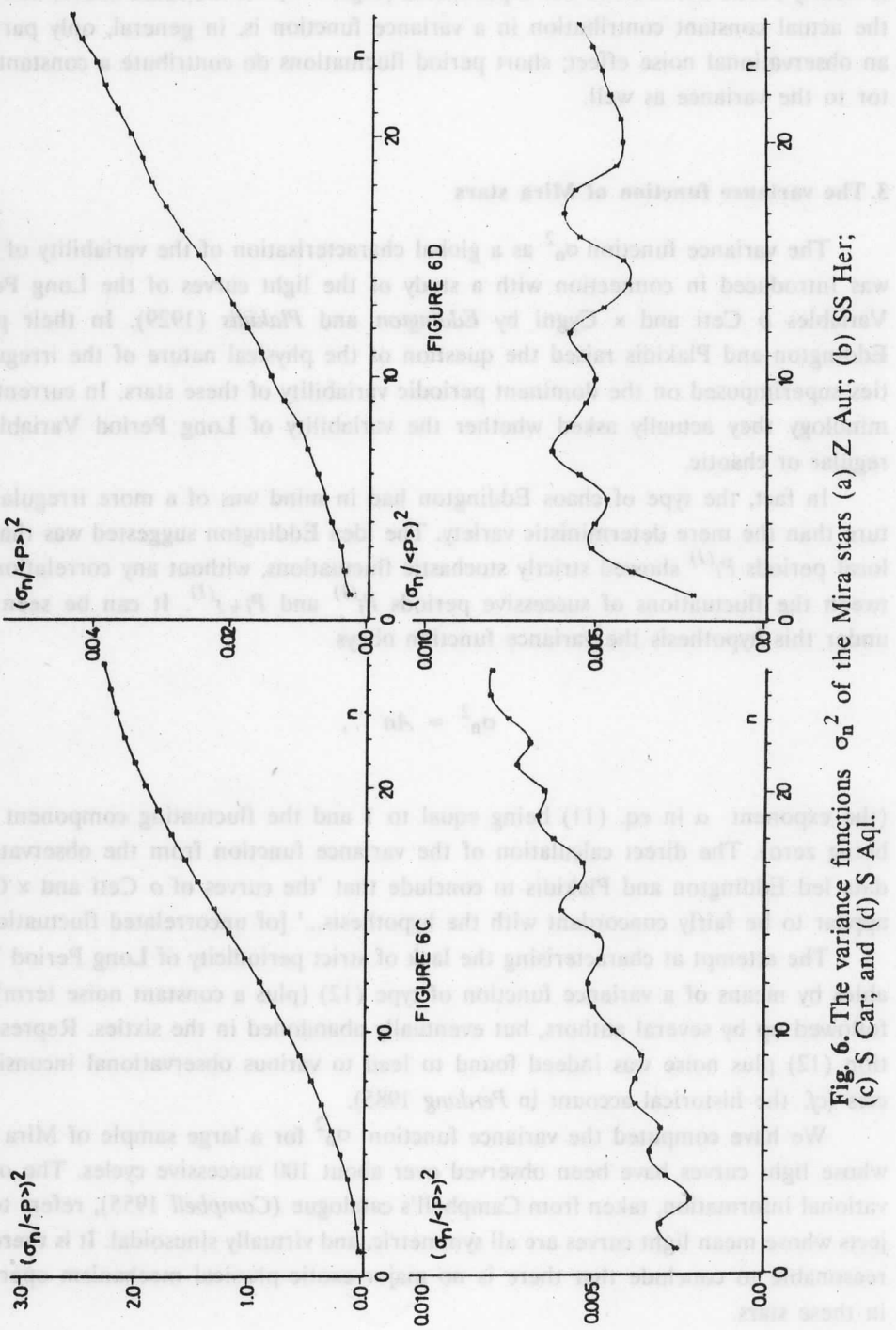

Fig. 6. The variance functions σ_n^2 of the Mira stars (a) Z Aur; (b) SS Her; (c) S Car; and (d) S Aql.

The typical patterns of observational σ_n^2 curves we encountered can roughly be divided into 3 types (*cf.* Figs. 6a,b,c,d).

(a) Miras with extremely *irregular* local period fluctuations from one cycle to the next, with very large relative changes in the cycle lengths, and with superimposed average *period switches.* For these stars the variance is regularly increasing, changing from a quadratic behaviour $\sigma_n^2 \propto n^2$ near the origin ($n < 10$), to a linear shape $\sigma_n^2 \propto n$ at intermediate values of n (from 10 to 20), and seemingly tending towards a plateau at higher n values (>20). We have observed this behaviour in the case of Z Aur (Fig. 6a), an object which shows extreme local period fluctuations (95–150 d over the observational time stretch); the averaged local periods display a jump from an average value of 110 d to 135 d. The large values of $(\sigma_n/<P>)^2$ found for this star are due to the period switches.

(b) Miras with very *irregular* local period fluctuations, and large relative changes in the cycle lengths, but without period switches over the observed time interval. The variance has essentially the same shape as for case (a), but with characteristic $(\sigma_n/<P>)^2$ values of a factor of 50 lower. The variable SS Her (range of the period fluctuations 95–120 d), shown in Figure 6b, and R Vir are examples of this class.

(c) Miras whose local period fluctuations as a function of the number of cycles, although irregular, exhibit some *pattern:* typically we observe a superposition of several seemingly independent waves. These objects have a variance of type (11) with α close to 1, together with a small amplitude fluctuation $P(n)$. As an example we quote S Car whose variance function fluctuates on a characteristic time scale of ~3–4 cycles (Fig. 6c); a similar behaviour is observed for R Vul, X Cam or T Her.

(d) Miras whose local periods, while fluctuating, remain strongly concentrated around an average value; a diagram of the local periods versus the cycle number shows again independent waves.

In this case we observe a variance of type (11) with $\alpha < 1$ and a large oscillatory contribution $P(n)$. S Aql (Fig. 6d) and W Pup are illustrative examples of this category.

If we compare these observational curves with the results of the numerical simulations we notice the following correspondences: Case (a) and case (b) behaviour of the variances can be reproduced by a signal with a uniform density of frequencies and a uniform distribution of amplitudes (*cf.* Fig. 3a); such a signal, if interpreted as chaotic, is presumably of a more irregular type than conventional deterministic chaos arising for instance out of successive period doublings.

Case (c) variances are similar to the simulation shown in Figure 4a, suggesting a type of chaos more irregular than for instance the common variety encountered in turbulence; we have here essentially uniform amplitudes over the region of accumulation of the frequencies.

Finally, case (d) variances are reminiscent of Hamiltonian chaos (Fig. 5), suggesting an interaction of two modes.

In any event, if we accept the idea that the time behaviour of these stars involves only a few effective degrees of freedom, the above results suggest that the observations cannot be interpreted as regular oscillations. Our simulations also rule out an interpretation of the irregularities as artifacts due to noise. The most plausible conclusion is therefore that we are witnessing chaos.

4. Conclusion

Our numerical study using just the epochs of the maxima of the observational light curves of a sample of Long Period Variables, indicates that the variability of these objects is consistent with *chaos* in all cases we have analysed. We wish to mention that we have also tried to construct return maps for these variables (*Perdang* and *Blacher* 1987). Unfortunately, the noise level in the observations does not enable us to isolate any clear cut pattern in those diagrams: the presence of noise merely produces a random scatter of the data points all over an area. It is the virtue of the procedure outlined in this paper to isolate noise (or high frequency fluctuations) from the main signal.

We wish to remind the reader once more that an observationally given signal can always be interpreted by a simple or a multiple Fourier series, so that we can never definitively conclude that the signal is 'intrinsically' chaotic. It may well have been generated by a dynamical system involving a huge number of degrees of freedom.

References

Auvergne, M. 1987, Communication presented at the CECAM Preparatory Meeting on *Nonlinear Hydrodynamics and Magneto-Hydrodynamics in Stars,* Utrecht, September 9-11, 1987.

Auvergne, M., and Baglin, A. 1985, *Astr. Ap.,* **142**, 388.

Ben-Mizrachi, A., Procaccia, I., and Grassberger, P. 1984, *Phys. Rev.,* **A29**, 975.

Blacher, S., and Perdang, J. 1981, *Physica* **3D**, 512.

Buchler, J. R., and Kovács, G. 1987, *Ap. J. Letters,* **320**, L57.

Buchler, J. R., and Regev, O. 1982, *Ap. J.*, **263**, 312.

Campbell, L. 1955, *Studies of Long Period Variables*, AAVSO, Cambridge, Mass.

Däppen, W., and Perdang, J. 1984, *Mem. Soc. Astr. It.*, **55**, 299.

Eddington, A. S., and Plakidis, S. 1929 *M. N. R. A. S.*, **90**, 65.

Grassberger, P., and Procaccia, I. 1983, *Physica* **9D**, 189.

Hoffmeister, C., Richter, G., and Wenzel, W. 1984, *Veränderliche Sterne*, Springer, Berlin.

Perdang, J. 1979, *Stellar Oscillations:The Asymptotic Approach*, Lecture Notes, Third Cycle in Astronomy and Astrophysics, FNRS, Brussels.

Perdang, J. 1985, *Physicalia*, **7**, 239.

Perdang, J., and Blacher, S. 1982, *Astr. Ap.*, **112**, 35.

Perdang, J., and Blacher, S. 1984, *Astr. Ap.*, **136**, 263.

Perdang, J., and Blacher, S. 1987, (in preparation).

Plakidis, S. 1931, *M. N. R. A. S.*, **92**, 460.

Whitney, C.A. 1984, in *Proceedings of the 25th Liège International Colloquium: Theoretical Problems in Stellar Pulsations*, July 10-13, 1984, p. 454.

Wolfram, S. 1984, *Physica* **10D**, 1.

KULTURA Külkereskedelmi Vállalat közös kiadása
az MTA Csillagászati Kutató Intézettel
Felelős kiadó: Szeidl Béla, Szabó József
Szerzők: Kovács-Szabados-Szeidl
Lektorok: Dr. Paparó Margit, Harvey Shenker
Példányszám: 500 Törzsszám: 88-357
Készült a KFKI sokszorosító üzemében
Felelős vezető: Töreki Béláné
Budapest, 1988. julius hó
ISBN 963 8361 29 8